THE USE OF ENHANCED ANAEROBIC DIGESTION PROCESS FOR ENERGY RECOVERY AND PHOSPHORUS RELEASE FROM AGRO-INDUSTRIAL WASTES

by

UGWU SAMSON NNAEMEKA (61342947)

submitted in accordance with the requirements
for the degree of

DOCTOR OF PHILOSOPHY

in the subject

ENGINEERING

at the

UNIVERSITY OF SOUTH AFRICA

SUPERVISOR: PROFESSOR CHRISTOPHER C. ENWEREMADU

DECEMBER 2020

Title page

The use of enhanced anaerobic digestion process for energy recovery and phosphorus release from agro-industrial wastes

The financial assistance of the National Research Foundation (NRF) towards this research is hereby acknowledged. Opinions expressed and conclusions arrived at, are those of the author and are not necessarily to be attributed to NRF.

Publications during candidature (included in this thesis)

Journal Publications

Ugwu, S. N., and Enweremadu, C. C. (2020). Ranking of energy potentials of agro-industrial wastes: Bioconversion and thermo-conversion approach. Energy Reports, 6, 2794-2802.

Ugwu, S. N., and Enweremadu, C. C. (2020). Enhancement of biogas production process from biomass wastes using iron-based additives: types, impacts, and implications. *Energy Sources, Part A: Recovery, Utilization, and Environmental Effects*, 1-23.

Ugwu, S. N., Biscoff, R. K. and Enweremadu, C. C. (2020). A meta-analysis of iron-based additives on enhancements of biogas yields during anaerobic digestion of organic wastes. *Journal of Cleaner Production*, 122449. DOI: 10.1016/j.jclepro.2020.122449

Ugwu, S. N. and Enweremadu, C.C. (2020) Enhancing anaerobic digestion of okra waste with the addition of iron nanocomposite (Ppy/Fe_3O_4), Biofuels, 11:4, 503-512
DOI: 10.1080/17597269.2019.1702796

Ugwu, S. N. and Enweremadu, C. C. (2019). Biodegradability and kinetic studies on biomethane production from okra (Abelmoschus esculentus) waste. *South African Journal of Science*, *115*(7-8), 1-5. DOI: 10.17159/sajs.2019/5595

Ugwu, S.N. and Enweremadu, C.C. (2019). Effects of pre-treatments and co-digestion on biogas production from Okra waste. Journal of Renewable and Sustainable Energy 11, 013101 (2019); DOI: 10.1063/1.5049530

Ready for submission

Ugwu S.N. and Enweremadu C.C. Life cycle assessment of enhanced anaerobic digestion of agro-industrial waste for biogas production. *Journal of cleaner production.*

Ugwu S.N. and Enweremadu C.C. Optimization of iron enhanced anaerobic digestion of agro-wastes for biomethane production and phosphate release. *Renewable energy.*

Conference papers presented

Ugwu, S.N. and Enweremadu, C.C. (2019). Comparative Studies on the Effect of Selected Iron-Based Additives on Anaerobic Digestion of Okra Waste. In *ASME 2019 13th International Conference on Energy Sustainability* American Society of Mechanical Engineers. Bellevue, Washington, USA. July 14-17,2019. DOI: 10.1115/ES2019-3820

Ugwu, S.N. and Enweremadu, C.C. (2019). Ranking of Energy Potentials of Agro-Industrial Wastes: Bioconversion and Thermo-conversion Approach. Book of Abstracts of the 3rd International Conference on the Sustainable Energy and Environmental Development. 16-18 October 2019 Krakow, Poland.
http://www.ize.org.pl/wydawnictwo/materialykonferencyjne/2019/seed2019-book-of-abstracts.pdf

Ugwu, **S. N.,** Ugwuishiwu, B. O., Nwoke, O. A., Echiegu, E. A and Enweremadu, C. C. (2018). Kinetic Studies on Methane Production from Okra Wastes Using Growth Functions. Proceedings of the 3rd NIAE-SE Regional Conference, Univ. of Nig., Nsukka 27th-30th August, 2018. 63-71. (**won the best paper presentation award**)

Declaration

I, **UGWU, SAMSON NNAEMEKA (61342947)** declare that .. **The Use of Enhanced Anaerobic Digestion Process for Energy Recovery and Phosphorus Release from Agro-Industrial Wastes** is my own work and that all the sources that I have used or quoted have been indicated and acknowledged by means of complete references. I further declare that I submitted the thesis/dissertation to originality checking software and that it falls within the accepted requirements for originality. I further declare that this work is being submitted for the degree of Doctor of Philosophy and that I have not previously submitted this work, or part of it, for examination at University of South Africa for another qualification or at any other higher education institution.

Signature:  **Date:** 7th December, 2020

Dedication

This thesis is dedicated to the Lord Almighty, my supportive family and true friends

Acknowledgement

My profound gratitude goes to my PhD supervisor, Professor Christopher Chintua Enweremadu for his invaluable support throughout my doctoral degree program in the Department of Mechanical and Industrial Engineering (DMIE), University of South Africa (UNISA). I am sincerely grateful for your diligent guidance, encouragement and advice. Your belief in me inspired the confidence needed to get this work to this final stage. Thank you most sincerely Prof.

Prof. D.C. Baruah is immensely acknowledged for his professional advice and contributions to this research at the conception stage. Special thanks to Dr. Nyoni of Nanotechnology and Water Institute, University of South Africa for his help during the characterization phase of this research. Prof. Kevin Harding, your timely intervention and assistance at the life cycle assessment component of my study will never be forgotten. Thank you Dr. Uyiosa Aigbe for making chemicals and other consumables readily available for my use. I appreciate the support of the Chair of Department, Ms. Nelly Nkambule, Gugulethu Dubase, other academic and administrative staff of DMIE; your sincere support was instrumental to the success of this program.

The bodies behind the funding and scholarships I received during my doctoral program are deeply appreciated. I want to thank The World Academy of Science (TWAS) and South Africa's National Research Foundation (NRF) (2017-2019), University of South Africa and NRF S&F-Extension Support for Scholarships and Fellowships (2020) for financing this research. I would also like to thank DMIE-UNISA for the Research Assistantship offered to me during this program.

I want to sincerely thank Chinenye, my wife. Your unconditional love, prayers and doggedness were a great source of strength. I also want to extend my appreciation to my brother (JohnFirstday), in-laws and friends for their support and encouragement. Thank you all.

Most importantly, I wish to thank my Lord and Savior, Jesus Christ for his protection, preservation, mercy, favor and guidance throughout this doctoral program.

Abstract

Enhancement of anaerobic digestion process is an established strategy for ensuring the usability of diverse substrate-types, overcoming the recalcitrance of substrates to biological conversion and increasing biodegradability. It aids the supplementation of deficient but vital nutrients useful to methanogenic activities and constituting cofactors in anaerobic digestion enzymes as well as increasing both biogas production and biomethane content. Although these enhancements especially the use of iron-based additives aid substrate solubilization and improve biomethane yield, the iron ions react with other available ionized nutrients such as phosphate (P) to form non-degradable complexes and hinder recoverability of P or its release for plant usage. In response, this thesis investigates an integrated approach to biomethane recovery and P release using different enhancement options (accelerants and antagonists) as well as an assessment of the environmental impacts of the enhanced processes. Mixed methodological approach was employed in this study to select a novel substrate (okra biomass) and additive (Ppy/Fe_3O_4 NPs) for anaerobic digestion and assessment of the impacts of enhancement options on the environment. From all the enhancement options, most of them increased biomethane yield, but 20 mg/L of Ppy/Fe_3O_4 NPs gave the highest biomethane yield. The optimization of additives (accelerants and P antagonist) supplementation achieved the maximum biomethane yield of 502.743 mLCH4/gVS and P release of 168.674 mg/L at the optimum conditions of Ppy/Fe_3O_4 (20.0014 mg/L), HA (5.0018 mg/L), As (1.448 mg/L) and co-digestion (25.0001%). In considering the energy-environmental trade-offs of the enhancement options, a comparative assessment of the impact categories showed that co-digestion+Ppy/Fe_3O_4 NPs and Ppy/Fe_3O_4 only options improved biomethane productions and recorded lower impact category values.

Keywords: anaerobic digestion, enhancement, biomethane, biogas, iron-based, life cycle assessment, pretreatment, biogas, wastes, additives, optimization, antagonists, accelerants.

Table of Contents

List of Tables

List of Figures

Chapter one

Introduction

This chapter is partly adapted from: Ugwu, S. N., and Enweremadu, C. C. (2020). Enhancement of biogas production process from biomass wastes using iron-based additives: types, impacts, and implications. *Energy Sources, Part A: Recovery, Utilization, and Environmental Effects*, 1-23.

Ugwu, S. N., Biscoff, R. K. and Enweremadu, C. C. (2020). A meta-analysis of iron-based additives on enhancements of biogas yields during anaerobic digestion of organic wastes. *Journal of Cleaner Production*, 122449.

1.1 Overview of global energy status

The need to achieve 50% reduction in global emissions by 2030, carbon-neutral economies by 2050 and restrict the rise of global mean temperature to 1.5^{o}C more than the pre-industrial levels has necessitated the global efforts aimed at reducing CO_2 and other emissions (BP,2019; IPPC, 2018). One of such efforts is succinctly captured as sustainable development goal (SDG) 7, which targets increasing access to reliable, affordable and sustainable energy, energy efficiency and the share of renewable energy in the global energy mix (UNDP 2020; UNSTAT, 2019; IPCC, 2018). Aside from the environmental and climate change issues associated with the use of fossil energy types, their imminent depletion coupled with the rising energy demand gap is a source of concern. The global primary energy consumption rose by 2.9 % in 2018, doubling the 10-year average value of 1.5% per year and expected to rise to about 18 BToE in 2040 as shown in Fig. 1.1a (BP, 2019). In contrast, the global proven oil reserve is estimated to sustain global demands for barely 50 more years (BP, 2019). The same pattern of increasing consumption and constant depletion applies to both coal and natural gas, which are also major conventional energy sources (BP, 2019). The increased global fossil energy usage caused the unprecedented rise of carbon emission to 2% in the last seven years and would be about 42.4 billion tons in 2035(BP, 2019) However, with the sustenance of the 17.8% renewable energy growth in 2018 as shown in Fig.1.1b, this continuous menace to the environment could be mitigated (WBA, 2019).

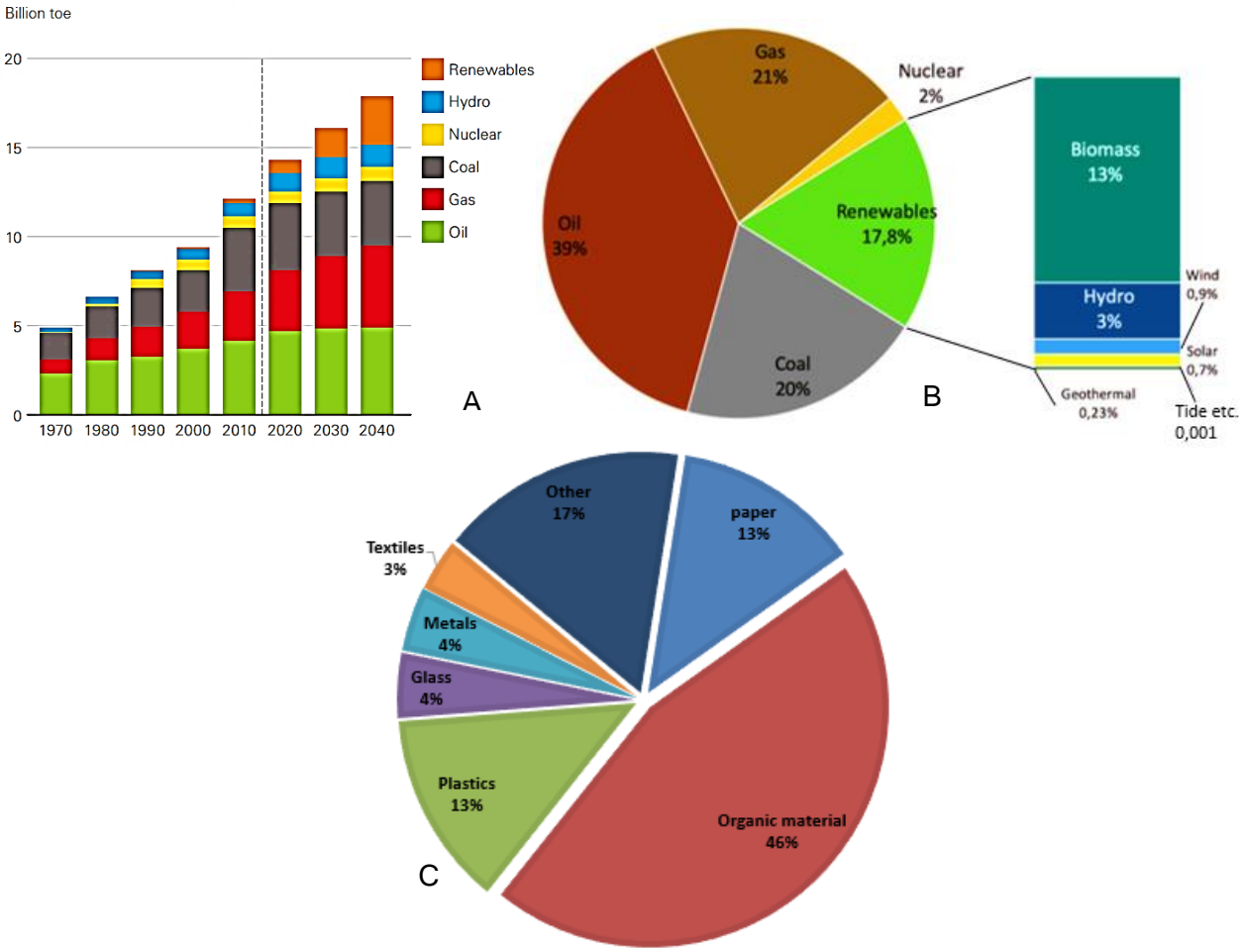

Fig. 1. 1 (a) Global Primary Energy Demand (BP, 2019), (b) Global Final Energy Consumption (WBA, 2019) (c) Global Composition of Municipal Waste (Adapted from UNSTAT, 2020)

On the other hand, renewable energy sources are clean and affordable with capabilities of bridging the global energy demand-gap and ensuring environmental sustainability. Bioenergy is a renewable energy type, involving the conversion of biomasses and organic fraction of wastes (Basu, 2018; Maletta and Díaz-Ambrona, 2020). Most biomass emanates from varying stages of agro-industrial and other human activities and can be utilized in energy generation via pyrolysis, gasification, combustion, anaerobic digestion or fermentation into solid, gaseous or liquid biofuels (Gao et al. 2018). Depending on their origin, these biomasses grouped into generations (first, second, third and fourth) as shown in Fig. 1.2 (Chauhan, 2020). According to WBA (2019) and Maletta and Díaz-Ambrona (2020), total biomass potential of the world is about 55.6 EJ/year, which accounts for about 70% of the gross renewable energy usage and projected to rise to 100-300 EJ by 2050. Currently, energy from biomasses constitutes more than 13% of all primary energy supplied globally, 90% of which is used mostly for heating purposes in developing countries (WBA, 2019; Maletta and Díaz-

Ambrona, 2020). Similarly, while the total food wastes currently stand at 3.6 million tons/day, it is expected that the organic fraction of the daily global waste generations will amount to 46% of the 6 million tons/day of the total wastes in 2025 as shown in Fig. 1c (UNSTAT, 2020; Huang et al., 2020).

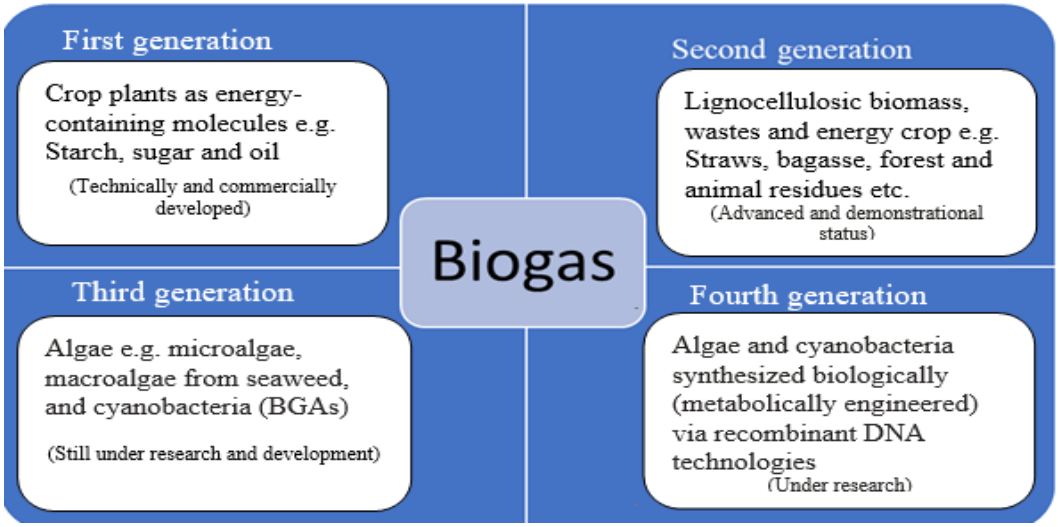

Fig. 1. 2 Classification of biomasses for biogas production based on their generations.

The enormous organic fraction of all the biomass generations for energy production purposes shown in Fig. 1.2 can be anaerobically digested for biogas production. Anaerobic digestion is an established biomass-to-energy and waste management technology that uses various biochemical stages (hydrolysis, acetogenesis, acidogenesis and methanogenesis) to achieve waste volume reduction, treatment and clean energy recovery (Cai et al. 2017). Biogas yield is projected to grow by 40% in 2040 at an annual growth rate of 9.7% (IEA, 2020a). The organic (biodegradable) component for anaerobic digestion are composed of biopolymers (lignin, cellulose, hemicellulose, starch, lipids, keratin, elastin and collagen), monomers and synthesized polymers (polypropylene, polyethylene and polyesters) (Akunna, 2018; Cai et al. 2017). The lignocellulosic polymers (lignin 0-40%, cellulose 15-99% and hemicellulose 0-85%) form the major organic fraction of biodegradable biomass, unlike monomers, which are easily broken-down in an anaerobic digestion process, the polymers have structures that take a long time to breakdown (Akunna, 2018; Li et al. 2018). Aside from the challenges associated with structural degradation of lignocellulosic biomasses, slow syntrophic metabolism of intermediate products, low acidification rate, difficulties in removing humic substances and bacterial cell disintegration also inhibits methanogenic activities during the anaerobic digestion processes (Liu et al., 2016; Hao et al., 2017, Bharathiraja et al., 2018, Zhang et al., 2019). These identified challenges with ease of substrate degradation and hampered methanogenic activities necessitate some forms of substrate pretreatments and enhancements during anaerobic digestion

(Akunna, 2018; Li et al. 2018).

1.2 The need for anaerobic digestion enhancement and biogas yield

The organic fraction of wastes, which are largely lignocellulosic, limits the viability of substrates for biogas production. Lignocellulosic biomasses have complex and compact structures, resulting in low hydrolysis rate and low substrate biodegradability (< 70%) (Li et al. 2018). Previous studies showed that pretreatment of these lignocellulosic polymers (substrates) mechanically, thermally or chemically for anaerobic digestion, improves overall process performance vis-à-vis increased methane yield, solids and hydraulic retention-time reduction (Carlsson, 2015; Kreuger et al. 2011; Ward et al. 2008). Alkaline pretreatment was reported in Zhang et al. (2014a) and Ugwu and Enweremadu (2019) to degrade cellulose and hemicellulose as well as the three-dimensional network of lignin by promoting methanogenesis during acetogenesis. Li et al. (2018) and Zhang et al. (2014), showed that in the pretreated substrate, hemicellulose and cellulose content decreased with improvement in the hydrolysis and methanogenic phase, unlike the lignin content with low pretreatment effect, resulting in a slow and incomplete degradation process. Although alkaline and acid pretreatments improve the degradation of lignin-rich biomasses, extreme pH values and a large amount of salt formation inhibit the activities of methanogens (Zhang et al. 2014a; Abdelwahab et al. 2020).

While pretreatment aids degradation of lignocellulosic substrates, Abdelsalam et al. (2016) posited that utilization of additives is a less expensive and increasingly effective enhancement method for improving the performance of biodigesters. However, additives enhance the efficiency of the anaerobic digestion process, ranging from an increase in the startup speed, improved production rate, reduction in the hydraulic retention time (HRT) and higher methane content (Hao et al. 2017; Ward et al. 2008). Additives have been grouped based on their main compositions and roles such as increased stability of the digestion process, reduction of toxin impacts and supply of deficient nutrients and for performance improvement (Kim et al. 2017; Baredar et al. 2016). The addition of nanoparticle to anaerobic digestion caused a reduction of lag phase (Abdelsalam et al. 2016). Additives can be either organic or inorganic or biological or chemical and are in macro, micro or nanoscale (Mao et al. 2015; Romero-Guiza et al. 2016; Abdelwahab et al. 2020).

Various additives essential for enhancement of anaerobic digestion process are as follows Ni, Fe, Co, Mo, Se, C, N, P, S, etc. (Abdelsalam et al. 2016; Mao et al. 2015). Among all the broadly utilized

additives, iron-based additives have merits of being viable in H_2S toxicity control, nutrient supplementation, improvement of biomethane yield and content, enablement of substrate solubilization, etc. (Chen et al. 2018; Mao et al. 2015). Iron is an important element for biological activities of methanogens like energy acquisition and DNA multiplication, it is crucial for the survival of cells and serves as an electron acceptor and due to its ability to ionize to Fe^{2+} and Fe^{3+} (Chen et al. 2018; Casals et al. 2014). It has been noted that iron-based additives reduce oxidative-reductive potentials (ORP), enhance the activities of hydrolysis-acidification enzymes and improve the anaerobic digestion conditions (Feng et al. 2014). In general, it was reported in Ugwu et al. (2020) that the pooled results of iron-based additives supplementation had an overall significant influence on the enhancement of anaerobic digestion and increase in biogas yield.

Based on the above adduced positive enhancing impacts, lots of iron-based additives have been used in many environmental management processes, nutrient supplementation, and digestion enhancement in an anaerobic digestion operation either singularly or in combination with organic and inorganic substances as shown in Table 1.1 (Kim et al. 2017; Zhang et al. 2015). Most used iron-based additives for anaerobic digestion purposes were classified in this study largely into 4 groups. This classification is based on: their types, whether they occur naturally or synthetically manufactured, as well as their enhancement or inhibition capabilities.

Table 1. 1 Classification of iron-additives and their influence on biogas production

S/N	Groupings	Types	Source	Remarks	Reference
1.	Iron Scraps	Waste Iron Scraps (Rusty and clean waste iron scraps) WISs	By-product of iron industries	Enhanced were reported for both types of WISs	Hao et al, 2017; Zhang et al, 2014b
		Zerovalent Scrap Iron (ZVSI)	Waste scraps from the ironwork doped with metal	Addition of 1 g/g VSS enhanced Biogas yield	Yadav et al, 2012; Zhen et al 2015
2.	Iron Powder	Fe powder	Produced and commercially obtained	Increased methane yield	Suanon et al 2017
		ZVI	Synthesized/ commercial	At the optimum range, ZVI recorded enhancement	Kong et al, 2018 Zhang et al, 2013
		Hematite (Fe_2O_3)	Red mud is a by-product from the alumina refining of bauxite ore	Biomethane yield was promoted	Ye et al, 2018
		Magnetite (Fe_3O_4)	Commercially procured	Enhanced process	Zhao et al, 2018
		Iron salts e.g. $FeSO_4$, $FeCl_3$, etc. or Fe with other trace metals e.g. Co, Mo, Ni etc.	Commercially procured as synthesized	$FeSO_4$ inhibited $FeCl_3$ and $FeCl_2$ enhanced Fe + other trace elements enhanced	Thiruselvi et al, 2018 Qin et al. 2019 Zhang et al, 2015
3.	Iron Nanoparticle	Fe_3O_4-NP	Synthesized from Fe hydrate, NH_3 and KI	At optimum dosage, the yield was enhanced	Noonari et al, 2019

		Hematite NPs	Commercially procured as synthesized product	Enhancement of biogas was observed	Ambuchi et al, 2018; Wang et al, 2016
		Green NPs	Synthesized with plant extracts (in place of reducing agents) and iron source	Enhancement was recorded at dosage ≤300 mg/L	Thiruselvi et al, 2018
		NZVI	Synthesized Iron source and $NaHB_4$	Biogas yield increased at dosages ≤ 1000 mg/L	Jia et al, 2017
		Fe-NP coated or mixed with Zeolite (nZVI, ICZ, IMZ, CU)	Synthesized ferric salt, zeolite and $NaHB_4$	Increased biogas yields were recorded at optimum dosages ≤ 1000mg/L	Amen et al, 2017 Amen et al, 2018
4	Advanced Oxidation Process (AOP)	Fenton process (Fe and H_2O_2)	A mixture of Ferrous iron and hydrogen peroxide	No consensus (more studies on AOP enhanced digestion needed)	Uman et al, 2018; Taha et al, 2014

Studies have revealed that increasing biogas recoverability with iron additives supplementation is effective, but wields menacing effects on the bio-solids and the environment at very high additive concentrations (Xie et al., 2017; Eduok et al., 2017; Dwivedi et al., 2015). Addition of excess Fe^{2+}, produces reactive oxygen (by Fenton reaction), raising pH and cytotoxicity occurring and ultimately causing inhibition to biogas production (Ganzoury and Allam, 2015; Tang and Lo, 2013). Iron-based additive, when in excess forms non-biodegradable precipitates like siderite ($FeCO_3$), pyrite (FeS_2), vivianite ($Fe_3(PO_4)_2$), etc., which threatens the ecosystem (Puyol et al. 2017; Peeters et al. 2016).

1.3 Relevance of enhancement approach to increased phosphate release

There is a need to attenuate the impacts of the nutrient-rich digestates from iron enhanced anaerobic digestion process on the ecosystem by preventing iron complexing with P in digestates for ease of recovery. Phosphorus is an important resource in life for crop production, human and animal growth, (Ashley, 2011). Naturally occurring phosphorus exists as phosphate rocks in few countries and is estimated to be used up in less than a 100-year time (Gurtekin, 2014). Consequently, the indispensability of P to life's existence justifies the search for alternative P sources. Anaerobic digestion of biomasses facilitates the solubilization of substrates and decomposition of the protein content of the substrate to release P as well as other elements into the digestate (Zheng et al. 2013; Zhang et al. 2014b; Puyol et al. 2018). As reported in Cucina et al. (2017) and Campos (2014), the release of trapped P in the organic matrix and insoluble P can be increased using methanogenesis enhancing additives.

Notwithstanding the hopes of releasing P from substrates during anaerobic digestion, it is established that iron additives decrease P availability in digestates (Puyol et al., 2017). This is due to

immobilization of available inorganic phosphate (P_i) forming insoluble iron-P precipitates in the liquid fraction of the digestate (Puyol et al., 2017). According to Elijamal et al. (2020), Mokete et al. (2020), Suanon et al. (2016) the immobilization of P to form iron-P precipitation occurs more with limited availability of oxygen (anaerobic condition). The iron-P precipitates, which are non-biodegradable accumulates in the digestate to constitute serious environmental concerns and increasing plant operational costs (Puyol et al. 2018; Puyol et al. 2017). However, the iron reduction-induced phosphate precipitation during anaerobic digestion of waste can be mitigated with the addition of chelating additives or Fe-P antagonists, etc.

Past studies have shown that some elements like Fe, Ca, Mg, etc. have a synergistic relationship with P, others such as arsenic (As) compounds with similar properties wield antagonistic influences on P as well as a chelating substance like humic acid (HA) which affects P availability in solution (Puyol et al. 2018; Liu et al. 2011). Humic acids are the most abundant substance on earth mainly from putrefying organic matters, they are complex biomolecules, very soluble at wide pH range and acts like weak polyelectrolytes (Azman et al. 2015a; Giasuddin et al. 2007). According to Liu et al. (2011) and Jeong (2017), HA and iron can coexist, and bind reasonable amounts of As to form Fe-bridged As-Fe-HA complexes and surface complexation of As on HA-Fe stabilized colloids. This interaction alters their ability to absorb nutrient like phosphate due to the phosphate/arsenate exchange leading to the availability of Fe^{3+} and PO_4^{3-} in solution as well as the formation of HA-Fe and As-Fe precipitates (Lenoble et al. 2005). Although, it has been reported in Yap et al. (2018) and Azman et al. (2015b) that at high concentration of As and HA, anaerobic digestion is inhibited due to the decrease in the hydrolysis of cellulose, but the addition of Fe mitigated the inhibitory influences of HA and As. Consquently, this study, which is aimed at optimizing the HA, Fe and As dosages and understanding their impacts on both soluble phosphate availability and biogas yield is necessary.

1.4 The need for lifecycle assessment of the integrated enhancement approach

Although the proposed simultaneous enhancement of anaerobic digestion is expected to increase both biomethane yields (in quantity and quality) and phosphate release, the environmental footprints of the vast processes and inputs should be evaluated. Lifecycle assessment (LCA), an international standard ranging from ISO 14040 to ISO 14044 (ISO, 2006), is multi-criteria, multi-stage modelling framework aimed at evaluating the potential environmental impacts of processes like the integrated approach to enhanced methane and P release from agro-industrial waste (Esteves et al. 2019; Hiloidhari et al. 2017). Different versions of LCA software (e.g. SimaPro, OpenLCA, GaBi,

Umberto, etc.) have four planned iterative steps, from the definition of goal and scope, inventory analysis, impact assessment to impact interpretation (Duan et al. 2020; Acero et al. 2014). Energy and P release processes pose both direct and indirect health and environmental challenges. These concerns are linked to energy, chemical and other resources used, necessitating the application of sensitivity analysis in determining the response of the impact assessment and changes to the recovered products and environment (Giwa, 2017; Amini, 2014). However, LCA is essential in avoiding inadvertent consequences of novel technologies and environmental mitigation strategies (Ghosh et al.2020; Pant et al., 2011).

In previous LCA studies, Cremiato et al. (2017); Desmidt et al. (2015) revealed that in a simultaneous approach to energy and P release/recovery processes via anaerobic digestion had lower environmental impacts, produced renewable energy and performed better than those using the pure composting or other waste disposal means. Giwa (2017) reported in LCA studies of biogas production using cow dung and algae, that eco-friendly inputs in biogas production and P recovery reduce the process impact on the ecosystem. Remy and Jossa (2015) showed that biogas production and P recovery pathways/methods vary majorly in the quantity of P recovered, biogas produced, energy used, and impacts on the environment. In the LCA assessment of five different nanoparticles (Ni NPs, Co NPs, Fe NPs and Fe_3O_4 NPs). Hijazi et al. (2020a) noted that the nano-additives, when compared with the control (without additives), were most effective in greenhouse gas emission mitigation, lower ozone layer depletion, human toxicity potential, acidification, human toxicity potential and eutrophication values.

On the other hand, Puyol et al. (2018) and Xie et al. (2017) reported that due to the use of additives like iron nanoparticles biogas production was enhanced but had both positive and negative effects on P content of the digestate as well as the environment. Hence the suggestion of Remy and Jossa (2015) that evaluation and selection of most suited strategies for integrated resource recovery with additives from agro-industrial wastes using life-cycle based tools are to be studied. In the same vein, Mayer et al. (2016) recommended that integrated technological trade-offs (systems-level analyses) should be focused on evaluating impacts of resource recovery strategies on varying products and the ecosystem should be researched.

Summarily, most research addressing the intensification of biogas production using various strategies already exist (Arif et al. 2018; Li et al. 2019; Koniuszewska et al. 2020; Ugwu et al. 2020). They

largely focused on either biogas production enhancement with additives or the release of phosphates from digestates for phosphorus recovery or direct land application of digestates (Campos, 2014; Abdelsalam et al., 2017; Melia et al., 2017; Xie et al., 2017). It was also observed in previous studies that while nano-additives enhances biogas yield, it inhibits P availability in the digestate mixed liquor (Mayer et al., 2016; Melia et al., 2017; Puyol et al., 2017). Therefore, further studies on an integrated approach to enhancing biogas production and the increasing availability of phosphate content in the liquid fraction of the digestates with the addition of iron additives as well as antagonists is needed. Knowledge on these suggested potentials for simultaneous enhancement of both biogas yield and phosphate release is largely lacking and deserves assessment. Due to the processes involved in this proposed approach shown in Fig.1.3, the assessment of the environmental impacts becomes necessary.

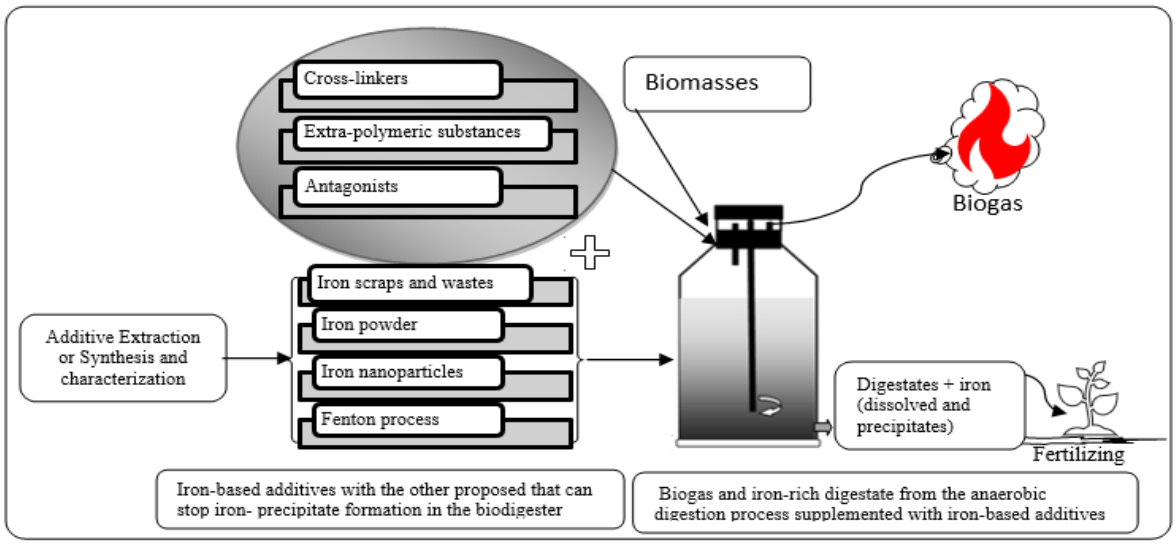

Fig. 1. 3 A proposed integrated approach of iron additive and P antagonist supplementation of anaerobic digestion.

1.5 Justifying the integrated approach to enhancement of biogas production and P recovery

The global population is growing, leading inevitably to increased consumption of food and depletion of virgin raw material resources such as phosphorus which is a very essential non-renewable resource in crop production (Worldometer, 2020; Zahra et al. 2020; FAO, 2019; IEA, 2020a;). The depletion of resources such as mined phosphate ores, which is used for fertilizer production and has about 90% of its known reserves located only in five countries (the U.S., China, South Africa, Jordan and Morocco), is already at an unsustainable level and estimated to be consumed in about 100 years

(Steven, 2010; WERF, 2011; Gurtekin, 2014).

The energy-demand gap is on the increase in most countries; it is expected to rise by 30% in 2040. In South Africa, the peak demand is estimated to rise to 57, 274MW in 2030, with 17,800MW expected to be from renewable energy sources (IEA, 2019; CSIR, 2016; DoE, 2016). Currently, about 90% of the energy supply is from non-renewable sources, making South Africa one of the 15 largest emitters of CO_2 worldwide (IEA, 2019). However, the energy crisis in 2008 and the need to close this gaps in 2030 made South African Government to start investing largely in renewable energy sources, more in solar and wind energy, but biogas (waste-to-energy) technologies remain largely untapped (IEA, 2019; CSIR, 2016; DoE, 2016).

The currently used resources for alternative energy (biogas) and phosphorus are unsustainable and compete with other humans/animal uses (Kampman et al., 2017). Owing to this, the Food and Agricultural Organization's 2008 report in Kigozi et al.,(2014) noted that food insecurity is imminent due to heightened food crop-to-bioenergy conversion. To avert this impending doom, identification of non-food feedstocks (e.g. agro-wastes, and other energy crops/novel substrates) as alternative sources for energy and phosphorus recovery becomes imperative and should be prioritized (Boulamanti et al, 2013; Elbeshbishy et al., 2012). Cheerfully, countries like South Africa has annual generation capability of above 108MT total waste, 50% of which is from the entire agro-industrial value chain with potentials for meeting both energy and phosphorus demand when properly harnessed (DEA, 2012; ARC, 2016).

Anaerobic digestion process, which is the most suited technology for recovering both energy and phosphates from wastes according to Hijazi et al. (2020a) and Puyol et al. (2018) is faced with process drawbacks connected to the complex molecular nature (lignin and hemicellulose) and the entrapment of P in the organic matrices. Hijazi et al. (2020a) and Abdelsalam et al. (2016) stated that the use of additives (e.g. trace metals and nanoparticles) can alter the substrate matrix of the complex molecules to enhance methanogenic bacteria growth during enzyme synthesis, increase biogas yield and P release.

Matter-of-factly, while these additives improve biomethane production, on the one hand, they reduce P availability on the other hand (Puyol et al. 2018). It was mentioned in Puyol et al. (2018) that the high affinity of Fe and P results in non-biodegradable precipitate formation during anaerobic

digestion, reducing both dissolved P and Fe availability in bioreactors. However, because of the environmental implications of these Fe-P complexes, it was reported in Jeong (2017) that addition of P antagonists (As) and chelating substances (HA), can form As-Fe-HA complexes and stable colloids ensuring more P availability in the digestate mixed liquor. In line with these propositions, the favourable alteration of anaerobic digestion processes via this integrated approach could lead to the achievement of increased biogas production without the inhibition of P availability for recovery.

However, Mayer et al. (2016) and Amini (2014) argue that the trade-offs between environmental and economic impacts of this integrated approach to enhanced biogas and P release, just like other novel techniques should be determined through the conduct of. LCA. The enormity of processes and inputs to this resource recovery approach as well as their possible environmental impacts justifies the need for LCA studies aimed at enabling the decision making on the most environmentally friendly enhancement option.

1.6 Alignment to the university and national/international strategies

United Nations Sustainable Development Goals (SDGs) 6, 7 and 13 are aimed at achieving clean energy and ensuring environmental sustainability (UNSTATS 2019; Osborn et al. 2015). These they hope to achieve among other ways through ensuring proper waste management to avoid eutrophication in water bodies, achieving affordable and clean energy (waste-to-energy) production, manage enormous waste generated properly, etc. However, after the 2008 energy crisis, South Africa with over 108 million tonnes of wastes generation capacity, started investing in large scale renewable energy sources like biogas (waste-to-energy) technologies (DoE, 2016). To achieve the targeted 6000MW renewable energy input to South Africa's energy mix and ensure a sustainable environment, integrated approach to recovery in waste-energy-P nexus should be enhanced (IEA, 2019; DoE, 2016; DEA, 2012).

1.7 Research questions

The global quest for energy sufficiency, sustainable environment amidst the rise in global population, increasing waste generation, depletion of available resources as well as the paucity of information on the integrated resource recovery strategy from wastes have elicited some concerns. This research is targeted at addressing the following questions and contributing to the body of knowledge on biomass-resource recovery:

i. What are the biomethane and P potential of identified agro-industrial wastes?

ii. Which enhancement method can increase biomethane production from anaerobic digestion of selected substrate?
iii. What appropriate dose of iron-additive and antagonist can achieve optimum biogas yield and P release during anaerobic digestion of selected substrate?
iv. How can environmental footprints of the anaerobic digestion enhancement process be evaluated?

1.8 Research objectives

This research is aimed at enhancing anaerobic digestion processes of agro-industrial wastes for increased biomethane yield and phosphorus release with the use of additives and nutrient antagonists, and evaluation of process impacts on the environment. The specific objectives are:

i. To identify, characterize and rank potential agro-industrial wastes based on their energy and phosphorus potentials.

ii. To identify the most suitable enhancement techniques for increased biogas production during anaerobic digestion of selected agro-industrial waste.

iii. To optimize the iron enhanced anaerobic digestion of selected agro-waste for biomethane production and phosphate release with the addition of antagonists.

iv. To use Lifecycle Assessment (LCA) tool in evaluating the environmental footprints of different enhancement types for anaerobic digestion of selected agro-industrial waste.

1.9 Scope and outline of the thesis

The desire to achieve resourceful waste-to-energy has necessitated studies aimed at optimizing per kilogram resource recovery. Anaerobic digestion is an established means of energy and other resource recovery are confronted with issues of biodegradability emanating from the nature of substrates, presence of inhibitors or operational challenges. However, enhancement of anaerobic digestion process mitigates inhibition of microbial activities, increases substrate solubilization and methane yields. Addition of iron-based additives for enhancement of anaerobic digestion facilitates biogas production, but forms complexes and precipitates with other available nutrients. The formation of non-biodegradable precipitates, which causes environmental pollution upon disposal have been studied, but an approach aimed at ensuring increased biogas yield and nutrient availability are largely not researched.

The integrated approach to enhancing anaerobic digestion for increased biogas yields and phosphate release is the major focus of this thesis. This study investigates the substrate viability for anaerobic digestion in south Africa, enhancement potentials of some anaerobic digestion intensification strategies (pretreatment, co-digestion and additive supplementation), the possibility of releasing and maintaining more soluble phosphate in the digestate with the addition of P antagonists (As) and chelating substances (HA) to during anaerobic digestion for easy recoverability or usage plants as well as understanding the environmental impacts of this integrated approach with LCA tools. Special emphasis was given to novel substrate identification and novel iron-based additive type usage. Despite the concerns around the formation of non-biodegradable iron-phosphate complexes during iron-additive supplemented anaerobic digestion processes, little or no information on integrated approach towards holistic energy and P release is available.

Therefore, **Chapter 1**, which is the introductory chapter aims at identifying research gaps from available scientific information on anaerobic digestion enhancement for increased biogas yield and phosphate released per kg of substrate digested. Possible ideas of an integrated strategy for increasing biogas yield and phosphorus release from wastes with additive supplementation was identified. In **Chapter 2,** the mechanisms of anaerobic digestion enhancement for resource recovery is reviewed. A brief overview of relevant concepts of anaerobic digestion, enhancement options, influences of enhancement on anaerobic digestion and phosphate release, etc. were described. From the review, there is a possibility of ensuring integrated enhancement of biogas production and phosphorus release. **Chapter 3** describes the screening (characterization and ranking) of identified agro-industrial wastes for their energy recovery and phosphate release potentials through a mixed-method approach. Novel substrate (okra wastes) with good biomethane potential was selected for enhancement (pretreatment, co-digestion or additives supplementation). **In Chapter 4,** various anaerobic digestion enhancements (NaOH pretreatment, co-digestion with sheep slurry, and iron supplementation) of okra wastes was carried out. This chapter shows that the use of Ppy/Fe_3O_4 nanocomposite enhanced biogas yield more than other options. An attempt at achieving optimized biogas yield and phosphate release via the addition of antagonists (As and HA) and accelerants (Ppy/Fe_3O_4) to the co-digestion of okra wastes and pig manure was studied in **Chapter 5**. The maximized value of responses (biomethane yield and phosphate release) were simultaneously obtained. In **Chapter 6**, the trade-offs between enhanced energy recovery and environmental sustainability were considered for different enhancement options studied using LCA tool. A combined enhancement (co-digestion + Ppy/Fe_3O_4) scenario with high

energy output and low environmental impact is preferred. Finally, conclusions from this thesis were discussed in **Chapter 7**. Future research outlooks were stated in this chapter.

Chapter Two

Literature Review: Mechanisms of Anaerobic Digestion Enhancement for Resource Recovery

This chapter is partly adapted from: Ugwu, S. N., and Enweremadu, C. C. (2020). Enhancement of biogas production process from biomass wastes using iron-based additives: types, impacts, and implications. *Energy Sources, Part A: Recovery, Utilization, and Environmental Effects*, 1-23.

2.1 Overview and relevance of anaerobic digestion

Vast biodegradable wastes from agro-industries are available for biogas production but had remained under-exploited globally amidst visible energy demand gaps especially in developing climes (UNSTAT, 2020; WBA, 2019). The amount of waste generated globally is enormous and posing serious environmental challenges if not properly disposed or re-channeled to more sustainable reuse. When indiscriminately disposed of, these agro-industrial wastes (e.g. food wastes) emits annually about 3.3 billion tonnes of CO_2 equivalent of GHG carbon footprint into the atmosphere (FAO, 2013). It was reported in USEPA (2017) and Lee et al. (2017), that waste landfills recorded greenhouse gas emission of about 115.7 $MtCO_2e$ per year. Similarly, in South Africa, emissions from solid wastes will be above 50 $MtCO_2$ by the year 2050 (DEA/GIZ, 2014). Given these threats, European Union's (EU) baseline studies in 1995 issued a "Landfill Directive", setting mandatory targets for a total reduction of 25%, 50% and 65% of biodegradable waste meant for landfill by 2010, 2013 and 2020 respectively (Pazera et al., 2015).

These GHG emissions can be mitigated by minimizing waste generation, recycling or reusing and sending less waste to landfills or ensuring that released methane from the landfills is captured (Lee et al. 2017; UNSTAT, 2020). According to Lee et al. (2017), it was stated that waste reuse/treatment options like waste-to-energy (WTE) process have several merits, which includes cheap feedstocks, zero/reduced GHG emissions and sustainability. Leveraging on these advantages, several WTE technologies have evolved, these include thermochemical (gasification, pyrolysis, hydrothermal liquefaction, etc), biochemical (fermentation and anaerobic digestion) and mechanical (densification etc) (Crolla, 2017; Lee et al. 2017). Although the WTE technology of choice is based on the waste type and energy need, most thermochemical WTE technologies are most frequently used, but the cost-effectiveness of the biochemical WTE strategy like anaerobic digestion distinguishes it from others (Lee et al. 2017).

Furthermore, anaerobic digestion is a more sustainable resource recovery strategy which involves the systematic diversion of wastes intended for disposal via a return of material flows to a specific and sustainable next use (DEA, 2000; Sharp et al., 2015). This process is of environmental importance, cost-effective, decreases the amount of waste for disposal, saves space in landfills, and conserves natural resources (Gurtekin, 2014). Kampman et al. (2017) advocated that the sustainable diversion of these wastes for biogas production will contribute to renewable energy, environmental sustainability, decarbonization, and energy security objectives. In the same vein, disposable waste (digestate) from anaerobic digestion processes has environmental benefits which include reduced methane and nitrogen-based gas (N_2O) emission capability, reduced pathogens, odours and volatile fatty acids (VFAs), hence making its land application to conform to the environmental laws and regulations (Crolla, 2017). In lieu of this, substrate solubilization during anaerobic digestion process results in nutrients availability in their ionized states (Org-P, Inorg-P, N and NH_4^+) (Campos, 2014).

The biogas which is an end-product of anaerobic digestion is composed of 50-75% methane, 25-50% carbon dioxide and other minor compositions (often lower than 1%) of hydrogen sulfide, nitrogen, ammonia and hydrogen (Kougias and Angelidaki 2018; Obileke et al. 2020). As shown in Fig. 2.1, biogas is used for electricity generation using combined heat and power system (30-40% electricity, 35-45% heat and 15% energy loss), house lighting, heat production (cooking and other heat usages) and when upgraded to bio-natural gas (BNG) or compressed biomethane used in transportation (Surendra et al. 2014; Sun et al. 2015; Zheng et al. 2020a). However, the digestion process aids the release of minerals trapped in the organic matrix of substrates due to carbon transformation, which are readily available in the effluent streams (digestate) and used as fertilizers for soil amendment.

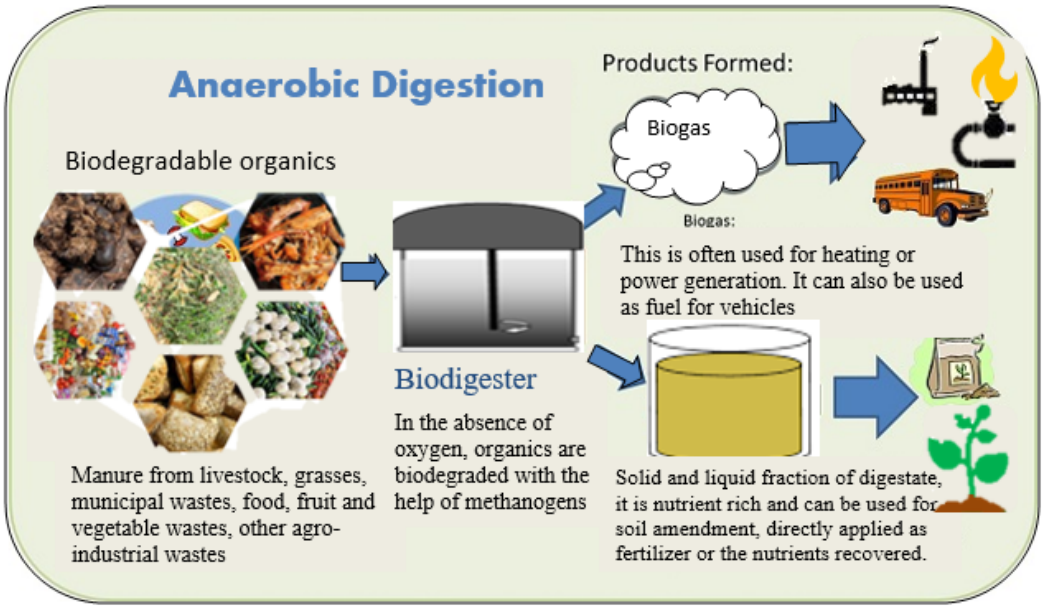

Fig.2. 1 Anaerobic digestion processes, products and by-products

Technological advancements in biogas generation have been responsible for the development of improved anaerobic digestion with modifications in the pretreatment of feedstock methods, economical biogas upgrading systems, enhanced biochemical process and conditions, sophisticated digesters with monitoring and data acquisition components, inclusion of nanotechnology and other novel technologies (Ugwu and Enweremadu 2020; Kampman et al. 2017). Furthermore, the growing relevance of anaerobic digestion enhancement for increased biogas yield and phosphate release or recovery nowadays will be discussed later.

2.2 History and global status of biogas production

Anaerobic digestion has a rich history surrounding its development, implementation and advancement when compared to other alternative energy sources. Between 10^{th} and 16^{th} century B.C, anecdotal facts on primeval use of biogas for bath water heating in India, China, Persia and Assyria existed, but it was about three thousand, five hundred years later that evidence of the methodical scientific approach to biogas production started (Obileke et al.2020; Lusk, 1998). Jan Baptita van Helmont in 17^{th} century determined that flammable gases could evolve from decaying organics (Kougias and Angelidaki, 2018). In a descriptive dossier from Benjamin Franklin to Joseph Priestly in 1764, the flammability of emitting gas from a wetland in New Jersey, USA was reported, but the substantiation of this incidence was only scientifically done by Alessandro Volta in 1776 (Oechsner et al. 2015; Lusk, 1998). In 1801, Cruikshank through his work demonstrated the absence of oxygen molecules in methane, while between 1804 and 1808, John Dalton and Humphrey Davy

independently proved the inflammable gas was methane and determined the correct formula of methane (Kougias and Angelidaki, 2018; Abbasi et al. 2012). With the growing interest in the anaerobic digestion process in the later part of 19th century, Béchamp in 1868 first proved that microbial process was responsible for methane production from putrefying organics, thereafter, enzymatic hydrolysis of polymers and intermediate production organic acids were established (Kougias and Angelidaki, 2018). A French journal Cosmos in 1881 was the first to cite the usage of full-scale biodegradation of domestic wastewater in an air-tight compartment known as Mouras Automatic Scavenger. Similarly, in 1895, Donald Cameron constructed a model of the Mouras Automatic Scavenger (septic tank) at Exeter, England, the biogas collected from the designed septic tank was used for heating and lighting (Oechsner et al. 2015; Abbasi et al. 2012). However, in 1859 at a leper colony in Bombay, it was reported that the first anaerobic digester was constructed in India (Kougias and Angelidaki, 2018). Similarly, according to Oechsner et al. (2015) and Abbasi et al. (2012), tanks for waste disposal were designed with biogas collection system at a leper colony in Matunga, Mumbai, India in 1897, this digester was fed with human wastes and the gas was used on gas engines and to augment electricity demand.

More so, at the inception of 20th century, Omelianski (1906) and Söhngen (1906) reported that during fermentation of cellulosic materials, methanogens facilitate the release of acetic acid, butyric acid, formic acid, ethanol, hydrogen, carbon dioxide). In 1910, Söhngen in his experiment with enriched cultures reported that the reaction of hydrogen and carbon dioxide forms methane via hydrogenotrophic methanogenesis as shown in equation 2.1 and that decarboxylation of acetic acid could form methane (Kougias and Angelidaki, 2018; Abbasi et al. 2012).

$$CO_2 + 4H_2 \rightarrow CH_4 + 2H_2O \qquad 2.1$$

Subsequently, according to Buswell and Boruff (2002), the theoretical calculations for biomethane potential of substrate determination was discovered in 1933. However, the first reported isolation of methane-producing microbes (*Methanobacterium formicicum, Mathanobacillus omelianskii, Methanococcus vannielli and Methanosarcina barkerii*) was in 1936 (Barker, 1956). In 1921, the construction of an $8m^3$ biodigester fed with wastes for commercial supply of energy for lighting and cooking was carried out by Guorui Luo in China, a similar report in 1920 of biogas supply via the gas grid from the first sewage treatment plant was reported in Germany about 1920 (Obileke et al. 2020). The developments and research in biogas climaxed in the 1970s (1973-1979) in most

developed countries during the global oil price hike (Oechsner et al. 2015). Shortly after, the concerted interests and investments in biogas technology development declined especially in developed climes, but there seems to be a renewed interest in biogas production as stated in Table 2.1. There has been uneven development of biogas across the globe, based on the feedstock availability, polices that supports biogas production and utilization (IEA, 2020b; Zeng et al. 2020a; Zheng et al.2020b). According to IEA (2020b), 90 per cent of the global biogas production are from Europe, China and the United States. The technological advancements and market-oriented policies can be the reason for having more biogas output from Europe than China (Xue et al. 2020). It is noteworthy that early support is vital to achieving economically viable and cost-effective biogas production. The biogas technology policies and incentives are at global, regional and country-specific level as shown in Table 2.1.

Table 2. 1 The biogas technology status and policies of selected countries

S/N	Country	Status and advances	Current policies and incentives	References
1	**China**	China has an annual theoretical biogas potential of about 73.6 billion m^3, about 41.93 million biodigesters (serving over 200 million persons) and about 110,975 MLBPs (18.92million m^3 volume capacity and 2.225billion m^3 annual biogas production) and about 15.8bcm of upgraded biogas. She has in the last 10 years invested more than CYN 42 billion in biogas projects with the aim of completing 194 bio-natural gas (BNG) plants by 2020.	China has lots of pro-biogas development policies, but in 2015, Ministry of Agriculture and Rural Affairs (MARA) and the National Development and Reform Commission of the People's Republic of China (NDRC) published a Working Plan of Upgrading and Transforming Rural Biogas Project 2015-2030. Although the household digesters are no longer subsidised, the Medium-large scale biogas plants (MLBPs) and BNG projects would still enjoy subsidy.	Zeng et al. 2020a; Zheng et al. 2020b; Xue et al. 2020
2	**Europe**	Biogas highly industrialized and commercialized in European countries with above 18,202 biogas installations (which represents 53% (31.24bcm) of the global and may rise to 70bcm in 2030), installed electric capacity (IEC) of 12,010 MW, and 63,511 GWh of biogas produced. Germany with more than 8700 operating commercial-size plants and generating more than 3.4 GW of electrical power. Under the Gas for Climate: a path to 2050 directive, above 660 BNG plants producing 2.28bcm per annum.	Lots of policies like Gas for Climate: a path to 2050 directive aimed at achieving an estimated 98 bcm per annum contributing to approximately 22% of the current natural gas market There is also a RED II, with the overall EU target for Renewable Energy Sources consumption to be raised to 32% by 2030. The EU States must require fuel suppliers to supply a minimum of 14% of the energy consumed in road and rail transport by 2030 as renewable energy. The European Regulation on Fertilising Products (FPR) recognizing digestate as bio-fertiliser was approved and published in the Official Journal of the EU in June 2019.	EU-RED, 2018; Xue et al, 2020; EBA, 2019

3	**United States**	The biogas recovery systems in the US are diverse from livestock, Landfill gas (LFG) from municipal solid wastes (MSW) and gas from wastewater treatment plants. There are about 1,250 municipal WRRFs in the United States with anaerobic digesters that treat wastewater solids for biogas production. With the potentials for sustaining 14,000 biodigesters or 8000 livestock manure digesters and capability of generating 16 million MW/h per year, there are currently more than 2,200 operational systems in all 50 states. 173 BNG producing plants are being built As of March 2020, about 288 farm-based biodigesters are documented, 255 are currently in use and others are under construction. 19 of which are BNG/RNG producing plants and 20 RNG plants are being built. There are about 634 MSW-LFG operational energy plants in 2020 (72% for the generation of about 17 billion kWh of electricity and 10% for producing about 2.27bcm RNG). Above 60 stand-alone biogas plants are used for the treatment of food-based wastes.	In the US, policies and incentive programs for biogas systems are at both the federal and state levels. US Environmental Protection Agency (EPA) established the AgSTAR program, which provides technical assistance to agricultural producers on biogas recovery and increases biogas plants from 300 to 1300 by 2020 The US Department of Agriculture (USDA) created the Rural Energy for American Program (REAP), which provides guaranteed loan financing and grants to agricultural producers and small rural businesses of up to $545 million to 8800 biogas projects for improving energy efficiency and producing renewable energy. There is also a support program of USDA Section 9003 for Biorefinery, Renewable Chemical and Biobased Product Manufacturing. The USDA NRCS has a cost-sharing program called the Environmental Quality Incentives Program (EQIP) aimed at encouraging waste-to-energy. The Feed-in tariffs (FIT) are a policy tool used to encourage renewable electricity technologies. FIT-eligible renewable electricity generation facility will receive a set price from their utility for all of the electricity they generate and provide to the grid.	Sam et al. 2017; American Biogas Council, 2020; AgSTAR-EPA 430-B-20-001 2020
4	**India**	There are about 5 million domestic NNBOMP digesters currently producing about 2.07bcm per year covering just about 0.4% of the energy need of rural Indians. However, India has potentials 12 million digesters for producing 48bcm per annum. The BPGTP digesters currently generate 86,595 m^3 of biogas per day and 8.753MW of power. The wastes from urban, industries and agro-industries have the potentials of generating 5690MW_{eq}, but currently achieved 330MW_{eq} (Industrial 65%, urban 34% and agro-wastes <1%). The SATAT initiative has can achieve of 62 million tonnes per year of BNG, with the set target of 15 million tonnes	In India, there are several biogas related policies and incentives. In the 1970s, the National Biogas and Manure Management Program (NBMMP) was promulgated and currently known as New National Biogas and Organic Manure Programme (NNBOMP) for domestic digesters (1-25m^3) and Biogas Power Generation (Off-grid) and Thermal energy application Programme (BPGTP) for digesters (30-2500m^3) and power capability (3-250kW). Other programmes and incentives include (a) Programme on Energy from Urban, Industrial and Agricultural Wastes/Residues, eg. Biogas, BNG, etc. (b) Sustainable Alternative Towards Affordable Transportation (SATAT) Initiative for support of the use of	Folk 2020; Kemausuor 2018; IRENA 2017; Bharti, 2019.

		per year of BNG from 5000 BNG plants by 2023. Only 344 BNG plants are being built or functional now.	compressed biogas (BNG) in transportation. (c) National Policy on Biofuels produced in 2018 advocates for the promotion of advanced biofuels. (d) Galvanising Organic Bio-Agro Resources Dhan (GOBAR-Dhan) Programme or biowaste-to-biowaste in villages targeting between 2018-2019 build 700 digesters in 350 districts but have achieved 381 already.	
5	**Africa**	Although Africa has the greatest biogas potentials, the biogas technology is still in its infancy and are mainly farm-size or domestic type systems. Recently, initiatives for promotion and adoption of the technology in Africa is gaining much traction. In East African countries (Ethiopia, Kenya, Uganda, Tanzania) and Burkina Faso (West Africa), about 46,000 digesters had been installed by the Africa Biogas Partnership Programme, a public-private partnership between Hivos and SNV Netherlands Development Organisation with the plans of extending the number to 100,000 households beyond 2016. However, it was reported that the current total number of functional biodigesters in Africa is about 28,404. The project aimed at bottling biogas for clean cooking is being planned to start in Africa (Ghana and Uganda for pilot purposes). The commercial biogas outfits in Africa currently generates 65.84 MW. The highest number of commercial biogas plants are in South Africa, Kenya and Ghana. In Kenya, one of the plants with a power capability of 2.2 MW supplies power about 6000 rural homes.	African Union (AU) and individual African countries have lots of policies and incentives on biogas production. Aside from the UN-SDG on affordable and clean energy, AU has other bioenergy policies like: (a) Agenda 2063 will be implemented through The African Union Bioenergy Development in Africa Programme ECREEE (ECOWAS), RCREEE (North Africa), EACREEE (EAC), SACREEE (SADC). (b) Bioenergy Development Strategy and Investment Plan for the Southern Africa Region under the African Bioenergy Framework and Policy Guidelines adopted by the AU Assembly in 2013. (c) the Energy Development Strategies and Initiatives in Africa by AU Energy Division is aimed at increasing energy access to the African people and ensuring a sustainable environment by (i. facilitating the implementation of the programme for infrastructure development in Africa (PIDA) – Priority Action Plan (PAP) energy projects (2012-2020 to 2040). (ii. Operationalizing the execution of the Africa Renewable Energy Initiative (AREI) adopted at the COP21 in Paris, December 2015. (iii. Aiding the implementation of Sustainable Energy for All (SE4ALL) Initiative adopted by the Conference of Energy Ministers of Africa (CEMA), in November 2012. (iv. Supporting the implementation of the Africa Bioenergy Policy Framework and Guidelines adopted by the CEMA in November 2012 and Heads of State and Government in January 2013. (v. expanding the Continental Harmonized Regulatory Framework for Energy Sector	So et al. 2020; IRENA 2017; AU 2019; Twinomunuji et al. 2020; Kemausuor 2018; Roopnarain and Adeleke 2017

			(CHRFES). (vi. The execution of the Africa-EU Energy Partnership launched at the Africa-EU Summit in Lisbon, Portugal in 2007.	
6	**South Africa**	South Africa has the largest electricity generation capacity installed in Africa, but one of the world's highest emitter of CO_2. There is low integration of bioenergy into the energy mix of the country and biogas technology is also at infancy level like other African countries. The total wastes in South Africa were estimated to be capable of generating about 148GWh. However, the total electricity generation potential of biogas from available agro-industrial wastes is about 2.800 GWh per annum. It is reported that out of the 700 registered/installed biogas plants in South Africa, only about 300 may be in operation currently. Out of this number, 90% of the biodigesters are of household scale. Others are commercial-scale plants (about 22 biogas plants projects in South Africa) with power generation capabilities ranging from 30kW to 19MW and biogas potentials of 118 million m^3 per annum based on available feedstock estimation. Although there plans and policies for the upgrading of biogas, their little activities around the BNG developments in South Africa. The BNG potentials are approximately 3million Nm^3 per day. CBG as a transport fuel in South Africa is currently not economically viable, despite benefitting from an informal subsidy provided.	There are many policies and incentives for the facilitation of biogas technology developments. South Africa supports commercial biogas plants with grants. Some of these policies include: (a) The Integrated Resource Plan (IRP) 2010-2030 is the approach to energy provision in South Africa (b) Integrated Pollution Waste Management for South Africa Policy on Pollution Prevention, Waste Minimization, Impact Management and Remediation, provided for resource recovery and diversion of waste for energy generation. (c) The National Regulator of South Africa (NERSA) registers and regulates the ownership of biogas projects in conjunction with South African Biogas Industry Association (SABIA), Biogas SA and the South African National Energy Development Institute (SANEDI) (d) various incentives are provided by the Department of Trade and Industry for investors in biogas projects under the Manufacturing Competitiveness Enhancement Programme (MCEP). (e) The government has also made significant investments in bioenergy development through the Renewable Energy Independent Power Producer Procurement (REIPPP). (f) South African government supports BNG via the Industrial Development Corporation (IDC) via the provision of subsidy in the form of a soft loan for the conversion of petrol and/or diesel vehicles to BNG vehicles employing an exemption from fuel taxes and levies. But there is no regulatory framework and licences as well as an absence of stable medium-to-long term demand policy. (g) There is Feed-in-Tariff policy, but was replaced by a competitive tender or auction-based-tariff (ABT) system in 2011 under the REIPPP Programme	Kemausuor et al. 2018; So et al. 2020; DOE 2020; Roopnarain, and Adeleke. 2017; DOET 2000; ARC, 2006.

2.3 Anaerobic digestion: concepts, inputs and influences of process parameters

2.3.1 Anaerobic digestion process and stages

Anaerobic digestion is a collection of complex biological process in which a consortium of microorganism breakdown biodegradable organic matter in the absence of oxygen to produce biogas and nutrient-rich bio-solid (Levis and Barlaz, 2013). This reaction is said to be a slow process that occurs under anaerobic conditions by different groups of bacteria;it is also a waste to energy technology (Obileke et al. 2020). Anaerobic digestion processes exist naturally in marine sediments, peat bogs and stomach of ruminants (Al-Seadi et al. 2008). Currently, most (over 25%) biodegradable wastes generated especially in Europe and energy crops are treated anaerobically (EBA, 2019; Kampman et al. 2017). It also reduces mass and volume of waste streams, pathogens and odours, requires little land space for treatment, and may treat solid, wet and pasty wastes into stabilized and improved biofertilizer that are readily available to plants (Kampman et al. 2017; Gurtekin, 2014; Weiland, 2010). Anaerobic digestion can generally be summarized with Equation 2.2.

$$C_6H_{12}O_6 \rightarrow 3CO_2 + 3CH_4 \qquad 2.2$$

Anaerobic digestion process involves four stages and they include hydrolysis, acidogenesis, acetogenesis and methanogenesis. These stages describe the biochemical reactions vital for biodegradation organic materials by anaerobes as shown in Fig.2.2. (Borja and Rincón 2017; Wang 2016).

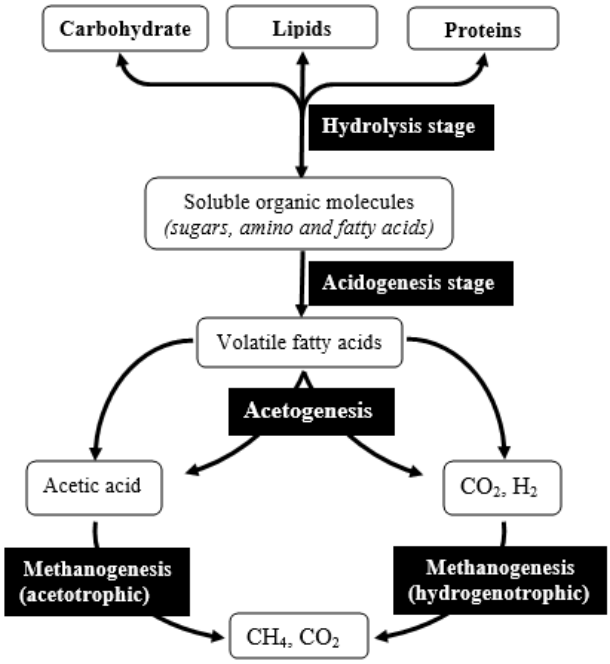

Fig.2. 2 The stages involved in anaerobic digestion (adapted from Abbasi et al. 2012)

Hydrolysis stage

Bacteria hydrolysis of feedstock is the beginning of anaerobic digestion by breaking down insoluble organic polymers (carbohydrate, proteins and fat) into soluble oligomers and monomers (simple sugar, amino acids and fatty acids) and availing them for activities of microbes. The hydrolytic extracellular enzymes excreted by hydrolytic microbes are responsible for substrate solubilization at the hydrolysis phase of anaerobic digestion (Obileke et al. 2020; Kougias and Angelidaki 2020). As the most rate-limiting step, hydrolysis (hydrolysis rate) depends on feedstock types and composition, surface enzyme production and adsorption (Rea, 2014). According to Borja and Rincón (2017), hydrolysis is referred to as the rate-limiting stage when the substrate has a lot of insoluble contents like cellulose compounds, etc. Equation 2.3 depicts the conversion of organic materials to glucose during the hydrolysis stage.

$$C_6H_{10}O_4 + 2H_2O \rightarrow C_6H_{12}O_6 + 2H_2 \quad (2.3)$$

Acidogenesis stage

Acidogenesis is the second stage of anaerobic digestion which involves acidogenic (fermentative) bacteria that convert monomers from the activities of hydrolytic bacteria into volatile fatty acid (Propionic acid, Butyric acid, Acetic acid, Formic acid, Lactic acid, Ethanol (30%), Methanol, etc.), CO_2, hydrogen (70%), ammonia, and other organic compounds which decreases pH (Dobre et al. 2014). At this stage, less than 50% of feedstock is converted into alcohols or volatile fatty acids Approximately, less than 50% of the substrate is transformed into alcohols or short-chain fatty acids (Obileke et al. 2020). Acidogenic bacteria commonly associated with an acidogenic stage in biodigesters are *Propionibacterium, Butyrivibrio, Bacteroides, Ruminococcus, Clostridium, Bifidobacterium, Eubacterium, Peptococcus, Streptococcus, Selenomonas, Acetivibrio, Lactobacillus* and other species of the Enterobacteriaceae (Borja and Rincón 2017). Acidogenesis phase is a pH-sensitive stage, the activities of fermentative bacteria cease at pH lower than 4, but high pH (greater than 5) favours the production of VFAs and lower pH (less than 5) facilitates more ethanol production (Chasnyk et al. 2015). The acidogenesis reactions are represented in Equations 2.4-2.6 (Obileke et al. 2020):

$$C_6H_{12}O_6 \rightarrow 2CH_3CH_2OH + 2CO_2 \quad \text{(glucose to ethanol)} \quad (2.4)$$

$$C_6H_{12}O_6 + 2H_2 \rightarrow 2CH_3CH_2COOH + 2H_2O \quad \text{(glucose to propionate)} \quad (2.5)$$

$$C_6H_{12}O_6 \rightarrow 3CH_3COOH \text{ (glucose to acetic acids)} \quad (2.6)$$

Acetogenesis stage

In the third stage, acetogenic bacteria transform the organic acids to acetic acid, CO_2, hydrogen and more ammonia (Dobre et al. 2014). Increased production of hydrogen increases the hydrogen partial pressure during acetogenesis reactions, but the activities of hydrogen scavenging bacteria lower the partial pressure and facilitate the formation of acids (Obileke et al. 2020). Higher hydrogen partial pressure inhibits metabolism of acetogenic bacteria. According to Al-Seadi et al. (2008), a symbiotic relationship exists between acetogenesis and methanogenesis stages of anaerobic digestion.

Species of acetogenic bacteria are grouped into non-obligate proton-reducing acetogens, obligate proton reducing proton to hydrogen and hydrogen-producing during acetogenesis. Non-obligate proton reducing acetogens are many and includes homoacetogens, which produces acetate from carbon dioxide and hydrogen (Obileke et al. 2020). Species of homoacetogens has these genera *Pelobacter, Acetobacterium, Eubacterium, Butyribacterium, Acetoanaerobium, Clostridium and Acetogenium*. These homoacetogens have the competitive ability for hydrogen and thrives under mildly acidic conditions (Borja and Rincón 2017). The electron-removing environment is most convenient for the growth of obligate proton-reducing acetogens, this kind of mutualistic interaction exists in the mixed culture of acetogens and hydrogen-removing microbe like methanogens (Borja and Rincón 2017). Obligate proton-reducing acetogens include *Desulfovibrio spp*. (metabolizes ethanol or lactate in the absence of Sulfur), *Syntrophobacter wolinii* (breakdown propionate), Syntrophus buswelli (degrades benzoic acid) and *Syntrophobacter wolfei* (degrades butyric acid), Syntrophococcus sucromutants (aids growth in co-culture with methanogens) and *Methanobacterium thermoautotrophicum* grows together with thermophilic butyric acid metabolizing acetogens (Borja and Rincón 2017). According to Archer and Kirsop (1990), obligate proton-reducing acetogens are associated with the methanogenesis from 3-chlorobenzoic acid and long-chain fatty acids. Some of the reactions at the acetogenesis stage are as shown in equations 2.7 (propionate to acetic acid and glucose), 2.8-2.9 (ethanol to acetic acid) (Obileke et al. 2020).

$$CH_3CH_2COO + 3H_2O \rightarrow CH_3COO + H + HCO_3 + 3H_2 \quad 2.7$$

$$C_6H_{12}O_6 + 2H_2O \rightarrow 2CH_3COOH + 2CO_2 + 4H_2 \quad 2.8$$

$$CH_3CH_2OH + 2H_2O \rightarrow CH_3COO + 2H_2 + H \quad 2.9$$

Methanogenesis stage

In anaerobic digestion processes, the first three phases are referred to as acid-producing phase. (van

Haandel and van der Lubbe, 2007). In this final stage of methanogenesis, methanogens make use of intermediate products (hydrogen, acetic acid and some CO_2) of other stages and transform them to methane, CO_2 and other trace gases (Rea, 2014; Abbasi et al. 2012). Methanogenesis phase is the slowest step and its bacteria is sensitive to operating parameters like pH (acidity), temperature, oxygen, substrate-type, organic loading rate (Crolla, 2017). Methanogens are obligate anaerobes and unicellular microbes that are varying archaebacteria groups with the capability of producing energy from methanogenesis (Borja and Rincón, 2017). A lot of methanogens use H_2 and CO_2 to form methane, but only these genera of Methanosarcina and *Methanothrix* species converts acetic acids to methane (Obileke et al. 2020). The species of methanogens mostly known for utilizing CO_2 and H_2 during anaerobic digestion are of these genera: *Methanobacterium, Methanobrevibacter Methanothermus, Methanococcus Methanomicrobium, Methanogenium Methanospirillum, Methanoplanus, etc.* (Borja and Rincón, 2017). These methanogens through the process of methanization, which is a biochemical process involving three pathways produces methane. These pathways as described by the reactions in equations 2.10, 2.11 and 2.12 are acetotrophic, hydrogenotrophic and methylotrophic pathways respectively (Obileke et al. 2020; Abbasi et al. 2012):

$$4CH_3COOH \rightarrow 4CO_2 + 4CH_4 \quad (2.10)$$

$$CO_2 + 4H_2 \rightarrow CH_4 + 2H_2O \quad (2.11)$$

$$4CH_3OH + 6H_2 \rightarrow 3CH_4 + 2H_2O \quad (2.12)$$

Generally, these reactions and products are formed due to the activities of microorganisms during the anaerobic digestion process. These microbes aid in maintaining stability and a balanced reaction rate in biodigesters by ensuring that H_2 and acid usage are faster than H_2 and acid production stages. At all the stages of anaerobic digestion, H_2 and acid are involved, but VFAs accumulation at acidogenesis stage affect the pH of the biodigester and inhibits methanogenesis. During anaerobic digestion, insoluble substrates, hydrolysis is the rate-limiting, but for soluble substrate like acetate, the rate-limiting is either methanogenesis or acetogenesis (Borja and Rincón, 2017). Calculations of theoretical methane yield are often based on the acetotrophic pathway, which is the primary pathway in methanogenesis (Abbasi et al. 2012).

2.3.2 Operational conditions for anaerobic digestion process

The operational conditions that categorize anaerobic digestion include temperature, total solids, pH,

C/N ratio, hydraulic retention time (HRT), mixing and substrate particles size, as well as their optimum ranges, are outlined in Table 2.2.

Temperature

The temperature regimes for the operation of anaerobic digestion determines the type of methanogens (mesophiles or thermophiles) that will be involved. These regimes are psychrophilic (<25°C), and more frequently, mesophilic (25–45°C) which takes place optimally around 35 to 37^{o}C, and thermophilic (45–65°C) which occurs optimally at 49-57^{o}C (Kougias and Angelidaki, 2018). Very low or very hot temperatures annihilate the anaerobes, causing the entire anaerobic digestion processes to be inhibited (Edwiges et al., 2017; Elbeshbishy et al., 2012; Kim et al., 2017; Cioabla et al., 2012). The fluctuations in temperature denature enzymes activities and cause process imbalance resulting in VFA accumulation and reduced biogas yield (Kougias and Angelidaki, 2018; Ghasimi et al. 2015; Labatut et al. 2014). Aside from the energy cost for satisfying the thermal needs, increased risk of process instability associated with rising ammonia stresses, reduced digestate dewaterability, as well as start-up challenges, thermophilic temperature has overwhelming advantages over other digestion temperature ranges (Kougias and Angelidaki, 2018). These advantages include the following: (a) improved energy balance, requiring smaller sized reactor and resulting in overall lower initial investment capital cost (b) accommodates higher organic load due to rapid digestion rates (c) attains improved effluent sanitation and quality (d) achieves shorter digester hydraulic retention time (HRT), unlike other temperature ranges as shown in Table 2.2 (e) facilitates improved biodegradation of Long-Chain Fatty Acids (LCFA) (f) produces lower amount and more qualitative effluent digestate depending on the chemical composition of the used substrates. In addition, it has been established that temperature properly correlates with HRT and kinetic rate constant (Obileke et al. 2020).

Table 2. 2 Operating parameters and optimum ranges for the anaerobic digestion process

S/N	Operational parameter	Optimum Dosage range	References
1	pH -overall -hydrolysis -acidogenesis -acetogenesis -methanogenesis Alkalinity	6-8.5 (preferably between 6.8–7.2) 5.5-6.5 5.5-6.5 6.6-8.0 6.8-8.0 1500-3000mg/L as CaCO3	Xu et al. 2020; Ghosh et al. 2019; Kougias and Angelidaki, 2018
2	Carbon to nitrogen ratio (C/N)	20-30:1	Crolla, 2017
3	Temperature -psychrophilic -mesophilic -thermophilic	< 25^{o}C 35 - 37°C 52 - 55°C	Kougias and Angelidaki, 2018

4	Hydraulic retention time (HRT)	70-80days at a psychrophilic temperature 30-40days at mesophilic temperature 15-20days at thermophilic temperature	Kougias and Angelidaki, 2018. Al-Al-Seadi et al. 2008
5	Organic loading rate (OLR)	0.5 – 4.8 kg VS/m^3d	Obileke et al. 2020
6	Solid content, Dry Wet	15-35% 10%	Kampman et al. 2017
7	Particle size	Less than 10mm (0.088 - 0.40mm is recommended)	Obileke et al. 2020 Raposo et al. 2011
8	Unionized ammonia Total ammonia nitrogen	Less than 80 mg/L Less than 1.7g/L	Kougias and Angelidaki 2018, Crolla, 2017

Solid content, particle size and C/N ratio

Anaerobic digestion is also divided into dry and wet digestion processes based on the total solids content of the mixed liquor. Dry digestion is done with solid content between 15% and 35%, while wet digestion uses solid content of below 10%. The wet process is the dominant process because it allows for continuous operation and complete stirring in the anaerobic digester (Kougias and Angelidaki, 2018; Kampman et al., 2017; Drosg et al., 2015; Dobre et al., 2014). Angelonidi and Smith (2015) reported that energy balance and economic performance of digesters running on the wet process were improved when compared to dry ones. More so, dry digesters have many merits like shorter HRT, water usage is reduced, flexibility in management and type of accepted feedstock as well as the end-product (Angelonidi and Smith, 2015). Kougias and Angelidaki (2018) concluded that the design of digester configuration, mixing type and transportation type depends on whether the digestion process is wet or dry.

The particle size of substrates influences the overall biodegradability and stability of the anaerobic digestion process (Raposo et al. 2011). Size reduction increases the specific surface area, enabling access to methanogenic bacteria for improved biodegradation rate of substrates and higher biogas production (Mshandete et al. 2006). In a study reported by Raposo et al. (2011), it was observed that the amount of methane produced is inversely proportional to the particle size. To support the views in Raposo et al. 2011, Obileke et al. (2020) and Yadvika et al. (2004) corroborated that smaller particle sizes such as 0.088mm and 0.4mm achieved more biogas yield than larger particle sizes, which can cause digester blocking or clogging and impede effective digestion processes, hence particle size of less than 10mm is suggested.

C/N ranges of 20:1 and 30:1 are ideal for anaerobic digestion because methanogenic bacteria in meeting protein needs uses nitrogen, with 25:1 as optimum C/N value (Mao et al., 2015). Higher C/N

ratio enables rapid depletion of nitrogen by bacteria, leaving excess carbon and resulting in reduced biogas yield (Kigozi et al., 2014). The excess nitrogen in the lower C/N ratio results into ammonia formation, increasing the digester pH beyond 8.5 and reducing gas production rate by microbe inhibition (Kigozi et al., 2014). Substrate for digestion should be bio-degradable and possess an increased surface area to aid the actions of methanogenic microbes (Montgomery and Bochmann, 2014). More so, mixing is an important parameter for the production of biogas, excessive mixing causes stress on the microorganisms and foam formation (Wang, 2016; Manyi-Loh et al., 2013).

pH, alkalinity, ammonia and VFA

The pH interval is relatively narrow within 6.5 and 8.5, with an optimum pH ranges of 6.8 and 7.2 for a stabilized anaerobic process as shown in Table 2.2 (Kougias and Angelidaki, 2018; Kigozi et al. 2014). Slight alkalinity and neutral pH enables methanogens to perform optimally, but acidic and high alkaline conditions kill microbes (Ward et al., 2008 and Weiland, 2010). Since pH depicts the stability and equilibrium of biodigesters, deviation from the allowable range results in process inhibition and sudden decrease in methane yield (Obileke et al. 2020; Kougias and Angelidaki, 2018). The hydrolysis rate constant is known to be dependent on pH, but the acidification phase is less pH-sensitive (Borja and Rincón, 2017). As indicated in Table 2.2, different stages of anaerobic digestion perform better at varying pH ranges.

Based on the substrate-type, the pH of reactors is lowered when there is an accumulation of organic acids, while CO_2 removal and/or increased ammonia concentration increases the digester pH (Mao et al. 2015). The pH of carbohydrate-rich substrate drops due to their rapid acidification, while protein-rich substrate results in pH rise due to increased ammonia (Obileke et al.2020). Although excess ammonia inhibits digestion process, it is needed for protoplasm growth and reproduction of microbial cells at an appropriate concentration (usually below 1500 mg/L) (Xu et al. 2020; Kougias and Angelidaki, 2018). Amount of free ammonia in reactors increases at a higher temperature, leading to toxicity, VFA accumulation, decreased pH and inhibited steady state.

Most times, accumulation of VFA in biodigesters is a symptomatic representation of inhibited process due to other operational parameter failures (such as pH of less than 5.5). VFAs are short carbon chained mid-product of anaerobic digestion, their concentrations serve as an indicator on the stability of the digestion process (Kougias and Angelidaki, 2018). An imbalance could be created when VFAs permeates the membrane of microbial cells and lowering the pH of the cell's cytoplasm, thereby

inhibiting the metabolism of anaerobes (Borja and Rincón, 2017). Challenges associated with low pH are salvaged through the addition of chemicals (bicarbonate, sodium hydroxide or ammonia) for the attainment of optimum alkalinity (1500-3000 mg/L as $CaCO_3$) (Kougias and Angelidaki, 2018).

Hydraulic retention time (HRT) and organic loading rate (OLR)

In addition, hydraulic retention time (HRT) is linked to the time taken for the quantity of volatile solids and organic matter remain in the digester before being discharged, it is vital because it describes the duration needed for anaerobes to grow/mature and degrade substrates to biogas (Obileke et al. 2020; Al-Seadi et al. 2008). Optimum HRTs are dependent on the temperature, substrate composition, digester technology and organic loading rate (OLR) of the process, (Mao et al. 2015; Abbasi et al. 2012). OLR is the quantity of organic matter in gCOD/L or gTS/L or gVS/L introduced to the anaerobic digester per time (Manyi-Loh et al., 2013). HRT is inversely proportional to OLR, it is noted that low OLR and long HRT leads to constant and maximum CH_4 yields (Mao et al., 2015). Most wastewater sludges run with HRT of 15-30 days under mesophilic conditions and other agricultural residue digester stay for a minimum of 10-15 days (Deublein and Steinhauser, 2010; Shi et al., 2017). Lignocellulose wastes require a long time because of low degradability by microbes, substrates of polymers take about 60-90 days to complete the digestion processes, maize requires 20 days is needed for digestion (Shi et al., 2017). Succinctly put, CSTR and plug flow bio-digesters need HRT of 20-30 days for animal manure digestion, while shorter HRT (long hours or few days) is attained with fixed film bioreactors (Mao et al., 2015). Methane yield and effluent quality and quantity (nutrient content and microbial load) increase with increased HRT (Manyi-Loh et al., 2013).

Mixing/agitation process

In the anaerobic digestion process, mixing provides a uniform environment for microbial proximity to available substrates, fluid homogeneity to increase biodegradation and process stability (Xu et al. 2020; Raposo et al. 2011). Reactor agitation can increase the reaction rate, stop scum formation, avert the emergence of noticeable temperature and pH gradients within the reactor, promote mass transfer, aid methane escape from the mixed liquor in the digester and encourage further size reduction of substrates (Borja and Rincón, 2017). Optimum mixing intensity and duration are needed to avoid disruption of the microbial community via rapid mixing, short-circuiting or improper mixing due to very slow mixing. It is also needed to improve the efficiency of anaerobic digestion (Xu et al. 2020; Yadvika et al. 2004). It was reported in Xu et al. 2020 and Liao and Li (2015) that enhanced mixing technology improved biogas yield and slightly enhanced the methane content by increasing mixing

intensity. However, they suggested that for cost-effectiveness, optimum mixing intensity is desirable. Agitation in biodigesters is achieved using either the propeller or scraper stirring mechanism (Yadvika et al. 2004). Choice of mixing duration and intensity largely depends on the bioreactor in use.

2.4 Agro-industrial wastes: availability, methane potentials and phosphorus content.

Biogas production from waste streams across the entire value chain of the agro-industrial sector is generating increased interest in most parts of the world. Different kinds of animal and plant biomass containing cellulose, hemicelluloses, carbohydrates, fats, and proteins as their dominant constituents wield potential for biogas generation (Weiland, 2010; Khan et al., 2015). The quantity and quality of biogas produced and the digestate composition are largely dependent on the type of feedstock, pH, carbon-to-nitrogen ratio (C/N), reactor temperature, retention time and type of digestion system (Khan et al., 2015). Strong lignified feedstocks such as woods which decomposes slowly under anaerobic conditions are few exceptions to biomass for biogas production (Weiland, 2010). The capability of feedstocks to produce biogas is evaluated either theoretically or experimentally.

2.4.1 Feedstocks for anaerobic digestion

Agricultural based waste streams abound both in liquid and solid forms and are characterized to determine the recoverability of valuable products like biogas, etc. (Campos, 2014; Khan et al., 2015). These include wastes from animal and crop production stages (farmlands, greenhouses, potting sheds, cattle houses, pig houses, milking houses, etc.), processing sections (slaughterhouses and butcheries, dairy firms, crop processing, animal feed production, fruit and food processing, sugar milling wineries and breweries, silage making, etc.), microalgae, macroalgae, etc. and others (agricultural produce storage, packaging and transportation) (Borja and Rincón, 2017). Agro-industrial waste contributes about 72% of the biogas produced in anaerobic digesters, 9% of sewage sludge and 18% of landfill globally (Kampman et al., 2017; Khan et al., 2015). They are anaerobically digested singularly or co-digested in either small and large scales (Kougias and Angelidaki, 2018, Weiland, 2010).

In countries like South Africa, canning, juicing, winemaking and drying processes in fruit industries, about 50% of citrus, 25–35% the dry mass of processed apples, 20% of grapes and emerging crop (olives) are generated as wastes with the ability to produce 213033803m^3/a of biogas (ARC, 2016; Khan et al., 2015). ARC (2016) reported that wastes from one cattle, one pig and 20 birds produce

785 m^3/a, 32m^3/a and 300m^3/a of biogas respectively. It is also estimated that in most parts of the world, energy crops (mostly maize) offers more than 50% of the biogas yield (318 PJ) in the EU. Others are from landfill, organic waste, sewage sludge and manure with 114 PJ, 86 PJ, 57 PJ and 46 PJ respectively (Kampman et al., 2017). Co-digestion of agro-industrial wastewater and other waste streams has high potentials for more bioenergy production and phosphate recovery (Kampman et al., 2017). Co-digestion of food wastes and grey/black water yielded 70% biogas increase (Kjerstadius, et al., 2015).

2.4.2 Biomethane potential of feedstocks

The biochemical methane potential (BMP), largely divided into experimental (BMP) and theoretical (TBMP) methods is the maximum volume of methane yield per g of volatile solids (VS) or chemical oxygen demand (COD) of feedstock which provides an index of biodegradability and potential of substrates to generate methane in anaerobic digestion (Angelidaki et al., 2009). The BMP test which measures methane yield avails the baseline data for determination of anaerobic digestion operational requirements and methane yield optimization as well as economic and technical feasibility studies for the construction of bioreactors (Hollinger et al. 2016; Elbeshbishy et al. 2012). The non-uniformity in the results of various BMP methods necessitated the inter-laboratory standardization of biomethane potential testing procedure (Holliger et al., 2016). They outlined that factors like pH, temperature, inoculum to substrate ratio (ISR), inoculum preparation, substrate (concentration, age and type), chemical composition, mixing, presence of inhibitors, etc. affects BMP determination (Edwiges et al., 2017; Wang, 2016). BMP is expressed in mL CH_4 at the standard temperature and pressure (STP) per amount of organic component added or removed (VS or COD basis).

However, the experimental BMP has a harmonized standardized protocol of determination and is dependent on inoculum sources, quality and preparation, substrate types, preparation and storage; inoculum to substrate ratio (with crucial influence on the kinetics), test setup, etc. (Holliger et al., 2016; Strömberg et al. 2014). However, the TBMP is a quick method of determining the BMP of substrates through the estimation of elemental compositions (C, H, O, N, S) using Buswell/Boyle's equation, organic fraction compositions (lipids, proteins, and carbohydrates) or chemical oxygen demand (COD), etc. (Raposo et al., 2011). The experimental BMP often has lower yield values than the TBMP. Both the experimental and the theoretical BMPs are used to calculate the biodegradability based on biomethane yield (BD_{CH4} %= Experimental BMP/TBMP *100).

It is noteworthy that based on the chemical compositions of different substrates, their BMPs varies significantly. Generally, the BMPs of substrates mostly reported in the literature range from 77 to 900 m^3/ton.VS (Borja and Rincón, 2017). For instance, in an inter-laboratory study, BMP of cellulose is found to be from 175 to 412 mL CH4/g VS (Holliger et al., 2016). Similarly, significant variations across agro-based waste on specific methane yield showed that maize waste with its low lignin and high starch content had a high methane potential of 399 NL kg/ VS (Elbeshbishy et al., 2012). BMP ranges of other agro-based wastes as captured in Fig. 2.3 include floatable oil from food waste (608-847 L CH_4kg/VS), grass sludge (227-400 L CH_4kg/VS), okra waste (270-444 L CH_4kg/VS) orange peels (297-502 L CH_4kg/VS), pineapple waste (357-400), cabbage waste (291-382), water hyacinth (130-350 L CH_4kg/VS), sugarcane bagasse (77-200 L CH_4kg/VS), Rapeseed oil (704-900 L CH_4kg/VS), etc. (Holliger et al., 2016; Elbeshbishy et al., 2012; Kampman et al., 2017). Wang (2016) advocated for more studies to know the impact of inoculum and substrate concentration on BMP, based on substrate types, inoculum types and varying conditions.

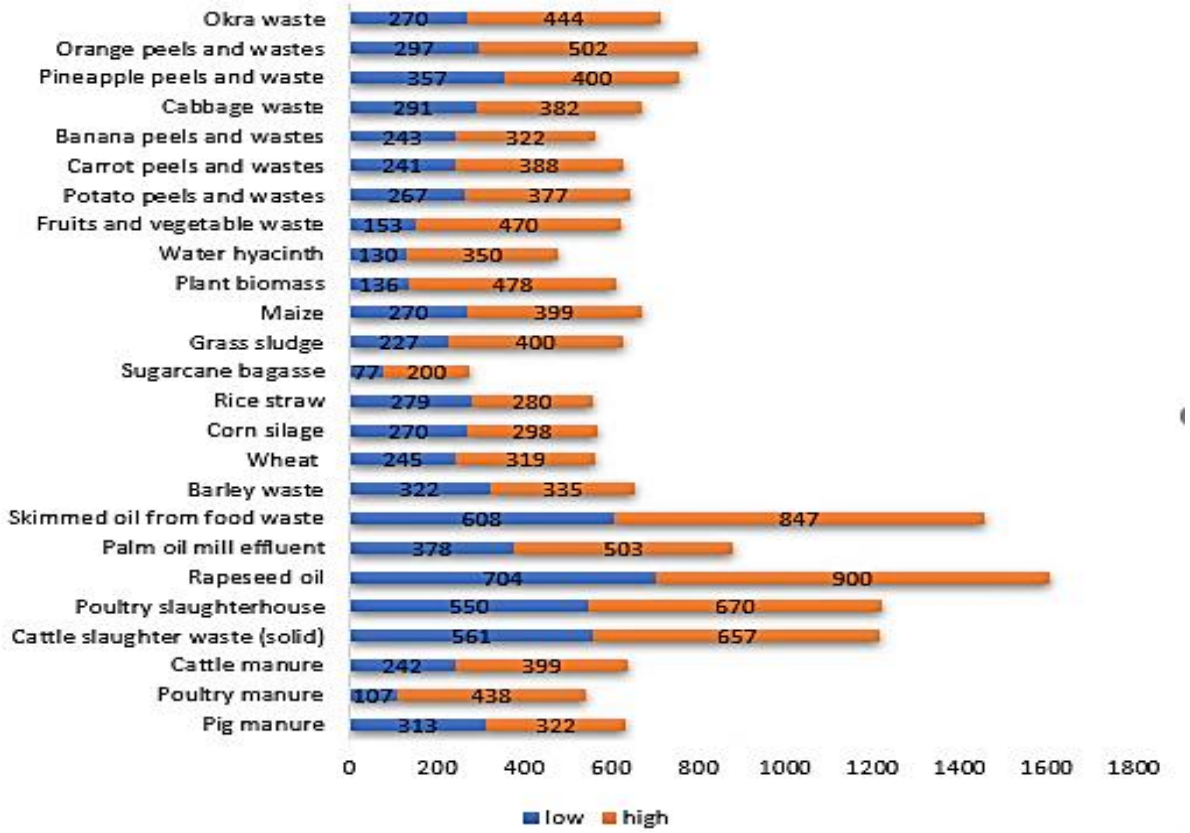

Fig.2. 3 The plot of biomethane methane potentials of some agro-industrial wastes (compiled from Ugwu and Enweremadu, 2019; Kougias and Angelidaki, 2018; Kampman et al. 2017; Holliger et al. 2016; Elbeshbishy et al. 2012; Raposo et al. 2011)

2.5 Enhancement of biogas production processes

Biogas yield which is widely associated with the economic feasibility of anaerobic digesters has gained increased interests in process technique enhancements. Varying ways aimed at achieving enhanced biogas generation include: (a) modification of the reactor operational conditions and configuration; (b) co-digestion aimed at increasing organic loading rate of the digester (OLR); (c) waste biodegradability enhancement via varying pretreatments; (d) accelerants or supplemental additives for microbial activity stimulation (e) antagonism to inhibitory agent concentrations (Braun et al., 2010; Romero-Guiza et al., 2016; Kim et al., 2017). The anaerobic digesters configuration currently used seems optimized and limited to Up-flow Anaerobic Sludge Blanket (UASB) reactor and Continuous Stirred Tank Reactor (CSTR) for soluble and particulate organic wastes respectively, hence enhanced biogas production now focuses on feedstock pretreatments and accelerants (Romero-Guiza et al., 2016). Antagonists which has barrier effects are substances or organisms used to lower the individual effects of compounds or microbes when combined (Braun et al., 2010). In an anaerobic condition, arsenate can antagonise the formation of Fe-P precipitate in the presence of humic acid (Wilfert et al., 2015). Accelerants are either chemical and/or biological additives that enable substrate surface adsorption and aid or immobilize microbial growth conditions for quicker biogas yield (Kim et al., 2017; Mao et al., 2015). The co-digestion process was reported in Li et al. (2017) to have led to high OLR of 11.1 and 30.2 gVS/L/d in a CSTR digester at mesophilic and thermophilic conditions respectively. This was achieved because the ratio of protein to ammonia conversion was high and the specific methanogenic activity was enhanced (Li et al., 2017; Mao et al., 2015).

2.5.1 Co-digestion

Co-digestion, as the name implies, is the anaerobic digestion enhancement option involving the digestion of more than one substrate with dissimilarity in characteristics at the same time in one bioreactor for increased biogas yield and other complementary gains (Chow et al. 2020; Kougias and Angelidaki, 2018). Due to the numerous benefits, most anaerobic digestion processes are carried out as co-digestion as against very few cases of mono-digestion operation. The co-digestion operation provides nutrient balance (C, N, P, etc. ratios), improves bioreactor economics and achieves higher methane yield, enhances mitigation of inhibitory substances, provides synergistic effects that aids degradability and better stability, promotes buffering ability of the mixed liquor to maintain pH values within methanogenesis tolerable range, the yield of properly digested digestate, etc. (Kougias and Angelidaki, 2018; Crolla, 2017). Co-digestion processes in bioreactors are influenced by combining ratio and nutrient balance of substrates, mixing, organic loading rate, operating temperature and

hydraulic retention time (Chow et al. 2020). However, attainment of optimum operating conditions for co-digestion is desirable.

Most energy crops have been co-digested successfully with liquid manure or wastewater to improve biogas yield (Crolla, 2017). According to Weiland (2000), co-digestion of energy crop with manure can enhance biogas production by more than 2 times. In the study of co-digestion of other substrates with wastewater, Chow et al. (2020) concluded that methane enhancement of between 13 to 176% is achieved in comparison to the mono-digestion operation. In Crolla (2017), high methane yield of 730m^3/t.VS from co-digestion of substrates (energy crop) with high (96%) volatile solid ratio and another feedstock (liquid dairy manure) of low (4%) VS ratio was produced. While reviewing more studies on the co-digestion operation, anaerobic digestion enhancement patterns were largely observed in a broad range of substrates as shown in Table 2.3.

Table 2. 3 Review of Co-digestion of Some Agro-industrial Wastes

Co-substrates	**Mixing ratio and OLR**	**C/N ratio**	**VS%**	**Biogas Yield /Remark**	**References**
Cow manure + pre-treated rape straw	80:20	26.1		382.9 mL/g VS. Increased by 11.1%	Gaballah et al. 2020
,,	60:40	30.4		535.4 mL/g VS. Increased by 55.4%	Gaballah et al. 2020
,,	40:60	36.9		516.2 mL/g VS. Increased 49.8%)	Gaballah et al. 2020
,,	20:80	47.5		500.5 mL/g VS. Increased by 45.2%	Gaballah et al. 2020
Grape marc wastes + Pedro lees	4.58	27	-	77.40 m^3 $_{STP}$ CH_4/tonne waste. Rose by 40.44%	Hungría et al. 2020
Grape marc wastes + Verdejo lees	5.10	496	-	44.30 m^3 $_{STP}$ CH_4/tonne waste. Declined by 4.06%	Hungría et al. 2020
Olive mill wastewater (OMW) + Poultry manure (PM) + liquid pig manure (LPM)	30% (OMW): 70%PM+LPM 2.2 kg.VS/m^3/d	-	59.8	0.8797 L/g $VS_{removed}$ Increased	Thanos et al. 2020
Olive mill wastewater (OMW) + Poultry manure (PM)+ cheese whey (CM)	40% (OMW): 60%PM+CW 2.2 kg.VS/m^3/d	-	62.1	1.0899 L/g $VS_{removed}$ Increased	Thanos et al. 2020
Sugar beet root waste (BW), cow dung (CD), and poultry manure (PM)	0.25:0.5:0.75	26.24	-	347.48 mL/g VS. Increased by 41.2%	Dima et al. 2020
Food wastes (FW), cow dung (CD) and piggery dung (PD)	40:40:20	16:1	86	0.64 L/g.VS. Increased by 23.44%	Oladejo et al. 2020

Food wastes (FW), cow dung (CD)	50:50	15:1	88.6	0.62 L/g.VS. Increased by 20.97%	Oladejo et al. 2020
Food wastes (FW) and piggery dung (PD)	50:50	15:1	90.615	0.58 L/g.VS. Increased by 15.52%	Oladejo et al. 2020
Swine manure (SM) and corn stover (CS)	1:1 3 g.VS/L.d	17.10	64.92	90.04 L/g.VS. Increased	Wang et al. 2020
Swine manure (SM) and corn stover (CS)	2:1 3 g.VS/L.d	13.93	64.92	96.72 L/g.VS. Increased	Wang et al. 2020
Swine manure (SM) and corn stover (CS)	1:2 3 g.VS/L.d	22.73	64.92	99.51 L/g.VS. Increased	Wang et al. 2020

2.5.2 Pretreatment

Most substrates are seemingly very slow to be degraded for biogas production owing to their chemicals compositions which are growth inhibiting to microbial activities. These compositions create physical problems such as foaming, floating and blockage in nozzles and impellers in digesters. More so, molecular structure, crystalline structures and small surface area of these substrates make them inaccessible to enzymes of microorganisms (Montgomery and Bochmann, 2014).

In anaerobic digestion, hydrolysis is the rate-determining step for the breakdown of complex organic matter. In achieving a faster breakdown of complex molecules, pretreatment methods to facilitate the anaerobic digestion is involved. This increase the rate of organic matter hydrolysis and enhances the production of biogas as well as aid in waste stabilization and disposal (Salihu and Alam, 2016).

Pretreatment methods are meant to achieve such purposes such as an increase in porosity, reduction of feedstock size, elimination of inhibitors, increase substrate solubility and degradability and low energy input requirement as well as cost-effectiveness (Atelge et al. 2020). The pretreatment choice depends on the characteristics of the substrate of interest and the required outcome. Pretreatments methods as shown in Fig. 2.4 include biological with the notable benefits of low or no chemical and energy inputs, but it is largely a slow process. The examples of biological pretreatment are anaerobic and aerobic, microbial pretreatment, fungal pretreatment and enzyme addition. The physical methods (mills, shredders, thermal, ultrasonic, microwave, high pressure homogenizing, freezing/thawing and electro-kinetic) facilitates fast size reduction process, improves degradability and enzyme accessibility, reduces pathogens, decreases the time of digestate dewaterability etc. Others include chemical (alkali, acid, oxidative pretreatment, etc.), hybrid or combined pretreatment methods (involves more than one pretreatment options e.g. physicochemical, thermochemical, etc.) (Baredar et al., 2016; Zhang et al., 2010).

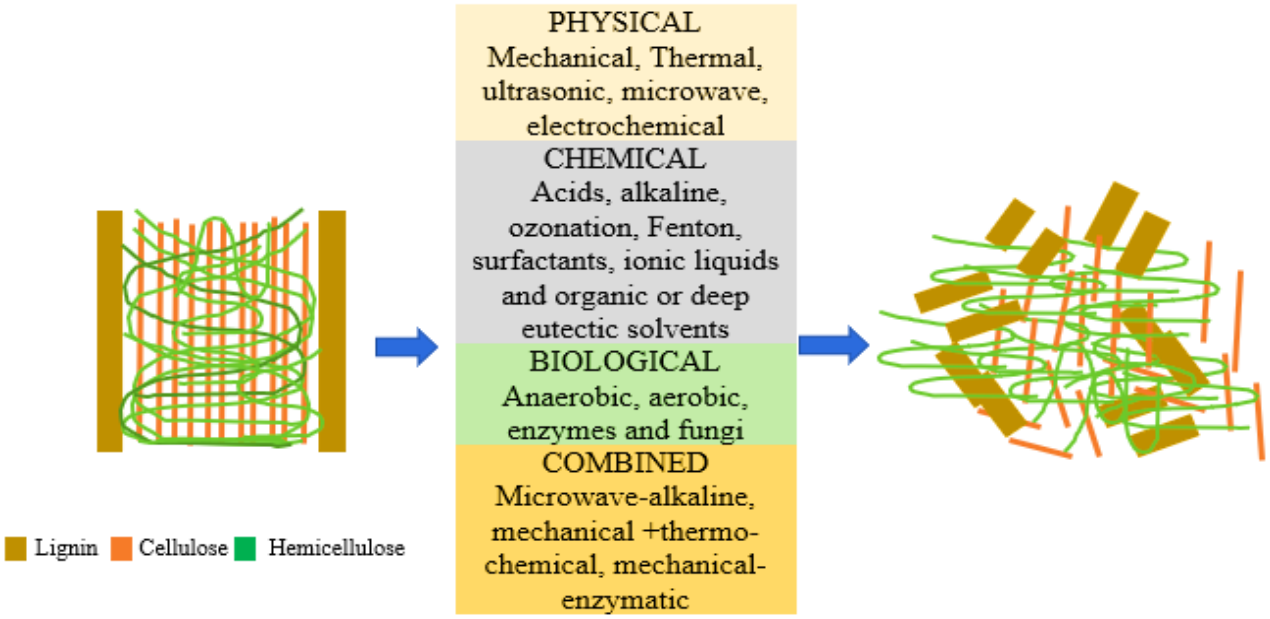

Fig.2. 4 Depiction of lignocellulosic substrate pretreatment mechanism of degradation

These pretreatments are also in the form of inoculation (seeding) and generally enhances solubilization of waste and anaerobic digestion (Zhang et al., 2010; Rodriguez et al., 2017). It was advocated by Salihu and Alam, (2016) that economic implications like energy consumption, operational costs and other output benefits (biogas produced and waste treatment) should drive the choice of pretreatment methods during anaerobic digestion. However, although pretreatment is an essential means for enhancing anaerobic digestion, production of some aliphatic acids and furans, which are toxic to biodegradation process and the attendant cost of ameliorating their impacts are the downsides of this enhancement option (Atelge et al. 2020).

2.5.3 Additives

Additives (accelerants or antagonists) for enhancing anaerobic digestion processes have recently been the cynosure of most researchers nowadays. Additives can be grouped based on their major constituents and` functions such as reduction of toxin impacts, the supply of deficient nutrients, control of specific digestion activities, performance improvement and increased stability of the anaerobic digestion process (Kim et al., 2017; Baredar et al., 2016; Kuttner et al., 2015). These additives when in higher concentration causes cytotoxicity affects the pH and inhibits biogas production (Mao et al., 2015). They are further divided into organic and mineral additives (Kim et al., 2017) or biological and chemical additives (Mao et al., 2015) or biological and inorganic additives (Romero-Guiza et al., 2016). Mineral additives include the following: (i) micro- (e.g. Ni, Fe, Co, Mo, Se and W) and macro- (e.g. N, P and S) nutrients additives, (ii) waste incineration ashes, (iii) ammonia

inhibition compounds, (iv) biomass immobilizing substances, (v) H_2S toxicity controlling compounds and (vi) nano-additives (NZVI, ZnO, CuO, Mn_2O_3, Al_2O_3 and CeO_2). Organic or biological accelerants include enzymes addition for enhanced solubilization of waste streams, bioaugmentation and addition of biological inoculum with biogas production potentials (Mao et al., 2015). Additives can also be subdivided into conductive (magnetite, hematite, granular activated carbon (GAC), biochar, carbon fiber, etc.) and non-conductive additive (metal hydroxides, N, S, etc.) types (Chiappero et al. 2020; Wu et al. 2020).

Conductive additive types have been several times used for enhancement of anaerobic digestion and methanogenic activities, facilitation of syntrophic metabolism for increased electron transfer and maintenance of high hydrogen partial pressure etc. (Wu et al. 2020). As shown in Table 2.4, they are largely divided into metal-based (NZVI, ZVI, iron (nanoparticles, oxides, chlorides, etc.), Manganese, etc.) and carbonaceous (biochar, graphene, carbon (nanotubes, felt, fiber or cloth), etc.) conductive materials (Wu et al. 2020). According to Chiappero et al. (2020), conductive additive like biochar achieves biogas production enhancement via promotion of syntrophic metabolisms, increasing of digestion system buffering ability, reduction of inhibitors or antagonists, enhancement of digestate quality, scrubbing and upgrading of biogas, etc. However, some conductive additives (e.g. magnesium oxide, ferrihydrite, nano-silver, carbon black, etc.) inhibits anaerobic digestion processes due to limitation of mass transfer, toxicity on microbes, etc. (Wu et al. 2020).

Nano-additive materials with either positive or negative impacts on biogas production already researched are grouped into (a) carbon-based materials, (b) zero-valent metals, and (c) metal oxides (Ganzoury and Allam, 2015; Rahman et al., 2016). As reported in Table 2.4, while some nano-additives like ZnO and Ag showed negative effects on the biogas production due to toxicity, all the reported trace elements, carbon-based additives, biological additive, fullerene and most nanoparticles especially nano-iron oxide (Fe_3O_4) recorded enhancements. Similarly, other additives like micro/nano bottom ash (MNBA) and micro/nano fly ash (MNFA) was reported in (Rahman et al., 2016) to have enhanced considerably biogas generation. In the research of Al-Ahmad et al., (2014) on the effects of 10^{-5} mol/l Pd, Fe, Ni, Pt, Ag, Cu and Co nanoparticles entrapped in SiO_2 with 5 mg/l arsenate concentration on anaerobic digestion at 55^{o}C, observed a notable increase in biogas production as follows: Pt (6%), Fe (7%), Co (48%), and Ni (70%). To optimize biogas yield Ganzoury and Allam, (2015) suggested the need for: bioactive nano-metal oxides use to eliminate cytotoxicity on bacteria; exploring particle sizes, shape and concentrations of varying nano zero-valent metals

(NZVMs); harnessing the combined merits of NZVMs and ashes at varying ratios; and the use of visible-light photoactive metal oxides capable of enriching the photo-fermentation anaerobic reactor for increased hydrogen quantity and subsequent methane generation enhancement.

Table 2. 4 Impact of additives on biogas production processes

Additive type	Optimum Dosage mg/L	Substrate type	Biogas yield (mL/g.VS)/ Remarks	Reference
Metals: Trace				
Fe	≤ 1000 (100)	Food waste	414 enhanced by 11.3%	Zhang et al. 2015
Co	1	Food waste	418 enhanced by 12.4%	Zhang et al. 2015
Se	≤ 0.04	Food waste	580 enhanced by 34.1%	Ariunbaatar et al. 2016
Ni	5	Food waste	424 enhanced by 14%	Zhang et al. 2015
Mo	≤ 5	Food waste	415 enhanced by 11.6%	Zhang et al. 2015
Zero-valent iron	10000		Biogas yield was increased by 20.6%	Wang et al. 2018
Nanoparticles				
Fe	20	Livestock manure	511.27, increased by 1.45 times	Abdelsalam et al. 2017
Fe_2O_3	20000	sludge	1.4mmol/g.VSS, increased by 35.52%	Ye et al. 2018
Fe_3O_4	20	Livestock manure	584, increased by 1.66 times	Abdelsalam et al. 2017
Ni	2	Cattle dung	Enhanced by 1.8 times	Abdelsalam et al. 2016
Co	1	Cattle dung	Enhanced by 1.7 times	Abdelsalam et al. 2016
ZnO	5-500	Waste activated sludge	Biogas yield decreased by 63.68% as the dosage increased	Zhang et al. 2017
CeO_2	10	Sludge	Increased by 11%, but decreased when dosage rose	Nguyen et al. 2015
TiO_2	100	Cattle manure	Biogas production was enhanced by 9.7%	Ajay et al. 2020
Al_2O_3	250mg/g	Waste activated sludge	Maximum 14.8% rise in biogas yield was noticed	Ajay et al. 2020
NZVI	1000		30% rise was observed	Wang et al. 2018
Ag	1-10 mg/kg	Municipal solid waste	Methane yield declined from 10 to 80% as dosage rose	Ajay et al. 2020
Carbon-based				
Biochar	8000 -25000	Biomass	Average enhancement of 25% biogas yield and better digestate quality	Chiappero et al. 2020
Graphene	120	Sludges	54.1% rise in biogas yield	Abdelwahab et al. 2020
Multi-walled Carbon nanotube	500	Liquid manure	Biogas production was enhanced by 48.6%	Abdelwahab et al. 2020
Fullerene	500	Liquid manure	Methane yield increased by 33.6%	Abdelwahab et al. 2020
Biological				
Enzymes (lipases)	0.33 % v/v	Grease and sludge	Higher methane yield from 365 to 452 and higher solubilization of substrates	Donoso-Bravo et al. 2013

2.6. Influences of iron-based enhancement on anaerobic digestion

Amongst all the enhancement studies, iron additive types remain invaluable to the improvement of anaerobic digestion processes due to their affordability and conductive properties. Various iron-based

additives have been used in many environmental management processes, nutrient supplementation, and digestion enhancement in an anaerobic digestion operation either singularly or in combination with organic and inorganic substances (Kim et al. 2017; Zhang et al. 2015). Some of the other alluring properties of iron include their oxidative-reductive potential (ORP) decreasing capacity, cofactor role for lots of enzymatic activities, electron donation and accepting capability, etc. (Hao et al. 2017). As stated in Table 1.1, so many iron types have been used to enhance the anaerobic fermentation of substrates. Based on several studies, the following iron-based additives have been used for enhancement of anaerobic digestion process; Waste Iron Scraps (WISs) (Hao et al. 2017), Zero-Valent Iron (ZVI), Zero-Valent Iron Scraps (ZVSI), Nano Zero Valent Iron (nZVI) (Wang et al. 2018; Zhen et al. 2015). Also hematite+red mud (Ye et al. 2018), Fe and other trace metal supplementation (Zhang et al. 2015), Fe_3O_4 (Chen et al. 2018). These iron-based additives have varying impacts on the entire anaerobic digestion processes (biogas composition, VFAs, solid reduction, pathogen remediation, digestate quality, etc.).

2.6.1. Biogas yield and methane content

The viability of iron additives in anaerobic digestion has ensured enhanced biogas production in both quality and quantity of the methane content. Several studies on the enhancement of methane production have shown that above 60% CH_4 could be achieved (Hao et al. 2017). In Suanon et al. (2017), the presence of iron powder (1.6%) and nZVI (0.1%) during the anaerobic digestion process increased biogas yield by 40.8% and 25.2%. In Feng et al. (2014), an increase of 43% in methane production was recorded when sludge pretreated with alkaline were digested with WISs. While analyzing the anaerobic digestion of sludges with 10 g Fe/L of WISs at the acidogenic and methanogenic phases in, Hao et al. (2017), reported that methane production in both acidogenic and methanogenic phases was respectively enhanced by 10.1% and 21.4%. Rusty and clean iron scraps were added to enhance anaerobic digestion of sludge in Zhang et al. (2014b), 21.28% rise in methane yield was reported for clean scrap due to its better mass transfer efficiency, rusty scrap increased methane yield by 29.51%. The addition of red mud (45% Fe_2O_3) when compared to the control, promoted methane yield by 35.52 ± 2.64% (Ye et al., 2018). Amen et al. (2017) compared the influence of pristine nZVI, nZVI coated (ICZ), nZVI mixed with zeolite (IMZ) supplemented anaerobic reaction with the control bioreaction. It was observed that the supplementation of ICZ with 1000mg/L iron-based nanoparticles aided the attainment of maximum cumulative methane volume. However, the addition of nZVI and IMZ, upward stimulation of highest methane content was recorded respectively at 88 and 74%. Similarly, the extra hydrogen given out from the nZVI (30

mol/L) oxidation, stimulated the hydrogenotrophic methanogenesis process and resulted in 30% biogas yield enhancement (He et al. 2017). On the contrary, the addition of a higher dosage of nZVI/CU^{o} (>1500mg/L) inhibited biogas production (Amen et al. 2018).

The effectiveness of the advanced oxidative processes (AOPs) in enhancing biogas production and increasing substrate degradation, have been previously studied (Michalska et al. 2012; Lozano, 2010; Shahriari et al. 2012). Bhange et al. (2015) reported that the Fenton's reagent was effective on garden biomass and that higher H_2O_2 concentration in Fenton reaction resulted in a noticeable increase in the rate of cellulose and lignin degradation in contrast to a higher concentration of Fe^{2+} ion. Michalska et al. (2012) while advocating the necessity of applying a chemical pretreatment such as oxidation with Fenton's reagent reported 75% rise in methane content when Fenton process was used in the anaerobic digestion of Sorghum Moensch. In a full-scale digester, Lozano (2010) showed that the use of Fenton process in recycled substrate digestion improved digestibility of sludge and increased biogas production by 13%. In the conduct of batch biochemical methane potential (BMP) tests by Maamir et al. (2017), it was observed that the overall biogas and methane yields were although more without Fenton enhancement at 699 and 416 mL/g VS, respectively, but the Fenton pre-treated Olive Mill Solid Waste (OMSW)increased by 24% methane yield. In contrast, while questioning the work of Lozano (2010), Uman et al 2018 observed no difference in biogas yields of 0.280 and 0.279 LCH_4/gVS respectively for both Fenton process and control after 280 days of digestion. It was therefore concluded that Fenton reaction has no noticeable effect on biogas yield (Uman et al. 2018).

2.6.2. Volatile fatty acids (VFAs)

During anaerobic digestion processes, intermediate products like volatile fatty acids (VFAs) are very vital in the processes of biogas. They are fatty acids with carboxylic short-chains (C2-C6) and are produced after hydrolysis of biomass by syntrophic bacteria (Kim et al. 2018; Meng, 2013; Wan et al. 2013). Some factors such as pH and addition of iron-based additives can affect VFAs in an anaerobic digestion process. Propionic acid and butyric acid as two main VFA forms in the acidification stage are decomposable into the only acetate at a pH below 2 (Feng et al. 2014; Hao et al. 2017). The high rate of propionate production and low decomposition rate (much lower than other VFAs) causes propionate accumulation and disruption of pH balance between acidogenesis and methanogenesis, but according to Zhang et al. (2015), the addition of trace iron could stabilize anaerobic digestion processes. In the anaerobic digestion of wastewater, Meng et al. (2013) demonstrated that the addition of ZVI powder could contribute to the decomposition of propionate to

acetate by decreasing the Gibbs free energy and enhancing the activities acetogenesis-related enzymes homoacetogenesis which reduces H_2 content to aid propionate conversion to acetates. It is obvious that when substrates are hydrolyzed, excess VFAs that could inhibit methanogenesis by lowering pH is produced (Zhang et al. 2016). This anomaly can be remedied by the addition of iron additive (Ferric chloride) in the anaerobic digester, thereby enriching functional strains to avert inhibition from VFAs (Zhang et al. 2016). Acetate and maximum VFAs respectively at 24.9 and 49.3mg/L were obtained in Yang et al. (2013) with the addition of 30 mM nZVI. In a study, Zhen et al. (2015) reported that ZVSI provoked increasing VFA and acetate production, the addition of 0 to 1g-ZVSI/g VSS on the 12th day enhanced VFAs from 2059.9 ± 110.8 to 2340.4 ± 73.0 mg/L and the corresponding acetate increased from 779.6 ± 18.2 to 865.5 ± 24.8 mg/L respectively. On the 30th day, propionate attained maximum range, while there was a general decline of VFAs and acetate. Therefore, it can be inferred that the higher production of acetate with the addition of ZVSI, may have thermodynamically favoured the methanogenesis phase.

More so, after the mesophilic digestion state, maximum acetate and VFAs yield were recorded on the 15th and the 30th day, production of VFAs declined until no trace of acetate was noticed, suggesting completion of acetate degradation (Zhen et al. 2015). Differing from acetate, propionate at the same time exhibited peak yields between 1242.4 and 412.4 mg/L depending on the ZVSI dosage used and may be attributable to conversion of VFAs to propionate. Similarly, in Hao et al. (2017), a drastic decline in TVFA from 730 mg $CODL^{-1}$ to 30 mg $CODL^{-1}$ on the addition of WISs was observed, contrary to the control, which recorded an increase in VFAs (1080 mg COD/L). In the same vein, Feng et al. (2014) reported a similar VFAs decline from 534 mg $CODL^{-1}$ to 20 mg $CODL^{-1}$ in a digestion process aided by ZVI, but the addition of 4 g of ZVI increased VFAs by 37%. While observing the dominance of acetate and propionate at the acidogenesis phase, Liu et al. (2012) reported a propionic acid-type of fermentation amounting to 70% acetate and propionate. In a Fenton process aided digestion, Michalska et al. (2012), showed that after chemical hydrolysis, the concentration of VFA was low, resulting in overall low biogas yield. Uman et al. (2018) also reported low TVFA concentration of 75 mg/L throughout the digestion process, this was attributed to the low substrate solubilization resulting in low soluble COD (sCOD).

2.6.3. Solid reduction (VS/COD)

The reduction of solids during anaerobic digestion is as a result of substrate degradation by microbes, it is expressed as either chemical oxygen demand (COD) or volatile solids removed. Past studies

reported on the influences of iron-based additives on solid reduction (Volatile suspended solids (VSS), Volatile solids (VS) and COD) during anaerobic digestion. The substrate COD is released in the medium on account of microbial activities and their subsequent consumption as carbon sources (Suanon et al. 2017). In anaerobic digestion, COD could fluctuate (increase or decrease) the solid substrate particles that are not readily available to microbes are converted into soluble organics (VFAs), leading to soluble COD (sCOD) increase in the solution (Wan et al. 2013). In the work of Suanon et al. (2016), the addition of nZVI and iron particles (IP) during the anaerobic digestion process improved the removal of COD from initial COD of 6651 mg/L in digesters A (control), B (5 g of IP) and C (0.3 g of nZVI) respectively to 3683 mg/ L (44.6), 3032.1 mg/ L (54.4%) and 2247.5 mg/L (66.2%) at the end. Ye et al, (2018) observed that the introduction of 20 g/L red mud (45% Fe_2O_3) achieved the reduction of total COD (TCOD) from 30.15 to 14.35 g/L and 19.49 in the control reactor, showing that the solubilization of biodegradable organics for methanogenesis was aided by the addition of red mud.

Substrate solubilization is a vital step to hydrolysis and changes in sCOD dynamics during anaerobic digestion. As reported in Zhen et al. (2015), increased dosage of ZVSI (0 to 1.00 g-ZVSI/g VSS) respectively resulted in an average rise of sCOD concentration from 178.2 ± 3.5, to 199.2 ± 19.1 mg/g VSS on day 12 at 20^{o}C. This rise is attributable to the sustained endogenous decay of biomass, releasing more soluble compounds, slowing methanogenesis rate and retarding conversion of organics to methane (Zhen et al. 2015). The rise of digestion temperature from 20^{o}C to 35^{o}C accelerated ZVSI corrosion, substrate solubilization and attainment of maximum sCOD (306.9 to 351.3 mg. g^{-1} VSS), corresponding to the increasing dosage from 0 to 1.00 g.ZVSI.g^{-1}VSS after three days of mesophilic digestion stage. Enhanced solubilization due to the addition of ZVI and Fe_3O_4 resulted in increased TCOD. Zhao et al. (2018), reported that Fe_3O_4 solubilized waste more than ZVI. Ambuchi et al. (2018) corroborated the previous research on the influence of iron additives on substrate solubilization, resulting in increased sCOD and subsequent COD removal, it was reported that after the initial 6 hours, the reactor with hematite recorded a quick substrate degradation and showed higher removal efficiency of sCOD than the control reactors after 72hrs. Similarly, the use of nZVI and bimetallic NPs (IMZ, and ICZ) for anaerobic digestion enhancement as reported in Amen et al. (2017), showed that the sludge sCOD increased quickly throughout the digestion period in all the used bio-digesters. The initial concentration of sCOD was 3873 mg L^{-1} and upon digestion, the average sCOD of the zero-enhanced reactor, ICZ 1000, ICZ 500, IMZ and nZVI were 12,256, 20,110, 22,050, 28,640 and 28,936 mg L^{-1} respectively.

However, the use of H_2O_2 activated by iron salts in Fenton peroxidation process disintegrated sludges and broke the cellular constituents, which lead to greater sCOD concentration (Salihu and Alam, 2016). Uman et al. (2018) reported the relatively low sCOD concentration of approximately 250 mg/L all through the digestion period. Maamir et al. (2017) reported that as soon as the concentration of H_2O_2 concentration rose from 125 to 1000 mM, COD of Fenton-treated substrate when compared to the control COD value of 1123 mgO_2/L, increased from 1133 to 5594 mg/O_2 (56%) till attainment of optimized working conditions. These working conditions (pH 3, 120 min, H_2O_2/ $[Fe^{2+}]$ = 1000 and $[Fe^{2+}]$ = 1.5 mM), showed that the optimal Fenton process pretreated olive mill solid waste achieved 82% increase in sCOD (Maamir et al. 2017).

Although VS or VSS removal is regarded as the yardsticks for performance evaluation of anaerobic digestion, the presence of refractory materials hampers the complete degradation of organics (Elsayed et al. 2016). Addition of iron-based substrate has proven to be effective in overcoming the hurdles of refractory materials to enhanced solid removal. In the studies conducted by Hao et al. (2017) at both acidogenic and methanogenic phases of anaerobic digestion, the addition of WIS was reported to have improved the removal of VSS respectively by 4.5% and 14.0% of the added raw substrate VSS. In Zhu et al. (2014), a similar report of solid removal by the addition of iron shavings resulting in 75% to 98% carbohydrate consumption. Zhang et al. (2014b) also reported that the iron-enhanced reactors with rusty scraps, Fe powder and clean scrap achieved the highest VSS reduction rate of 48.27%. Amen et al. (2017) stated that the substrate digestion of volatile solid fraction with the addition of nZVI, IMZ and ICZ, resulted in the volatile solid reduction of up to 23.8% and suggested that for up-scaling, 1 g of volatile solids will need 2.67 g of ICZ particles to achieve maximum solid removal and methane yield. In full-scale digestion of Fenton reaction, Lozano (2010) reported 11.5% biosolid reduction. Furthermore, Uman et al. (2018) indicated high solid removal efficiency (58.5%) when compared to the control (53.2%).

2.6.4. Methanogens/microbial population

The anaerobic digestion processes involve complex activities of the microbial population. There are optimal operating conditions for methanogens at each stage of anaerobic digestion. Amongst all the stages, hydrolysis is the rate-limiting step, after the hydrolysis of biological polymers, H_2, VFAs and acetate are produced (Zhang et al. 2015b). Through syntrophic bacteria, under low partial pressure, VFAs are converted to H_2, acetate and H_2 are converted to methane (Zhang et al. 2015; Feng et al.

2014; Lv et al. 2010. Microbial activities are sensitive, enhanced or inhibited by functioning parameters like H_2, pH, VFAs and others (Feng et al. 2014). Wan et al. (2013) posited that the consumption and degradation of organic matter by microbial activities are responsible for the decrease or increase of COD in anaerobic digestion. In the case of low availability of trace elements like iron in anaerobic digestion, the enzymatic biochemical reactions of methanogenesis are often interrupted due to the shortage or reduction of metalloenzymes activity, which often results in process instability and ultimately low methane production (Zhang et al. 2015; Meng et al. 2013). Feng et al. (2014) reported that when the iron gets reduced, it lowers the ORP, which favours acetate production and serves as a direct substrate for methanogens and homoacetogens.

Anaerobic methanogenesis is significantly affected by the interspecies transfer of electron amongst methanogenic archaea and secondary fermenting bacteria (Stams and Plugge, 2009). Direct interspecies electron transfer (DIET) is another electron transfer type reputed as a vital interspecies electron transfer pathway between species via physical electrical networks from cell to cell (Lovley, 2017). DIET-linked microorganisms create biological electrical links with others and serve as the basis for the advancement of innovative biotechnologies (Ye et al., 2018). More so, extracellular polymeric substances (EPS), which are natural big molecular-weight polymers defaecated by microbes could store via electrochemical means, active substances like c-type cytochromes (c-Cysts) with the capability of improving the DIET process and responsible for 80 per cent of the activated sludge mass (Zhang et al., 2017b, Xiao et al., 2017). Carboxyl, hydroxyl and phosphoric functional groups can facilitate EPS to promote microbial aggregate formation to the benefit of DIET involved in syntrophic anaerobic metabolism (Ye et al., 2018). EPS can be affected by the external conditions due to the complex environment in anaerobic digestion (Ye et al., 2018).

Several studies have demonstrated that materials with conductive properties like iron can serve as solid channels for stimulating methane yield via direct electron transfer (Zhao et al., 2017). Ye et al. (2018) in studying the interaction between conductive material (red mud consisting of hematite (45 %)) and EPS on sludge aggregation, methanogenesis and EPS redox activities, discovered that the Fe_2O_3 multivalent cations aided successfully the creation of compact, big aggregates and probably assisted the quick transfer of direct electron at the time of the DIET process. It was also noted that more redox-active mediators, c-Cysts, tightly bound EPS (TB-EPS), humic substances, and addition of extra Fe with reduction-oxidation capabilities were involved in the process of interspecies electron transfer amongst methanogenic archaea and syntrophic bacteria, hence the higher methane yield

enhancement when compared to the control (Ye et al., 2018). Similarly, Ambuchi et al. (2018) observed that hematite enriched the bacteria Firmicutes and suggested that the communities of syntrophic microbes probably have more direct electron exchanged, and hematite playing the role of electron channels between the methanogens and homoacetogens, hence creating a DIET pathway.

Past studies have raised antimicrobial concerns on the use of iron-based additives, particularly nZVI on pure microbes, like Pseudomonas fluorescens, Escherichia coli, Cyanobacteria, Bacillus subtilis-varniger, effective removal of MS2 and aX174 viruses via cell membrane structural reductive disruption and strong adsorption (He et al., 2017). More so, the toxicity mechanisms of nZVI partly damages and inactivates respectively the DNA and enzyme due to the unconstrained iron ions from nZVI (He et al., 2017; Yang et al., 2013; Lee et al., 2008). According to He et al. (2017), the oxidation of nZVI resulted in the release of extra hydrogen gas and stimulation of the hydrogenotrophic methanogenesis process. This process is a complex biological concept involving about five coenzymes and ten reaction steps that converts H_2 and CO_2 to methane (Wagner et al. 2018). In the case of iron (ZVI or WISs, etc.) supplementation, hydrogenotrophic methanogenesis and homoacetogenesis are promoted either through the evolution of H_2 from iron corrosion or directly served electron donation from iron. (Hao et al. 2017). It was further observed that nZVI toxicity to anaerobic microbes can be weakened when it reacts with EPS, resulting in accelerated nZVI corrosion and slowing down the release of H_2 from the dissolution of nZVI. The report of the hydrogenotrophic microbial rise and the reduction in bacteria involved in glucose degradation cum acetoclastic methanogens showed H_2 facilitated tilt in the direction of the hydrogenotrophic pathway improving the methane yield. Feng et al. (2014), Zheng et al. (2013) and Zhang et al. (2015b) posited that ZVI provides a more favourable environment for necessary methanogens via ORP reduction of the anaerobic digestion systems for stimulation of hydrolysis/acidogenesis and enrichment of H_2-utilizing methanogens, accelerating the H_2 consumption and facilitating the entire digestion processes. The use of iron oxide powder as additives increased the activities of the hydrolysis–acidification related enzymes between 2 and 34 times (Meng et al. 2013).

According to Cheng et al. (2015), effective reduction of ferrihydrite-Fe(III) in the anaerobic digestion of sludge vials was reported. This could be attributable to either a dissimilatory iron-reducing bacteria (DIRB) direct mediation or circuitously by DIRB equivalents from the substrate anaerobic degradation. In a similar report by Zhang et al. (2014b), rusty iron could induce microbial Fe(III) reduction, polymerase chain reaction – denaturing gradient gel electrophoresis (PCR–DGGE) showed

that the enhancement of acetobacteria diversity and enrichment of iron-reducing microbes to accelerate digestion of composite wastes was based on the addition of rusty scrap. In similar research, Hao et al. (2017) added WIS respectively at the methanogenic phase (MP) and acidogenic phase (AP) during anaerobic digestion of sludge. It was revealed as detected with fluorescence in situ hybridization (FISH) that the WISs stimulated the anabolism and catabolism of anaerobes and might be responsible for higher (96.3%) methane yield, facilitating enhancement of electron transport rate (ETR) and hydrolysis of refractory wastes.

In a comparative study, Zhao et al. (2018) discussed the impacts of Fe_3O_4 and ZVI on the microbial communities during the anaerobic digestion process. It was observed that the Fe_3O_4, which is an electron acceptor, competes for electrons with methanogens, inhibited methanogenesis, while ZVI-added reactor enhanced the processes of hydrogenotrophic methanogenesis, thereby causing about 70% rise in methane production than in the control. In other words, processes of solubilization, acidification and hydrolysis enhancement could be achieved through a dissimilatory iron reduction process of Fe_3O_4 and availing the methanogens of the much-needed substrate for overall promotion of anaerobic digestion. Similarly, Wang et al. (2018) noted that the addition of 0.6 and 1.0 g. L^{-1} nZVI effectively disrupted the microbial cell membranes and promoted methane production, while the higher dosage of 4.0 and 10.0g/L nZVI addition due to substantial H_2 accumulation, inhibited the methanogenesis. This is because H_2, which is seen as an unfavourable thermodynamic intermediate product of microbial reduction (acidification/hydrolysis) or iron corrosion when accumulated in biodigesters, increases the H_2 partial pressure, causes pH instability, inhibits methanogenic activities and impede organic acids decomposition (Feng et al. 2014).

2.6.5. Antibiotics, pharmaceuticals and personal care products (PPCPs)

Antibiotics, pharmaceutical and personal care products are emerging pollutants of concerns to the ecosystem that are not easily treated. They are mainly from diverse human activities (animal production, etc.). Various sections of the environment can be occupied by antibiotic resistance genes (ARGs) (Pruden et al. 2006). Antibiotics are used generally for growth promotion, prevention and control of diseases in livestock farms. Approximately 30%–90% of antibiotics are not absorbed, but often excreted via urine or faeces, thereby making livestock manure a big antibiotic resistance genes (ARG) reservoir (Zhang et al. 2015b; Selvam et al. 2012). ARGs in the environment has been identified to be predominantly from activated sludge (Gao et al. 2017). The process of anaerobic digestion has widely been applied in pathogen and ARG removal/reduction, it is suggested that during

substrate anaerobic digestion, there are distinct responses from different ARGs to the operational conditions, hence the emergence of varying ARG carrier bacteria and fate (Zhang et al. 2016b). It has been shown from past studies that in the presence of iron additives (eg. ZVI), microbial consortia housing ARGs most likely perform differently during anaerobic digestion. It has been proven that ZVI and natural zeolite advance the removal of ARGs during composting and sludge digestion (Zhang et al. 2015b). The exposure of gut microbiota of mouse to iron additives might cause variations in ARGs (tet(O), tet(M) and tet(Q)) due to the adjustment of gut microbiota (Guo et al. 2014; Gao et al. 2015).

While investigating the influence of thermophilic co-digestion of wastes from kitchen and sludges with the addition of ZVI on the attenuation of the integrase gene intI1 and other seven typical resistant genes of tetracycline (tet(G), tet(M), tet(O), tet(A), tet, tet(W), tet(C) and tet(X)), Gao et al. (2017) stated that with the exclusion of tet(W), the entire tet and intI genes showed a significant decrease at the addition of 5g/l ZVI dose. It was noted that at thermophilic conditions with ZVI, the intI1 and tet genes in mixed liquor can be attenuated. Remarkably, different mechanisms of resistance encoded by tet genes enable its different behaviour in bioreactors, but the use of iron oxide improves their removal (Gao et al. 2017). In a similar bid to understand the ARGs fate during anaerobic digestion of swine at both mesophilic and thermophilic conditions with natural zeolite, ZVI and Dnase to clarify the influencing factors such as intI1, heavy metal resistance genes (MRG), microbial community changes and virulence factors, ARGs reduction could be realized (Zhang et al. 2018). The reduction of ARGs was more at the thermophilic condition than in mesophilic condition, but generally, ZVI enhanced the reduction of ARGs by 33.3%. It was further noted that except sulII and tet(M), other ARGs may have been efficiently removed (Zhang et al. 2018). Both partial redundancy and network analysis among treatments showed that the concurrence of MRGs and microbial consortia led to the differing fate of ARGs (Zhang et al. 2018).

Akin to the ARGs, PPCPs are a varied group of chemical substances for human or animal use, such as drugs, fragrances, disinfectants and other household chemicals, their disposal poses threat to ecological safety and human health, hence necessitating proper treatment when found in sludges (Santos et al. 2010). Suanon et al. (2017) reported that during anaerobic digestion with iron-based additives, many PPCPs might be fully or partially reduced. The use of IP and NZVI positively influenced chlorinated PPCPs reduction (Suanon et al. 2017). Other PPCPs did not record significant PPCP removal. In conclusion, iron additives (IP and nZVI) application in sludge anaerobic digestion

process has low removal efficiencies or degradation of most PPCPs (Suanon et al. 2017).

2.6.6. pH, total alkalinity and H_2S

pH and total alkalinity are crucial indicators, hence the importance of monitoring their values to ensuring anaerobic digestion operational stability and maintenance of appropriate metabolic status. Maximum methane yield and bacteria growth during anaerobic digestion is attainable at the most favourable pH range of 6.8–7.2 (Ogejo et al. 2009). The anaerobic digestion enhancement alters the stability, affects microbial activities and pH/alkalinity (Lu et al. 2016). According to Mokete et al. (2020) and Eljamal et al. (2018), pH affects the availability of iron ions when nZVI is dissolved in an aqueous solution. During anaerobic digestion, Amen et al. (2017) reported that the addition of iron-based additives (ICZ, nZVI or IMZ) resulted in the final pH variation of between 5.81 and 7.32 from the initial pH of 6.2. The presence of zeolite, which acts as a proton donor/acceptor (amphoteric character) in the pristine iron, tend to keep the digester pH at the neutral range. Due to the slow degradation in the control bioreactor, lower final pH was recorded. At the hydrolysis and acidogenesis stages in digesters with iron additives, the solubilization of degradable organics to VFAs decreased the pH and subsequently increased the initial pH value due to the uptake of H^+ by nZVI cations through ion exchange/adsorption by zeolite pore structures (Eljamal et al. 2018; Amen et al. 2017).

Unlike in Amen et al. (2018), Suanon et al. (2017) showed that pH increased at the inception of the anaerobic digestion and later decreased (within 7.0) till the process termination, the highest pH values of 7.8, 7.6 and 8.5 respectively for control, nZVI and IP were observed. The sudden early rise in pH value of the digester supplemented with IP (1.6%) maybe as a result of Fe^0 hydrolysis in an anoxic condition (insufficient dissolved O_2) for iron oxidation (Mokete et al. 2020; Eljamal et al. 2018; Suanon et al. 2017). However, as shown in equation 3, water serves as iron oxidant (Chen et al. 2011; Elijama et al. 2018). It is noted worthy that following the formation of VFAs, the pH decreased, and the microbes adapted to better activity (Zhai et al. 2015).

$$Fe^0{}_{(s)} + 2H_2O_{(aq)} \rightarrow Fe^{2+}{}_{(aq)} + H_{2(g)} + 2OH^-{}_{(aq)} \qquad 2.13$$

ZVSI is both direct and indirect H^+ electron donor, leading to low H_2 concentration and favourable pH environment (Zhen et al. 2015). Different dosages of ZVSI gave varying pH values, Zhen et al. (2015) reported that due to the accumulation of VFAs, at 20^{o}C, an overall drop in the values of pH

lower than 6.0 in the entire digestion was observed. This continued in the first 3 days at 35ºC and afterwards, a pH rise was noticed, which increased from 6.3±0.1 to 7.3±0.1 as the ZVSI dosages increased from 0 to 1.0 g-ZVSI/g-VSS on the 30th day. These according to Zhen et al. (2015) shows the important ZVSI buffering capacity, which induces stability in the bioreactors and could prevent a decrease in pH values.

In a Fenton process, the pH of anaerobic digestion can be remarkably affected. In the analysis of OMSW degradation with Fenton process at varying pH values and 1.5 mM (Fe^{2+}) at 25ºC, the pretreatment at pH value of 3 gave the best waste digestion, which is in line with Michalska et al. (2012), where it was demonstrated that at pH of 3, the finest result of the Fenton process was achieved (Maamir et al. 2017). At neutral pH, substrate solubilization is often lower, due to $Fe(OH)_3$ precipitation, which prevents Fe^{3+} and H_2O_2 reaction. After the precipitation of $Fe(OH)_3$, the H_2O_2 breakdown to O_2 and water is facilitated, leading to oxidative capacity reduction, iron complexes (at pH greater than 8) and subsequent precipitation after $Fe(OH)_4$ formation (Maamir et al. 2017; Michalska et al. 2012). Uman et al. (2018) reported system stability and a neutral pH range for all reactors throughout the duration of anaerobic digestion of a Fenton process treated sludge.

The dynamics of total alkalinity (TA) changes during anaerobic digestion, shows the positive impacts of iron additives on VFA consumption (Amen et al. 2017). Similar alkalinity profile to that of pH was reported in Suanon et al. 2017, to have attained the highest level on the 7th day between 943.3 and 1234.0 mg L^{-1} $CaCO_3$ in the reactors (Control, nZVI and IP) and later decreased due to the yield as well as the buildup of VFAs. At the end of digestion, the slight rise may be attributed to the consumption of available VFAs (Ahn et al. 2010). As a result of rapid biomass degradation, the total alkalinity dramatically increased from the initial concentration of 494 mg/L $CaCO_3$ to 776, 1480, 1549, 2456 and 1721 mg L^{-1} $CaCO_3$ for control, nZVI, IMZ, ICZ 1000 and ICZ 500 respectively (Suanon et al. 2017). The increase in the total alkalinity of digesters was because of the use of VFAs by anaerobic microbes Suanon et al. (2017) and Ahn et al. (2010). In a Fenton process, Uman et al. (2018) reported that the alkalinity level of 2,530– 5,890 mg/L $CaCO_3$ was seen during the entire operating period of the bioreactors. Maamir et al. (2017) further reported that carbonates (CO_3^{2-}) and bicarbonates (HCO_3) ions presence in basic media might take-up the hydroxyl radical, thereby increasing the total alkalinity.

The iron-based additives influenced the removal of sulfur or H_2S from the sulfur-containing substrate

which could be converted to sulfide during anaerobic digestion processes (Zhang et al. 2016). Yu et al. (2015) reported the successful adoption of ferric chloride for the removal of H_2S from anaerobic digesters. Suanon et al. (2017) also demonstrated that the addition of nZVI and IP remove H_2S from reactors as shown $Fe^0 + H_2S \rightarrow FeS + H_2$, eliminating/reducing odour (mostly from H_2S) and stabilizing the substrate in the bioreactors and subsequent enhancement of microbial activities as well as stabilizing the rate of methane production (Li et al, 2007). Del Valle-Zermeno et al. (2015) reported that ash incorporated with iron was used for immobilization of adsorbed H_2S from a biogas stream.

2.6.7. Fate of iron-based additive in digestate

Among the different additives used in the remediation of the contaminated environment and anaerobic digestion, iron-based additives are the most frequently used. However, these iron additives remain in the digestates or sludges after the treatment, forming complexes that are hazardous to the environment (Peeters et al. 2016). The redox potential of iron additives is the core reaction mechanisms as it relates to enhancement of anaerobic digestion or removal of contaminants via ionization, corrosion, reductive changes, adsorption and co-precipitation (Peeters et al. 2016). According to Noubactep (2010), Eljamal et al. (2018) and Eljamal et al. (2020) the redox potential and pH value of iron additives are responsible for the stability of oxidized iron (eg. nZVI) to Fe^{2+}, then to Fe^{3+} on reacting with O_2, before being further hydrolyzed and precipitated respectively as FeOOH and $Fe(OH)_3$, in this manner, the nano characters of Fe NPs are lost. Jiang et al. (2015) and Hotze et al. (2010) stated that because of the passivation levels of oxides on the surfaces, the reactivities of nZVI is more than that of most iron additives like nano-FeO and nano-Fe_3O_4. In an anaerobic environment, ions of iron additives are ferrous (Zhang et al. 2014b).

In Maamir et al. (2017), it was indicated that during the Fenton process pretreatment, amorphous cellulose of OMSW, most probably transforms into less digestible cellulose crystalline by methanogens and Fe^{3+} forms complexes in the digestate. Suanon et al. (2016) researched the impact of nZVI and Fe_3O_4 on the fate of metals after the bio-digestion process and reported changes in speciation of heavy metals (Co, Cd, Cr, Zn and Ni), which were mostly bonded to initial biodegradable substances and carbonates. The application of 0.5% dose of iron nanoparticles, positively influenced the equilibrium of metals in the digestate than compared to digester without iron nanoparticles (Suanon et al. 2016). The addition of Fe NPs controls the deployment of metals when anaerobic digestion process takes place and concentrate metals in sludge around the bound fraction of Fe-Mn (Suanon et al. 2016).

As shown in Amen et al. (2017), the entire species of iron dissolved were in ferrous ion forms, but low iron dissolution was reported for the bio-digester supplemented with ICZ 1000 and zeolite respectively at 205.2 and 147.3 mg L^{-1}. In line with the quick reactivity views of Noubactep (2010), nZVI and IMZ reactors had high total iron concentrations, attributable to the large number of cellular parts containing iron being freed during the entire endogenous digestion. The nZVI reactor released the largest amount of total iron, greater than the total iron released by a combination of ICZ and IMZ bioreactors (Amen et al. 2017). Zhang et al. (2014b) demonstrated that the rusty scrap recorded high dissolution iron due to the microbial reduction of Fe(III), resulting in about 1116.6 mg L^{-1} of dissolved iron in the digestate after removing the remaining iron scraps. The amount of dissolved iron obtained in clean scrap is 949.9 mg L^{-1}, but the solid phased iron in sludge was higher than in the solution. The iron precipitate formation may be the reason for higher iron content in the solid digestate fraction.

As reported in Zheng et al. (2013), Zhang et al. (2014b) and Puyol et al. (2018), decomposition of the protein in the substrates produces phosphate, which upon reaction with ions Fe forms iron phosphate precipitates and may be responsible for the variation in phosphate concentration. In line with this, the experiments Elijama et al. (2020), Mokete et al. (2020) and Elijama et al. (2018) with nZVI and bimetal of nZVI at varying supplies of oxygen, pH, etc, corroborated the precipitation of phosphate mostly at limited oxygen supply. Phosphate concentrations in the liquid portion for control, rusty scrap and clean scrap respectively varied from 1.13 to 0.47 (58.3 %) and then 0.9 (19.96 %) g /L. It was recommended that since the amount clean and rusty scrap dissolved were 0.584 g/L/batch and 0.766 g/L/batch respectively after addition of 10g/L of WISs, the digestate would effectively be recycled for more batches of up to 228 and 376 days respectively for clean and rusty iron scraps if the retention remains 22 days for each batch. Similarly, Puyol et al. (2018) reported the ZVI corrosion has a strong influence on physicochemical properties bioreactor during the released of iron ions. As reported in Puyol et al. 2017 and Zhang et al. (2016), biogenic sulfide can be reduced by Fe^{2+} to pyrite (FeS_2) precipitate, phosphate and bicarbonate react with Fe^{2+} to yield vivianite ($Fe_3(PO_4)_2 \cdot 8H_2O$) and siderite ($FeCO_3$) precipitates respectively. In anaerobic digestion, ZVI ionized to Fe^{2+}, entrapped soluble phosphate to form vivianite precipitate, reducing phosphorus release and making its accumulation in sludge very difficult/costly to recover, hence constituting environmental menace (Puyol et al. 2018; Puyol et al. 2017). Suanon et al. (2016) reported that the addition of nZVI and nano-Fe_3O_4 could promote the phosphorus immobilization within the substrate. WIS facilitated the precipitation of phosphorus, sulfides etc. from sludges during anaerobic digestion (Zheng et al. 2013).

2.7. Phosphorus release

The indispensability of phosphorus (P) is due to its limited geographical concentration (with about 90% of the estimated world's phosphate rock deposit in Morocco, China, South Africa, Jordan and the U.S.), non-renewability and increasing demand for global food security via plant growth, animal growth and microbial regeneration (Guedes et al., 2017; Karunanithi et al., 2015; WERF, 2011). Aside scarcity, P rich liquid and solid wastes from man's activities pose serious environmental concerns leading to eutrophication (Podstawczyk et al., 2017; Wong, 2016). Bridging the P supply gap and its abundance in wastes necessitate efficient recovery and reuse of phosphorus (Desmidt et al., 2015). Recovery of P ensures environmental sustainability, biofertilizer availability, as well as food sufficiency, efficiency in waste treatment and management (Sikosana et al., 2016). However, inhibitions in P recovery processes due to the presence of organic or inorganic or nano constituents of waste streams demands an integrated approach for holistic recovery and reuse.

2.7.1. Phosphorus sources

The enormous amount of P rich waste streams such as animal excreta, urine, greywater, animal carcasses, crop residues, food waste, abattoir wastes, municipal wastewater, industrial effluents, biosolids, sludges and other wastes of animal and plant origin are being yearly produced (Karunanithi, et al., 2015; Kataki et al., 2016). Urine and faeces are the largest sources of phosphorus in municipalities and can be directly reused for agriculture. Averagely, urine and faeces excreted per person are estimated to 0.9 g-P/day and 0.4 g-P/day respectively (Wong, 2016). The total P concentration in municipal wastewater is typically 6−8 mg-P/L but can be higher depending on the source (Parsons and Smith, 2008). Human excreta have been widely researched and found to be contributing 60-70% (0.3 kg of P per year) and 30-40% (0.16kg of P per year) respectively for urine and faeces fractions in Uganda, China, South Africa, India, Sweden and Haiti (Wong, 2016).

The phosphorus concentration (P wt% dry basis) of some agro-industrial wastes include: Meat (1.09), cow dung (0.04-0.07), farmyard manure (0.07-0.88), bones (8.73-10.91), oil cake (0.39-1.27), activated sludge (1.4), digestates (0.48-0.77), animal urine (0.02-0.07), etc (Sikosana et al., 2016; Drosg et al., 2015). However, Campos (2014) in the studies of P recoverability from agricultural residues, pig, cow and poultry manure, found that after anaerobic digestion of these wastes, about 55-65% of P remains in the solid fraction, but with enzyme or acid or carbonate treatment over 80% of trapped P is recovered. Digestate of food wastes co-digested with greywater 92% of P was recovered

(Kjerstadius, et al., 2015)

The global population of livestock is estimated to be about 65 billion and generates a large amount of manure yearly (Campos, 2014). The yearly manure generated contains P of about 10 times the annual P demand for agriculture (Naidu et al., 2012). EU member nations in 2009 are estimated to have produced 1,285 million, 88.5 million and 153.2 million tonnes of manure respectively from chicken, cattle and pigs (FAOSTAT, 2013). In view of these data, Foged et al. (2011) calculated that about 1.382 billion tonnes per year of manure production in Europe, amounting to approximately 25.071million tonnes of P yearly.

However, effluents from agro-industries like fruits and beverages processing firms, dairy, piggery, animal washing, flushed feed spills, urine, liquid manure and others are great sources of P. For example, about 0.52million and 0.291million megaliter (ML) respectively of dairy and piggery effluent are produced in South Africa, containing aside other vital nutrients, about 18,729,000 tonnes of P from dairy and 4.233,000 tonnes of P from piggery annually (Karunanithi, et al., 2015).

Other sources of P include the nano-sludges/digestates, this is because of increase in industrial and consumer use of nano-enabled materials due to its novel properties on processes and products enhancement (Mayer et al., 2016; Romero-Guiza et al., 2016). The use, reuse and disposal increase nanoparticles (NPs) release to the waste stream (accumulated in biosolids) and environmental risks (Barton et al., 2015). Recently, NPs (Co, Ni, Fe, ZVI, Ce, Fe_3O_4, etc.) are used for anaerobic digestion or wastewater treatments, effluents and biosolids (digestates) from these processes are rich in nano-P precipitates, toxic to microbes and reduces soluble P for recovery (Otero-González, et al., 2014; Eduok et al., 2017). Digestate from other anaerobic processes contains available nutrients in the substrate matrix for easy P recovery. The amount of P recoverable from digestate of anaerobic processes depend on the digestion method and type of substrate (Campos, 2014).

2.7.2. Release of adsorbed and insoluble P

Inorganic P at an interaction with organic P in agro-industrial wastes may become insoluble as phosphate salt or due to adsorption by the biomass matrix (Campos, 2014). This necessitates the need for solubilization of both absorbed and insoluble P through various means including acidification (humic acid, arsenate buffer, citric acid, sulfuric acid, etc.), the addition of alkaline (sodium hydroxide, CaO, etc.) or carbonate ions (sodium carbonate, etc.). Aside from solubilizing P, chemical

processes aid in reducing ammonia and inactivation of pathogen risks. Thermal and pressure treatments are important for pasteurization and sterilization of pathogens as well as solubilization of insoluble P (Campos, 2014). Campos (2014) reported that at pH between 6 and 7, acid addition resulted in the release of over 90% of P in the mixed liquor. It was further advocated in accordance with DIN 38409-7 in Campos (2014), for mild acid usage due to the possible effects of strong acids (low pH and strong oxidizing influence) on enzymes operation.

Solubilization of P increases with the addition of carbonate at pH 9.2. The P concentration in solution increases by the addition of carbonate ions. This also causes Mg^{2+} and P ions to increase and Ca^{2+} to decrease in the mixed liquor. Likewise, alkaline (e.g. sodium hydroxide of >0.1% weight) addition increases the pH value needed for increased struvite precipitation (Campos, 2014). It was also observed that thermochemical treatment of substrates with heat, acids and carbonates can possibly increase P recoverability.

As stated earlier, existing technologies in P recovery are limited by the solubility of the inorganic P in liquid solutions. The solid-liquid separation of agro-industrial waste digestates leaves over 80% of P in the solid fraction (Campos, 2014). Unlike other macronutrients such as nitrogen and potassium which are more soluble in water. In harnessing insoluble P (organic or inorganic or absorbed in biomass matrix or nano-biosolids, metal-rich digestate) content, specific microorganisms with solubilizing potentials for different forms of phosphates is needed (Campos, 2014). Enzymes of phosphate solubilizing microorganisms (PSMs) like Pseudomonas, Bacillus, Rhizobium, Enterobacter Aspergillus and Penicillium transform P from insoluble to soluble forms via the acidification processes.

2.8 Influence of antagonist and iron on anaerobic digestion and phosphates availability

The use of iron additives for enhancement of anaerobic digestion process is a cheap means of increasing biodegradability of substrates and achieving increased biogas yield. However, when in excess, iron additives form non-biodegradable and non-environmentally friendly polyatomic complexes such as vivianite ($Fe_3(PO_4)_2$), strengite ($FePO4.2H_2O$), siderite ($FeCO_3$), pyrite (FeS_2), etc. with other dissolved nutrients in bioreactor during anaerobic digestion (Puyol et al. 2017; Peeters et al. 2016). Furthermore, iron ions have a great affinity for some phosphate, sulfate, carbonate as well as humic acid and arsenic compounds. According to Giasuddin et al. (2007), the presence of competing anions such as NO_3^-, SO_4^{2-}, $H_2PO_4^{2-}$, HCO_3^-, etc., $H_2PO_4^{2-}$ showed the most antagonistic

relationship with humic acid in competing for iron (NZVI) adsorption. In Wilfert et al. (2015) it was reported that humic substances (humic acids, humins, and fulvic acid), which contains carboxyl and hydroxyl groups have vital relevance in the chemistry of iron and phosphorus. Buttressing the antagonistic relationship, in a humic rich digested sludge, about 30% iron reacted with pyrophosphate and an estimated 22% bonding of iron to the humic rich organic matter in activated sludge (rich in P) (Wilfert et al. 2015; Karlsson and Persson, 2012). The capacity of HA to transfer or transport electrons to Fe has prompted the theory that anaerobic microbes, sulfate-reducing bacteria, or methanogens could reduce Fe (Piepenbrock et al., 2014). HA can be restored on exposure to oxygen after its behaviour as an electron acceptor (Klüpfel et al., 2014).

During the oxidation of organic compounds, HA can be used by iron-reducing bacteria as electron acceptors, hence increasing iron reduction and making available inaccessible iron oxides (Wilfert et al. 2015). There are various bonds with different strengths between iron and humic acids (HA), these variations determine the type of complexes formed and affect iron speciation. The formation of different Fe-HA species involves processes like iron hydrolysis, polymerization and binding of arsenic (of similar reactivity and structure like orthophosphate) (Karlsson and Persson, 2012). Similarly, the existence of HA-Fe binding of arsenic exists, hence the possibility of HA-Fe-P complexes too, but by chelating iron from Fe-P, humic acid can dissolve P (Wilfert et al. 2015; Karlsson and Persson, 2012). On the other hand, during anaerobic digestion, sulfate-reducing bacteria-induced sulfide inhibits Fe-P formation and releases Fe-bound P, however, due to limited sulfate availability in the digester, FeS formation does not prevent vivianite formation (Wilfert et al. 2015)

Furthermore, Lenoble et al. (2005), stated that in a system containing iron, arsenic (As(III) and As(V)) and phosphate, As(III) oxidation by iron (III) to iron (II) and due to the similarity is properties, phosphate is substituted by As(V), this is because the adsorption capacities of As(III) thermodynamically favoured the formation of Fe^{2+} and $HAsO_4^{2-}$, leaving $Fe^{3}+$ and PO_4^{3-} in solution and various precipitates (Fe2+ as $Fe_3(AsO_4)_2 \cdot 8H_2O(s)$, Fe^{3+} as $FeAsO_4 \cdot 2H_2O(s)$, etc) of As(V) as shown in Equations 2.14-2.16. These processes enable phosphate release for easy recovery.

$$H_3AsO_3^0 + 2H_2O \Leftrightarrow \mathrm{HAsO_4^{2-}} + 4H^+ + 2e^- \quad 2.14$$

$$3Fe^{2+} + 2\mathrm{HAsO_4^{2-}} \Leftrightarrow \mathrm{Fe_3(AsO_4)_2} + 2H^+ \quad 2.15$$

$$Fe^{3+} + \mathrm{HAsO_4^{2-}} \Leftrightarrow \mathrm{FeAsO_4} + H^+ \quad 2.16$$

Moreover, it was reported that the surface normalization rate constant of 2mg/L As(III) and As(V) was reduced from 100% to 43% and 68% respectively on the addition of 20mg/L HA (high concentration) (Giasuddin et al. 2007). However, the addition of 0.1mM of $H_2PO_4^{2-}$, HCO^{3-}, $H_4SiO_4^0$ did not affect HA adsorption on NZVI, but further addition of anions resulted in reduced HA adsorption on NZVI, for instance, only 20% HA adsorption was recorded on the addition of 1mM $H_2PO_4^{2-}$ and at 10mM, there was no adsorption (Giasuddin et al. 2007). Jeong (2017) concluded that increased HA addition led to reduced arsenic adsorption in this order As-Fe > (HA-As) + Fe > (HA-Fe) + As.

Although there had been lots of contradictory reports in previous studies, certainly the influences of both iron additive and P- antagonists (HA, As) on anaerobic digestion processes are substantial and deserves further probe. Arsenic compounds abound in several livestock wastes and wastewater treatment facilities, the same goes for humic substances. Several studies on the valorization of arsenic compounds and the influence of HA on anaerobic digestion exists. Yap et al. (2018) observed that HA addition below 5g/L did not decrease the hydrolysis rate of cellulose, but higher dosage inhibited hydrolysis. Hydrolysis of protein and acetotrophic methanogenesis was not affected by 5g/L HA addition, but a dosage of up to 10g/L and 20g/L HA respectively inhibited partially and completely the acetotrophic methanogenesis (Yap, 2018). Similarly, Liu et al. (2015) reported that HA improved solubilization of carbohydrate and protein sludge as well as the activities of hydrolysis enzymes but inhibited the activity of acetoclastic methanogens because of the competition for electrons resulting in low VFA conversion to methane and encouraged short-chain fatty acid production from sludge. On the contrary, Li et al. (2019b) showed that although HA addition improved promoted acidogenesis by 101.5%, both hydrolysis (38.2%) and methanogenesis (52.2%) were inhibited.

As it relates to the influence of arsenic compound on anaerobic digestion, Zhai et al. (2017), revealed that through PCR (qPCR) during anaerobic digestion, metabolism genes suitable for the valorization of arsenic were in abundance, hence the biotransformation of As from swine wastewater and total As reduction of up to 33 to 71%. Similarly, Banerjee (2010) reported that co-digestion of liquid market waste, liquid water hyacinth and primary sludge containing As and 99.69% of As was removed within 50 days digestion period. This maximum reduction indicates that with adequate As dosage and properly acclimatized feedstock may not inhibit anaerobic digestion process significantly (Banerjee, 2010).

In conclusion, according to Azman et al. (2015) and Wilfert et al. (2015), ICP-AES revealed the binding ability of chelating and antagonistic substances, hence the mitigation capability of iron addition on HA and As ultimately results in phosphate release. However, the optimum combination of iron additives (accelerant) and P-antagonists (HA and As), will enhance anaerobic digestion as well as achieve P release, which is the focus of this study.

2.9 Summary

The literature review has revealed the current global energy status, demand-gap and the corresponding population rise and the need to energy recovery from alternative energy sources like anaerobic digestion. There abounds waste, energy crop sources and emerging substrate types for anaerobic digestion, but most of them need some form of enhancement to achieve maximum energy recovery. Process enhancement, which includes substrate pretreatment, co-digestion and additive supplementation, can aid biodegradability, provide deficient nutrient for microorganisms, destroy pathogens, increase methane quantity among others. Previous studies state that iron-based additives are a cheap and effective additive type widely used for anaerobic digestion enhancement. Although iron-based additives improve biogas yield and other anaerobic digestion activities. They react when in ionic forms with other soluble nutrients, resulting in the formation of complex non-biodegradable substance and low soluble P-availability in the digestate. However, research gaps in achieving both optimum biogas yield and phosphate release were found. Although varying influences of these additives had been studied individually with contradictory results. The dosage optimization and simultaneous supplementation of these chelating substances and antagonists seem to hold some potentials in achieving the identified research gap.

Chapter Three

Characterization and Ranking of Agro-industrial Wastes Based on Their Energy and Phosphorus Potentials

This chapter is adapted from: Ugwu, S. N., and Enweremadu, C. C. (2020). Ranking of energy potentials of agro-industrial wastes: Bioconversion and thermo-conversion approach. Energy Reports, 6, 2794-2802.

3.1 Introduction

Over the last two decades, the population of the world has incrementally risen by about 1.5 billion people (Ashraf et al. 2019; World Bank, 2015). This continuous population rise has widened the energy demand-supply gap and hastened the depletion of non-renewable resources like phosphorus (P), leaving over 1.2 billion without access to conventional energy and threatening the continuous P availability globally (Leng et al. 2019; World Bank, 2015). This energy-gap is predominantly satisfied with energy from fossil sources (Natural gas, oil and coal), which its usage rose by about 2.2% in 2017 and is expected to reach 49% by 2035 (Ashraf et al. 2019; BP, 2018; Nhuchhen and Abdul Salam, 2012). According to BP (2018) and Energy Information Administration (2010), the reliance on these fossil fuel sources for about 87% of the global energy need amounted to 1.6% rise in carbon release in two years and is projected to reach 42.4 billion tons in 2035. Amidst the projected extinction of global oil reserves in the next 52 years, the remarkable growth of 17% in renewable energy utilization if improved upon continuously, will reduce the current energy crisis and curb environmental degradation occasioned by the use of fossil fuels (BP, 2018; Nhuchhen and Abdul-Salam, 2012).

The widening energy insecurity and environmental concerns favour the need for alternative energy sources and attainment of energy mix diversification (Ashraf et al. 2019). The worldwide annual potential of biomass-based energy resources is about 56 EJ and has the highest chance of reducing the reliance on fossil energy sources (Hiloidhari et al. 2014). According to Fox and Fimeche (2013), about 30 to 50% of global food production are lost through postharvest operations. However, about 27 to 52kg/d of cattle manure with P potentials of between 8.4 to 64.2g/d can be generated per animal, in the United States with about 89.3million cattle, an estimated 1.17 billion Mg of manure are generated (Pagliari et al. 2020). Similarly, other livestock generates an appreciable amount of manure and P but varies from each other based on their breeds, diets, body sizes, performances and other variables (Pagliari et al. 2020). Moreover, the biomass-based energy with a capacity of zero net balanced CO_2 emissions and low carbon footprint, exists plentifully at cheaper prices, mostly

generated across the agro-processing value chain and can be combusted, pyrolyzed, fermented, gasified or anaerobically digested to form a liquid, solid or gaseous energy sources (Ashraf et al., 2019; Gao et al., 2018; Hiloidhari et al. 2014). This biomass for bioenergy and residues from energy generation are sources for P and could be applied directly to the land, composted or treated for P recovery (Leng et al. 2019).

In South Africa, one-third of the 31 million tonnes of food produced per annum are lost as food wastes. Of this number, only 10% are currently recycled (StatsSA, 2018). It is estimated that a large amount of agro-industrial waste (from livestock, meat processing, crop processing, among others.) is generated annually with combined energy generation potential of 2.800 GWh per annum when digested anaerobically (ARC, 2016). Currently, most of these agro-based wastes and other biodegradable wastes are either burnt or disposed of in the landfills, emitting ozone-depleting substances like methane and CO_2 (Browne and Murphy, 2013). South Africa is one of the top 15 globally in CO_2 emission. This is because about 90% of her energy supply is of fossil origin (mainly coal) (DoE, 2016; CSIR,2016). Ashraf et al. (2019) suggested that retrofit solution of partially substituting coal with biomass/organic wastes could reduce the emission of greenhouse gases.

Anaerobic digestion and controlled thermal degradation of these biomasses/organic wastes for energy recovery is a strategic way of averting the unsafe disposal (incineration or landfills). Renewable energy production from anaerobic digestion of biomass is a sustainable means of waste reuse. It is an efficient means of converting waste biomass to biomethane and nutrient-rich digestate (Cai et al. 2019; Ugwu and Enweremadu, 2019; Browne and Murphy, 2013). Biochemical methane potential (BMP) test which is divided into experimental and theoretical BMP (TBMP), is a method for assessing the maximum upper range of methane yield from biodegradable biomass; it provides an index for biodegradability and baseline for optimizing methane production (Angelidaki et al. 2009). Estimates from BMP of substrates are also used in the economic and technical feasibility studies prior to construction of anaerobic digesters and determination of other operational requirements (Holliger et al. 2016). BMP is expressed in mL CH_4 at STP per amount of organic component added or removed (VS or COD basis).

The experimental BMP has a harmonized standardized protocol of determination and it is dependent on inoculum sources, quality and preparation; substrate types, preparation and storage; inoculum to substrate ratio (with crucial influence on the kinetics), test setup, etc. (Holliger et al. 2016; Strömberg

et al. 2014). However, the TBMP is a quick method of determining the BMP of substrates through the estimation of elemental compositions (C, H, O, N, S) using Buswell/Boyle's equation, organic fraction compositions (lipids, proteins, and carbohydrates) or Chemical Oxygen Demand (COD), etc. (Raposo et al. 2011). The experimental BMP often has lower yield values than the TBMP. Both the experimental and the theoretical BMPs are used to calculate the biodegradability based on biomethane yield (BD_{CH4} %= Experimental BMP/TBMP *100).

Unlike in biochemical conversion, which involves slow degradation of substrates during anaerobic digestion into minute molecules with minimal energy, the thermal conversion is an energy-demanding and destructive means of recovering energy from biomass (Shi et al. 2016). The thermal conversion involves the determination of the biomass heating/calorific values and processes like dehydration, deoxygenation and dihydroxylation (Chen et al. 2017). The heating values of biomass are fundamental in selecting the biomass for energy generation and evaluating its potential for economic viability (Akhtar et al. 2019). However, biomass calorific values are determined through computational models or direct measurements (Shi et al. 2016). According to Hosokai et al. (2016), there are many computational models for evaluation biomass calorific values, but the Dulong and modified Dulong are mostly used based on their precision and adaptability.

Adequate information on the properties of biomass aids the prediction of its thermal processes and environmental impacts (Braz and Crnkovic, 2014). Biomass is thermochemically transformed at a temperature range between 200 and 320^{o}C into more dense, hydrophobic solid fuel in a process called torrefaction. Its product serves as a great renewable fuel source for both off-grid power and heat application (Gent et al. 2017). Similarly, a complex thermochemical process which in the absence of oxygen and a temperature greater than 250^{o}C facilitates the volatile compounds release, liquid formation (bio-oil), and high energy-dense biochar with higher calorific value is known as pyrolysis (Shi et al. 2016). These thermal decomposition techniques of biomass or associated materials are referred to as thermal analysis or thermogravimetry, it reveals the behaviours of biomass during thermal decomposition and exhibits multiple steps with varying activation energies (Ashraf et al. 2019). According to Braz and Crnkovic (2014), the knowledge of biomass thermogravimetry provides valid insights into the complex reactions throughout the entire thermochemical conversion (torrefaction, pyrolysis, etc.). However, aside from the beneficial products of the thermal conversion process, an enormous amount of nutrient-rich wastes (Leng et al. 2019).

These agro-industrial wastes and wastes from energy recovery processes (digestates, ashes, chars, etc.) are rich in phosphorus and if not properly characterized and managed before disposal, they constitute serious environmental menace (Li et al. 2020; Pagliari et al. 2020). Phosphorus is an essential, but limited element for plant, animal growth and biochemical reactions (Li et al. 2020). It is originally obtained from phosphate-bearing rock and is estimated to depleted in the next few years and not evenly distributed (71% in Morocco and Western Sahara) (Leng et al. 2019; USGS, 2019). However, organic matters of plant and animal origin are nutrient resource banks, mainly phosphorus, potassium and nitrogen (Li et al. 2020). Similarly, since the quantity of P content of these wastes is not known, they are excessively applied on lands for agricultural purposes leading to P buildup hence the adverse environmental impacts like surface water eutrophication and groundwater contamination via P-leaching (Pagliari et al 2020; Komiyama and Ito 2019). Waste types and sources, handling, storage and treatments (physical, chemical and biological and composting) affect P contents and bioavailability. According to (Komiyama and Ito 2019), the characterization of P content is essential for both agricultural and environmental management purposes. As reported in Komiyama and Ito (2019) and Leng et al. (2019), determination of phosphorus composition in waste streams help in the design and selection of appropriate technologies for precise usage or recovery, hence this study.

In this study eighteen identified waste biomasses from South African agro-processes were characterized based on their elemental compositions and solid compositions, both the theoretical and experimental biomethane potential of biomass via biochemical conversion, the calorific values, the thermal degradability (at torrefaction and pyrolysis stages) of these biomasses were also determined. Based on the results of all the characterizations and analyses, the biomasses were ranked on their energy generation capabilities and phosphorus recovery potentials.

3.2 Materials and methods

The eighteen (18) biomasses of both plant and animal origin were selected based on their availability and waste generation capacity *(*Ogejo, et al., 2010; StatsSA, 2018; FAOSTAT, 2017; ARC, 2016). They were sampled from different areas of Gauteng Province, South Africa as shown in Table 3.1. About 0.5 kg of each waste sample were collected and divided into portions for biomethane potential test (BMP), chemical analysis, proximate and ultimate analysis and the last portion were used for thermogravimetry studies. The inoculum was collected from an active anaerobic digester at the Department of Mechanical Engineering, University of Johannesburg. All samples were dried, ground and sealed or stored in a 4^{o}C cold room before use.

Table 3. 1 Biomasses parts used and their sources

S/N	Substrates	Used parts	Source	Waste generation Capacity in South Africa
1	Egg	Shells and spoilt content	ARC, Irene	155750 Mg/a
2	Chicken	Droppings	ARC, Irene	2 853751 Mg/a Solid manure 289140 Mg/a Slaughterhouse
3	Fish	Fish processing wastes	Fresh Produce Market, Johannesburg	62400 Mg/a
4	Avocado	Seed, Mesocarps and pomace	Fresh Produce Market, Johannesburg	34562 Mg/a
5	Cow	Dung	ARC, Irene	259894 Mg/a (Slaughterhouse) 1764000 Mg/a (Solid manure) 10238743 Mg/a liquid manure (Diary)
6	Pumpkin	Spoilt whole part and peelings, seeds	Fresh Produce Market, Johannesburg	130189.80 Mg/a
7	Okra	Pods and stalks	Organic Farm Centurion	*2892385 Mg/a
8	Potatoes	Peelings	Fresh Produce Market, Johannesburg	906700.20 Mg/a
9	Pineapple	Peelings and pomace	Fresh Produce Market, Johannesburg	74272 Mg/a – Pomace
10	Pig	Dung	ARC, Irene	1 368 946 Mg/a (Solid manure) 45019 Mg/a (Slaughterhouse)
11	Goat	Dung	ARC, Irene	735475 Mg/a
12	Sheep	Dung	ARC, Irene	15137280 Mg/a
13	Carrot	Pomace and peelings	Fresh Produce Market, Johannesburg	103715.80 Mg/a
14	Grapefruit	Peelings and pomace	Fresh Produce Market, Johannesburg	187724 Mg/a
15	Garlic	Dried bulbs and stalks	Organic Farm, Centurion	900 Mg/a
16	Chilis	Leaves and spoilt fruit	UNISA Greenhouse, Florida	6743.25 Mg/a
17	Meat	Beef fat (processing)	Abattoir, Bronkhorstspruit	36593 Mg/a
18	Peanut	Spoilt nuts and chaffs	Black Cat Peanut Butter, Johannesburg	53389 Mg/a

ARC: Agricultural Research Council, UNISA: University of South Africa, * = Global data, (FAOSTAT, 2017, StatsSA, 2018, Ogejo et al. 2010*)*

Portions of the ground biomass samples in triplicates were subjected to proximate analysis as described in Akhtar et al. (2019) for ash, volatile matter (VM) and moisture content determination. The percentage composition of the fixed carbon (FC) was calculated from the balance difference as shown below.

$$FC\ \% = 100 - (Ash\ \% + VM\ \%) \quad [3.1]$$

Prior to the BMP test, total solids and the volatile solids of both the inoculum and substrates were determined using the APHA standard methods (Barbeau et al. 2014). The Thermo scientific Flash

2000 Organic Elemental Analyzer was used for ultimate (CHNS) analysis of the biomass samples. The Analyzer with oxygen combusting at 250 ml/min and helium as carrier gas flowing at 140 ml/min, had its maximum temperature set at 950^{o}C and retention time of 610 sec. The oxygen content of the substrates was determined thus based on VS %: C+H+N+S+ Ash = 99.5 (Rincón et al. 2012).

Thermogravimetric analysis (TGA) of the biomass samples were conducted as described in Shi et al. (2016) with PerkinElmer Pyris 1 TGA. The TGA operated from switching gas to Nitrogen at a flow rate of 20.0 ml/min. The weight of the samples kept in the ceramic crucibles was between 10.37 and 13.92 mg. The system was configured to hold temperature at 105.0°C for 30.0 min, then the heat of the chamber rose from 105.0°C to 800.0°C at 10.0°C/min. This heating rate was used to understand the thermal degradation pattern at both the torrefaction and pyrolysis stages.

With the aid of the AMPTS II BMP Assay (Bioprocess Control, Sweden) and its standard procedures, the BMP of the eighteen substrates listed in Table 3.1 were performed in triplicate and at mesophilic temperature (37±1^{o}C) for 30 days. The batch processes were carried out with 500 mL capacity reaction bottles, each reactor was filled to 400 mL of the total volume with inoculum and substrate at inoculum to substrate ratio (ISR) 2:1). Nitrogen gas (Afrox gas, South Africa) was used to flush out oxygen from the reactors. The results from the data logging platform of the reactors were retrieved and processed.

The chemical compositions some anion determination, samples were dried, ground, mixed with 0.035M of carbonate/bicarbonate buffer extraction for 2hours, centrifuged and filtered with 0.45 µm x 28mm syringe filters membranes (Glassworld, South Africa). The filtrates were injected in triplicates via automatic sampler into intelligent Metrohm ion chromatograph 882 Compact IC plus 1 – Anion (Herisau, Switzerland) equipped with a conductivity detector and Metrohm suppressor module (MSM) was used for the chromatographic determination of anions via automatic integration. The separation was carried out on a Metrosep A Supp 5 (150 /4 mm) anion exchange column. Briefly, 50 mmol L^{-1} of sulfuric acid (H_2SO_4) was used for continuous regeneration of the suppressor. A mixture of 1.0mMol $NaHCO_3$ + 3.0mMol Na_2CO_3 was used as eluent, the flow rate of 0.7 mL/min while the total run time was 17 minutes. Multi-anionic standard solution (PerkinElmer, USA) containing the target anions (Fluoride, Bromide, Chloride, Nitrate, Phosphate and Sulfate) with a stock concentration of 100 mg L^{-1} was used to prepare calibration curve in the range of 0.16 to 100 mg L^{-1}. After the analysis, MagIC Net 2.3 (Metrohm) software was used for data acquisition and

data analysis.

25mg of organic wastes were digested with digestion reagent (4M HNO_3 + 1M H_2O_2) in a microwave-assisted oven for total digestion time 50minutes (20mins for heating and 30mins for cooling) and maximum temperature of 180ºC. The digested sample for chemical compositional analysis was filtered with 0.45 µm x 28mm syringe filters membranes (Glassworld, South Africa). A total of eight analytes (P, K, Ca, Mg, Fe, Zn, Na and As) were determined by directly introducing samples into the Inductively Coupled Plasma Mass Spectrometry (ICP-MS) (NeXION 350D, PerkinElmer, USA) in triplicates. Analytes were determined under the following conditions: Cyclonic spray chamber, RF power of 1400 kW, 1.2 L/min auxiliary gas flow rate, 15.5 L/min plasma gas flow rate, 6 mL/min sample uptake and 50 ms dwell time. Standard solution for PerkinElmer NeXION set up containing many cations was used for checking standard performance. 1 mg/L of P standard solution was prepared from KH_2PO_4 in 1% HNO_3 and combined with the other standard solution. The masses used for analyzing the analytes were P (31), K(39), Ca(43), Mg(24), Fe(57), Zn(66), Na(23) and As(75) atomic mass unit. Using 1% HNO_3, the multi-element standard solution (PerkinElmer, USA) was serially diluted from 0.1mg/L to 1mg/L, were later used to obtain the calibration curve for quantification. ICP-MS Syngistix software was used for acquisition and analysis of data.

Theoretical biomethane potential (TBMP) of each substrate was calculated based on their elemental composition using Buswell's Equation (Buswell and Mueller, 1952; Browne and Murphy, 2013). The TBMPs and biodegradability were also calculated as shown in Equations 2 to 4.

$$C_nH_aO_bN_c + \left(n - \frac{a}{4} - \frac{b}{2} + \frac{3c}{4}\right)H_2O \rightarrow \left(\frac{n}{2} + \frac{a}{8} - \frac{b}{4} - \frac{3c}{8}\right)CH_4 + \left(\frac{n}{2} - \frac{a}{8} + \frac{b}{4} + \frac{3c}{8}\right)CO_2 + cNH_3 \quad [3.2]$$

$$TBMP = \frac{22400\left(\frac{n}{2}+\frac{a}{8}-\frac{b}{4}-\frac{3c}{8}\right)}{12n+a+16b+14c} \quad [3.3]$$

$$BD_{CH_4} = \frac{BMP}{TBMP} * 100 \quad [3.4]$$

Where Methane Energy content = 37.78 MJ/m^3 at STP

C, H, O, N, S = Carbon, Hydrogen, Oxygen, Nitrogen, Sulfur (VS %)

TBMP = Theoretical biomethane potential at STP $\left(\frac{mLCH_4}{gVS}\right)$

BD_{CH4} = Anaerobic biodegradability (%)

According to Archinas and Euverink (2016), TBMP assumes that microbial condition is ideal, that all substrates were used-up, complete mixing and that constant temperature; substrate compositions are restricted to only C, H, O, N, S and CH_4, CO_2, NH_3 as its output.

The efficacy of fuels is not only dependent on proximate and ultimate analysis but also the atomic ratios (Sing et al., 2017). These atomic ratios as reported in Chen et al. (1986) and Basu, (2010) include the effective hydrogen to carbon molar ratio, hydrogen to carbon and oxygen to carbon ratio which is determined using equation 5 and 6. The calorific values (High heating values (HHVs)) of the biomass samples were calculated with the elemental composition using modified Dulong's equation for HHV estimation (equation 7) as stated in Shi et al. (2016), Akhtar et al., (2019) Browne and Murphy (2013).

$$H/C_{eff} = (H - 2O)/C \quad [3.5]$$

$$H/C = 1.4125(O/C) + 0.5004 \quad [3.6]$$

$$HHV\left(\frac{kJ}{kg}\right) = 337[C] + 1419[H] - 0.125[O] + 93[S] + 23[N] \quad [3.7]$$

Where H/C_{eff} = Effective hydrogen to carbon molar ratio

O/C = Oxygen-to-carbon molar ratio

H/C = Hydrogen-to-carbon molar ratio

HHV = Higher heating value (kJ/kg)

The BMP results of the eighteen substrates were predicted with both first-order kinetic and modified Gompertz models in this study. The first-order kinetic model assesses the biomethane production kinetics, while the modified Gompertz model is based on the view that the biogas production rate corresponds to the rate of methanogenic bacterial growth rate during anaerobic digestion processes (Ugwu and Enweremadu, 2019; Cai et al. 2019). Both models are stated below as equations 8 and 9.

$$Y = ym(1 - \exp(-kt)) \quad [3.8]$$

$$Y = ym.exp\left\{-\exp\left[\frac{R_{max}.e}{ym}(\lambda - t)\right] + 1\right\} \quad [3.9]$$

Where:

- Y is the accumulated bio-methane at the time t, mL/g VS
- ym is the potential methane production, mL/g VS,
- k is the methane production rate constant (day^{-1})
- R_{max} is maximum methane production rate, mL/g VS·day
- λ is lag-phase, day (d)
- t is measured digestion time, day and e, exp (1) =2.718282.

All the data used in this study were processed, curve-fitted and graphs plotted with Origin 9 Pro, MATLAB R2015b, PAST 3.26 and Microsoft Excel software.

3.3 Results and discussions

3.3.1 Characterization of chemical compositions

The choice of reuse, recycling and treatment for disposal are largely dependent on waste characteristics. The chemical characteristics analysis of 18 agro-industrial wastes were conducted as described above to determine three soluble anions (orthophosphate (o-P), N and S), Total P and seven cations (K, Na, Ca, Mg, Fe, As and Zn). From the results obtained, variations in the chemical compositions of all substrates were observed as presented in Table 3.2. From the soluble analysis, pig and peanut wastes had the highest orthophosphate, the highest nitrate content was observed in both pumpkin waste and potato peels, sulfate contents of pineapple and meat wastes were higher than others. However, based on the total chemical analysis, it was revealed that wastes derived from animal remains and manures had higher chemical compositions (especially P and cations), this observation was consistent with the studies of Haroon et al. (2018). Total P (1007.64mg/kg) and o-P (167mg/kg) in pig manure were very high, this agrees with the report in Campos et al. (2014), that pig manure contains a high amount of P and is suitable for P recovery.

Table 3. 2 Chemical characteristics of different types of agro-industrial wastes

Substrates	Phosphate (mg/kg)	Total P (mg/kg)	N (mg/kg)	S (mg/kg)	K (mg/kg)	Ca (mg/kg)	Mg (mg/kg)	Fe (mg/kg)	Zn (mg/kg)	Na (mg/kg)	As (mg/kg)
Egg	47.45	97.01	4.50	17.02	44.54	88606.86	1623.47	26.76	0.19	156.17	40.83
Chicken	8.52	394.65	4.98	7.88	575.09	7584.07	5093.50	1224.43	78.84	389.36	6.17
Fish	13.65	2309.25	5.04	17.74	354.80	23194.40	2199.42	477.86	64.24	831.31	15.72
avocado	16.62	69.05	6.28	8.12	535.07	118.20	657.34	51.30	6.30	14.95	0.44
Cow	44.44	260.51	4.04	2.04	248.13	2475.47	3325.26	974.32	80.85	137.55	2.06

Pumpkin	9.61	262.58	13.09	26.36	1504.87	837.91	2931.28	136.54	20.82	182.09	0.36
Okra	54.53	213.08	6.57	13.77	765.15	3144.28	5445.05	95.30	17.95	59.52	2.08
Potato	22.45	148.96	13.69	11.76	1270.50	261.96	1040.67	323.92	6.87	41.50	0.21
Pineapple	8.70	78.51	10.76	36.04	1484.64	418.37	1186.81	183.33	2.76	15.10	0.05
Pig	167.36	1007.64	4.04	2.70	860.24	5667.70	5352.22	1774.41	251.12	220.86	4.62
Goat	4.67	224.82	3.15	26.55	459.23	6144.41	4968.31	1509.25	30.23	354.42	4.68
Sheep	2.82	787.24	3.38	33.93	631.44	8432.20	6576.77	2880.17	181.24	684.39	7.98
Carrot	44.51	157.28	7.61	3.84	1574.00	4568.31	1126.49	167.35	10.00	461.85	2.77
Grape	1.28	55.69	5.04	17.74	537.16	1242.46	568.64	8.53	1.64	19.89	0.36
Garlic	2.82	124.68	3.38	33.93	1139.45	3122.88	1847.59	4133.68	14.05	65.47	4.12
Chilis	11.60	218.12	2.50	11.76	1358.31	613.88	1567.06	156.29	15.64	8.21	0.09
Meat	74.53	109.10	3.63	35.14	104.70	48.04	138.84	59.99	7.17	162.36	0.66
Peanut	140.28	203.28	3.99	16.47	562.78	228.86	1502.48	125.13	10.81	0	0.12

3.3.2 Characterization results

The ultimate and proximate properties of all the biomass samples studied are displayed in Tables 3.3 and 3.4. From the results, low TS % and VS % (wet basis) was observed in biomasses of fruit and vegetable origin with chilis having the lowest TS % and VS % respectively at 7.03 % and 6.51 %, while oil-bearing biomasses like peanut having the highest TS % (97.6 %) and VS % of (91.7 %). Except for egg waste, high biomass VS % (dry basis (VS/TS)) were recorded in all the samples with the highest value of 95.6 % from peanut, indicating the high availability of organic matter and energy content, which according to Zhao et al. (2016) and Li et al. (2013) are essential for anaerobic digestion and energy recovery process.

Among the evaluated biomasses, meat waste with higher carbon content (70.95 %), had higher heating value (36.64 MJ/kg). This is in line with the view of Braz and Crnkovic (2014) that biomass with high carbon content has high heating values. The high nitrogen contents observed in fish, chicken, and egg wastes resulted in the noticed lower C/N ratios. These values are below the recommend optimum C/N range of between 15 and 30 % for higher biomethane yields, hence the need for co-digestion with carbon-rich substrates (Li et al., 2013). The ash contents of fourteen biomass samples were below the 8 % recommended in Shi et al. (2016) as being beneficial in enhancing combustion facility operation and reducing energy consumption in transportation. The egg had the highest ash content of 62 %. The garlic and egg wastes had the highest fixed carbon content among biomasses with the potential of generating more solids during the thermal degradation process.

Table 3. 3 Proximate and Ultimate values of Biomasses

Substrates	N	C	O	H	S	Ash content	C/N	TS %	VM %	FC %
Egg	3.03	23.49	7.65	2.311	1.02	62.50	7.75	58.76	18.90	18.60
Chicken	3.94	37.16	45.01	4.81	0.96	8.13	9.44	28.60	77.90	13.97
Fish	7.41	44.42	28.67	7.90	1.25	10.35	5.99	34.21	75.56	14.09
Avocado	1.26	47.41	44.04	6.28	0.00	1.01	37.61	35.95	97.78	1.21
Cow	1.98	44.11	45.63	5.53	0.00	2.76	22.31	18.80	88.27	14.49
Pumpkin	3.50	48.85	39.33	6.67	0.00	1.65	13.95	16.71	92.32	6.03
Okra	3.21	45.30	45.94	5.39	0.00	1.17	14.13	7.82	88.36	10.47
Potatoes	2.15	42.20	48.05	5.84	0.00	1.76	19.64	17.99	93.39	4.85
Pineapple	1.08	41.88	50.23	5.43	0.00	1.40	38.93	13.48	92.29	6.31
Pig	1.97	40.39	45.53	5.29	0.00	6.82	20.54	31.56	81.54	11.63
Goat	2.15	45.75	33.56	5.50	0.87	12.18	21.26	37.43	87.10	0.72
Sheep	1.99	43.80	40.47	5.33	0.85	7.56	22.07	51.90	87.70	4.74
Carrot	2.17	42.45	47.63	5.55	0.00	2.19	19.57	9.88	81.86	15.95
Grape	2.15	41.99	49.42	5.49	0.00	0.95	19.57	15.84	94.82	4.23
Garlic	1.08	42.96	37.40	5.49	0.88	12.20	39.82	28.97	67.64	20.17
Chilis	2.31	33.32	59.50	4.23	0.00	0.65	14.43	7.03	92.61	6.74
Meat	0.70	70.95	16.90	11.01	0.00	0.44	101.69	75.52	99.50	0.06
Peanut	3.30	59.27	22.39	8.18	0.00	6.86	17.96	97.56	93.95	0.81

Among other things, classification based on the C, H, O atomic ratios (O/C and H/C) as estimated with Equation 6 is vital for understanding the heating values of substrates as fuels (Sing et al., 2017). It is also a yardstick for determining gasification process efficiency (Yadav and Jagadevan, 2014). The higher O/C ratio resulted in lower HHV as seen in Table 3.4, Chilis waste samples with high O/C ratio of 1.35 showed the lowest HHV value of 6.82 MJ/kg. Similarly, meat waste with low O/C ratios 0.11 to recorded high energy density and HHV of 36.64 MJ/kg. This trend was akin to the report of Basu (2010), which showed that HHV reduced from 38 MJ/kg to 15 MJ/kg as the O/C increased from 0.1 to 0.7. However, most of the substrates in this study were within the Van Krevelen's diagram recommended biomass H/C (1.26 – 1.58) and O/C (0.4 – 0.8) ranges. These values are higher than those of coal (Quan and Gao, 2016). The H/C ratios observe similar trends as O/C among all the substrates studied. The predominantly low heating values of biomasses in this study is attributed to the high oxygen contents, which does not enhance combustion, but adversely affect biomass conversion to liquid fuel (Basu, 2010; Shi et al., 2016). However, high H/C results in low effective heating value, leading to release of more energy at the oxidation reaction, but in the presence of high O and H content, the H/C does not translate to high HHV (Braz and Crnkovic, 2014). This is because high oxygen consumes available hydrogen in biomass to yield water, which is not beneficial in the thermo-conversion process (Basu, 2010).

$H/C_{eff,}$ ratio estimates the economic viability and possibility of biomass conversion into hydrocarbons. The $H/C_{eff,}$ ratios in Table 3.4 as calculated with Equation 5 ranged between 1.15179 and -2.59471. Except for biomasses with rich oil contents, egg waste and highly fibrous pineapple waste, the H/C_{eff} of all other biomasses were within the limit of ≤ 0.5 as suggested in Basu (2013). The negative ratios as seen in most of the fruits and vegetable (moisture-laden wastes) suggest insufficiency of biomass hydrogen content for oxygen removal, hence achievement of high-quality fuel will necessitate the addition hydrogen or deoxygenation during torrefaction (Shi et al., 2016). Similarly, Chen et al. (1986) stated that substrate with less than 1.0 H/C_{eff} ratio is very difficult to upgrade the hydrogen-deficient feedstocks for premium product yields, hence most of the substrates are either co-pyrolyzed with coal or better suited for other forms of bioenergy conversion.

The heating value of a fuel is the amount of energy released per unit mass of such fuel when completely combusted (Sing et al., 2017). The suitability of the biomass sample for energy generation is dependent on its heating values and viability economically (Akhtar et al., 2019). In Table 3.4, the heating values (HHV and HHV based on VS %) are shown for all the biomass samples, HHVs are the gross heating values and in this study, it ranged between 6.815 (chilis) and 36.64 MJ/Kg (meat/fat) and based on VS %, the egg waste had the lowest HHV of 1.91 MJ/KgVS. The low calorific value based on VS % is attributable to the high solid content (ash % and FC %), which may affect the ease of operation (Shi et al., 2016). It could be deduced that the wastes from the animal carcass and oil-bearing crop had the highest HHVs and lower output of solid content after thermal processes, thus enabling the reduced cost of operation.

Table 3. 4 Summary of Energy Content, BMP and TBMP Parameters.

Biomass	**HHV (MJ/Kg)**	**HHV based on VS % (**MJ/kgVS)	**BMP** (mL/gVS)	**TBMP** ($mLCH_4$/ gVS)	**B_{CH4} %**	**Substrate Formula**	**H/Ceff ratio**	**O/C**	**H/C**
Egg	10.09	1.91	477.30	630.48	75.70	$C_{61.4}H_{72}O_{15}N_{6.8}S_1$	0.68	1.24	1.17
Chicken	11.63	9.06	281.10	323.47	86.90	$C_{103.7}H_{159.8}O_{94.3}N_{6.8}S_1$	-0.28	0.91	1.54
Fish	15.20	11.48	532.03	542.82	98.01	$C_{95}H_{201.5}O_{46.04}N_{13.6}S_1$	1.15	0.49	2.12
Avocado	17.19	16.81	302.23	459.27	65.81	$C_{43.9}H_{69.2}O_{30.6}N_1$	0.18	0.70	1.58
Cow	14.75	13.02	176.28	404.28	43.60	$C_{26}H_{38.8}O_{20.2}N_1$	-0.06	0.78	1.49
Pumpkin	19.12	17.65	320.32	490.09	65.37	$C_{16.3}H_{26.5}O_{9.8}N_1$	0.423	0.60	1.63
Okra	12.02	10.62	349.73	487.21	71.78	$C_{16.8}H_{23.4}O_{12}N_1$	-0.04	0.71	1.39
Potatoes	14.12	13.18	295.05	381.18	77.40	$C_{22.9}H_{37.7}O_{19.6}N_1$	-0.07	0.86	1.65
Pineapple	13.02	12.01	324.93	464.98	69.88	$C_{45.4}H_{70.1}O_{20.3}N_1$	0.65	0.45	1.54
Pig	13.18	10.74	249.80	378.13	66.06	$C_{45.4}H_{37.4}O_{77.6}N_1$	-2.60	1.11	0.82
Goat	17.49	15.23	127.74	509.33	25.08	$C_{140.9}H_{201.8}O_{77.6}N_{5.7}S_1$	0.33	0.55	1.43
Sheep	15.36	13.47	213.02	434.24	49.05	$C_{137.1}H_{198.8}O_{95.1}N_{5.3}S_1$	0.06	0.69	1.45
Carrot	13.88	11.36	295.42	378.64	78.02	$C_{22.8}H_{35.6}O_{19.2}N_1$	-0.12	0.84	1.56
Grape	13.32	12.63	291.42	361.63	80.59	$C_{22.8}H_{35.6}O_{20.2}N_1$	-0.21	0.89	1.56

Garlic	15.83	10.71	267.06	471.67	56.62	$C_{130.5}H_{198.8}O_{85.3}N_{2.8}S_1$	0.22	0.65	1.52
Chilis	6.82	6.31	344.07	407.33	85.70	$C_{16.8}H_{25.4}O_{22.6}N_1$	-1.18	1.35	1.51
Meat	36.64	36.46	780.92	907.87	86.02	$C_{188.6}H_{219.4}O_{21.2}N_1$	0.94	0.11	1.16
Peanut	27.77	26.09	561.99	731.71	76.80	$C_{21}H_{34.4}O_6N_1$	1.067	0.29	1.64

3.3.3. Biochemical conversion

3.3.3.1 Biomethane potential and biodegradability

After 30 days of digestion, the results of the experimental BMP are shown in Table 3.4. The BMPs of waste samples ranged from 780.915 to 127.735 mL/gVS. The highest yields were from the animal part and oil crop biomass; next to it was the BMP of fruits and vegetables with okra having the highest BMP (349.7304 mL/gVS) in that category. The least results were recorded from BMP of animal dungs, these patterns of results agree with Li et al. (2013) and Yan et al. (2017). Elemental compositions of biomasses in Table 3.3 were used to compute theoretical biomethane potential (TBMP) and the predictions were higher (907.8738 - 323.4703 mLCH4/gVS) than the experimental BMP results but followed the same trends in yields. These higher values of TBMP over those of experimental BMP were in line with the suggestions that TBMP calculations are predicated on the complete substrate degradation assumptions (Holliger et al., 2016; Strömberg et al., 2014). Wastes from the animal carcass and oil crops estimated higher methane yields than the lignocellulosic materials (Cai et al., 2019 and Li et al., 2013). The biodegradability (BD_{CH4}) of organic substrates were calculated with Equations 4 and shown in Table 3.4. The animal manure and most of the lignocellulosic substrates recorded lower BD_{CH4} % (*<70*) as suggested in Raposo et al. (2011). This low BD_{CH4} in animal manure and lignocellulosic substrates is consistent with previous studies (Cai et., 2019; Li et al., 2013; Yan et al.,2017).

3.3.3.2 Kinetic models (First-order kinetic and modified Gompertz model)

The accumulated biomethane yield from the experiment was predicted with first-order kinetic and modified Gompertz equation. Vital model parameters (Y_m, k, R_{max} and λ) and model fitness indices (RMSE and R^2) resulting from the model-fitting were evaluated from Equations 8 and 9 and presented in Tables 3.5 below. In the first-order kinetic model, all the model parameters and fitness indicators were generally low (Li et al. 2013). It was observed that nine out of the eighteen substrates, their experimental results could not be predicted by the first-order model. The *k* value, which is the hydrolysis constant and measures the biomethane production rate per time, nine substrates predicted successfully with positive *k* values ranging from 0.084 d^{-1} to 0.292 d^{-1}, indicating swiftness in biogas production rate (Kafle et al., 2013). According to Cai et al. (2019), the failure to properly predict all

the substrates shows that the model may not be well suited for simulating anaerobic digestion process of some substrates.

In the modified Gompertz model, the model kinetic parameter R_{max} value, which is the rate of methane production was in the range of 16.582 mL/(g VS·d) to 116.424 mL/(g VS·d). According to Zhao et al. (2016) and Cai et al. (2019), higher value R_{max} mostly suggests higher biomethane yield. R_{max} is the methane production rate and the R_{max} values were in the range of 8.6 mL/(g VS·d) to 60.4 mL/(g VSd). The lag phase (λ) shows the adaptation time of methanogens for the substrate usage in anaerobic digestion process (Cai et al., 2019), as shown in Table 3.5, λ values ranged from 0.14 d to 4.99 d, the substrates with lower λ value suggests early commencement of biodegradation. Meat/fat waste with the highest λ value may be as a result of its organic components or activeness of the inoculum (Xu et al., 2014; Cai et al., 2019).

Table 3. 5 Kinetic parameters of cumulative biomethane production

Substrate	Y_t (mL/g VS)	First-order kinetic model					Modified Gompertz model					
		Y_m mL/gVS)	Predict Difference %	k (d^{-1})	R^2	RMSE	Y_m (mL/gVS)	Pred. Difference %	**R_{max}** mL/(g VS·d)	**λ (d)**	R^2	RMSE
Egg	477.30	NP	NP	NP	NP	NP	474.13	0.67	64.668	3.52	0.9961	13.85
Chicken	281.1	287.30	2.16	0.243	0.9657	14.89	281.4	0.11	55.425	0.80	0.9975	19
Fish	532.03	NP	NP	NP	NP	NP	536.94	0.92	46.144	1.01	0.9975	11.12
Avocado	302.23	320.18	5.61	0.084	0.9577	21.33	302.49	0.09	25.574	1.49	0.9828	13.85
Cow	176.30	180.49	2.34	0.132	0.9917	4.914	174.09	1.24	16.582	0.14	0.9936	4.385
Pumpkin	320.32	331.73	3.44	0.138	0.9079	32.37	318.18	0.67	45.466	2.19	0.9651	19.59
Okra	344.73	338.45	1.86	0.292	0.979	12.34	332.7	3.49	69.177	0.23	0.9842	11.1
Potatoes	295.05	302.96	2.61	0.218	0.9055	27.33	298.3	1.10	50.469	0.99	0.9524	19.74
Pineapple	324.93	333.53	2.58	0.181	0.941	32.01	323.2	0.53	60.496	1.95	0.966	19.42
Pig	249.80	249.93	0.051	0.134	0.984	9.52	239.26	4.22	25.144	0.42	0.9856	9.196
Goat	125.74	NP	NP	NP	NP	NP	131.16	4.32	17.518	0.98	0.9787	8.34
Sheep	213.02	NP	NP	NP	NP	NP	221.83	4.14	26.928	1.12	0.9685	16.78
Carrot	295.42	301.71	2.09	0.182	0.8975	29.95	293.1	0.79	53.697	1.94	0.9602	19
Grape	291.42	NP	NP	NP	NP	NP	293.0	0.54	60.448	1.51	0.9418	21.94
Garlic	267.06	NP	NP	NP	NP	NP	271.12	1.52	30.201	2.54	0.9947	7.11
Chilis	349.07	NP	NP	NP	NP	NP	350.5	0.41	82.948	0.86	0.9725	23.88
Meat	780.92	NP	NP	NP	NP	NP	779.22	0.22	116.42	4.99	0.9914	28.82
Peanut	561.99	NP	NP	NP	NP	NP	564.32	0.42	85.829	0.8	0.993	20.55

NP: Not successfully predicted

The R^2 values were in the range of 0.9418 and 0.9975 and the RMSE values were also from 4.385 to 28.82. The biogas production potential (Y_m) of 779.22 mL/gVS was observed in the meat/fat substrate, while the least value of 131.16 mL/gVS was obtained from goat dung substrate. These values were close to those of the experimental biogas yield. The prediction difference, which is one of the model fitness indicators (prediction difference, R^2 and root mean square (RMSE)) ranged from

0.09 % to 4.32 %. All biomethane yield predictions were within the recommendation of Raposo et al. (2011), which stated that the prediction difference must be ≤10, above which the model is deemed unfit.

It is evident from the results, that the modified Gompertz model was more suited for predicting the anaerobic digestion process of the 18 selected substrates than the first-order kinetic model.

3.4. TG and DTG results of pyrolysis and torrefaction

The polymeric composition of biomass at different percentages, such as lignin (10 – 40%), cellulose (40 – 50%), hemicellulose (25 – 35%) and other inorganics are responsible for the different thermal degradation patterns and reactions in these temperature ranges; cellulose (240 – 350^{o}C), hemicellulose (180-260^{o}C) and lignin (280 – 500^{o}C) (Akhtar et al., 2019; Jin et al., 2013).

The results of the thermal decomposition process are shown in the plots of TG (normalized weight loss), the DTG (rate of weight loss) and Char yields from torrefaction and pyrolysis of biomasses in Figs. 3.1 and 3.2. It could be observed that there was a significant weight loss between 50 and 105^{o}C, it continued up to 150^{o}C. These losses could be attributed to the volatilization of the remaining surface and chemically bound moisture as well as low molecular weight volatiles (Shi et al., 2016). Most of their transition points were between 230 and 250^{o}C, except for the egg waste which was not denatured till 620^{o}C. The associated weight loss within this range (230 - 250^{o}C) is typical of cellulose and hemicellulose degradation phase or loss of short-chain hydrocarbons phase and it is also the torrefaction temperature (Akhtar et al., 2019 and Shi et al., 2016).

Pyrolysis which is a biomass upgrading process lowers atomic H/C and O/C ratios, enhances heating values and achieves better solid fuel production (Braz and Crnkovic, 2014). The remains of the biomasses after the torrefaction and pyrolysis process are shown in Fig. 3.1. From the torrefaction result, the egg waste sample had the highest yield of 96.49% and the least value was from carrot waste of 59.43%. Aside wastes of fruit origin with highest weight losses, all other samples had relatively insignificant weight loss after torrefaction, making them good feedstocks for co-pyrolysis processes with coal, thus decreasing greenhouse emissions (CO_2 and NO_2) which is synonymous with coal combustion (Quan and Gao, 2016). The observed high char yields and brittleness of samples after torrefaction were corroborated in the report of Shi et al. (2016). Similarly, after the pyrolysis process, the meat/fat and peanut yielded (3.4%) and (16.37) respectively the lowest char, while the egg waste

had a yield of 50.42% highest char content was recorded. It is suggested that biomasses with low char yield after pyrolysis may have been converted into gases or bio-oil (Shi et al., 2016). Although the egg wastes had higher char yield after torrefaction, the oil-bearing wastes are better suited for pyrolysis because of their higher energy output and low operation cost on char yield management.

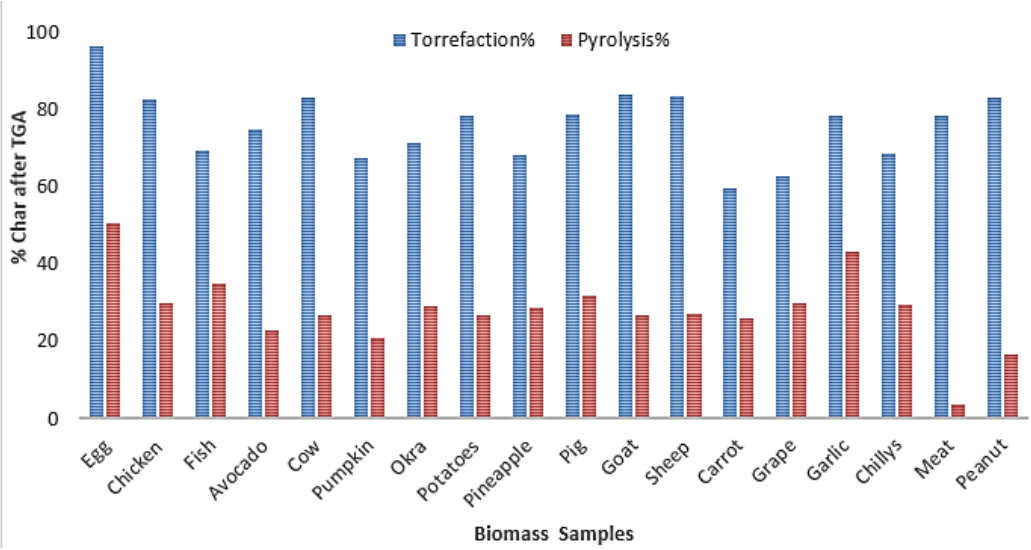

Fig.3. 1 Char yield of Torrefaction and Pyrolysis of the Biomass Samples

The TG and DTG curves in Fig. 3.2 describe the degradation behaviours of the samples tested. According to Shi et al. (2016), the curve variations are dependent on the nature of the analyte. The meat/fat and peanut had similar degradation peak between 312 and 430^{o}C. Except for egg waste with degradation peak at a high temperature of 713^{o}C, the significant losses of all other samples happened between 250 and 480^{o}C, which shows that large amount cellulose, hemicellulose and lignin were decomposed, while remaining part represents gradual degradation of other polymers (Ashraf et al., 2019; Shi et al., 2016).

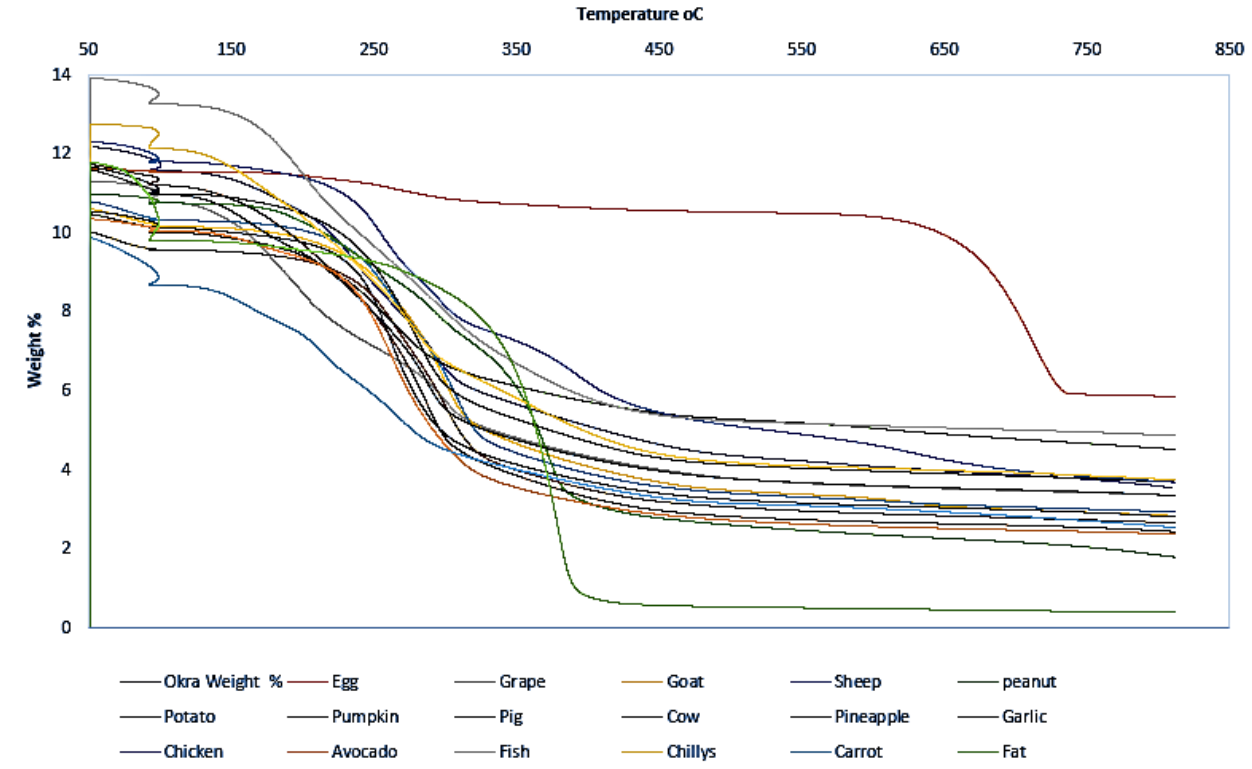

(A)

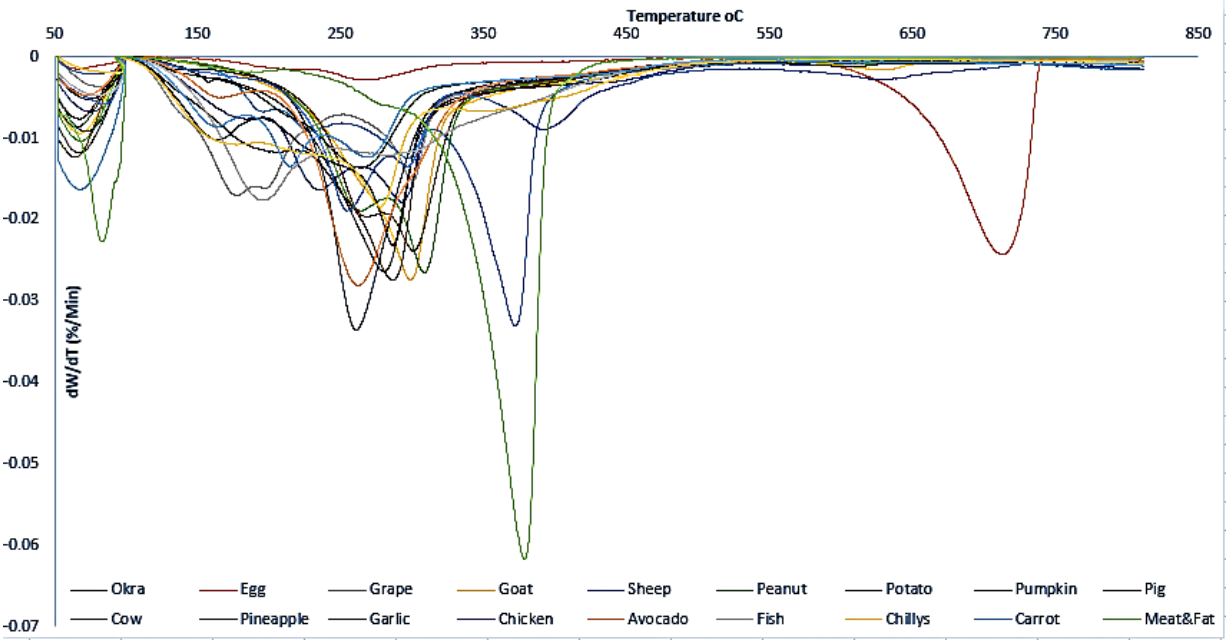

(B)

Fig.3. 2 TG and DTG curves of Biomass Samples

3.5 Ranking of substrates

Ranking and classification is a vital way of evaluating properties of fuel and grouping the same based on similarity in characteristics (Basu, 2010). Biomasses used in this study were classified based on their biomass-to-energy (thermochemical or biochemical) conversion strategies. The suitability and

efficacy of fuel are not based on only the ultimate and proximate analysis, but it is also dependent on the atomic ratios H/C_{eff} and (H/C and O/C), which is represented in Fig. 3.3 as Van Krevelen plot and C, H, O ternary diagram (Sing et al, 2017; Basu, 2010). Other ranking criteria are energy content (BMP and HHV) and energy conversion (biochemical and thermochemical).

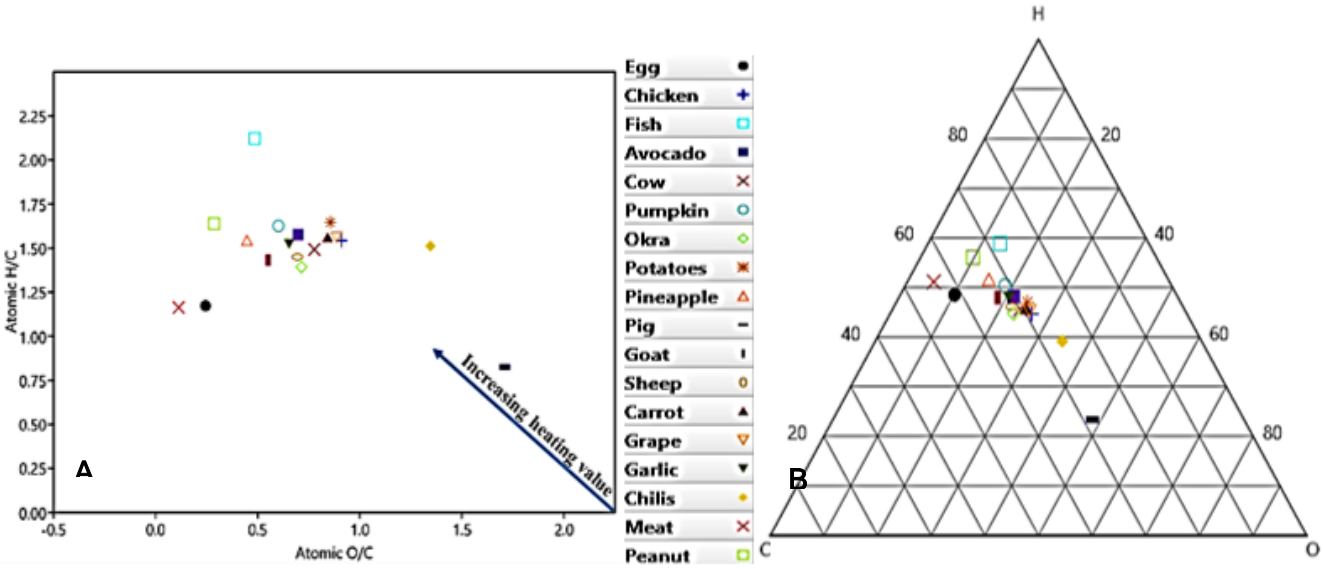

Fig.3. 3 (A)Van Krevelen diagram showing the atomic ratio of H/C versus O/C. (B) C-H-O ternary plot of biomass showing the gasification process

Based on the atomic ratios, the H/C and O/C ratios of the 18 substrates were plotted in the Van Kerelen diagram (Fig.3.3). According to Shi et al. (2016) and Sing et al. (2017), higher energy content, energy density and HHV are achieved at lower O/C and H/C ratios, resulting from more C-to-C bonds than C-to-O bonds. The peanut waste has high HHV (27.77383), higher H/C_{eff} value (1.06667), lower O/C ratio (0.28571) and from the Van Krevelen and ternary diagram, it also showed high calorific values and lower oxygen content. According to the recommended bases for classification in Basu (2010), Shi et al. (2016) and Singh et al. (2017), it is evident that peanut waste met all the criteria for ranking like the meat/fat and fish wastes than other feedstocks. Cow dung with low H/C and O/C also showed great potentials. The least performance on all the ranking indices of atomic ratio was observed in the pig waste.

From Table 3.4, the meat/fat waste with higher BMP (780 mL/gVs) and higher HHV (36.64356 MJ/kg) is ranked top on the energy content (Biomethane potential (BMP) and higher heating value (HHV)) bases. Generally, all other animal parts and oil crops have high energy contents. Similarly, the thermochemical and biochemical performances were predicated on substrate degradability either anaerobically or thermally and char yield. Based on a suggestion in Shi et al. (2016), that low char

yielding biomasses have better gas and oil yield, it can be deduced from Fig. 3.1, that egg waste with higher char yield at both torrefaction and pyrolysis states ranked least in the thermal conversion criteria. The dung from goats with the lowest $\%BD_{CH4}$ of 25.07923, which is lower than the recommended $\%BD_{CH4}$ (<70) in Raposo et al. (2011) is ranked least for biochemical conversion purposes.

As shown in Fig 3.2, the chemical compositions of plant-based wastes were lower than those of the animal-based wastes. Aside carrot (plant-based) waste with highest K of 1574.00 mg/kg, animal wastes showed higher cations values, the same trend was true for Total P. Although, Fish waste had the highest Total P and low o-P, but the pig manure had highest o-P and second-highest Total P. Based on the Olsen's method (extraction with sodium bicarbonates) reported in Leng et al. (2019) as being used for evaluation of P bioavailability and ease of release/recoverability, pig manure with higher o-P (bioavailable P) is ranked top.

3.5 Summary

The characterization and analysis of eighteen identified agro-waste biomasses in South Africa have been studied to categorize and rank them based on their energy contents and phosphate release potentials. In terms of phosphate recovery potentials, pig waste with highest o-P and second-highest Total P ranks top. Based on the results, wastes from the animal carcass and oil crop ranked best in energy conversion (thermal and biodegradability), energy content and minimal waste generation. Okra waste in the fruit and vegetable category, which was the second in rank, performed better than the others. Although the animal manure had high HHVs, it recorded very poor BMP yields. The modified Gompertz model predicted all substrates within acceptable limits with the goodness of fit. However, due to the low suitability of most biomass studied for thermo-conversion, bioconversion is recommended as the appropriate strategy for conversion of these wastes to energy. Co-digestion of high performing substrates with others (e.g., okra and pig wastes) is also suggested as well as pretreatments or enhancement of substrates before resource recovery should be encouraged.

Chapter Four

Enhancement of Anaerobic Digestion of Selected Agro-industrial Waste for Biogas Production

This chapter is adapted from: Ugwu, S. N. and Enweremadu, C.C. (2020) Enhancing anaerobic digestion of okra waste with the addition of iron nanocomposite (Ppy/Fe_3O_4), Biofuels, 11:4, 503-512

Ugwu, S. N. and Enweremadu, C. C. (2019). Biodegradability and kinetic studies on biomethane production from okra (Abelmoschus esculentus) waste. South African Journal of Science, 115(7-8), 1-5.

Ugwu, S.N. and Enweremadu, C.C. (2019). Effects of pre-treatments and co-digestion on biogas production from Okra waste. Journal of Renewable and Sustainable Energy 11, 013101 (2019)

Ugwu, S.N. and Enweremadu, C.C. (2019). Comparative Studies on the Effect of Selected Iron-Based Additives on Anaerobic Digestion of Okra Waste. In ASME 2019 13th International Conference on Energy American Society of Mechanical Engineers Digital Collection.

4.1 Introduction

The rapid population and energy demand have significantly increased in most emerging economies, triggering global concerns regarding the depletion rate of fossil fuel sources, their adverse impacts on the environment and the need to reduce the emission of greenhouse gases (Achinas and Euverink, 2016; Deepanraj et al. 2015; Shafiee and Topal, 2008). These have engendered more interest in the development of renewable/alternative energy from biomasses and biodegradable wastes (Talha et al. 2018). Biogas technology is a renewable energy type, which combines sustainable waste management and efficient biofuel production (Ding et al. 2017). This waste-to-energy process is an established technology for biogas production and waste volume reduction that operates through microbial-aided degradation of substrates under anaerobic condition involving different stages of hydrolysis, acidogenesis, acetogenesis and methanogenesis (Bharathiraja et al. 2018; Muvhiiwa et al. 2017). Anaerobic digestion has been underexploited in most developing climes like South Africa. According to the South African Biogas Industry Association (2015) and Damm and Triebel (2008), more than 2.328 million households (about 25% of all families in South Africa) use local fossil fuel sources like charcoal and firewood to meet their energy demands. The high cost and unavailability of electricity in most informal and rural settlements has increased both the demand for and development of biogas technologies (Muvhiiwa et al. 2017).

Although biogas production involves low-cost technology, availability of cheap feedstocks remains the major incentive for sustained investment in biogas production (Bharathiraja et al. 2018). The quest to ensure feedstock sustainability has necessitated the aggressive search for novel energy crops with

high biogas potentials, while optimizing methane generation potentials of existing feedstocks via enhancement processes (Bharathiraja et al. 2018; Li et al. 2018b; Aguilar-Aguilar et al. 2017; Tsapekos et al. 2017). The viability and degradability of wastes or otherwise for biogas production is determined through its biochemical methane potentials (BMP), which is a simple but reliable procedure for determining maximum methane volume produced per gram of the substrate's volatile solid and indicates rate and extent of conversion of biodegradable organics to methane in an anaerobic digestion set-up (Jingura and Kamusoko, 2017; Raposo et al. 2011). BMP is either determined theoretically or experimentally. The BMP and biodegradability of most agro-industrial wastes have been evaluated with Buswell's and modified Dulong's equations among other BMP theoretical equations with the results of ultimate (carbon, hydrogen, nitrogen, sulfur and oxygen) (Jingura, and Kamusoko, 2017; Browne and Murphy, 2013; Li et al. 2013; Buswell and Mueller, 1952).

Maximum biodegradability of substrates are not often attained because most feedstocks are composed of natural polymers such as starch, lignin (0-40 %), cellulose (15-99 %), hemicellulose (0-85 %), lipids, collagen, elastin, etc., monomers and synthesized polymers are the major components of biodegradable substrates (Akunna, 2018). For instance, lignocellulosic wastes like okra (*Abelmoschus esculentus*) waste are polymeric in nature containing lignin (7.1 %), hemicellulose (15.4 %), cellulose (67.5 %), pectin (3.4 %), protein and waxes (18%), fat (3.9 %) and crude fiber (25 %) (Alam and Khan 2007; Olaniyan and Omoleyomi 2013). Okra is an allopolyploid vegetable plant, grown predominantly (96%) in Asia and Africa (FAOSTAT, 2016), with waste generation capability of above 27 tons of biomass per hectare from foliage and stems (National Research Council, 2006). Similarly, just like other vegetables, wastes from harvest okra pods can be up to 30-50% of the total yield (Bharathiraja et al. 2018). In Duman et al. (2017), it was reported that there is a State's development policy on okra waste utilization from about 36,000 tons of okra produced per annum in Turkey. Currently, most of the dried wastes are directly used as a solid fuel for heating and the wet okra wastes disposed of in the landfill, these disposal options are neither environmentally sustainable nor economically viable (Bharathiraja et al. 2018). However, anaerobic digestion (co-digestion or mono-digestion) has been described in Talha et al. (2018) as a more environmentally friendly means of treating biodegradable wastes and recovering biogas for beneficial uses. For energy purposes, bio-oil from okra seeds has been reportedly used for biodiesel production (Anwar et al. 2010), but prior to the studies which form part of this thesis, no previous report had been recorded on anaerobic digestion of okra waste for biogas production in any form (mono-digestion, co-digestion, pretreated or enhanced).

Akin to other biodegradable organics, okra wastes are lignocellulosic waste-type which achieves slow and partial degradation during anaerobic digestion (Akunna, 2018; Duman et al. 2017), this dense and complex lignocellulosic structures, lowers hydrolysis rate, resulting in low degradability of substrates and low biogas yield, necessitating pretreatment, use of additives for nutrient fortification and acceleration of the hydrolysis, which is the rate-limiting stage in anaerobic digestion process (Bharathiraja et al. 2018; Choi et al. 2018; Ding et al. 2017). Enhancements of the anaerobic digestion process are necessary to overcome the main limiting factors associated with the availability of most substrates for biogas production. These factors include instability from essential nutrient deficiency, presence of inhibitors and polymeric structures of most substrates (Wang et al. 2018; Abdelsalam et al. 2017; Zhang et al. 2015). Anaerobic digestion enhancements facilitate the breakdown of recalcitrant complex polymeric substrates for increased biodegradability, increase process efficiency, startup speed and stability of the digestion process, reduce impact toxins and inhibitors, supply deficient nutrients for microbial stimulation, reduce HRT and lag phase, increase organic loading rate, aid synthesis of necessary cofactors and coenzymes in methanogenesis, improve biogas yield and methane content (Akunna, 2018; Li et al. 2018; Kim et al. 2017; Baredar et al. 2016; Song et al. 2014).

Furthermore, co-digestion is an enhancement approach, which involves anaerobic digestion of more than one different, but complementary substrates to achieve increase organic loading rate of the digester, boast the C:N ratio, decrease biodegradation time and increase overall biogas production (Kougias and Angelidaki, 2018; Simth and Holtzapple, 2011). Previous studies have established that the interaction type within different waste streams affects the overall biogas yield positively (Mahanty et al. 2014). Bharathiraja et al, (2018) concluded that co-digestion of substrates enhances digestibility and gives the best biomethane yield both in quantity and quality.

Previously, several pretreatment options, which include physical, mechanical, biological, chemical, physicochemical methods, etc. have been used to increase biodegradability and accelerate the hydrolysis stage of anaerobic digestion (Bharathiraja et al. 2018; Talha et al. 2018). Other than for biogas purposes, the mechanical, thermal and chemical pre-treatment of okra have been studied (Adelakun et al. 2009; De Rosa et al., 2010; Olaniyan and Omoleyomi, 2013). It has been observed that all the pre-treatments resulted in a decrease in the mechanical properties, which may be attributable to the substantial delignification and degradation of cellulose chains (De Rosa et al. 2010;

Kalia et al. 2009).

Sodium hydroxide (NaOH), which is the most widely used type of alkaline, is reputed for delignification of lignocelluloses substrates, resulting in exposure of cellulose to microbes (Kalia et al. 2009; Talha et al. 2016). Talha et al. (2018) reported that in anaerobic digestion of lignocelluloses substrate, 6% NaOH pre-treatment gave the maximum yield. The combined effects of acid/alkali-assisted steam/microwave heating and enzymolysis were harnessed to increase methane yield (Ding et al. 2017). Microwave irradiation has been reported as a good method of accelerating the hydrolysis of lignocellulosic materials and enhances enzymatic hydrolysis significantly (Zhao et al. 2017b, Bharathiraja et al, 2018). Hu et al. (2012) reported that the microwave pretreatment of cattail enhanced yield by 32% when co-digested with rumen microbes. While optimizing microwave pretreatment of lignocellulosic waste for enhancing methane production and comparing with the water-heat pretreated substrate, Zhao et al. (2017b) reported that the microwave-irradiated substrate increased by 38.3% in yield at an optimum time of 14.6 minutes. Similarly, Yu et al. (2017) examined the effect of microwave-assisted with alkaline (MW-A) pre-treatment of swine manure and found that the manure disintegration degree was maximized by 63.91% and digestion period shortened. Consequently, most of these pretreatment methods accelerate substrate hydrolysis and improve biomethane yield from lignocellulosic-rich biomass, but the low cost-efficiency arising from high chemical input and extra energy consumption, extreme pH and large salt formation limit methanogenic activities and impacts the operational cost (Zhao et al. 2018; Zhang et al. 2014a; Hashimoto, 2004).

Moreover, additive supplementation is another form of anaerobic digestion enhancement, which involves the addition of trace elements such as Ni, Co, Mo, Fe, Se, etc. to increase microbial activities and ultimately achieve improved biogas yield (Chen et al. 2018; Mao et al. 2015). Additives are cheaper and more effective enhancement option for plant performance improvement (Abdelsalam et al. 2016). Among all the allochthonous additives like CO_2, H_2 and other trace elements (iron (Fe), etc.) previously studied for anaerobic digestion enhancement, the Fe supplementation showed better advantage (Zhao et al. 2018; Hao et al. 2017; Liu et al. 2016).

Iron (Fe^{2+} and Fe^{3+}) ions are vital for energy acquisition and DNA replication in biological activities of all living creatures (Casals et al. 2014; Banfield and Zhang, 2001). The role of iron as both electron donor and acceptor makes it an important cofactor for several proteins and its homeostatic capabilities

is also very essential for the survival of cells/methanogens (Emerson et al. 2010). Fe additives decrease oxidative-reductive potentials, improves the hydrolysis-acidification enzyme activities and enhances digestion environment (Feng et al. 2014). Excess ions of iron in the anaerobic environment can result in Fenton reaction from reactive oxygen produced, causing toxicity to microbes and generate deleterious radicals to biomolecules (Casals et al. 2014; Tang and Lo, 2013). The deficiency of Fe ions due to its consumption by methanogens and reduction in Fe supply reduces the growth rate of the digester microorganisms (Chen et al. 2018; Ram et al. 2000). However, Casals et al. (2014) suggested that maintaining optimum concentrations of iron in an anaerobic digester is a critical step to boost bacterial activity. Several iron-based additive types have been used for enhanced biogas production.

It was reported in Zhang et al. (2015) that the supplementation of Fe (100 mg/L) with other trace metals helped in achieving a great methane yield in the anaerobic digestion of food waste. Demirel and Scherer (2011) reported in their review that for both substrates (cow dung and poultry litter), the addition of $FeSO_4$ improved methane content and biogas production during a batch anaerobic digestion experiment. Hansen et al. (1999), also reported that an increase of about 60 % biogas yield was recorded when $FeCl_3$ was added to the anaerobic digestion of water hyacinth-cattle dung. Ambuchi et al. (2016) reported that Hematite (iron oxide (Fe_2O_3)) enhanced biogas production from beet-sugar industry waste (BSIW). Red mud (45 % Fe_2O_3) which also promoted methane production (35.52 ± 2.64 % increase compared with the control (Ye et al. 2018), iron powder (1.6 %) also increased biogas yield by 40 % (Suanon et al. 2017).

Although other sources of Fe ions accelerate anaerobic digestion processes, the evolution of nanotechnology has shown to be an attractive option due to its nano-sizes, which increases the penetrability of cell membranes in biological systems and facilitation of distribution, uptake, metabolism, etc. (Powell et al. 2010). Nanomaterials have unique properties such as self-assembly and dispersibility, high reactivity due to high surface area to volume ratio, large surface area and high specificity (Wang et al. 2018; Nassar, 2012). Kadar et al. (2012) suggested that the nanoparticulate form of iron nanoparticles made Fe more available for microalgae than other metals. Recently, the viability of nano-iron additives (nZVI, nano-Fe_3O_4, iron nanoparticle, etc.) in anaerobic digestion has ensured enhanced biogas production in both quality and quantity of the methane content (Abdelsalam et al. 2017; Wang et al. 2018; Casals et al. 2014; Suanon et al. 2017; Amen et al. 2017).

Conductive iron oxides like Fe_3O_4 nanoparticles (NPs) have been reported to promote the growth of methanogen, facilitates direct interspecies electron transfer in syntrophic methane production, improves hydrolysis, solubilization and acidification stages through dissimilatory process of iron reduction and wields great potential in the degradation of complex organics (Chen et al. 2018; Zhao et al. 2018; Tan et al. 2015; Zhuang et al. 2015). Although Fe_3O_4 is one of the superior types of iron oxide NPs in the anaerobic digestion process, the activities of excess Fe_3O_4 can inhibit methanogenesis, because it is an electron acceptor that can contend for electrons with methanogens (Noonari et al. 2019; Romero-Guiza et al. 2016; Auffan et al. 2008). Casal et al. (2014) reported the use of a novel, optimal and continued release Fe_3O_4 NPs to the digester to achieve 180% rise in biogas yield. The addition of 0.5% dose of Fe_3O_4 NPs to an anaerobic digestion process resulted in optimum biogas yield and improved stabilization of metals in the digestates Suanon et al. (2016). Abdelsalam et al. (2017) reported that the use of 20 mg/L Fe_3O_4 NPs gave the highest yield of 584 mL/gVS and 351.8 mL CH_4 g/VS for specific biogas and methane yield respectively. In Ali et al. (2017), a different optimum dose (75 mg/L) of Fe_3O_4 NPs resulted in the highest cumulative methane yield (5000 mL/gVS).

Akin to other Fe_3O_4 magnetic NPs previously applied in solving diverse environmental challenges, polypyrrole magnetic NPs (PPy/Fe_3O_4) with great qualities has attracted attention and has been extensively used in providing environmental solutions (Abdelsalam et al. 2017). These interesting properties include cheapness, charge neutrality, high dispersibility in water, high coercivity, biocompatibility, non-toxicity, superparamagnetic and low Curie temperature (Aigbe et al. 2018; Bhaumik et al. 2011; Kim and Kim, 2003). Summarily, although iron additives improve bacterial activity in the anaerobic digestion process, optimum dosages are needed for maximum yield (Casals et al. 2014).

The variation in the characteristics of okra waste from place to place, based on agronomical differences and storage conditions before digestion, necessitates the evaluation of its kinetic properties. Various kinetic (sigmoidal and other statistical) model types have been successfully used to simulate anaerobic digestion processes (Ware and Power, 2017; Kafle and Chen, 2016). Fitting kinetic functions to the cumulative methane production curves obtained from the BMP process enables information on anaerobic process performance to be gathered. This information includes whether the maximum methane yield (B_o) was attained, the maximum rate of methane production (R_{max}), the degradation rate constant (K) and the lag phase (λ) duration (Ware and Power, 2017). The

accuracy of biogas yield prediction in the model is dependent on the substrate that is used as the feedstock.

This study was motivated by the huge amount of okra waste that can be available for waste-to-biogas production and the quest to improve biogas recoverability from okra waste via pretreatment, co-digestion and additive supplementation at varying times. The determination of the BMPs (measured and calculated) and biodegradability were studied. The possibility of enhancing anaerobic digestion of okra with varying dosages of Ppy/Fe_3O_4 and previously determined optimum doses of nZVI, Ppy/Fe_3O_4, Fe and Fe_2O_3 was assessed (Wang et al. 2018; Abdelsalam et al. 2017; Ambuchi et al. 2016). Pretreatment of okra waste with alkaline (NaOH), microwave (MW) and microwave-assisted alkaline (MW-NaOH) pretreatment as well as co-digestion with sheep manure in accelerating the conversion of the organic component of okra wastes to biogas was also studied. The effects of these enhancements on biogas yields were evaluated. Finally, the suitability of the artificial neural network (ANN) model and other kinetic models (first-order, modified Gompertz, etc.) for evaluating/ predicting the kinetics of biogas production from okra waste were determined.

4.2 Materials and methods

4.2.1 Substrate and inoculum collection/preparation

In this study, okra waste and sheep slurry were collected from Organic Growers farm located in Centurion, Gauteng, South Africa at different times for the four BMP experiments. They were separately blended to achieve homogeneity, increase their surface areas and stored in the cold room at 4^{o}C until use for either characterization or anaerobic digestion. The inoculum containing consortium of anaerobes from an active food and vegetable waste continuous digester operating at mesophilic temperature (37±1^{o}C) at the Mechanical Engineering, University of Johannesburg, South Africa were collected, stored at 4^{o}C and further acclimatized at mesophilic temperature before use.

4.2.2 Substrate characterization

The entire analyses were conducted in triplicates and the mean values are presented in this work. The total solids (TS), volatile solids (VS), moisture content and ash content were determined by the standard procedures (APHA, 2005). The % VS removal was determined as a percentage between initial and final VS. The carbon (C), Hydrogen (H), Nitrogen (N) and Sulfur (S) contents were determined using a CHNS elemental analyser. Elemental composition (C, H, N, S) of the samples was determined using a LECO CHNS-932 combustion analyser (TruMac, Argon, LECO

Corporation) at 1050 °C, with sulfamethazine as a standard substrate in accordance with Raposo et al. (2011). Oxygen content was calculated by assuming C + H + O + N + ash = 99.5% (on a VS basis) (Rincón et al. 2012). pH was measured using a pH meter (HI 9828 Multi-parameter, Hanna Instruments). The volatile fatty acid (VFA) was determined using gas chromatography VFA centrifuged at 10 000 rev/min for 10 minutes. The supernatant after centrifuging was filtered off with 0.45µm filter and directly injected. VFA was determined as described in Liu et al (2018) by gas chromatography (Agilent 7890B, USA) equipped with a flame ionization detector and a fused-silica capillary column (HP-5, 30 mm x 320 µm x 0.25µm). Nitrogen was used as the carrier gas at a flow rate of 1.0mL/min. The injected sample volume for each GC analysis was 1µL and the run time of 28minutes. The injection port and detector temperatures were 250ºC and 270ºC respectively.

4.2.3 Theoretical biomethane potential and biodegradability

Methane production potential and biodegradability of okra were estimated using two theoretical biomethane potential (TBMP) approaches – Buswell and modified Dulong formulae – based on okra's elemental composition (Browne and Murphy, 2013; Buswell and Muller, 1952). The energy value of feedstock E^* (okra) and its theoretical biomethane potential ($TBMP_{E*}$) were estimated using the modified Dulong equation. Boyle's (modified Buswell) equation was used to determine the TBMP (Boyle, 1976) and biodegradability was calculated as shown in Equations 4.1 to 4.5. TBMP was predicated based on the following assumptions (Achinas and Euverink, 2016): ideal microbial condition and total substrate digestion; complete mixing and constant temperature; substrate composition limited to only C, H, O, N, S and output in the form of CH_4, CO_2, NH_3.

$$E^* = 337C + 1419\left(H - \frac{1}{8}O\right) + 93(S) + 23.26(N) \quad 4.1$$

$$TBMP_{E^*} = \frac{E^*(base\ on\ \%VS)}{37.78} \quad 4.2$$

$$C_nH_aO_bN_c + \left(n - \frac{a}{4} - \frac{b}{2} + \frac{3c}{4}\right)H_2O \rightarrow \left(\frac{n}{2} + \frac{a}{8} - \frac{b}{4} - \frac{3c}{8}\right)CH_4 + \left(\frac{n}{2} - \frac{a}{8} + \frac{b}{4} + \frac{3c}{8}\right)CO_2 + cNH_3 \quad 4.3$$

$$TBMP = \frac{22400\left(\frac{n}{2}+\frac{a}{8}-\frac{b}{4}-\frac{3c}{8}\right)}{12n+a+16b+14c} \quad 4.4$$

$$BD_{CH_4} = \frac{BMP}{TBMP} * 100 \quad 4.5$$

where E^* is the energy value of the substrate (MJ/Kg); methane energy content = 37.78 MJ/m^3 at

STP; CHONS = carbon, hydrogen, oxygen, nitrogen, sulfur (% TS); TBMP is the theoretical biomethane potential at STP $\left(\frac{mLCH_4}{gVS}\right)$; and BD_{CH4} is the anaerobic biodegradability (%).

4.2.4 Pre-treatment and co-digestion

The mechanical pretreatment (grinding) was first carried out to achieve substrate size reduction. The other pretreatments were conducted thus: the sodium hydroxide and hydrochloric acid used for okra waste pre-treatment and pH stabilization were purchased from (Sigma-Aldrich, South Africa). The de-ionized water (Milli-Q, Millipore) was used for the pretreatment processes and to complete the AMPTS II reactor headspace, flow meter as well as temperature water bath. The alkaline pretreatment process was carried out using 500 ml beakers containing 19.25 g total solids (TS) of okra was treated to 6% NaOH at room temperature for 15 min, samples already pre-treated with NaOH were further subjected to irradiation using a microwave (Russel Hobbs-RHMA20L, 700W, 2450 MHz) for 14.6 min. 500 ml beakers containing 14.61 g (TS) of okra waste only was also subjected to microwave pre-treatment. Different ratios of the sheep slurry (25%, 50% and 100%) were co-digested with okra waste. Un-pretreated okra waste samples were used as a control; all samples were in triplicates and shown in Table 4.1. The pre-treated samples were neutralized with hydrochloric acid immediately after pre-treatments before the commencement of the biochemical methane potential test.

Table 4. 1 Various pre-treatments on substrates

S/N	Identification	Substrate	Pre-treatments
1	O	Okra 100%	Nil
2	OA	Okra 100%	NaOH
3	OAMW	Okra 100%	NaOH and Microwave
4	OMW	Okra 100%	Microwave
5	OS25	Okra 75% + Sheep slurry 25%	Nil
6	OS50	Okra 50%+ Sheep slurry 50%	Nil
7	S	Sheep 100%	Nil

4.2.5 Iron-based enhancement

Based on our published meta-analysis studies and review paper on the impacts of iron-based on anaerobic digestion processes (see attached as annexes), the optimum dosages of some previously studied iron-based additives were selected alongside a novel iron-based additive (Polypyrrole magnetic nanocomposite (PPy/Fe_3O_4)) for anaerobic digestion enhancement. The Polypyrrole magnetic nanocomposite (PPy/Fe_3O_4) used in this experiment was synthesized in the Physics and Mechanical/Industrial Engineering Laboratory of University of South Africa as described and characterized by Aigbe et al. (2018). Because PPy/Fe_3O_4 had not been previously used for anaerobic

digestion, dosages of iron oxide nanoparticles (Fe_3O_4) from previous studies indicating maximum yields were used (Amen et al. 2017; Ali et al. 2017; Abdelsalam et al. 2017; Suanon et al. 2016). These four doses of the synthesized PPy/Fe_3O_4 (20, 75, 750 and 1000 mg/l) as shown in Table 4.2 were added to the substrate for the enhancement of microbial activities by the freeing-up of Fe ions from PPy/Fe_3O_4 in the anaerobic digestion process. These different doses were dispersed in deionized water and then sonicated for 10 min before being introduced into the bioreactors. The control experiment was conducted in a bioreactor containing only organic waste (OW) and inoculum, the BMP data from different dosages of iron-base additive.

Table 4. 2 Treatment levels of PPy/Fe_3O_4 NPs for substrate enhancement

Notation	**Treatment**	**Dosage mg/L**
O	Okra (control)	0
Oppy20	Okra + Polypyrrole-magnetic nanocomposite	20
Oppy75	Okra + Polypyrrole-magnetic nanocomposite	75
Oppy750	Okra + Polypyrrole-magnetic nanocomposite	750
Oppy1000	Okra + Polypyrrole-magnetic nanocomposite	1000

After the determination of the optimum dosage of PPy/Fe_3O_4, it was used alongside other iron-based additives to supplement anaerobic digestion processes. The other selected additives and their sources are as follows: nano-zero valent iron (nZVI), (mKnano, Canada), iron powder (Sigma-Aldrich, South Africa), and Hematite (iron mine, South Africa). The dosages used in this stage of the experiment are from previously determined optimum doses as reported in Wang et al. (2018); Abdelsalam et al. (2017); Ambuchi et al. (2016). These doses are as shown in Table 4.3. below

Table 4. 3 Different types of iron-based additives for substrate enhancement

Notation	**Treatments**	**Dosage, mg/L**
O	Okra (control)	0
Ppy/Fe_3O_4	Okra+Polypyrrole-magnetic nanocomposite	20
Fe_2O_3	Okra+Hematite	750
$nZVI_{20}$	Okra+nano-zero valent iron	20
$nZVI_{1000}$	Okra+nano-zero valent iron	1000
Fe	Okra+iron powder	750

4.2.5 Experimental setup

Four different batches of laboratory-scale anaerobic digestion of okra waste were performed with AMPTS II reactors (Bioprocess Control, Sweden) located at the Department of Mechanical and Industrial Engineering Lab, University of South Africa (UNISA) for 25, 25, 32 and 19 days of hydraulic retention time (HRT) respectively for biomethane and biodegradability, pretreatment and

co-digestion, PPy/Fe_3O_4 supplementation and comparative iron supplementation (nZVI, Fe, Fe_2O_3 and PPy/Fe_3O_4) batch experiments at mesophilic temperature (37 ± 1°C). The bioreactors assay of 500 ml capacity each were used for the anaerobic digestion processes with 400 ml as the working volume. The bioreactor headspace, temperature water bath and flow meter were filled up with de-ionized water (Milli-Q, Millipore). OW of 14.49 g (1.9 g VS) was added to 382.4 ml of inoculum (3.9 g VS) in each reactor at an inoculum to substrate ratio (ISR) of 2:1. Prior to the addition of additives, the pH of the mixed liquor in the bioreactor was adjusted to 7.0 with the aid of NaOH and HCl. To create an anaerobic environment in the bioreactors, nitrogen gas (N_2) from Afrox Gas, South Africa was used to purging each reactor before starting the stirrers. The daily and cumulative biomethane production of different enhancement options and the control experiment (without enhancements) were collected using an in-built data-logger in the AMPTS II. Results were retrieved from the data logging platform of the reactors and used for the calculation of daily biogas production, production rate and cumulative methane production. The entire process tests were performed as stipulated in the AMPTS II standard operational manual. The final pH, VFA and VS of the digestate from all reactors were measured. Percentages between the initial and final VS were used to determine the %VS removal. The scanning electron microscopy coupled to an energy dispersive spectroscopy (SEM-EDS) was used to determine the structural degradation of substrates. All the treatment levels were run in triplicates and the setup is shown in Fig. 4.1.

(a)

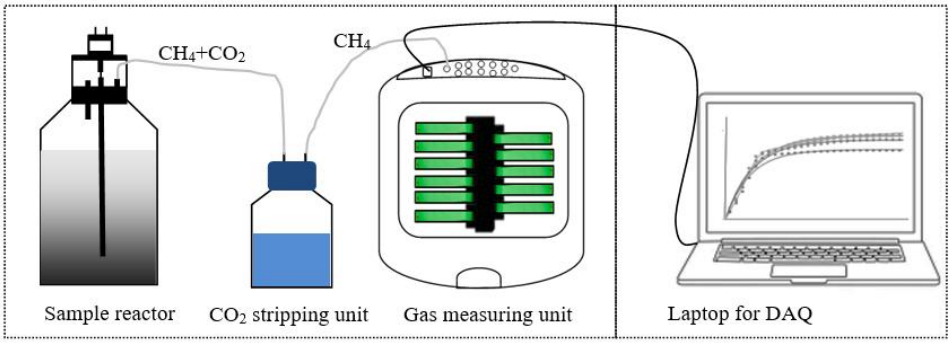

(b)

Fig.4. 1 (a) Picture of AMPTS II Biomethane potential assay with DAQ, (b) Schematic representation of Biomethane Potential Assay

4.2.6 Kinetic models for biogas production

In anaerobic digestion, kinetic modelling is a recognized technique for showing the specific performance of the system parameters (Kafle et al. 2013). Some of these models like the first-order kinetic are used to simulate the kinetics of anaerobic digestion processes, while others like modified Gompertz model assumes that biomethane yield rate is proportional to the growth of methanogens during anaerobic digestion (Talha et al. 2018; Mahanty et al. 2014). In this study, non-linear regression analysis was performed using the curve-fitting tool in Matlab R2015b with the least square method at $p < 0.05$ significant level to evaluate the growth functions (modified Gompertz, Stannard, transference, logistic and first-order kinetic models) shown in Equations 4.6 to 4.10. The average measured cumulative methane productions were used to evaluate the models (their parameters and fitness).

Modified Gompertz: $B = B_o Exp\left\{-Exp\left[\frac{R_{max}.e}{B_o}(\lambda - t)\right] + 1\right\}$ 4.6

Stannard $B = B_o\left\{1 + Exp\left[-\frac{(1+kt)}{p}\right]\right\}^{-p}$ 4.7

Transference $B = B_o\left\{1 - Exp\left[\frac{R_{max}}{B_o}(t - \lambda)\right]\right\}$ 4.8

Logistic $B = \frac{B_o}{\left\{1+Exp\left[\frac{4R_{max}}{B_o}(\lambda - t)+2\right]\right\}}$ 4.9

First-order $B = B_o(1 - Exp(-kt))$ 4.10

where B is cumulative specific methane production (mL/gVS); B_o is maximum specific methane production potential (mL/gVS); R_{max} is the maximum specific methane production rate (mL/gVS- d); e is Exp(1)=2.718282; λ is the lag phase in days; k is the methane production rate constant (day^{-1}); t is digestion time (days), and p is the slope of growth.

The kinetics of biogas production was evaluated using the five growth functions to determine the following parameters: B_o, B_p, k, λ p, R^2, adjusted R^2, R_{max} and root mean square error (RMSE). The entire experiment was performed in triplicate and the average of the three values was used. STATISTICA 12, Minitab 15 and OriginPro 9.1 were used for all statistical analyses and all inferences are at a 95% confidence.

4.2.7 Artificial Neural Network

In this study, an unperturbed batch lab-scale process was used to maintain a constant anaerobic condition in the reactors with the only one outlet for biomethane yield. Out of all the important input factors, T and RT were the only measurable input variables. T and RT were the input datasets, daily biomethane yield was the output (target) dataset and Artificial Neural Network was used to model and predict biomethane yields, just like observed in Najafi and Ardabili (2018), where %VS, %TS, temperature (T), C/N and retention time (RT) were noted as the most important variables in biogas production processes. The Neural Network Application in MATLAB 2015b (Mathworks Inc.) software was deployed for executing the predictive model of intricate non-linear systems with closed-form (black-box) equation.

The ANN model structure used were trained, tested and validated with an architecture of 10 neurons on the hidden layer and displayed in Fig. 4.2 as the best network with the highest performance, the best neural network structure and decreased error to the user-specified values were obtained (Najafi and Ardabili, 2018). Data percentages of 70 %, 15 % and 15 % respectively for training, testing and validating performed best out of other tested percentages. The sigmoid transfer function was used as the transfer function, the Levenberg–Marquardt back-propagation algorithm training (trainlm) was used for the training task and the Purelin transfer function, which is part of the output layer. It was used to calculate layer's output from its net input (Najafi and Ardabili, 2018). The performance of the network is indicated by the performance parameters (R^2 and RMSE) and the predicted outputs are as shown and discussed in subsequent sections.

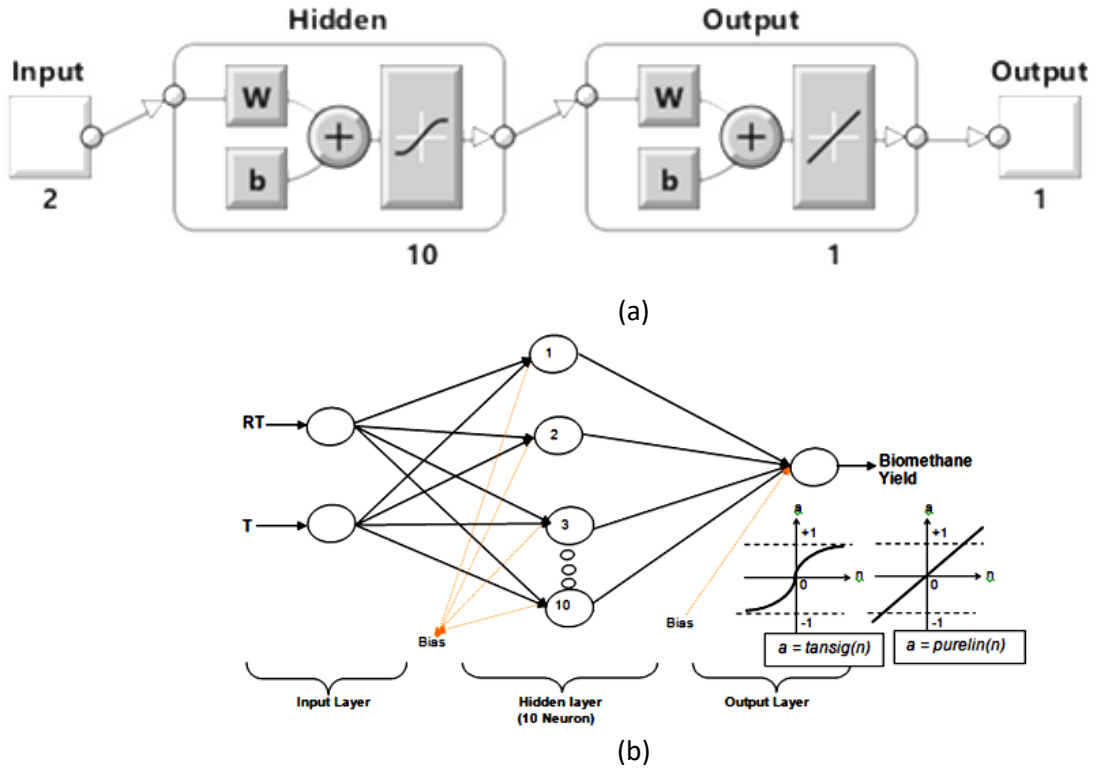

Fig.4. 2 (a) Artificial Neural Network Model Structure used in this study; (b) Neural network architecture for the training of experimental data of simplex-centroid mixture design.

4.3 Results and discussions

The results of the four different enhancement, biodegradability and kinetic studies on biogas production from okra wastes are captured in this section and are discussed separately. This is necessary because the substrates were not collected at the same time and the duration of digestion varies from each other.

4.3.1 Okra BMP, biodegradability and kinetic studies

The ultimate and proximate properties of okra waste are shown in Table 4.4. A mass of 27.55 g was determined based on 7.8157 %TS and 6.8945 %VS. Although a high substrate VS/TS ratio of 88.36% was recorded, 76.06% of it was removed during the anaerobic digestion process. This finding agrees with Li et al. (2013) who reported a high VS/TS to be desirable for biogas yield. The waste showed a C/N ratio of 12.24, which was outside the ideal range of 15–30, thus necessitating co-digestion or nutrient enrichment (Li et al. 2013).

Table 4. 4 Proximate and ultimate analyses of samples

Properties	**Inoculum**	***Abelmoschus esculentus***
Initial pH	8.08±0.02	8.13±0.01
Final pH	7.68±0.01	8.15±0.02
Moisture content %	98.50±0.01	92.36±4.402
Ash content %	0.03±0.00	15.87±0.006
Total solids (TS) %	1.50±0.01	7.82±0.005
Volatile solids (VS) %	1.02±0.04	6.90±0.001
VS of TS %	68±0.01	88.36±4.402
Removed VS of TS %	89.5±0.00	76.06±0.12
Carbon% TS	NT	39.30±0.012
Hydrogen% TS	NT	5.39±0.003
Oxygen% TS	NT	35.74±0.003
Nitrogen% TS	NT	3.21±0.003
C/N ratio	NT	12.24±0.003

NT, not tested

The result of experimental BMP test of okra waste yielded 270.98 mL/gVS of biomethane as shown in Table 4.5, this value concurs with other reports of low biomethane yields from lignocellulosic vegetable wastes (Yan et al. 2017; Li et al. 2013). Theoretical biomethane potential (TBMP) and biodegradability (BD_{CH4}) calculated with Equations 4.1 to 4.5 using elemental and energy content of the substrate are shown in Table 4.5. TBMP based on elemental composition (444.48 $mLCH_4/gVS$) was higher than that obtained based on energy content (342.06 $mLCH_4/gVS$). BD_{CH4} based on elemental composition (60.97%) was lower than that based on energy content (79.22). Raposo et al (2011) reported that BD_{CH4}<70% is considered an outlier or invalid. In view of this finding, TBMP based on energy content satisfied the criterion better. The low BD_{CH4} seen in elemental TBMP is consistent with the biodegradability of lignocellulosic vegetables (Yan et al. 2017; Li et al. 2013).

Table 4. 5 Summary of key energy production parameters

Parameter	**Result**
BMP (mL/gVS)	270.98
TBMP ($mLCH_4/gVS$)	444.48
$TBMP_{E*}$ ($mLCH_4/gVS$)	342.06
E* (MJ/kg) on %TS	14.63
E* (MJ/kgVS) on 88.36 %VS	12.93
BD (%)	60.97
BD_{E*} (%)	79.22
Substrate formula	$C_{14.3}H_{23.4}O_{9.8}N_1$

BMP, biomethane potential; TBMP, theoretical biomethane potential; E, energy; BD, biodegradability

The measured and predicted methane production results, as well as the determined parameters, are

shown in Fig. 4.3 and Table 4.6. The cumulative measured biogas was 270.8 mL/gVS; the models predicted cumulative biogas to be 267.38, 267.99, 270.89, 267.50 and 270.15 mL/gVS, respectively, for modified Gompertz, Stannard, transference, logistic and first-order models. These values are consistent with the assertion of Raposo et al. (2011), who recommended that the difference between B_o and B_t should not be more than 10%, above which this kinetic model is deemed invalid for predicting anaerobic digestion processes.

Table 4. 6 Kinetic parameters of average cumulative methane production curves

Parameter	**Modified Gompertz**	**Stannard**	**Transference**	**Logistic**	**First-order**
Measured biogas yield, $B_{(t)}$ (mL/gVS)	270.98	270.98	270.98	270.98	270.98
Predicted biogas yield, $B_{(P)}$ (mL/gVS)	268.38	267.99	270.89	267.50	270.15
Difference between $B_{(t)}$ and $B_{(p)}$ (%)	0.95	1.1	0.03	1.28	0.31
B_o (mL/gVS)	268.4	268.0	271.1	267.5	270.3
R_{max} (mL/gVS)	39.93	–	77.2	34.38	–
Lag phase, λ (days)	0.872	–	0.143	1.24	–
Degradation rate, K (per day)	–	1.449	–	–	0.2994
P	–	3.269	–	–	–
R^2	0.963	0.957	0.983	0.946	0.982
Adjusted R^2	0.96	0.953	0.982	0.941	0.981
RMSE	13.67	14.7	9.209	16.54	9.378

The lag phase (λ) of the growth functions, which is the time required for bacteria to adapt and start biogas production, is given in Table 4.6 and Fig. 4.3. The values are 0.872, 0.143 and 1.24 for modified Gompertz, transference and logistic models, respectively. The low λ values found in this study are in line with the report of Talha et al. (2018), who stated that lower lag phase is dependent on the activeness of the adapted inoculum and biodegradability of the organic part of the okra waste.

Most lignocellulosic substrates have cellulose as their main polymer component (about 68% in the case of okra). The hydrolysis rate of cellulose is normally the rate-limiting step, and the biomethane production rate is denoted by *k* (Dudek et al. 2019; Mao et al. 2016). The *k*-value of substrates can be determined via product formation (biomethane production or VFAs) and substrate depletion (VS, COD or DOC) methods (Angelidaki and Sanders, 2004). In this study, biomethane production (the product formed) was used to compute the *k*-values of both Stannard and first-order models of 1.449/day and 0.2994/day, respectively. The *k*-values obtained were both high and positive, which, according to Dudek et al. (2019), could be because of the higher bioavailability of cellulose, which results in a faster rate of biogas production (Budiyono and Sumardiono, 2014; Kafle et al. 2013). This observation agrees with that of Veeken and Hamelers (1999), namely that biomethane production

represents the hydrolysis rate of the bioavailable substrate which decreases with decreasing VS and can be best described with first-order kinetics.

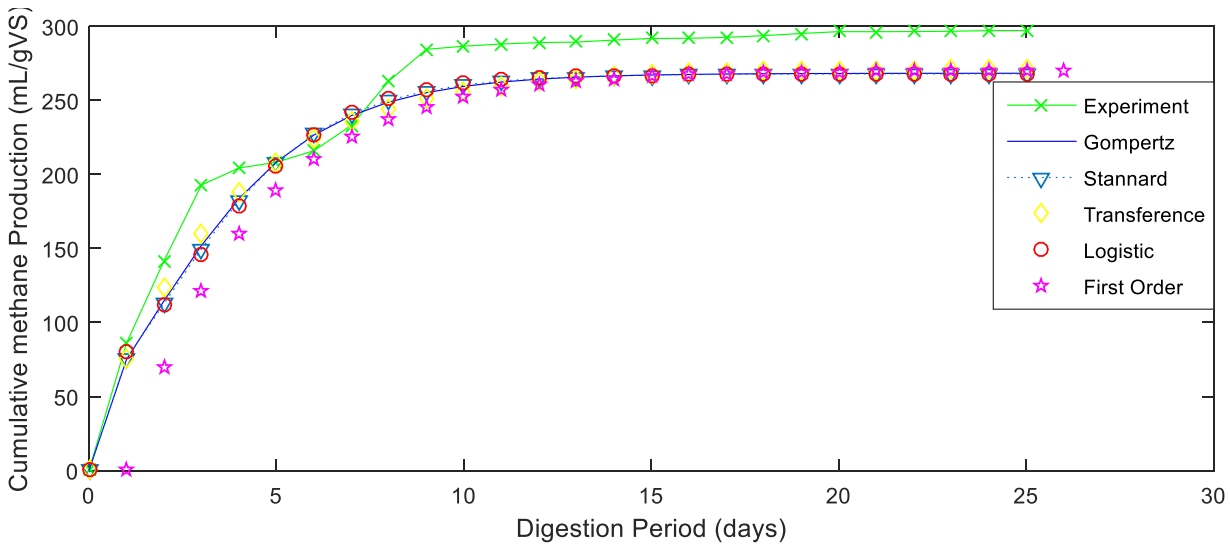

Fig.4. 3 Cumulative biogas production based on experimental and kinetic modelling results.

Transference and first-order models best-predicted okra waste digestion, with a prediction difference of 0.03% and 0.31%, respectively. This finding is consistent with the report of Kafle and Chen 2016), who showed that the first-order kinetic model was found to be the best model for predicting BMP. Li et al. (2018) reported that the transference model performed better than the modified Gompertz model. The statistical indicators of model fitness (as shown in Table 4.6) ranged from 0.946 to 0.983, 0.941 to 0.982 and 9.209 to 16.54 for R^2, adj. R^2 and RMSE, respectively. In line with the report of Budiyono and Sumardiono (2014), RMSE value <10 shows good model prediction. Based on this criterion, only transference and first-order kinetic models were within the accepted limit.

4.3.2 Pretreatment and co-digestion of okra waste

4.3.2.1 Characteristics of the substrate

Okra waste and sheep slurry substrates used for anaerobic digestion in this study were analysed for TS, VS, and C, pH, N and VFA as shown in Table 4.7. The per cent moisture content for all substrates, including inoculum ranged from 66.54 to 98.50. The TS and VS values of samples were respectively between 1.50% to 33.46% and 1.02% to 13.34%. The variation in the composition of substrates is dependent on substrate varieties, agronomic practices, soil quality and environmental factors (Talha, 2018). The carbon to nitrogen ratio as was analysed and calculated ranged from 15.90 to 16.73, which was lower than the recommended optimum value between 20-40 for biogas production (Smith and

Holtzapple, 2011). This shows that co-digestion of substrate studied with others of higher carbon values or nutrient supplementation is required for maximum output. All determined pH values were within the recommended values of between 6.5 and 8.5 (Capodaglio et al. 2016).

Table 4. 7 Proximate and Ultimate Analyses of Samples

Properties	Inoculum	O	OS25	OS50	OA	OMW	OAMW	S
Initial pH	8.08	8.13	8.18	8.24	8.50	8.20	8.44	8.10
Final pH	7.68	8.15	7.94	7.83	7.91	8.00	7.76	7.80
Moisture content %	98.50±0.0	84.85±0.2	81.18±0.2	79.72±0.02	80.55±1.02	80.55±1.02	80.55±1.02	66.54±3.36
Ash contents %	0.03	0.31	0.29	0.28	0.24	0.24	0.24	0.27
Total Solids %	1.50±0.01	15.15±0.2	18.5±0.00	20.28±0.00	15.15±0.24	15.15±0.24	15.15±0.24	33.46±0.00
Volatile Solids % (wet basis)	1.02±0.04	13.34±0.0	13.5±0.05	13.11±0.03	10.09±0.39	13.34±0.02	10.09±0.39	11.85±0.19
Final VS% of TS	60.86±1.6	64.52±1.0	62.3±0.06	61.76±1.12	47.87±1.28	62.40±1.95	56.99±6.03	59.99±0.00
Carbon %	NT	6.69±0.12	6.64±0.05	6.46±0.09	6.69±0.12	6.69±0.12	6.69±0.12	5.97±0.22
Nitrogen %	NT	0.42±0.02	0.41±0.02	0.39±0.01	0.42±0.02	0.42±0.02	0.42±0.02	0.373±0.00
C/N ratio	NT	15.9±0.35	16.16±0.7	16.73±0.81	15.90±0.35	15.90±0.35	15.90±0.35	16.00±0.44
Initial VFA g/l	0.19	2.1	1.9	1.7	2.1	2.1	2.1	1.3
Final VFA g/l	0.18	0.15	0.15	0.15	0.15	0.17	0.23	0.19

Note: NT = not tested, data expressed as the mean ± standard deviation.

The concentrations of VFA, which is a vital mid-product in the anaerobic digestion process, affect the population of methanogens, fluctuate pH and biogas yield (Talha et al. 2018). As shown in Table 4.7, the initial and final VFAs of substrates were analysed to determine the system's efficiency to reduce VFA. Initial VFA values of okra wastes for acetic, propionic and butyric were 1.0 g/l, 0.4 g/l and 0.7 g/l respectively, had the overall highest VFA of 2.1 g/l. The inoculum had the lowest value of 0.19 g/l. Contrary to previous works by Wang et al. (2009) and Talha et al. (2018) where higher propionic acid negatively impacted biogas yield and significantly inhibited the activities of methanogenic microbes, this study consistently recorded lower propionic acid.

4.3.2.2 Digestate characteristics

After 25 days of anaerobic digestion, digestates from each reactor were characterised to determine the VS based on TS, pH and VFA as shown in Table 4.7. The digestate VS/TS % value ranged from 47.87% to 64.52%, resulting in VS (TS%) reduction of 27.22, 77.15, 34.99, 11.68, 88.46, 79.16, 83.36 and 10.46% respectively for inoculum, O, OS25, OS50, OA, OMW, OAMW and S in the reactors. All the pre-treatments showed VS (TS%) reduction with OA achieving the highest reduction, this is in line with Wang et al. (2016), whose studies on alkaline pre-treated waste activated sludge (WAS) gave the highest removal of 45.6%. Zhang et al (2014b) also reported that the largest

reduction of about 60% substrate mass (VS) was noticed in the alkaline-pre-treated samples. The digestate pH values were generally lower than that of the pre-treated/co-digested substrates, which was between 7.76 and 8.15. This noticeable reduction, which according to Talha et al (2018) is due to a high removal of VFAs from the reactors. All samples in Table 4.7 showed high VFA reduction except for samples OMW, OAMW, S, which recorded lower VFAs. These lower VFA reduction in identified samples when compared to the control sample (O), may be responsible for the lower biomethane yield resulting from inhibition of methanogenic activities (Talha et al, 2018; Wang et al, 2009).

4.3.2.3 Methane production

The mean methane yield of all samples used in this study was statistically compared and their differences determined at the 95% probability level. The daily methane production and cumulative methane yield as can be seen in Fig. 4.4 and 4.5 respectively, showed that methane yield of OA was the most enhanced by 45.87% and was statistically different. Although OAMW was slightly increased by 0.95%, means of both OMW and OAMW were statistically the same with biogas yield of O. All samples co-digested with 25%, 50% and 100% sheep slurry respectively recorded decline in biogas yield by 9.92 %, 34.11% and 69.5% and were statistically different at $P<0.05$. The low biogas yield of the sheep slurry suggested the presence of inhibitors or low VS composition (Table 4.7), this was in line with Bharathiraja et al (2018), that operational parameters or feedstock and presence of inhibitors can reduce the activities of methanogens.

Although pre-treatment or co-digestion of okra waste within the reach of the researchers has not been studied, the enhancement of OA was in line with previous studies, Fu et al (2018) reported that pre-treatment of *Miscanthus* with NaOH resulted in 25.5% increase in yield. Unlike in this study, prolonged pre-treatment of water hyacinth by microwave resulted in 38% rise in yield (Zhao et al, 2017b), Tao et al. (2017) also observed that alkaline-microwave pre-treated swine manure at 54 J/g and pH 12, achieved 63.9% rise.

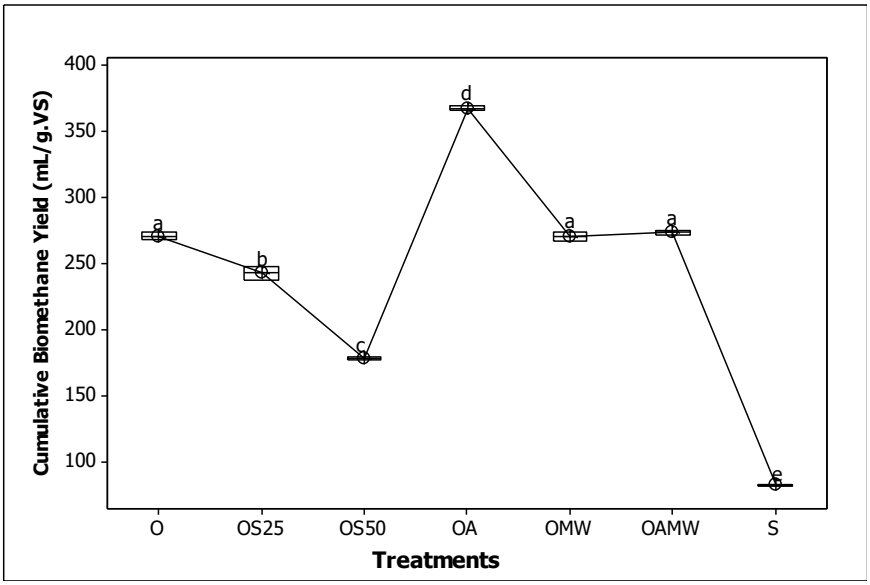

Fig.4. 4 Plot of treatment means and cumulative biomethane yield

From the graph of daily biogas production in Fig.4.5, the daily biogas flow from reactors O, OS25, OS50, OA, OMW, OAMW and S respectively can be seen and their time of flow terminations.

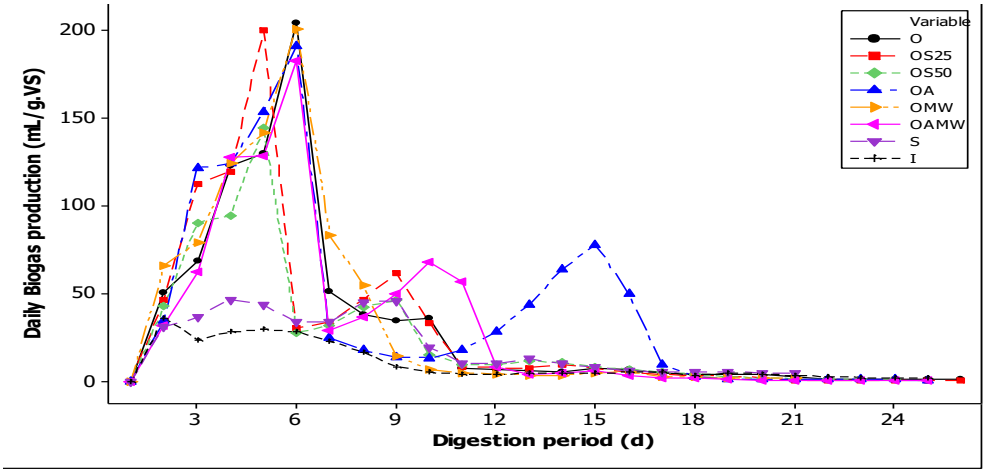

Fig.4. 5 Daily Biogas Production of pretreated and co-digested substrates

4.3.2.4 Kinetic study using first-order kinetic and modified Gompertz models

The experimental cumulative biomethane yield obtained from anaerobic digestion of pretreated and untreated okra waste was modelled based on first-order kinetic and modified Gompertz equation. Kinetic constants Y_m (biogas production potential), R_{max}, λ and k resulting from the model-fitting based on non-linear regression were determined and presented in Tables 4.8 and 4.9. In evaluating the model, predicted and measured mean yields were plotted against each other as shown in Fig. 4.6 and 4.7.

Table 4. 8 Results from using a modified Gompertz model

Parameter	**O**	**OS25**	**OS50**	**OA**	**OMW**	**OAMW**	**S**
Measured Biogas Yield- $Y_{(t)}$ (mL/gVS)	297.23	245.25	179.70	369.09	278.02	280.05	85.83
Predicted Biogas Yield -$Y_{(P)}$ (mL/gVS)	293.46	242.98	177.77	378.23	276.20	278.16	84.78
Difference between $Y_{(t)}$ and $Y_{(p)}$ (%)	1.27	0.93	1.07	2.48	0.66	0.68	1.22
Y_m (mL/gVS)	293.5	243	177.8	394.7	276.2	278.3	84.88
R_{max} (mL/gVS)	112.3	99.08	65.4	57.44	160.4	91.94	29.32
λ (d)	1.05	0.96	1.08	3.55	0.14	1.10	2.67
R^2	0.954	0.956	0.959	0.9265	0.9913	0.9575	0.992
RMSE	16.53	13.26	9.55	28.48	6.82	15.75	2.92

The lag phase λ is the time required for bacteria to adapt and start biogas production. λ in the modified Gompertz model in Table 4.8 and plotted in Fig. 4.6 was computed, the values were all between 0.09 day and 2.70 days, with higher lag phase noticed in the samples co-digested with sheep slurry. Lower λ values were suggested in Talha et al. (2018) to be dependent on the activeness of the adapted inoculum and biodegradable organic part of the okra waste. Y_m (biogas production potential) was the highest and was recorded by OA at 402.5 mL/gVS.

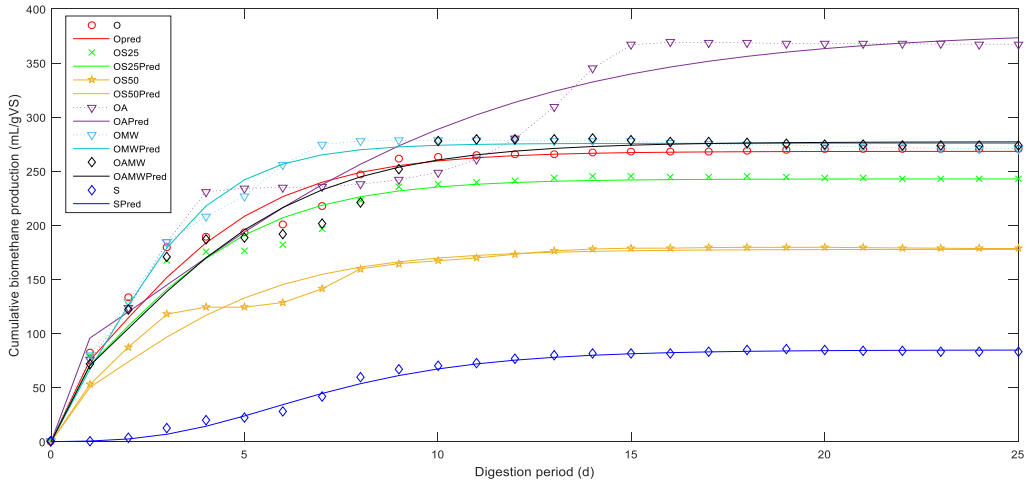

Fig.4. 6 Cumulative biogas production – experimental and modified Gompertz model

The root mean square (RMSE) value, which depicts the fitness of the model fell within the range of 2.92-28.48, All other samples expect OS50, OMW and S (9.55, 6.82 and 2.92 respectively) were outside the recommended value of 10 (Raposo et al, 2011), while others were outside the range. The R^2 value was within the range of 0.9265-0.992, this agreed with the R^2 of 0.92, which was adjudged a good fit and reported in anaerobic digestion of water hyacinth by Barua, et al. (2018). The difference between the modified Gompertz model-predicted and measured methane yields was in the range of 0.66%-2.48%. Budiyono, and Sumardiono (2014) and Talha et al. (2018) reported the differences in

the measured and predicted biogas yield to be 0.76-3.14 and 0.67- 10.86%, predicting this study to have performed well.

Table 4. 9 Results of using first-order Kinetic Model

Parameter	**O**	**OS25**	**OS50**	**OA**	**OMW**	**OAMW**	**S**
Measured Biogas Yield- $Y_{(t)}$ (mL/gVS)	297.23	245.26	179.70	369.09	278.02	280.05	**85.83**
Predicted Biogas Yield -$Y_{(P)}$ (mL/gVS)	294.82	244.10	178.74	370.33	279.16	280.01	**91.54**
Difference between $Y_{(t)}$ and $Y_{(p)}$ (%)	0.81	0.47	0.53	0.34	0.41	0.01	**6.65**
Y_m (mL/gVS)	295	244.2	178.9	384.4	279.2	280.0	**102.1**
k (d^{-1})	0.2957	0.3124	0.2819	0.1323	0.3543	0.2464	**0.0927**
R^2	0.9753	0.9768	0.9792	0.923	0.9945	0.9684	**0.931**
RMSE	9.88	9.416	6.647	27.82	5.298	10.04	**8.383**

The non-linear regression was used in fitting the first-order kinetic model and the results of parameters (k and Y_m) determined were presented in Table 4.9. The term k is a measure of the biomethane production rate per time in this study ranged between 0.0927 and 0.3653. Y_m calculated for all samples, ranging from 376.4 to 101.2 mL/gVS, with OA recording the highest Y_m value. Results of both k and Y_m computed were used in predicting yield. The measured and predicted yields were plotted as shown in Fig. 4.7. The positive k values seen in this study agrees with the reports of Budiyono and Sumardiono (2014) and Kafle et al. (2012) that positive values of k indicate, a faster rate of biogas production. Fitness errors (RMSE) for all samples ranging from 5.298 to 27.82 were all within the acceptable value of 10 except for OA at 27.82. The R^2 was between 0.923 and 0.9945. The model prediction difference between the measured and the predicted which is shown in Fig. 4.7 ranged from 0.01-6.65%.

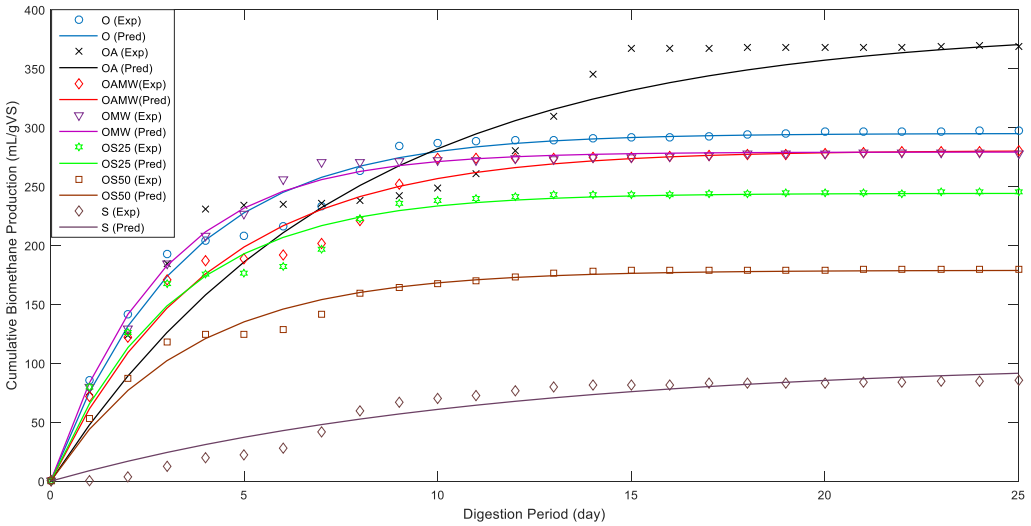

Fig.4. 7 Cumulative biogas production – experimental and first-order kinetic model

In comparing the predicted biomethane production from both models in Tables 4.8 and 4.9, the difference between measured and predicted gas yield was lower in the first-order kinetic model (0.01-6.65%) than with modified Gompertz model first-order kinetic model (0.66%-2.48%), this result was consistent with model comparisons made by Budiyono and Sumardiono (2014) and Deepanraj et al. (2015). The first-order kinetic model was better than the modified Gompertz model. Although modified Gompertz model predicted satisfactorily biogas production, the First-order kinetic model with higher R^2 and lower fitting errors (less than 10% for most samples) is better suited for predicting anaerobic digestion of okra waste.

4.3.2.5 ANN modelling and comparison with kinetic models

The neural network was trained to achieve a network with the capability to predict using dependent variables (RT and T), the independent variable (biomethane yield). The training stage, which is the most important process in determining the optimum neuron numbers of the hidden layer when the minimal performance factor (MSE) is attained. As described in Kipli et al (2012) and Najafi and Ardabili (2018), since MSE is the difference in factor between the estimator and the estimated, then smaller MSE value indicates higher prediction network accuracy. 70% of the dataset was used for training and the optimized training with smallest MSE values for O, OS25, OS50, OA, OMW OAMW and S at 10 hidden neuron layers were 0.0476, 0.0755, 0.0757, 0.0049, 0.6734 and 0.0310 respectively after several trainings were selected.

Table 4. 10 Results of using Artificial Neural Network

Parameter	**O**	**OS25**	**OS50**	**OA**	**OMW**	**OAMW**	**S**
Measured Biogas Yield- $Y_{(t)}$ (mL/gVS)	297.23	245.25	179.70	369.09	278.02	280.05	85.83
Predicted Biogas Yield -$Y_{(P)}$ (mL/gVS)	298.96	245.28	179.65	368.42	284.90	281.41	82.75
Difference between $Y_{(t)}$ and $Y_{(p)}$ (%)	0.00582	0.00013	0.0003	0.00182	0.02475	0.00486	0.03589
R^2	0.9998	0.99994	0.99986	0.99994	0.99994	0.99994	0.99997
RMSE	0.2182	0.2748	0.2752	0.7715	0.8206	0.4627	0.1762

On completion of network training, the developed network was tested. The network testing, which is a conventional way of comparing obtained output value with target values can be identified with the linearity of the coefficient of determination (R^2) as the indicator. In the network test results, the output values of O, OS25, OS50, OA, OMW OAMW and S respectively have 99.98%, 99.998%, 99.983%, 99.979%, 99.996%, 99.983% and 99.992% of linearity with target values. The R^2 and RMSE values between the output and target of the total result of the ANN process are shown in Table 4.10. Fig. 4.8

shows a plot of the overall coefficient of determination between the output and target from the input dataset.

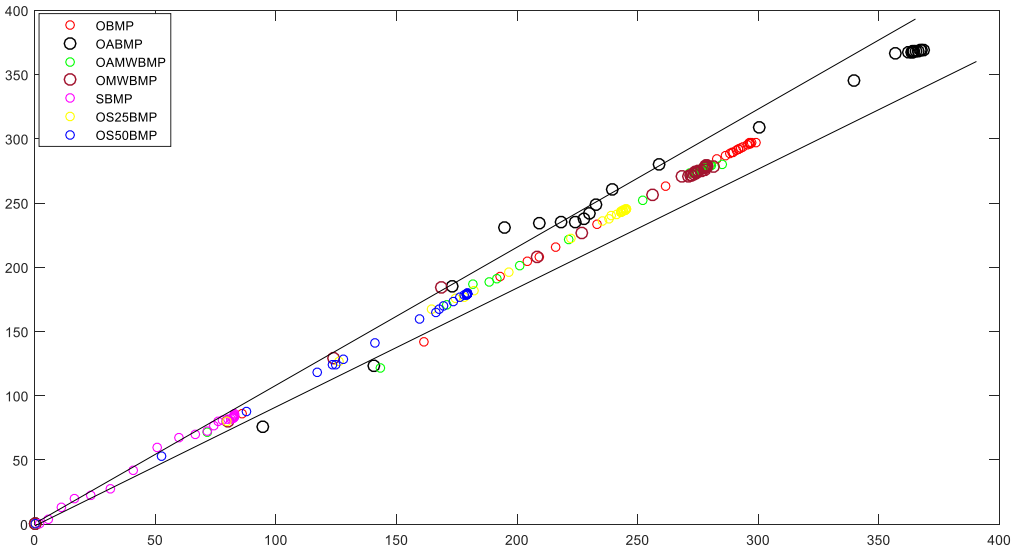

Fig.4. 8 Correlation of experimental Biomethane yields and ANN Predicted yields

In accordance with Raposo et al. (2011), which recommended that the % prediction between experimented and estimated data must not be more than 10% and the R^2 must be <70% for models to be deemed valid for in anaerobic digestion processes. Based on the results in Tables 4.8-4.10, comparing the R^2 of the three models, it can be observed that the ANN has higher linearity between target and output values (R^2 range of 0.9998 -0.99997), both the modified Gompertz and First-order kinetic models (with R^2 range of 0.9265-0.992 and 0.923-0.9945 respectively) have lower linearity between target and output values.

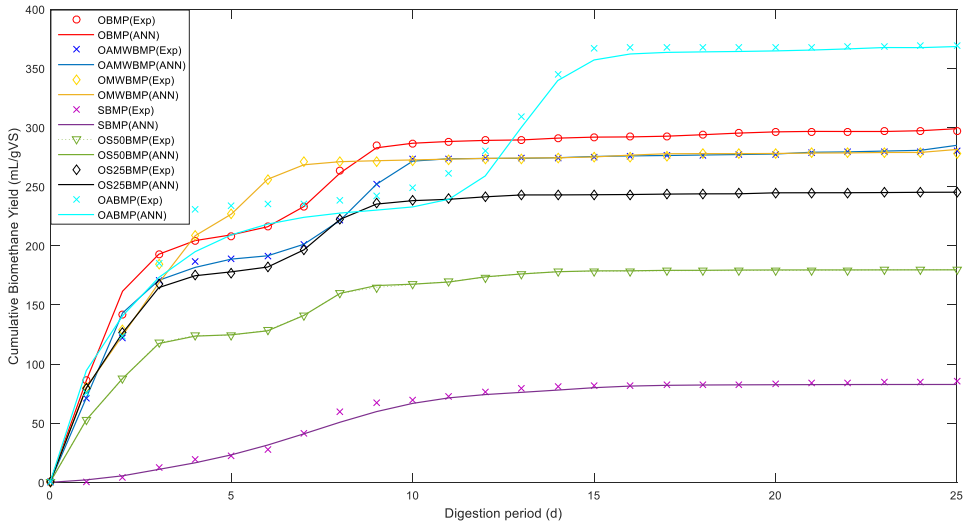

Fig.4. 9 Cumulative biogas production – Experimental and Artificial Neural Network

Prediction

The prediction difference between experimental and predicted biomethane yields, as well as the RMSE, showed the lowest values (Table 4.10) when compared to both the modified Gompertz model (Table 4.8) and first-order kinetic model (Table 4.9). This is in line with the results of Najafi and Ardabili (2018), which reported that ANN performed better than other regression model used in the study. Figs 4.6-4.9 showing the graph of both experimental and predicted cumulative biomethane yields over the digestion period of 25 days indicates that ANN fitted better than both modified Gompertz and first-order kinetic models.

4.3.3 Enhancement with PPy/Fe_3O_4

4.3.3.1 Substrate and digestate characteristics

The substrate (okra waste) pH, C, H, N and solid analysis (VS, VS/TS, TS, MC and AC) were determined as shown in Table 4.11. The initial and final pH values are between 7.00 and 7.90, the digestate pH values were lower than that of the substrates with iron-based additives ranging from 6.95 and 7.40, these values according to Kigozi et al. (2014) were within the recommended values (6.5 - 8.5). The determined carbon to nitrogen ratio (C:N) was 12.24, this according to Smith and Holtzapple (2011) the C:N value was below the recommend optimum ranges of 20 and 40 for maximum biomethane yield. This is suggesting that for the attainment of higher C:N values, co-digestion or nutrient supplementation is required. The oxygen and hydrogen contents (%) were 35.74 and 5.39 respectively. The substrate VS, TS and ash values of samples were between 13.11% to 13.74%, 15.15 % to 15.35% and 0.2329% to 0.2625% respectively. After 32 days of the anaerobic digestion process, the digestates were characterized and the VS/TS% reduction of 60.59, 61.52, 65.34, 62.76, 57.87 and 42.40% respectively recorded in reactors O, Oppy20, Oppy75, Oppy750 and Oppy1000. The highest removal of VS/TS% was observed in the Oppy20 reactor and the least reduction noticed in the Oppy1000 reactor. This may be attributable to inhibition effect of the higher dose of iron-based additives (Casals et al. 2014). The higher removal noticed in both Oppy20 and Oppy75 is in line with the report of Abdelsalam et al. (2017) and Ambuchi et al. (2016), that degradation of substrates was quicker in reactors containing optimum dosages iron additives.

Table 4. 11 Proximate and ultimate analyzes of samples

Parameter	Inoculum	O	Oppy20	Oppy75	Oppy750	Oppy1000
Initial pH	8.08	7.00	7.20	7.31	7.44	7.90
Final pH	7.68	6.90	7.05	7.16	7.15	7.40
Ash content (g)	0.03	0.2329	0.2452	0.2625	0.2401	0.2365
Total Solid (%)	1.50±0.01	15.15±0.2	15.48±0.00	15.28±0.00	15.25±0.24	15.35±0.24
Volatile Solid (%)	1.02±0.04	13.11±0.0	13.31±0.05	13.51±0.03	13.69±0.39	13.74±0.02
Final VS of TS %	60.86±1.6	61.52±1.0	65.34±0.06	62.76±1.12	57.87±1.28	42.40±1.95
Carbon % TS	NT	39.30±0.012	39.30±0.012	39.30±0.012	39.30±0.012	39.30±0.012
Hydrogen% TS	NT	5.39±0.003	5.39±0.003	5.39±0.003	5.39±0.003	5.39±0.003
Oxygen% TS	NT	35.74±0.003	35.74±0.003	35.74±0.003	35.74±0.003	35.74±0.003

NT = not detected, data expressed as the mean ± standard deviation

The morphology of the OW and the digestate were determined with SEM-EDS and the results are shown in Fig. 4.10. Although with visible observation, the morphological differences may be hard to estimate, the undigested OW appeared loose and rough, while morphologies of O, Oppy20 and Oppy75, Oppy750 and Oppy1000 digestates were densely packed, smoother and rigid. This is in line with Ambuchi et al. (2016). Digestates of Oppy750 and Oppy1000 showed more densely packed aggregates than O, Oppy20 and Oppy75. Xu et al. (2015) suggested that the more compact images connote tightly coated bacteria and EPS that inhibits Fe^{2+} penetration, hence resulting in lower biomethane production, this is true for samples for Oppy750 and Oppy1000.

Table 4. 12 Elemental compositions of undigested OW and digestates

Element	Undigested OW	O	Oppy20	Oppy75	Oppy750	Oppy1000
Fe (%wt)	0.1	0.3	0.5	0.6	0.9	3.9
Mg (%wt)	0.5	0.3	0.8	0.5	0.6	0.3
Ca (%wt)	1.5	1.4	1.7	1.8	1.7	1.3
C (%wt)	55.1	57.7	55.0	57.9	56.6	58.6
O (%wt)	38.3	31.2	30.8	30.6	30.5	28.4
K (%wt)	2.6	3.9	4.1	3.4	3.4	3.9
P (%wt)	0.4	0.4	1.1	0.8	0.9	0.3

The iron and other chemical composition were revealed through EDS analysis and shown in Table 4.12. The iron content in the digestate increased with the addition of Ppy/Fe_3O_4 NPs, which according to Zhao et al. (2018) was due to the activities of dissimilatory iron reduction with capabilities of utilizing recalcitrant substrate-types. Akin to the report of Suanon et al. (2016), the coexistence of C, O, Mg, P, Ca, K, etc. in the digestate was revealed by the elemental composition profile summarized in Table 4.12.

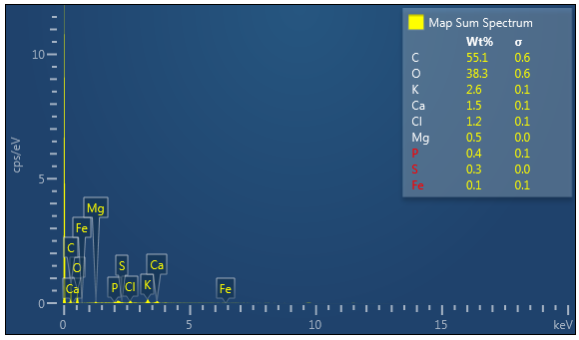

Undigested Okra waste

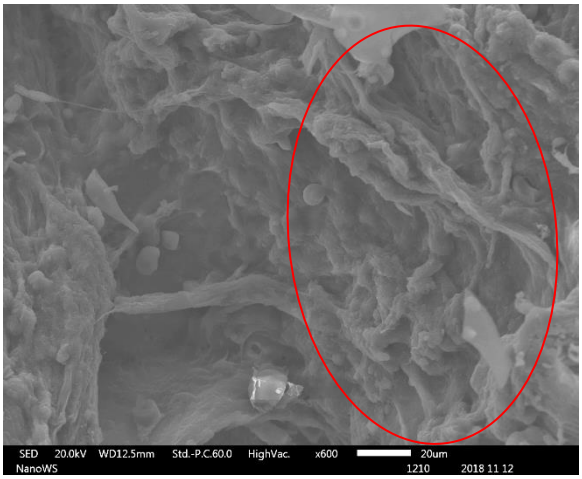

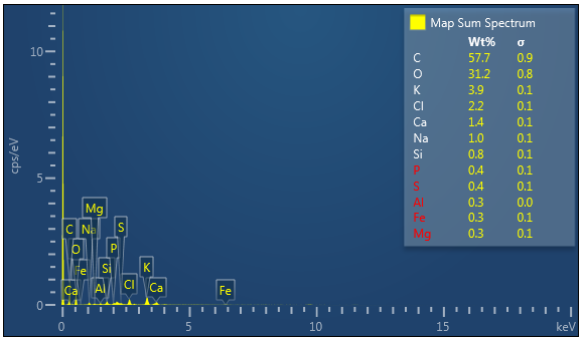

Digested Okra waste (O)

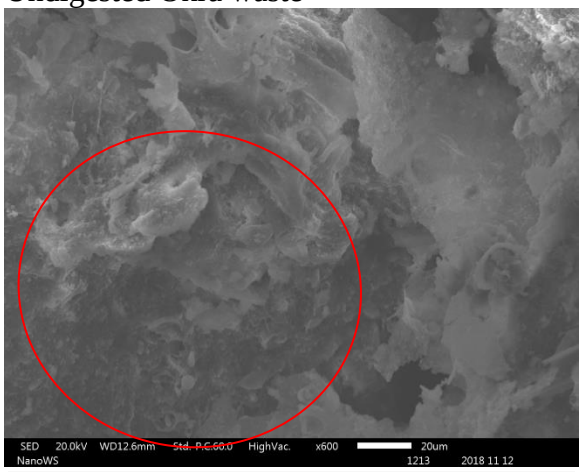

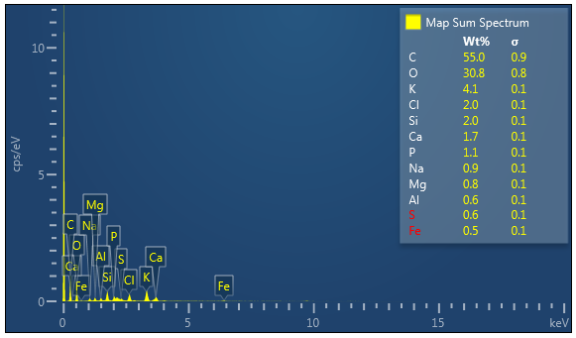

Oppy20

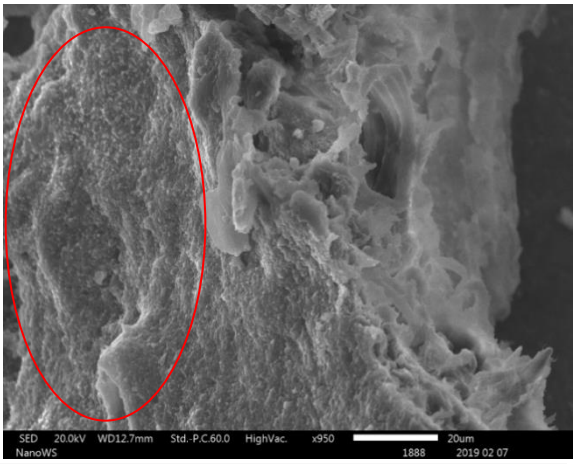

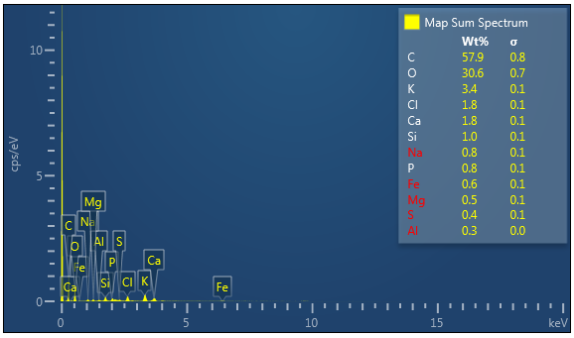

Oppy75

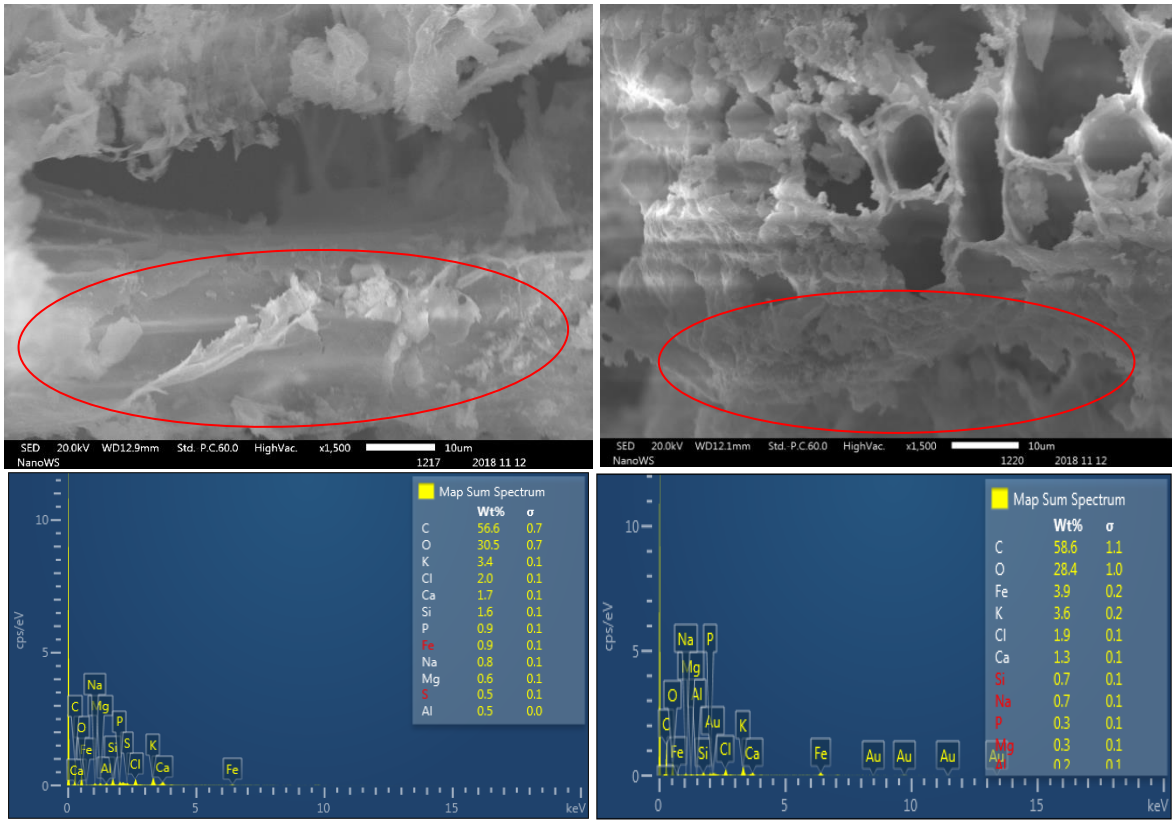

Oppy750 Oppy1000

Fig.4. 10 SEM-EDS images of Undigested and Digested Okra Waste Exposed to Different Doses of Ppy/Fe_3O_4 Nanoparticles.

4.3.3.2 Methane production

The effect of Ppy/Fe_3O_4 NPs on the cumulative biomethane yield and daily biomethane production at different dosages (Oppy20, Oppy75, Oppy750 and Oppy1000) were studied. The Ppy/Fe_3O_4 NPs has iron as the predominant element, which enhances methanogenic activities due to its Fe^{2+}/Fe^{3+} ionization capability and direct interspecies electron transfer (DIET) in syntrophic methanogenesis facilitation (Casals et al. 2014; Ali et al. 2017). In both Figs 4.11 and 4.12, it is indicated that when compared with the yields of the control sample (O), biomethane yield of Oppy20 was the most enhanced by 2.74%, followed by 0.8% enhancement by Oppy75. This result is akin to the stance of Abdelsalam et al. (2017), which reported an increased yield of 1.45% with the addition of 20 mg/l magnetic nanoparticles. More so, the noticeable increment achieved with the addition of 75mg/l of magnetic-Fe_3O_4 nanoparticles agrees with the results of Ali et al. (2017). The better results in both Oppy20 and Oppy75 may have been due to the enhancement of methanogenic activities and AD performance arising from the electron donor properties of reducing CO_2 into CH_4 as shown in equations 4.11 and 4.12 and low oxidation-reduction potential (ORP) (Ali et al. 2017; Abdelsalam et al. 2017). These resulted in the promotion of substrate solubilization, hydrolysis and acidification.

$$CO_2 + 4Fe^o + 8H^+ \rightarrow CH_4 + 4Fe^{2+} + 2H_2O \quad 4.11$$

$$CO_2 + 4H_2 \rightarrow CH_4 + 2H_2O \quad 4.12$$

The above-stated process in equations 4.11 and 4.12 has a balance of pH between hydrogen ion (H^+) and H_2CO_3 formed from CO_2, hence controlling the pH of the mixed liquor, which is key to the operations of methanogens. Statistically, biomethane potential of a substrate treated with 75 mg/l (Oppy75) and the control (O) is the same at the mean values of 887 mL/gVS and 880.3 mL/gVS and denoted with the same letter 'a' as shown in Fig.4.11, while others (Oppy20,750 and 1000) that are statistically different were denoted with different letters (b, c and d). The reactors with 750mg/l and 1000mg/l doses of Ppy/Fe_3O_4 recorded the least performance with a decrease of 5.99% and 21%. The lower yield at increased dosages may be as a result of inhibition and toxicity, which may arise from the electron acceptance contest between the Fe_3O_4 and the methanogens (Noonari et al. 2019; Zhao et al. 2018).

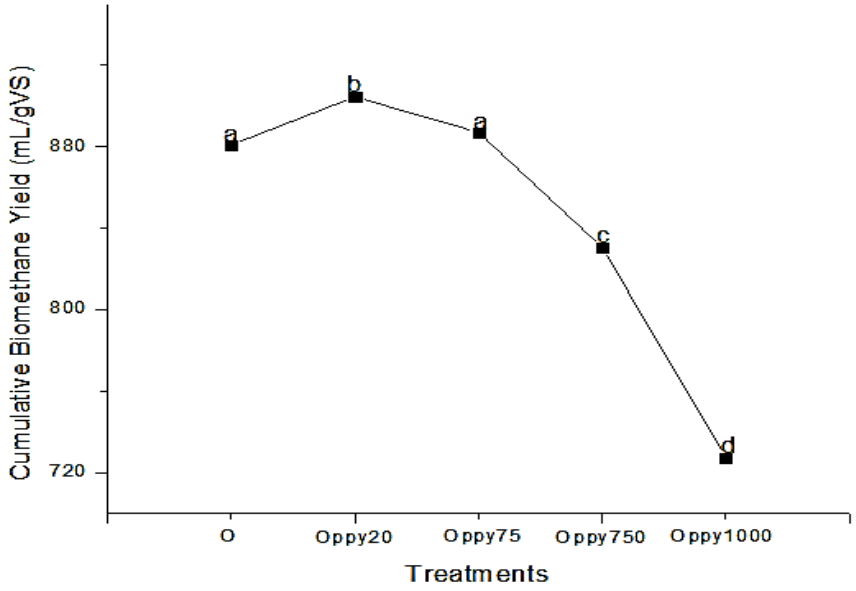

Fig.4. 11 Plot of Cumulative Biomethane Yield Indicating Significant Levels of Treatments @ $p<0.05$ (means with the same letter are statistically the same, while other shows difference in mean)

The graph of daily biomethane production in Fig.4.12. shows the daily biomethane flow from reactors O, Oppy20, Oppy75, Oppy750 and Oppy1000 and their time of flow terminations. The higher daily flow was observed within the first 5days, then daily decreased until termination at the 32nd day.

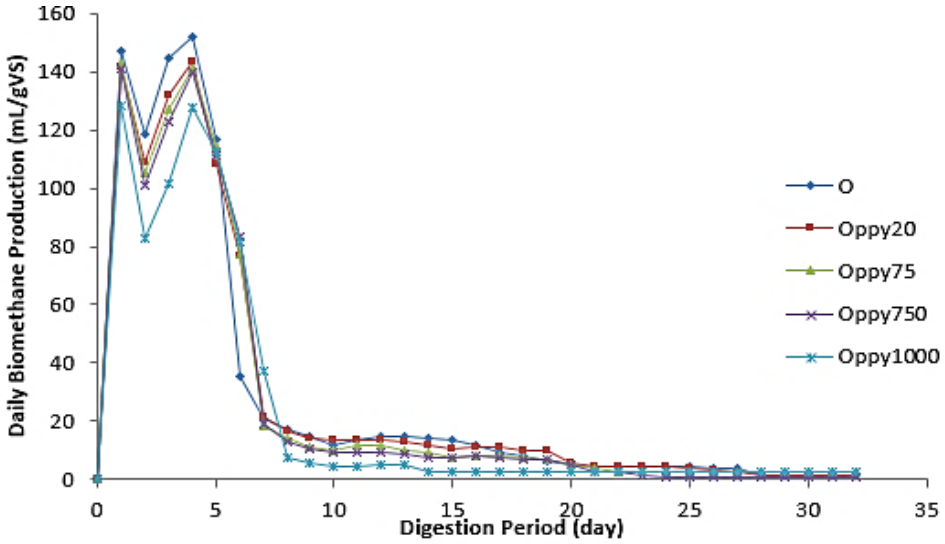

Fig.4. 12 Daily Biomethane Yields of Substrates With/Without Ppy/Fe_3O_4 Nanoparticles

4.3.3.3 Kinetic Models (First-order Kinetic Model and Gompertz Model) and ANN Model

Table 4.13 summarizes the predicted parameters of the two kinetic and ANN models studied. Among the three predictive models used in this study, the ANN model exhibited lowest difference (0-1.057%) between the measured and estimated biomethane production, then followed by the First order kinetic model modified (0.391-2.691%). Between the measured and the predicted biomethane yield, the modified Gompertz model showed the highest difference (0.508–4.753%). All the models showed low deviations between the estimated and experimental values (below 10%), signifying the accuracy of the models in predicting the reactor behaviour (Raposo et al. 2009).

The value of the kinetic constant (k) according to Kafle and Kim (2012) is used in determining the rate of biomethane production per time. In this study, k value ranged between 0.215 to 0.267 d^{-1} as shown in Table 4.13. These k values are higher than the previously reported ranges of 0.087-0.210 d^{-1} (Budiyono and Sumardiono, 2014), and 0.017-0.040 d^{-1} (Kafle and Kim, 2012) respectively for pretreated okra waste, vinasse with rumen and fish waste. The higher and positive k value obtained in this study concurs with observations of Kafle and Kim (2012) and Budiyono and Sumardiono (2014) that higher positive values of k are related to faster biomethane production rate.

The minimum time required for biomethane to be produced or for methanogens to acclimatize in the digester is lag phase λ (Kafle and Chen, 2016). The λ of all samples from the evaluated modified Gompertz model shown in Table 4.13 ranged from 2.328 to 2.505 days. The lack of swiftness observed in all samples resulting in high lag phase according to Talha et al. (2018), may be attributed

to inactiveness of the inoculum, other inhibitions to microbial activities on the biodegradable organic part of the okra waste, hence microbial enrichment of inoculum or microbial analysis of the mixed liquor is suggested. The maximum methane production rate (R_{max}) ranged from 59.74 to 63.75 mL/gVS.d, this describes the growth rate of methanogens specifically (Kafle and Chen, 2016).

Table 4. 13 Summary of results of two kinetic models and the ANN predictive model

First-order kinetic model	**O**	**Oppy20**	**Oppy75**	**Oppy750**	**Oppy1000**
Measured Methane Yield- Y(t) (mL/gVS)	880.3	904.45	887	830.55	727.3
Predicted Methane Yield -Y(P)mL/gVS)	870.667	883.99	863.128	827.307	734.355
Difference between Y(t) and Y(p) (%)	1.094	2.262	2.691	0.391	0.970
Ym (mL/gVS)	191.7	209	141.9	221.4	164.6
k (d-1)	0.231	0.215	0.224	0.239	0.267
R^2	0.988	0.988	0.986	0.987	0.977
RMSE	24.39	25.96	26.55	24.47	28.82
Modified Gompertz model					
Measured Methane Yield- Y(t) (mL/gVS)	880.3	904.45	887	830.55	727.3
Predicted Methane Yield -Y(P)mL/gVS)	853.536	864.677	844.838	811.406	723.607
Difference between Y(t) and Y(p) (%)	3.0403	4.398	4.753	2.305	0.508
Ym (mL/gVS)	314	318.1	310.8	298.5	266.2
Rmax (mL/gVS.d)	59.74	56.98	59.01	61.43	63.75
λ (d)	2.332	2.506	2.456	2.366	2.328
R^2	0.981	0.981	0.983	0.988	0.996
RMSE	32.12	32.65	30.13	23.79	12.74
ANN Predictive model					
Measured Methane Yield- Y(t) (mL/gVS)	880.3	904.45	887	830.55	727.3
Predicted Methane Yield -Y(P)mL/gVS)	880.824	904.45	885.49	839.330	727.739
Difference between Y(t) and Y(p) (%)	0.060	0	0.170	1.057	0.060
R^2	0.99999	0.99999	0.99994	0.99999	0.99999
RMSE	0.168	0.02	1.766	1.579	0.119

After evaluation of the kinetic models (first-order kinetic model and modified Gompertz model) via non-linear regression, the ANN achieved predictive capacity by training the network using a smaller value of MSE, higher value of R^2 and optimum neuron numbers are attained using dependent variables (RT and T) and biomethane yield (independent variables) to predict yields (Najafi and Ardabili, 2018). The first-order kinetic model, modified Gompertz model and ANN predictive model were plotted in Figs. 4.13-4.15 respectively.

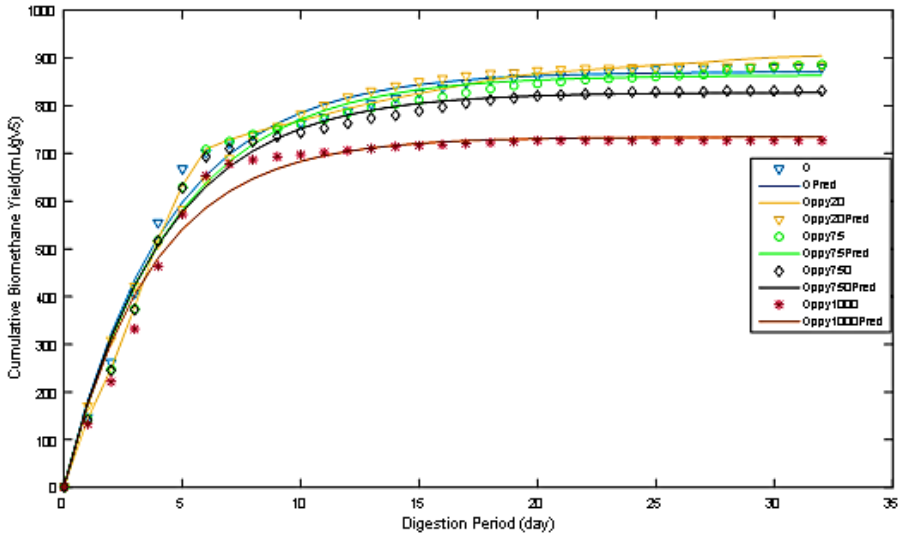

Fig.4. 13 Cumulative Biomethane Production-First-Order Kinetic Model and Measured Data

The model fitness indicators (RMSE and R^2) were reported in Table 4.13, RMSE and R^2 of the first-order kinetic model ranged from 24.39-28.82 and 0.977-0.988 respectively. For the modified Gompertz model, RMSE and R^2 have the ranges of 12.74-32.62 and 0.981-0.996 respectively. The best model fitness was observed from the ANN predictive model with the lowest RMSE (0.02-1.766) and Highest R^2 (0.99994-0.99999). However, based on the result, the ANN predictive model has the best performance followed by the First-order kinetic model.

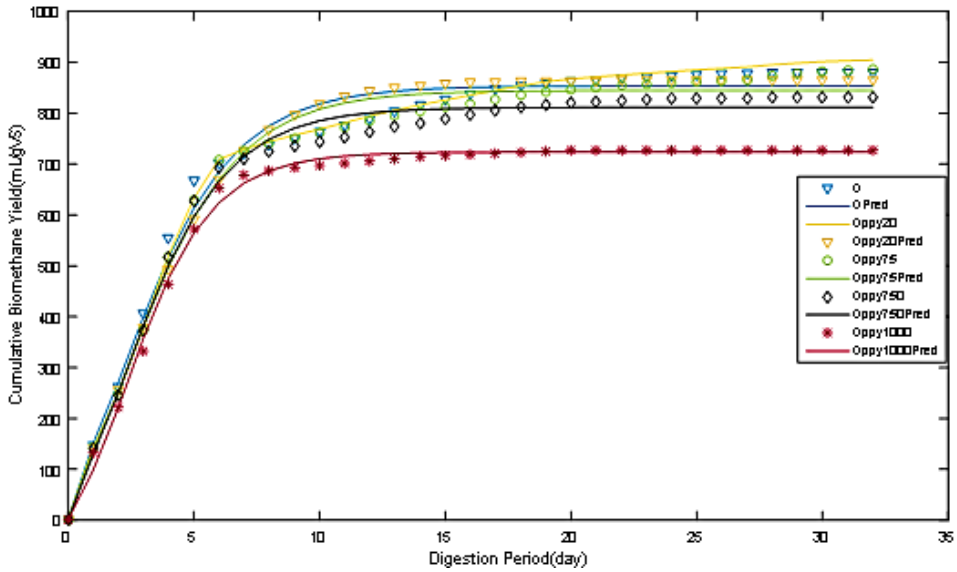

Fig.4. 14 Cumulative Biomethane Production-Modified Gompertz Model and Measured Data

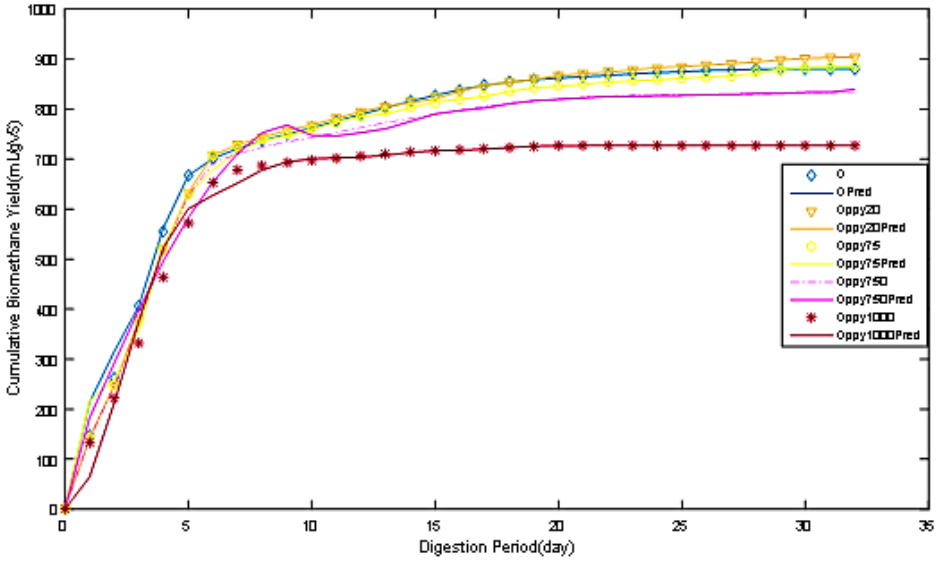

Fig.4. 15 Cumulative Biomethane Production- Artificial Neural Network Prediction and Measured Data

In comparing all the models (first-order kinetic model, Modified Gompertz and ANN), it can be observed that the ANN performed better than the kinetic models used in this study on all indexes (of the model fitness indicators and the difference between predicted and measured methane yield). Higher linearity of the ANN R^2 (0.99994 – 0.99999) when compared with R^2 of kinetic models, lower prediction differences and RMSE were observed in ANN model unlike in the kinetic models with higher differences and RMSE values, this is in line with previous studies of Najafi and Ardabili, (2018). The performance of the First-order kinetic model, which was the second-best agrees with the report of Kafle and Chen (2016); Kafle et al. (2013); Budiyono and Sumardiono (2014). As stated in Raposo et al. (2009), the difference between Y_m and Y_t must not be more than 10 %, above which such kinetic model is deemed not valid for predicting anaerobic digestion processes, all models predicted within the recommendation 10%.

4.3.4 Comparative studies on the effect of selected iron-based additives

4.3.4.1 Substrate and digestate characteristics

Solid analysis (VS, TS, VS/TS, etc.), C, H, N and pH were determined from the substrate (okra) as shown in Table 4.14. The VS, TS, VS of TS and ash values of samples were respectively between 1.50 % to 15.16 %, 1.02 % to 13.37 %, 68 % to 91.0347 % and 0.03 to 0.2625 %. The ratio of carbon to nitrogen calculated was 12.24; this is below the optimum recommended value of between 20 and 40 for biogas production, necessitating the need for co-digestion in subsequent operation with substrates of higher C: N value or nutrient supplementation (Smith and Holtzapple, 2011). The

hydrogen and oxygen contents (%) were 5.39 and 35.74 respectively. Both the initial and final pH values ranged between 7.68 and 8.44, which were within the recommended values of between 6.5 and 8.5 (Kigozi et al. 2014).

Table 4. 14 Proximate and ultimate analyzes of samples

Parameter	**Inoculum**	**O**	**Ppy-Fe_3O_4**	**nZVI-20**	**nZVI-1000**	**Fe_2O_3**	**Fe**
Initial pH	8.08	8.15	8.44	8.13	8.20	8.10	8.12
Final pH	7.68	8.20	7.76	8.15	7.91	7.80	8.00
Ash content (g)	0.03	0.23	0.25	0.263	0.240	0.237	0.237
Total Solid (%)	1.50±0.01	1.68±0.026	1.75±0.08	1.866±0.024	1.611±0.2	1.54±0.15	1.30±0.035
Volatile Solid (%)	1.02±0.04	1.17±0.027	1.225±0.06	1.31±0.066	1.201±0.1	1.182±0.07	1.182±0.005
VS of TS %	68±0.08	69.35±0.55	70.22±0.29	70.220±2.65	74.716±3.04	77.267±1.25	91.035±2.86
Carbon % TS	NT	39.30±0.01	39.30±0.01	39.30±0.012	39.30±0.01	39.30±0.01	39.30±0.01
Hydrogen% TS	NT	5.39±0.003	5.39±0.003	5.39±0.003	5.39±0.003	5.39±0.003	5.39±0.003
Oxygen% TS	NT	35.74±0.003	35.74±0.003	35.74±0.003	35.74±0.003	35.74±0.003	35.74±0.003

NT = not tested, data expressed as the mean ± standard deviation

At the end of 19 days' digestion process, the solid analysis of the digestates was conducted and characterized. The VS (TS %) reduction of 56.493, 60.59, 57.84, 58.599, 56.85 and 55.22 % respectively for O, Ppy-Fe_3O_4, nZVI-20, nZVI-1000, Fe_2O_3 and Fe reactors were recorded. All the highest VS (TS %) reduction was seen in the reactor containing 20 mg/L of Ppy-Fe_3O_4 additive, the least reduction was recorded in the reactor with 750 mg/L of Fe. It could be observed that all the nano-iron additives achieved higher solid reduction. This is in line with the assertion in Ambuchi et al. (2016), that microbes degrade swiftly the substrates in reactors containing nano-iron additives. The digestate pH values were generally lower than that of the pre-treated/co-digested substrates, which was between 7.76 and 8.15.

4.3.4.2 Methane production

The cumulative biogas yield with methane content and daily methane production as shown in Fig.4.16a, and 4.17 respectively, indicated that both biogas yield and methane content of Ppy-Fe_3O_4 were the most enhanced by 10.32 % and 25 % when compared with the yields of the control sample. Biogas yields from reactors with Fe_2O_3 and nZVI-1000 additives are statistically the same at the mean values of 429.35 mL/gVS and 424.2 mL/gVS. Least performance was seen in the nZVI-20 and Fe respectively with the yield of 377.55 mL/gVS and 373.85 mL/gVS, which are also statistically the same at $p < 0.05$, but with different methane compositions as seen in Fig 4.16b. The variations and low biogas yield was seen in most iron-based enhanced reactors suggested inhibition which, according to Bharathiraja et al. (2018) stated that feedstock or presence of inhibitors or operational

parameters can reduce the activities of methanogens and may be responsible for the variations in the daily production peaks.

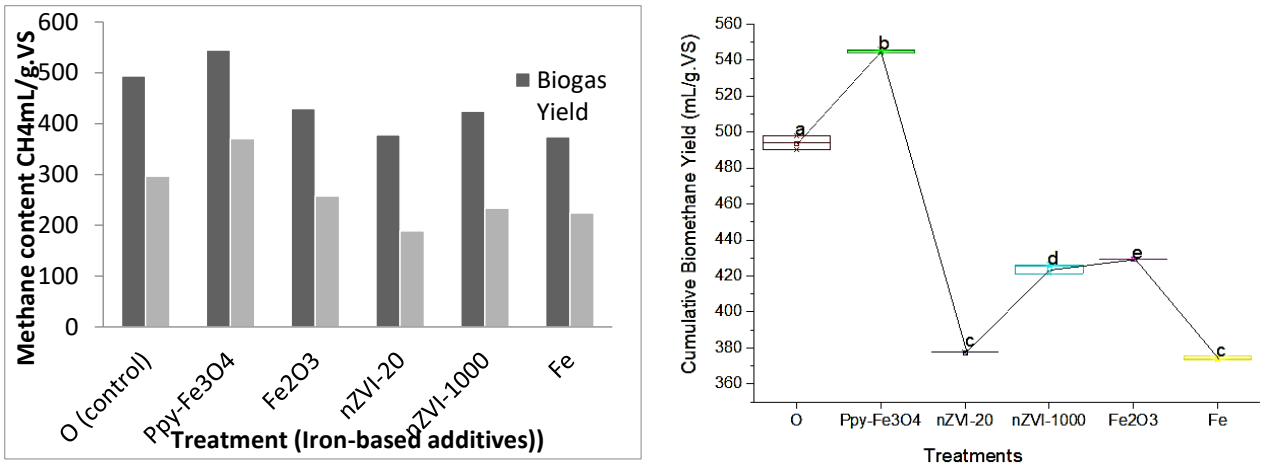

(A) (B)

Fig.4. 16 (a) Cumulative biogas yield and methane composition (b) Plot of treatment means indicating the level of significance @ $p<0.05$

Although the enhancement of okra waste with iron-based additives has not been previously studied (to the best of our knowledge), the result of the magnetic-Fe_3O_4 nanoparticles (Ppy-Fe_3O_4) used in this research was in line with other studies. Abdelsalam et al. (2017) reported that the use of 20 mg/L of nZVI and 20mg/L magnetic-Fe_3O_4 nanoparticles in anaerobic digestion of manure, achieved respectively 1.45 and 1.66 times increase in biogas volume. Wang et al. (2018) reported that 1000mg/L of nZVI gave the highest yield with 31 days of digestion of sludge, although the same dosage in our report underperformed, elongation of retention time is suggested.

The graph of daily biogas production in Fig.4.17 shows the daily biogas flow from reactors O, Ppy-Fe_3O_4, nZVI-20, nZVI-1000, Fe_2O_3 and Fe and their time of flow terminations.

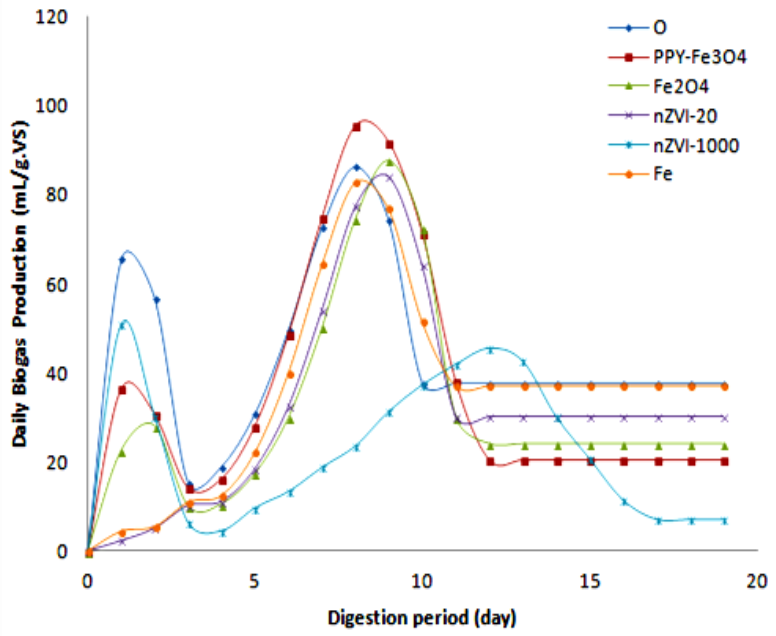

Fig.4. 17 Daily Biogas Yields of Substrates With/Without Iron-Based Additives

4.3.4.3 Impacts on substrate and digestate characteristics

After 19 days' digestion period, representative digestates from some reactors (O, Ppy-Fe_3O_4, Fe) were collected based on biogas yields, observed under SEM-EDS and compared with the undigested sample. The structural images of substrate and digestates from SEM-EDS in Fig 4.18 shows that the undigested okra waste (Fig 4.18a) appeared loose and rough, while digested samples showed a rigid and compact appearance. This in line with the reports in Zhang et al. (2018) and Ambuchi et al. (2018). Fig (4.18c and d) shows more densely packed aggregates. This according to Xu et al. (2015) suggests that those densely packed aggregates visible in all digestates are tightly coated bacteria and EPS that prevent penetration of iron additives, hence the low biogas yields in from them. More micropores were seen in Fig (4.18c), this goes to show that the addition of iron-additives aids the creation of micropores structures, which according to Zhang et al. (2018) aids the growth of acidogens and methanogens to grow, enhancing the interspecies mass and electron transfer.

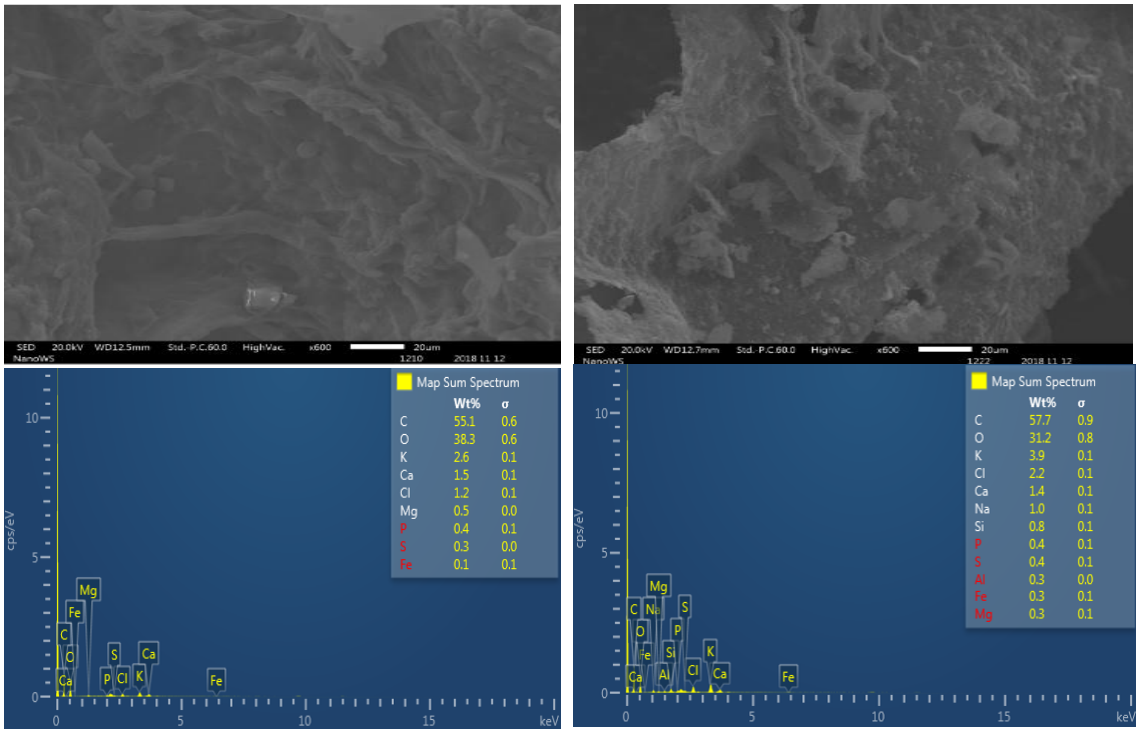

(A) (B)

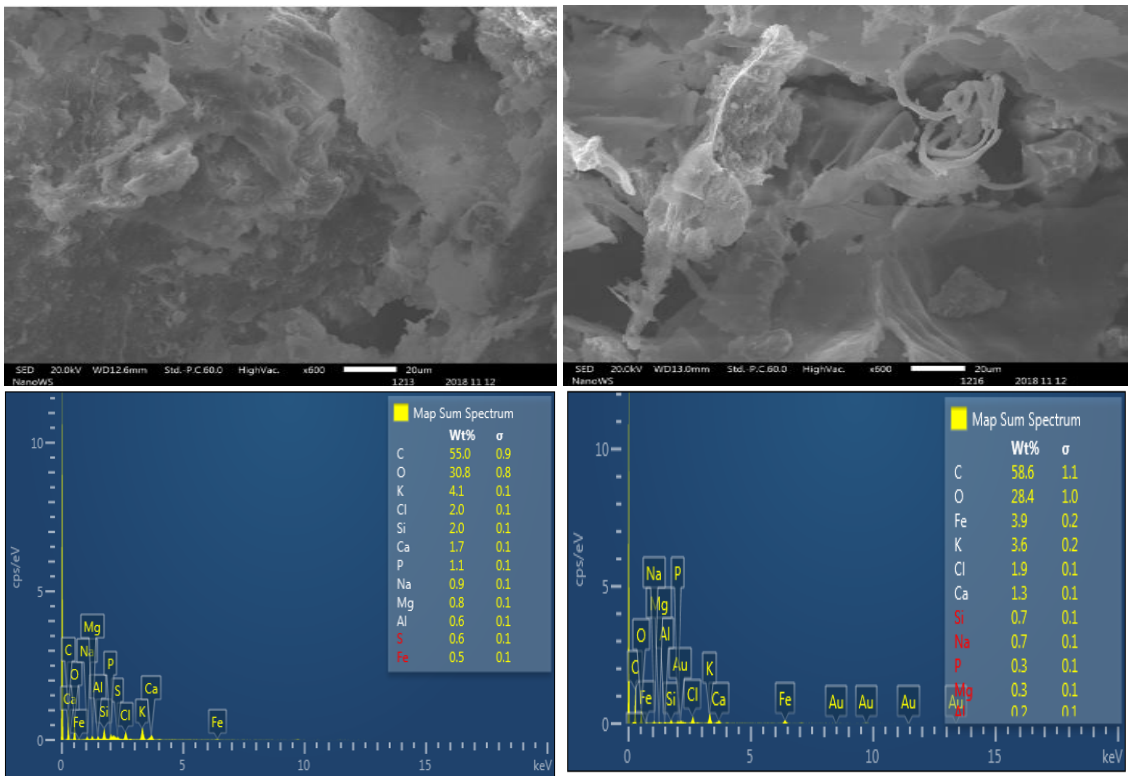

(C) (D)

Fig.4. 18 SEM and EDS of (A) Undigested okra, (b) O (control digestate), (c) PPy/Fe_3O_4, and (d) Fe. The size bar corresponds to 5μm

4.3.4.4 Kinetic study (Gompertz Models) and ANN Model

From the model-fitting of a non-linear regression and the network training, testing and validation of the experimental cumulative biomethane yield obtained from the anaerobic digestion process of okra waste enhanced with iron-based additives, model parameters (Y_m, R_{max} and λ) and model fitness indicators (RMSE and R^2) were determined and presented in Table 4.15 and Table 4.16. The plots of predicted and experimental mean yields were plotted together and shown Figs. 4.19 and Fig 4.20.

Table 4. 15 Results of using Artificial Neural Network

Parameter	**O**	**Ppy/Fe_3O_4**	**nZVI-20**	**nZVI-1000**	**Fe_2O_3**	**Fe**
Measured Biogas Yield- $Y_{(t)}$ (mL/gVS)	493.90	544.90	377.55	424.2	429.35	373.85
Predicted Biogas Yield -$Y_{(p)}$ (mL/gVS)	494.41	544.91	377.59	424.16	429.35	374.18
Difference between $Y_{(t)}$ and $Y_{(p)}$ (%)	0.10326	0.00184	0.01059	0.00943	0.000	0.08827
R^2	0.99914	0.99914	0.99986	0.99994	0.9989	0.99964
RMSE	9.2	3.3	0.2752	0.7715	3.6	0.25

The lag phase λ is the duration needed for the adaptation of bacteria before the commencement of biogas production. In the modified Gompertz model, λ of all the samples as were computed and shown in Table 4.16 and Fig. 4.19 ranged between 0.41 and 3.55 days, the higher lag phase observed in sample Fe and Fe_2O_3 shows lack of swiftness unlike in all the nanoparticles (Ambuchi et al. 2016). According to Talha et al. (2018), lower λ values suggest the activeness of the inoculum and that of the microbes on the biodegradable organic part of the okra waste.

Table 4. 16 Results from using a modified Gompertz model

Parameter	**O**	**Ppy-Fe_3O_4**	**nZVI-20**	**nZVI-1000**	**Fe_2O_3**	**Fe**
Measured Biogas Yield- $Y_{(t)}$ (mL/gVS)	493.9	544.9	377.55	424.2	429.35	373.85
Predicted Biogas Yield -$Y_{(P)}$mL/gVS)	521	534.3	385.7	445.8	447.4	381.2
Difference between $Y_{(t)}$ and $Y_{(p)}$ (%)	5.202	1.984	2.113	4.845	4.034	1.928
Ym (mL/gVS)	191.7	209	141.9	221.4	164.6	140.3
R_{max} (mL/gVS)	22.07	30.44	31.65	10.87	25.77	31.5
λ (d)	1.05	0.41	0.81	0.75	1.43	3.55
R^2	0.967	0.976	0.991	0.976	0.973	0.992
RMSE	34.33	34.11	16.36	24.52	30.16	15.4

The highest value of Y_m (biogas production potential) was obtained in the sample enhanced with nZVI-1000, the value is 221.4 mL/gVS. The model difference between the experimental biogas yield and model predicted ranged from 1.928 % to 5.202 %. This is in the ranges of previously reported differences of 0.67- 10.86 % (Talha et al. 2018). The fitness of models is dependent on the values of root mean square (RMSE) and in this study, it ranged between 16.36 and 34.11 for the modified Gompertz model and are all above the recommended value of 10. The R^2 value of between 0.967 and 0.992, agreeing with R^2 of 0.92 reported in Barua et al. (2018).

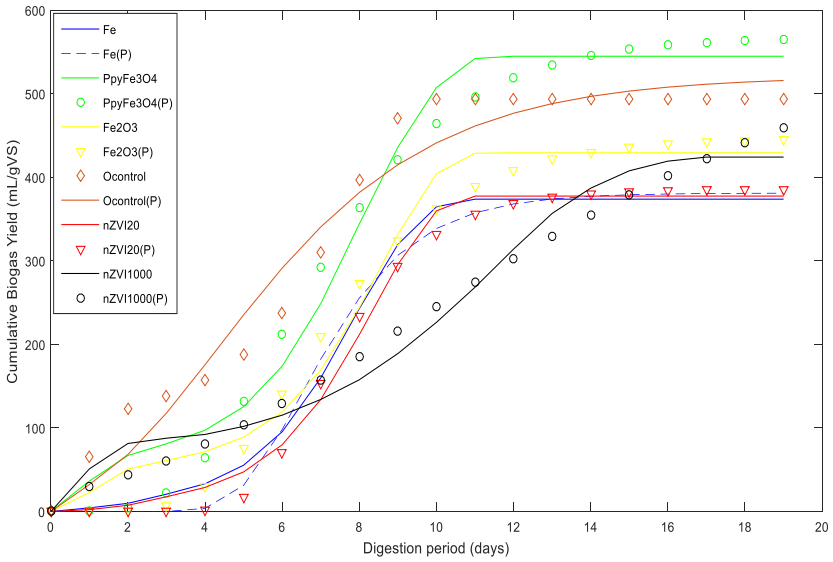

Fig.4. 19 Cumulative Biogas Production-Modified Gompertz Model and Measured Data

After attaining the capacity to predict by training the network, dependent variables (retention time (RT) and temperature (T)) and biogas yield (independent variables) were used to perform ANN tasks. According to Najafi and Ardabili (2018), the smaller value of MSE (minimal performance indicator) shows high prediction accuracy, low MSE and the optimum neuron numbers, is achieved during the training stage, since MSE is the difference in factor between the estimator and the estimated, then smaller MSE value indicates higher prediction network accuracy. At 10 hidden neuron layers, 70% of the input dataset (RT and T) was used to train the networks till optimized training with the smallest MSE values is attained. As shown in Table 4.15 and Fig. 4.20, these MSE values for O, Ppy-Fe_3O_4, nZVI-20, nZVI-1000, Fe_2O_3 and Fe respectively at 9.2, 3.3, 0.2752, 0.7715, 3.6 and 0.25 were selected after several trainings.

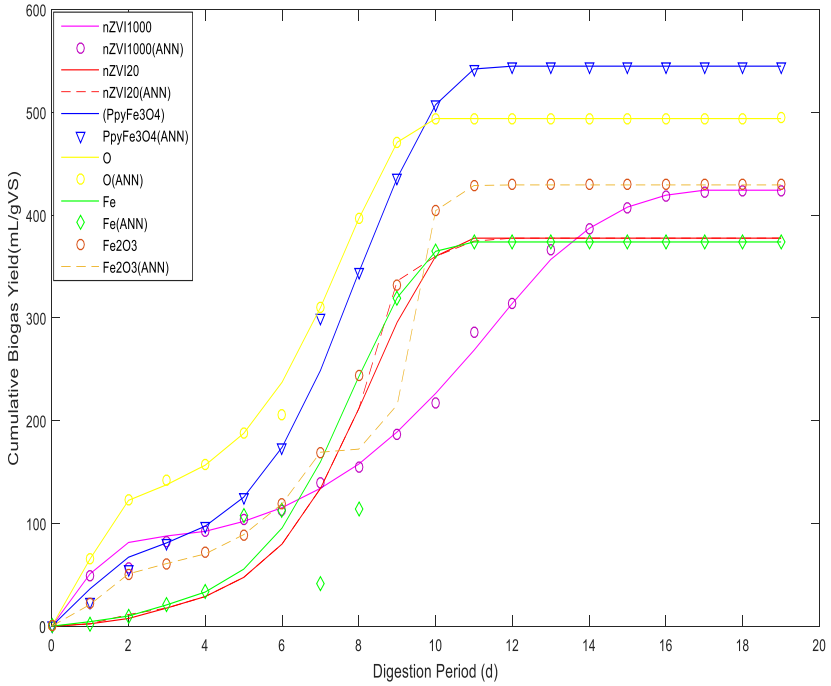

Fig.4. 20 Cumulative Biogas Production-Experimental and Artificial Neural Network Prediction

After the training stage, the network testing, which is a way of comparing obtained output value with target values, was performed. The testing indicator is identified with the linearity of the coefficient of determination (R^2). The values of O, Ppy-Fe_3O_4, nZVI-20, nZVI-1000, Fe_2O_3 and Fe output network test results respectively have 99.914 %, 99.914 %, 99.986 %, 99.994 %, 99.89, and 99.964 % of target linearity values as reported in Table 4.15 and Fig. 4.20. Low prediction differences were achieved with ANN ranged between 0.000 and 0.10326, it is evident that all enhanced samples were predicted better than the control sample.

In comparing both models (Modified Gompertz and ANN), it can be observed that the ANN performed better than the kinetic model used in this study on all indexes. Higher linearity of the ANN R^2 (99.89 – 99.994) when compared with R^2 of Modified Gompertz model (0.967 - 0.992), lower prediction differences and RMSE were observed in ANN model unlike in the kinetic model with higher differences and RMSE values. The result of this study is supported by previous works of Najafi and Ardabili (2018) where it was reported that the ANN model outperformed all the kinetic models studied. All models predicted within the recommendation of Raposo et al. (2011), which stated that the difference between Y_m and Y_t must not be more than 10 %, above which such kinetic model is deemed not valid for predicting anaerobic digestion processes.

4.4 Summary

Based on the different experiments conducted, the following conclusions were arrived at:

i. Okra waste was found to be a viable feedstock for biogas production. It also shows that both energy content and elemental composition evaluation methods could be reasonably used to calculate TBMP and BD_{CH4} of okra waste. The goodness of fit, good methane yield prediction and lowest percentage prediction difference showed that both transference and first-order models performed better than the other models evaluated. The positive kinetic constant and lower lag phase confirmed the high rate of degradation. Based on the goodness of fit, the logistic model had the worst performance.

ii. Due to the commendable BMP of okra and the need to increase its biodegradability in this study, pretreatment of okra waste with alkaline (NaOH) was found to have enhanced the anaerobic biodegradability of okra wastes by 45.87%. Other pretreatments were not statistically different from untreated okra wastes, the samples co-digested at varying ratios showed a decline in biogas yield. Initial and final results of parameters like VS and VFA were monitored during the digestion period. All samples recorded high VS and VFA concentrations removal. Results obtained from the experiment were used to fit modified Gompertz, First-order kinetic models and perform ANN. The ANN was observed to have "learned" the experimental data and to have most described cumulative biogas production with the better goodness of fit (R^2) and RMSE values compared to the first-order kinetic model and modified Gompertz models. Effects of prolonged pretreatment of okra with microwave and the declining biomethane yield noticed in the co-digested samples need to be further investigated.

iii. In order to achieve improved biogas yield, the study on the impact of adding iron magnetic nanoparticles (Ppy/Fe_3O_4) for enhancement of okra waste was successfully carried out. The bioreactor enhanced with 20mg/l of iron additives (Oppy20) gave the highest result of 2.74% rise in biomethane production when compared to the control sample. The lowest yield was recorded in the bioreactor enhanced with 1000mg/l of Ppy/Fe_3O_4 (Oppy1000). From the SEM images, higher disintegration was noticed in the structures of samples with additives, with higher availability of Fe ions (wt%) in the analyzed digestates. The prediction of biomethane from the experimental data using the kinetic models (first-order kinetic model and modified Gompertz model) and ANN predictive model, were all within acceptable limits, but ANN performed outclassed the other models. It can be concluded that Ppy/Fe3O4 nanoparticles

which are often used for water treatment can enhance the anaerobic digestion process. The high lag phase noticed should necessitate studies on the activeness of the methanogens or possible toxicity/ inhibition.

iv. Based on the results of previous enhancement processes by this author and other studies on the influence of iron-based enhancement on anaerobic digestion of wastes, the comparative assessment of the effect of iron-based additives on okra waste was successfully carried out. In Enhancement of okra waste with iron additives (Ppy-Fe_3O_4, nZVI-20, nZVI-1000, Fe_2O_3 and Fe), the best result of 10.32% and 25% rise in both biogas yield and methane content respectively was achieved from the sample with 20mg/mL of Ppy-Fe_3O_4. The yields from other additives were lower than that of the control sample. High solid (VS of TS%) removal was recorded, especially in samples enhanced with iron-based additives. From the SEM images, higher degradation took place in the structures of samples with additives. Both modified Gompertz model and ANN network, using the experimental data, predicted within acceptable recommendations, but ANN outclassed the other with better goodness of fit (R^2 and RMSE). Long retention time and other cause of a decline in the biogas yield of other additives are to be studied.

Chapter Five

Optimization of iron enhanced anaerobic digestion of agro-wastes for biomethane production and phosphate release

5.1 Introduction

The global waste generation is on the rise due to increasing population growth, just like agro-industrial wastes, municipal wastes are estimated to generate above 3.40 billion tonnes by 2050 with organic waste constituting above 50 per cent of the total global wastes and more than 33 per cent of these are improperly disposed of (World Bank, 2020). Anaerobic digestion is an established technology with dual capabilities of waste treatment and bioenergy production is most suited for handling the enormous organic wastes being generated annually while closing the widening global energy-supply gap (Puyol et al. 2018). In the absence of oxygen, complex polymeric biodegradable organics are broken down by microorganisms and enzymes to monomers and simple molecules via a four-stage process of hydrolysis, acidogenesis, acetogenesis and methanogenesis (Siami et al. 2020; Dobre et al. 2014). Hydrolysis phase which is known as the rate-limiting step in anaerobic digestion process aids substrate solubilization but is restricted by nature of substrate, presence of inhibitors, etc. (Choi et al. 2018; Bharathiraja et al. 2018). Generally, the efficiency of all anaerobic digestion stages and processes are influenced by factors such as digestion temperature, C/N ratio, pH, loading rates, hydraulic retention time, microbial biomass, etc. (Kumar et al. 2020; Dobre et al. 2014).

However, due to low biodegradability associated with substrates (especially lignocellulosic and most 4th generation bioenergy feedstocks), there have been notable efforts toward the achievement of high substrate degradability and ultimately increased biogas yield. Some of these intensification strategies include improvement of bioreactor operational conditions, types and configurations, advancements in alternative substrate usage, co-digestion, substrate pretreatment and nutrient or additive supplementation (Puyol et al. 2018; Bharathiraja et al. 2018). Anaerobic co-digestion is vital for the maintenance of digestion pH and C/N ratio, etc. as well as amelioration of adverse impacts of toxic substrates with the addition of non-toxic ones for improved biogas production (Ghaleb et al. 2020). It also increases the organic loading rate of the biodigester. Several pretreatment options for increased substrates degradability and hydrolysis rate through the disruption of extracellular polymeric substance (EPS), sludge flocs, intercellular organic matter, the cell wall of organisms and polyvalent cations (Siami et al. 2020). Any of these pretreatment methods, which are selected based on economic feasibility and effectiveness include physical (microwave, ultrasound or milling), thermal, enzymatic

or biological, chemical (alkali or acid) and combined methods (Zaidi et al. 2020). It has also been reported in Ding et al. (2017) the combined pretreatments like steam/microwave heating and enzymolysis assisted by acid/alkali assisted pretreatment achieved an increase in biomethane yield. Although the afore-mentioned enhancement techniques recorded a remarkable improvement in biomethane production, according to Zhao et al. (2018), the additional input (energy and chemical) cost may not be compensated for by the resulting yield increase. Similarly, extreme pH, salt formations and overall toxicity are serious concerns bedevilling the choice of chemical pretreatments (Zhang et al. 2014b; Hashimoto, 2004).

On the other hand, the use of other efficient, cheaper and environmentally friendly enhancement options such as additives are vital for cost-effective biogas production (Abdelsalam et al. 2016; Wang et al. 2018). Additives such as iron (Fe), selenium (Se), nickel (Ni), cobalt (Co), molybdenum (Mo), etc. are vital for nutrient augmentation, microbial growth and general biochemistry of anaerobic digestion (cell lysis, VFA usage and biogas production) as well as being important makeup of enzymes and cofactors needed to stimulate anaerobic digestion (Menon et al. 2017; Linville et al. 2016). These additives trigger higher organic loading rate by improving feedstock utilization and process stability (Zaidi et al. 2020; Zaidi et al. 2019). According to Menon et al. (2017), nutrient availability or additive supplementation (when scarce in substrates) eliminates the inhibitory influences of VFAs, ammonia, humic substances, among others. When compared to other additives, iron-based additives (nanoparticles, scraps, powder, liquid, etc.) have gained more prominence because they are mostly cheap, easy to apply and its ability to reduce oxidative reductive potential (ORP) of anaerobic digestion and cofactor capabilities with lots of proteins due to their role as electron donor and acceptor (Casals et al. 2014; Emerson et al. 2010). Studies on the viability of iron additives as a stabilizing agent for anaerobic digestion of waste confirmed its positive effects on improving the entire anaerobic digestion environment and its capability to enhance hydrolysis-acidification enzymes activities (Zhang et al. 2015; Feng et al. 2014).

Although iron supplementation enhances anaerobic digestion when in excess, the reactive oxygen can initiate Fenton reaction and create toxic environments capable of inhibiting microbial activities. However, when in low supply, it is easily used up by methanogens, thereby reducing the activities of microbes in the biodigester. Against this backdrop, optimum dosage supplementation is needed to maintain bacteria activities and stability (Casals et al.2014). Iron additives (eg. Fe_3O_4) with conductive properties aid methanogenic growth, direct interspecies transfer, degradation of polymeric

substrates and ultimately improve biomethane production (Tan et al. 2015; Zhuang et al. 2015). According to Zhang et al. (2015), the addition of 100 mg/L of trace iron to anaerobic digestion of food waste significantly enhanced biogas production. Puyol et al. (2018) reported that the addition of adding 2.5 kg ZVI m^{-3} resulted in a significant increase of the biomethane yield. Using nanoparticle of Fe_3O_4 to enhance anaerobic digestion of green microalgae Enteromorpha, Zaidi et al. (2018) reported the highest enhancement of 28% cumulative biogas yield. Similarly, the supplementation with 20 mg/L Fe_3O_4 nanoparticles gave the highest yield of 584 mL/gVS and 351.8 mL CH_4 g/VS for specific biogas and methane yield respectively (Abdelsalam et al. 2017). Casals et al. (2014) reported that the optimum application of Fe_3O_4 nanoparticle on a continuous release basis enhanced biogas yield by 180%. In our previous work on biogas production from the enhancement impact of anaerobic digestion of okra waste with 20 mg/L PPy/Fe_3O_4, 2.74% biomethane increase was reported (Ugwu and Enweremadu, 2020).

More so, iron additives release Fe^{2+}/Fe^{3+} in the course of the digestion processes which according to Jia et al. (2017) impacts the dynamics (physicochemical) of the bioreaction. These iron ions react with dissolved anions such as phosphate (P), carbonate, respectively to vivianite ($Fe_3(PO_4)_2 \cdot 8H_2O$), siderite ($FeCO_3$) and reducing biogenic sulfide to form pyrite (FeS_2) (Puyol et al. 2018; An et al. 2014). Phosphates released to the mixed liquor or digestate during the anaerobic digestion process are entrapped, reducing P availability and increasing cost of recoverability due to the formation of non-easily degradable vivianite (Heiberg et al. 2012). P is vital to both human beings and plants globally, it is a non-renewable resource that is estimated to be used up in the next few years, hence the need for alternative P recovery plans to ensure its sustainability (Sikosana et al., 2016). Due to the relevance of P to life on earth, the achievement of enhanced energy recovery from biodegradable organics with iron additives without sacrificing P release or recoverability is the focus of this study.

Furthermore, to achieve P release in an iron enhanced anaerobic digestion, Tian and Yu (2020) suggested the need to interrupt the interaction between Fe and P to avert Fe-P production. In line with this Takashima (2019) reported that the introduction of sulfate to iron enhanced anaerobic digestion improves phosphate release via sulfate to sulfide reduction. Although this method improved P release, methane loss and additional scrubbing cost pose valid concerns, hence the need for a new approach (Tian and Yu, 2020; Takashima, 2019). P shares similar properties with arsenic compounds (As) properties and an antagonistic relationship with humic acid (HA) (Lenoble et al. 2005). In line with this, Jeong (2017) reported that the reaction of HA, As and P with iron ions formed stable As-Fe-HA

colloid and released P into the solution. Similarly, Azman et al. (2015) and Wilfert et al. (2015) revealed that iron addition on HA and As ultimately results in phosphate release. In previous studies on HA addition to anaerobic digestion, Yap et al. (2018) observed that HA addition below 5 g/L did not decrease the hydrolysis rate of cellulose, but higher dosage inhibited hydrolysis. On the influence of arsenic compound on anaerobic digestion, Zhai et al. (2017), revealed that between 33 and 71% of As from swine wastewater and total As were removed without adversely affecting anaerobic digestion.

However, as stated in Zaidi et al. (2020), optimum concentrations of additives (accelerants and/or antagonists) are needed to avert ecotoxicity, inhibition and additional cost due to overdose. Therefore, the design of experiment aimed at achieving optimal biogas yield and P release from the supplementation of anaerobic digestion with iron additives (an accelerant) and P-antagonists (HA and As) can be achieved with response surface methodology (RSM). According to Box and Draper (1987), RSM involves sets of mathematical and statistical techniques used for evaluating the effects of independent variables and optimizing their effects on each response. RSM is generally aimed at determining the optimal conditions of operations to achieve expected output. Previously, RSM has been used for the optimization of enhanced anaerobic digestion with co-digestion, trace elements and nanoparticles (Zaidi et al. 2020; Dar et al. 2019; Menon et al. 2017; Linville et al. 2016; Liu et al. 2015b), however, no study has previously reported on the optimization of additives for simultaneous enhancement of biogas yield and P release/recovery.

In this study, the influence of variables such as co-digestion, iron nanocomposite (PPy/Fe_3O_4), humic acid and arsenic oxide on biomethane yield and phosphorus release from okra waste and pig manure was investigated using response surface methodology. The optimized variables for the attainment of maximum biomethane yield and P release with minimal additive input were arrived at.

5.2 Materials and methods

5.2.1 Substrates and Inoculum

For the enhanced co-digestion and optimization process, pig and okra waste used as substrates were respectively collected from Organic Farms and Agricultural Research Council in Centurion, Gauteng, South Africa. The particle size of these wastes were reduced, homogenized and then individually preserved in a cold room at a temperature of 4^{o}C within a short time before usage and characterization. The ultimate and proximate analysis of the processed wastes were conducted. The inoculum

containing microbial biomass from an active food and vegetable waste biodigester located at the Mechanical Engineering, University of Johannesburg, South Africa. Obtained inoculum from a continuous anaerobic digester operates at the mesophilic condition and was kept in the cold room with a working temperature of 4^{o}C before use.

5.2.2 Additive supplementation

The humic acid, Arsenic (V) oxide, hydrochloric acid (HCl) and sodium hydroxide were purchased from Sigma-Aldrich (South Africa). The polypyrrole magnetic nanocomposite (PPy/Fe_3O_4) used in this experiment was synthesized in the Physics and Mechanical/Industrial Engineering Laboratory of University of South Africa as described and characterized by Aigbe et al. (2018). The concentrations of these additives used were based on recommendations of previous studies. In our earlier study (Ugwu and Enweremadu 2020), we determine that 20 mg/L of PPy/Fe_3O_4 gave the highest biomethane. Ali et al. (2017) observed that the use of 75 mg/L of Fe_3O_4 nanoparticles resulted in the maximum biogas production. Yap et al. (2018) and Azman et al. (2015) demonstrated that humic acid concentration less than 500 mg/L does neither inhibit hydrolysis nor methanogenesis. Webster et al. (2016) and Banerjee (2010) suggested that Arsenic (V) dosage of less than 1% did not significantly inhibit the anaerobic digestion process. The different doses were dispersed in deionized water and then sonicated for 10 min before being introduced into the bioreactors.

5.2.3 Analytical method

Based on APHA (2005) standard methods, the results of the proximate analysis which are total solids (TS), moisture content (MC), volatile solids (VS) and ash content (AC) were obtained and the %VS/TS was calculated. Using the Thermo Scientific Flash 2000 Organic Elemental Analyzer, the ultimate analysis (CHNS) of the substrates were conducted. The analyzer with oxygen combusting at 250 ml/min and helium as carrier gas flowing at 140 ml/min, had its maximum temperature set at 950^{o}C and retention time of 610 sec. The oxygen content of the substrates was determined thus based on VS %: C+H+N+S+ Ash = 99.5 (Rincón et al. 2012). The pH was quantified with the use of pH meter (HI 9828 Multi-parameter, Hanna Instruments). For P determination, 25mg of organic waste was digested with digestion reagent (4M HNO_3 + 1M H_2O_2) in a microwave-assisted oven for total digestion time 50 minutes (20 mins for heating and 30 mins for cooling) and maximum temperature of 180^{o}C. The digested sample and digestates for chemical compositional analysis were filtered with 0.45 µm x 28mm syringe filters membranes (Glassworld, South Africa). Total P and others were determined by directly introducing the sample into the Inductively Coupled Plasma Mass

Spectrometry (ICP-MS) (NeXION 350D, PerkinElmer, USA) in triplicates. Analytes were determined under the following conditions: Cyclonic spray chamber, RF power of 1400 kW, 1.2 L/min auxiliary gas flow rate, 15.5 L/min plasma gas flow rate, 6 mL/min sample uptake and 50 mins dwell time. Standard solution for Perkin Elmer NeXION set up was used for checking standard performance. The mass used for analyzing the analyte was P (31) atomic mass unit. 1 mg/L of P standard solution was prepared from KH_2PO_4 in 1% HNO_3 and serially diluted from 0.1mg/L to 1mg/L. It was later used to obtain the calibration curve for quantification. ICP-MS Syngistix software was used for acquisition and analysis of data.

The volatile fatty acids were determined using a Gas Chromatograph (Agilent 7890) incorporated with a mass spectrometer (LECO Pegasus 4D Time of Flight) detection and a multipurpose (Gerstel) sampler as described in Moreroa et al. (2020). The column used was a 30 m × 0.25 mm × 0.25 µm Stabilwax-DA (Restek, USA). These system operational parameters include Helium operating a flow rate of 1.4 mL/min was the carrier gas, the initial oven temperature was set at 50 °C and held at the same temperature for 0.5 min before raising it to 240 °C by 10 °C/min and maintained for 2.5 min. With the aid of the autosampler, 1 µL of sample volume was injected at a split of 1:10 and the run time for each analysis was 22 min. The secondary oven and modulator temperature offset were set at 10 °C. The settings for the mass spectrometry are thus: Electron ionization at −70 eV, solvent delay of 0 min, the auxiliary temperature at the interface was 240 °C, the source temperature was 250 °C, stored mass range from 30 to 300 µ, acquisition rate of 8 spectra/second and a detector voltage offset of plus 250 V to the optimized detector voltage. Conclusively, all tests results were expressed as the mean of triplicate tests at 95% probability level.

5.2.4 Experimental design and statistical model

The batch experiments were carried out based on the two level-four factors central composite design (CCD) RSM ($n = 4, \pm \alpha = 2.0$) to analyze the relationship between independent variables and responses as well as to optimize both biomethane yield and P release. The independent variables and the responses are as shown in Table 5.1. The design of the experiment had a total of 30 runs including six centre points replications and twenty-four non-centre points. The CCD RSM was coded based on minimum (-1), central (0) and maximum (+1) levels as shown in Table 5.1.

Table 5. 1 Levels of variables and experimental design matrix for RSM

Independent variable codes	Parameters	Levels		
		-1 (Min)	0	+1 (Max)
A	Ppy/Fe_3O_4 (mg/L)	20	47.5	75
B	Humic acid (HA) (mg/L)	5	27.5	50
C	Arsenic (V) (As) (mg/L)	1	3	5
D	Co-digestion (%)	25	50	75
Run	**A**	**B**	**C**	**D**
1	47.5(0)	17.5(-2)	3(0)	50(0)
2	75(+1)	50(+1)	5(+1)	75(+1)
3	20(-1)	50(+1)	1(-1)	25(-1)
4	47.5(0)	27.5(0)	3(0)	50(0)
5	47.5(0)	27.5(0)	3(0)	50(0)
6	47.5(0)	27.5(0)	3(0)	100(+2)
7	47.5(0)	27.5(0)	3(0)	50(0)
8	75(+1)	50(+1)	1(-1)	25(-1)
9	75(+1)	5(-1)	1(-1)	25(-1)
10	47.5(0)	27.5(0)	3(0)	50(0)
11	47.5(0)	27.5(0)	7(+2)	50(0)
12	75(+1)	50(1)	5(1)	25(-1)
13	75(+1)	5(-1)	5(+1)	25(-1)
14	47.5(0)	27.5(0)	3(0)	50(0)
15	20(-1)	50(+1)	1(-1)	75(+1)
16	75(+1)	5(-1)	5(+1)	75(+1)
17	20(-1)	50(+1)	5(+1)	25(-1)
18	20(-1)	5(-1)	5(+1)	25(-1)
19	75(+1)	5(-1)	1(-1)	75(+1)
20	20(-1)	5(-1)	1(-1)	75(+1)
21	20(-1)	5(-1)	1(-1)	25(-1)
22	20(-1)	50(+1)	5(+1)	75(+1)
23	20(-1)	5(-1)	5(+1)	75(+1)
24	102.5(+2)	27.5(0)	3(0)	50(0)
25	7.5(-2)	27.5(0)	3(0)	50(0)
26	75(+1)	50(+1)	1(-1)	75(+1)
27	47.5(0)	27.5(0)	3(0)	13.64(-2)
28	47.5(0)	27.5(0)	3(0)	50(0)
29	47.5(0)	27.5(0)	3(0)	50(0)
30	47.5(0)	27.5(0)	1(-2)	50(0)

The data from the CCD RSM experimental were used to generate suitable second-order polynomial regression that describes system pattern as follows in Equation 5.1:

$$Y = \beta_o + \sum_{i=1}^{4} \beta_i X_i + \sum_{i=j}^{4} \beta_{ii} X^2{}_i + \sum_{i=j}^{4} . \sum_{j=i+1}^{4} \beta_{ij} X_i X_j + \varepsilon \qquad 5.1$$

Where Y represents the expected response of the variable (mL CH_4/g VS); β_0, β_i, β_{ii} and β_{ij} signifies regression coefficients of intercept, linear, quadratic and interaction respectively; X_i and X_j represent the independent variables; ε is used to express the prediction error and k which in this study depicts

the number of variables (Ppy/Fe_3O_4, HA, As and co-digestion) used in the analysis (Yılmaz and Şahan, 2020). The statistical significance of the quadratic models, interactions and the process parameters were determined through analysis of variance (ANOVA) at the 95% probability level. Coefficient of determination (R^2) and other fitness indices were used to evaluate the suitability of the entire statistics. The Design-Expert® software (version 12.0.11.0) was used for RSM design of experiment, analysis of parameters and optimization of variables.

5.2.5 Experimental setup

Batch laboratory-scale anaerobic digestions based on the CCD RSM shown in Table 5.1 were conducted with AMPTS II bioreactors (Bioprocess Control, Sweden) situated at Mechanical and Industrial Engineering Laboratory, the University of South Africa for 28 days digestion period at mesophilic temperature (37 ± 1°C). The bioreactors assay with working volume 500 mL capacity each were used for the biochemical methane potential tests (anaerobic digestion process). Okra waste of 40.06 g based on 6.90% VS was co-digested with pig manure of 11.4 g based on 25.72% VS at various combining percentages as shown in Table 5.1 and was respectively added to each bioreactor containing 460.56 mL inoculum (1.2% VS) at an inoculum to substrate ratio (ISR) of 2:1. Thereafter the mixed liquor (inoculum and substrates) were supplemented with different dosages of additives as shown in Table 5.1. De-ionized water (Milli-Q, Millipore) was used to top up the headspace of the bioreactors, temperature water bath, flow meter and for substrate dilution. The mixed liquor in each bioreactor was adjusted to pH of 7.0 with the aid of NaOH and HCl and absence of oxygen in the reactors was ensured by purging each bioreactor with nitrogen gas (from Afrox South Africa) before digestion process commenced. The biomethane production (daily and cumulative) of different additive doses as designed with CCD RSM and shown in Table 5.1 were measured and recorded with a data-logging platform of the AMPTS II as shown in Fig. 5.1.

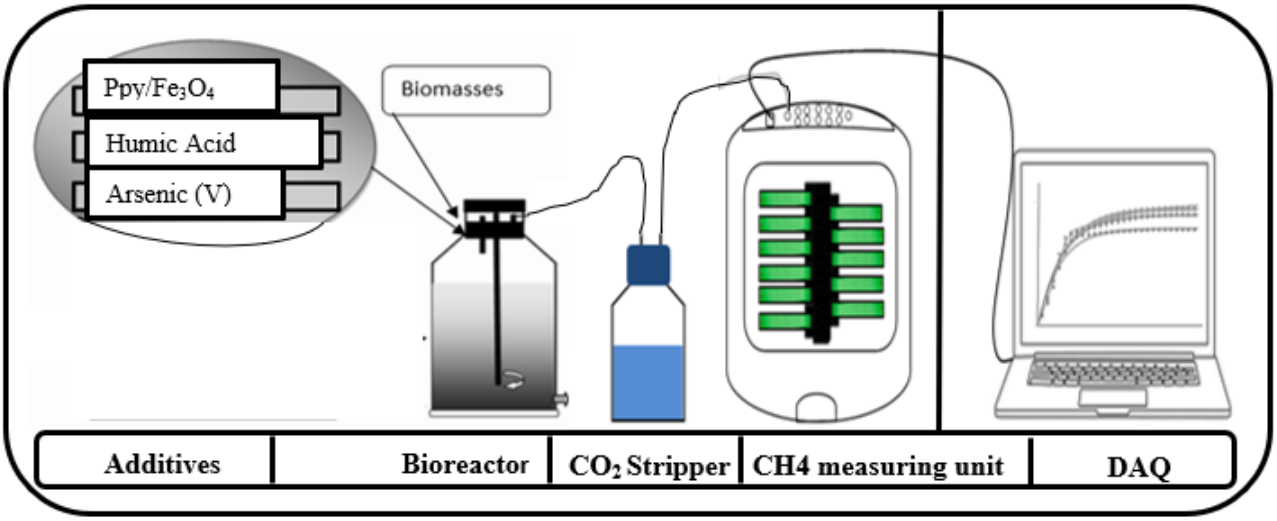

Fig.5. 1 Schematic diagram of additives enhanced anaerobic digestion with AMPTS II BMP assay

All the treatment levels and analysis were run in triplicates. The entire statistical analyses and plots in this study were done with STATISTICA 12 software and Microsoft Excel (version 2016). The statistical significance of all analysis was established at $p < 0.05$ level.

5.3 Results and discussions

5.3.1 Substrate characterization

The pH, proximate and ultimate contents of substrates (okra and pig wastes) were determined as listed in Table 5.2. The pH of okra and pig wastes were 7.20 and 7.57 respectively. These values were within tolerable limits (6.5-8.5) recommended in Kigozi et al. 2014 for optimum anaerobic digestion performance. However, based on evaluated carbon-to-nitrogen (C:N) ratio of substrates, okra waste has C:N ratio of 12.24. This low C:N value justifies the choice of co-digestion with a substrate of higher C:N ratio (pig waste with C:N of 20.50) in order to attain optimum C:N range (20-40) for enhanced biogas yield (Smith and Holtzapple, 2011). P (total P and soluble P) contents of the pig waste were higher than that of okra waste, this result agreed with the high P content reported in Campos (2014). Similarly, oxygen (45.53 %), arsenic (4.62 mg/L) and iron (1774.41 mg/L) contents were higher in pig manure than in okra waste. Consistent with vegetables, the moisture content (92.18) and volatile solid (88.36 %) of okra waste were higher than that of pig manure.

Table 5. 2 Characteristics of substrates studies

Parameters	**Okra waste**	**Pig waste**
Moisture content %	92.18	68.44
pH	7.20	7.57
TS %	7.82	31.56
VS %	88.36	81.54
C %	39.30	40.39
N %	3.21	1.97
H %	5.39	5.29
O %	35.74	45.53
C/N	12.24	20.50
Total P mg/L	213.08	1007.64
Soluble P	54.53	167.36
Fe mg/L	95.30	1774.41
As mg/L	2.08	4.62

5.3.2 Influence of different enhancement levels on volatile fatty acid

Volatile fatty acid which is an intermediate product influences pH and alkalinity levels. Its availability maintains digester performance and adversely impact digestion process when concentration is high (Wang et al. 2020). The VFA results of samples collected at intervals from different enhanced digestion runs are shown in Fig. 5.2a. The VFA concentrations of runs 1 to 30 showed a gradual rise in the first 6 days. This signifies that entire anaerobic digestion parameters and processes were performing well at this stage. However, digester 5 maintained the rise, but VFAs in the other digesters recorded substantial decline after the 12^{th} day and continued till the 28^{th} day. This trend was akin to what was reported in Liu et al. (2015b) that the peak VFA increase was recorded on the 5^{th} day and declined thereafter. The rapid consumption of VFA at the inception stage (hydrolysis and acidogenesis) where according to Liu et al. (2015b), produced VFAs like butyric and propionic are consumed quickly during the process of methanization. More so, the sustained total VFA reduction may be attributable to the low total solid (TS%) content, which is in line with the findings of Wang et al. (2020) that high TS content of 20% and above is responsible for VFA (acetic and propionic acid) accumulation in the digester. The VFAs in samples were quantified based on their compositions from C_2-C_6 and retention time as shown in Fig. 5.2b.

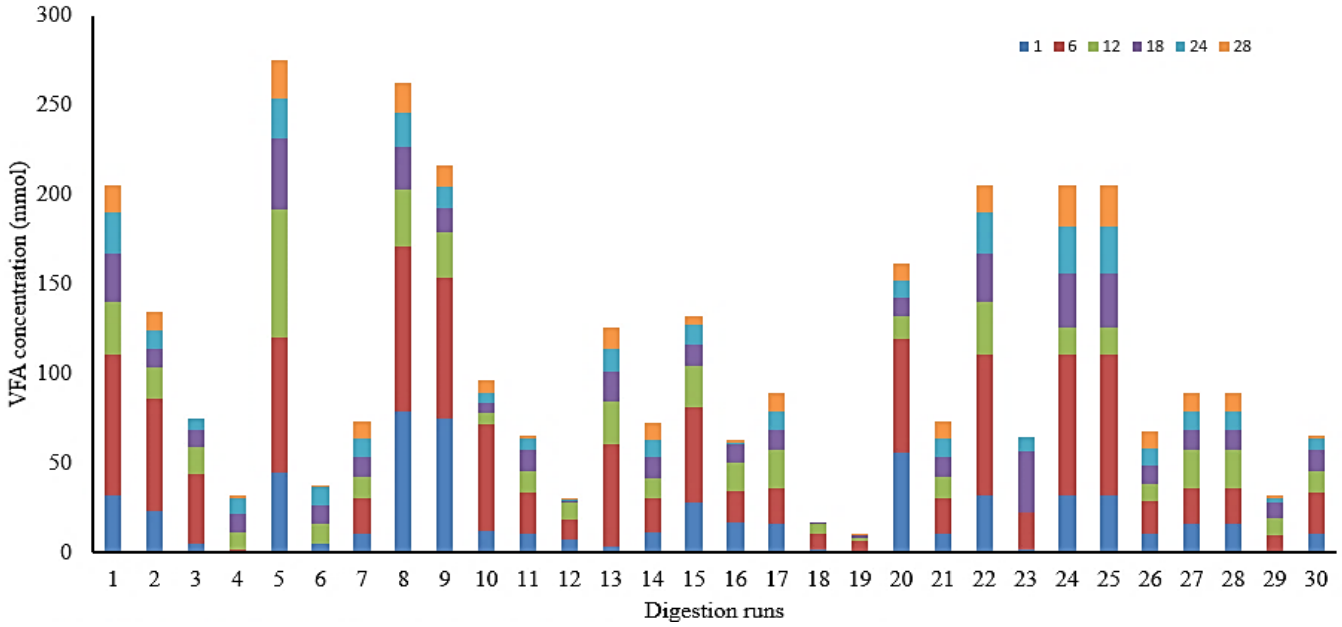

(a)

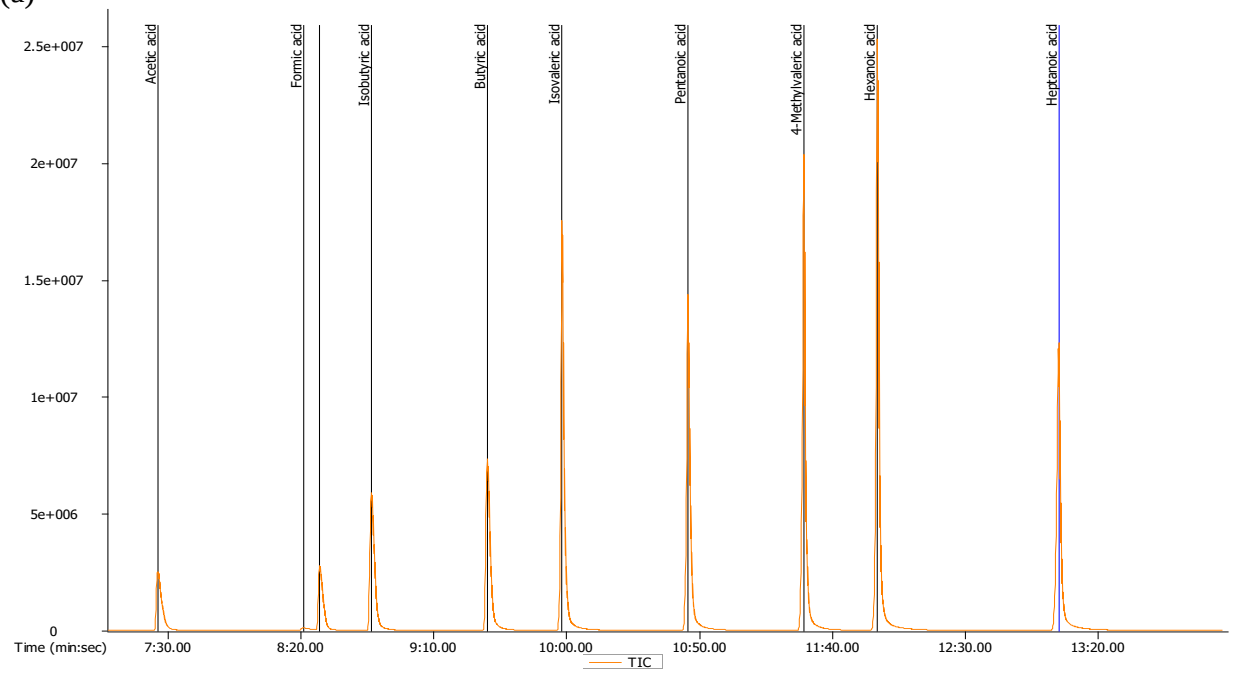

(b)

Fig.5. 2 (a)Volatile fatty acids of digestion runs on different days, (b) GC-MS chromatograms of the standard solution of each VFA (C_2 to C_6) in mmol

5.3.3 Biomethane production from enhanced anaerobic digestion

Biomethane yield maximization as a response parameter was part of the study objectives. The influence on cumulative biomethane yields of different enhanced digester runs was measured and shown in Table 5.3 and Fig. 5.3. When compared to the control run, the highest combined enhancement in biomethane yield of 53.35% was from digester run 21. This is a significant

improvement in biomethane production over previously reported single enhancement efforts (Ugwu and Enweremadu, 2020; Abdelsalam et al. 2017; Ali et al. 2017).

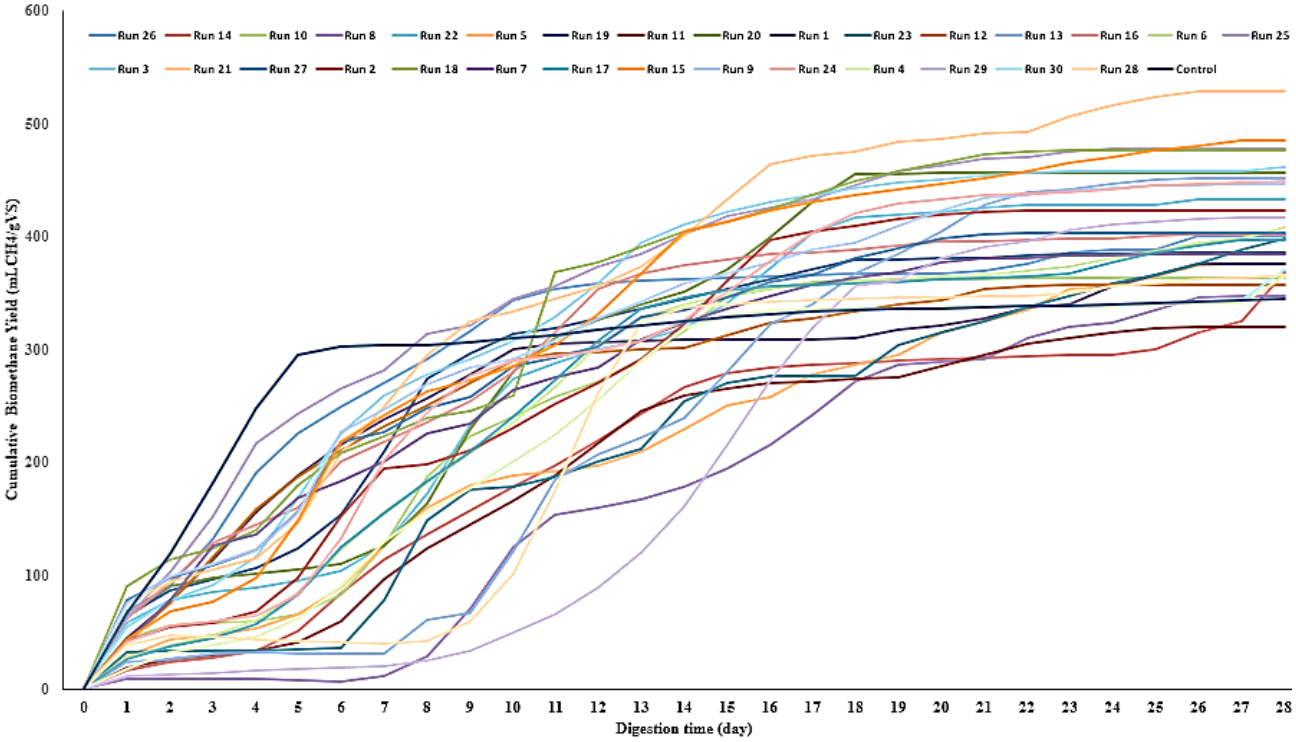

Fig.5. 3 Plot of cumulative biomethane yield of different enhancement processes

Table 5. 3 Experimental design with response surface methodology and the results

Std order	Run order	Input variables				Output responses	
		Ppy/Fe_3O_4 (mg/L)	HA (mg/L)	As (mg/L)	Co-digestion (%)	Biomethane Yield ($mLCH_4/g.Vs$)	P Release (mg/L)
19	1	47.5	17.5	3	50	376.117	235.813
16	2	75	50	5	75	423.563	181.662
3	3	20	50	1	25	461.278	138.013
28	4	47.5	27.5	3	50	364.741	241.188
29	5	47.5	27.5	3	50	376.733	240.188
24	6	47.5	27.5	3	100	409.027	160.691
30	7	47.5	27.5	3	50	384.729	242.188
4	8	75	50	1	25	347.603	93.9933
2	9	75	5	1	25	446.97	102.304
27	10	47.5	27.5	3	50	363.928	252.425
22	11	47.5	27.5	7	50	320.171	143.463
8	12	75	50	5	25	357.89	114.803
6	13	75	5	5	25	451.679	107.865
26	14	47.5	27.5	3	50	368.723	246.11
11	15	20	50	1	75	485.62	122.268
14	16	75	5	5	75	402.709	153.003
7	17	20	50	5	25	397.034	145.641
5	18	20	5	5	25	477.31	146.116
10	19	75	5	1	75	386.074	125.631

9	20	20	5	1	75	456.831	116.273
1	21	20	5	1	25	528.632	153.737
15	22	20	50	5	75	433.301	151.708
13	23	20	5	5	75	398.934	130.463
18	24	102.5	27.5	3	50	449.309	110.286
17	25	7.5	27.5	3	50	478.49	186.025
12	26	75	50	1	75	401.351	139.04
23	27	47.5	27.5	3	13.6364	403.625	180.731
25	28	47.5	27.5	3	50	366.731	242.425
20	29	47.5	72.5	3	50	416.744	144.114
21	30	47.5	27.5	1	50	371.437	204.559

Using RSM to further analyze the cumulative biomethane yield in Table 5.3, a quadratic model was suggested, and the second-order equation of selected parameters was chosen. From the statistical analysis in Table 5.4, F-value of the model was significant at 150.16 and the *p*-value was less than 0.0001, indicating that the model is significant (Anderson and Whitcomb, 2017). Based on the established criteria, the significant model terms include A, B, C, D, AB, AC, AD, BD, A^2, B^2, C^2, D^2. The F-value of this model's lack of fit is not significant at 0.21 relative to the pure error, this implies that the model is good (Anderson and Whitcomb, 2017). The model fitness indicator showed that the R^2 is 0.9929 and that the predicted R^2 of 0.9795 reasonably agrees with the Adjusted R^2 of 0.9863 since the difference between both is less than 0.2, indicating the suitability of the model. Low coefficient of variation (CV %) of the model was 1.37 %, which implies that the experimental data is highly reliable, reproducible and accurate (Lu et al. 2019).

Table 5. 4 ANOVA for the quadratic model of biomethane yield

Source	**Sum of Squares**	**DF**	**Mean Square**	**F-value**	***p*-value**	
Model	66618.73	14	4758.48	150.16	< 0.0001	significant
A-Ppy/Fe3O4	14680.24	1	14680.24	463.24	< 0.0001	
B-HA	3892.67	1	3892.67	122.84	< 0.0001	
C-As	2120.00	1	2120.00	66.90	< 0.0001	
D-Co-digestion	546.03	1	546.03	17.23	0.0009	
AB	328.97	1	328.97	10.38	0.0057	
AC	4886.91	1	4886.91	154.21	< 0.0001	
AD	614.07	1	614.07	19.38	0.0005	
BC	0.9071	1	0.9071	0.0286	0.8679	
BD	12104.05	1	12104.05	381.95	< 0.0001	
CD	53.30	1	53.30	1.68	0.2143	
A^2	21029.59	1	21029.59	663.60	< 0.0001	
B^2	5870.07	1	5870.07	185.23	< 0.0001	
C^2	773.08	1	773.08	24.40	0.0002	
D^2	2993.60	1	2993.60	94.46	< 0.0001	
Residual	475.35	15	31.69			
Lack of Fit	141.43	10	14.14	0.2118	0.9821	not significant
Pure Error	333.92	5	66.78			

Cor Total	67094.08	29		
Std. Dev.	5.63		R^2	0.9929
Mean	410.24		Adjusted R^2	0.9863
C.V. %	1.37		Predicted R^2	0.9795
			Adequate Precision	53.6428

In Fig. 5.4, the normality probability plot is shown indicating the compliance of residuals to a normal distribution, that is having points in a straight line and scattered on both sides. The biomethane yield residual plot showed less dispersion of data, which according to Siami et al. (2020) justifies the closeness of the results to the normal line. Similarly, another residual plot (residual versus experimental runs) which showed random scatter in Fig. 5.4 is used according to Deepanraj et al. (2020) to check lurking variables capable of influencing response during the experiment. The plot of predicted vs actual data (Fig 5.4) indicates that there is less difference between both as numerically estimated as R^2 in Table 5.4.

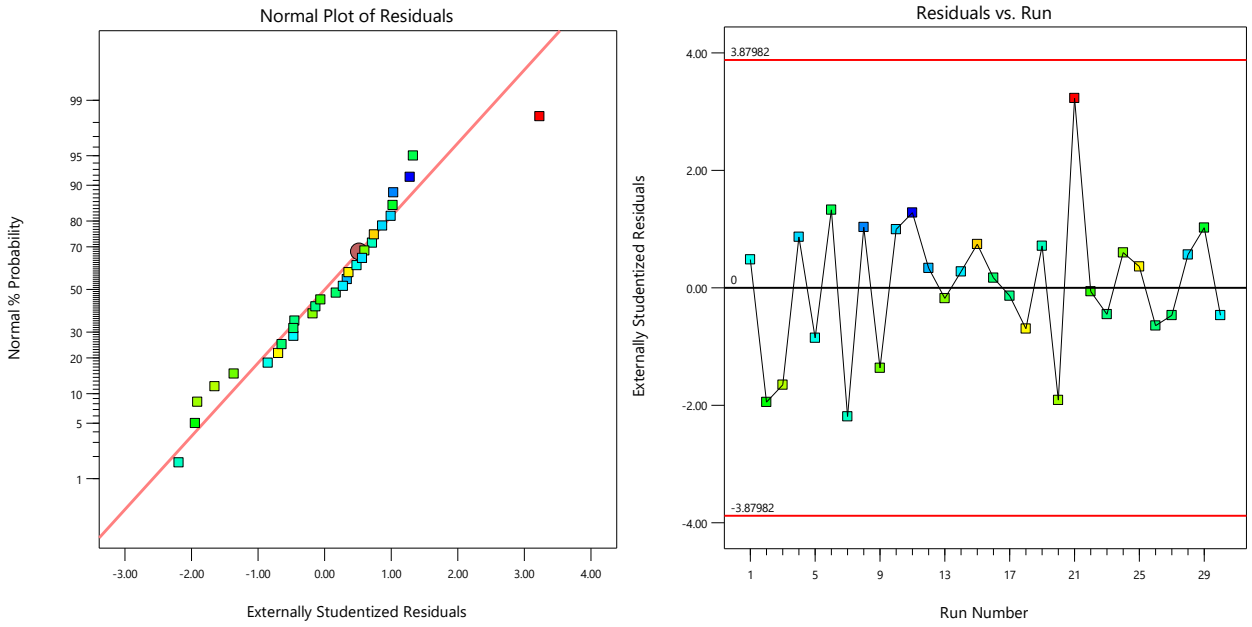

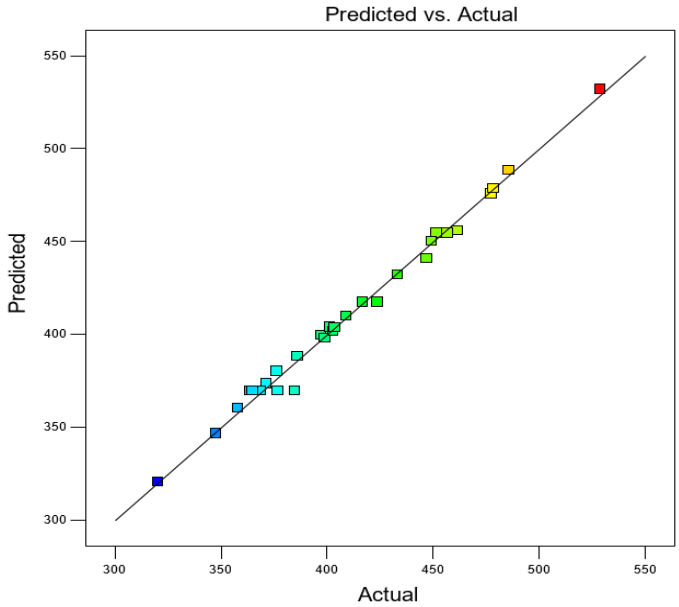

Fig.5. 4 Plot of Residuals and Predicted vs Actual of enhanced biomethane yield

The multi-regression of input variables analysed through RSM and showed in the ANOVA table (Table 5.4) resulted in an empirical model for biomethane yield represented by Equation 5.2. However, non-significant terms of the regression equation are considered irrelevant and discarded to achieve Equation 5.2 below.

$$\text{Biomethane Yield (mL CH4/g VS)} = 369.92 - 26.41A - 15.08B - 5.09D - 4.53AB + 17.48AC + 6.20AD + 27.50BD + 33.29A^2 + 19.47B^2 - 6.96C^2 + 12.56D^2 \quad 5.2$$

From the model coefficients (Equation 5.2), the linear effect of A, B, C and D, the quadratic effect of A^2, B^2, C^2 and D^2 as well as interaction effects AB, AC, AD, BD are significant, BC and DC were removed because they are non-significant (p-value > 0.05). All the linear terms are negatively correlated with biomethane yield, this implies that if any input variable is held constant and the other increases, biomethane yield decreases (Lu et al. 2019). Except for term C^2, other second-order coefficients A^2, B^2 and D^2 had a positive correlation with biomethane. This shows that the parabola of the surface plot opens upward and, in this study, the vertex had the highest biomethane yield on the surface plots (Fig. 5.5). Similarly, the significant interaction effect at $p < 0.05$ indicates that selected variables synergistically influenced biomethane yield (Lu et al. 2019). The influence of the four independent variables on biomethane yield is described using both surface and contour plots as shown in Fig. 5.5. These plots represent the influence of two variables on one response (biomethane yield) while keeping the other two variables constant (Pei et al. 2014). Fig 5.5 showed that biomethane yield increased with decreasing additives concentration.

According to the model result Ppy/Fe_3O_4 additive had the most impact at both linear (F= 463.24) and quadratic level (F= 663.60) and are highly significant at $p < 0.0001$. This agrees with the fact that supplementation of anaerobic digestion with iron-based additive (Ppy/Fe_3O_4) aid substrate solubilization, increases methanogenesis and ultimately enhances biomethane yield (Ugwu and Enweremadu, 2020; Bharathiraja et al. 2018; Ali et al. 2017). In this study, the highest biomethane yield (528.632 mLCH_4/gVS), was obtained when 20 mg/L of Ppy/Fe_3O_4 was added in Run 21, but increasing the dosage caused a decline in biomethane yield (Fig. 5.5). This result agrees with Ugwu and Enweremadu (2019) that the addition of 20 mg/L Ppy/Fe_3O_4 recorded the highest enhancement when compared with other iron additives used.

However, the increasing effects on biomethane yield with the decreasing dosage of humic acid (HA) concur with the reports of Azman et al. (2015) and Yap et al. (2018) that lower HA (< 500 mg/L) concentrations do not inhibit anaerobic digestion process. Similarly, higher biomethane yield was observed in presence of low arsenate (As) concentration. This agrees with Webster et al. (2016) that low dosage (< 5 mg/L or < 1%) of As in a bioreactor did not inhibit anaerobic digestion process, but higher As concentration inhibited it. More so, the increasing addition of pig waste to the co-digestion factor as an enhancement option resulted in decreasing biomethane yield as shown in Fig.5.5. The decline in biomethane yield with increasing co-digestion suggests the presence of inhibition, hence substrate pretreatment is suggested (Lu et al. 2019).

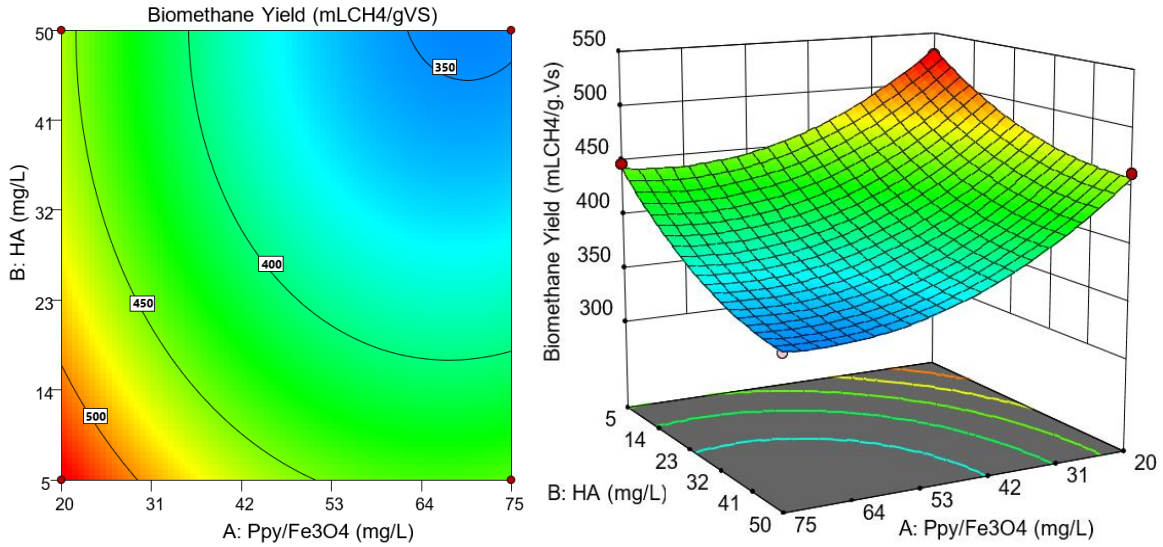

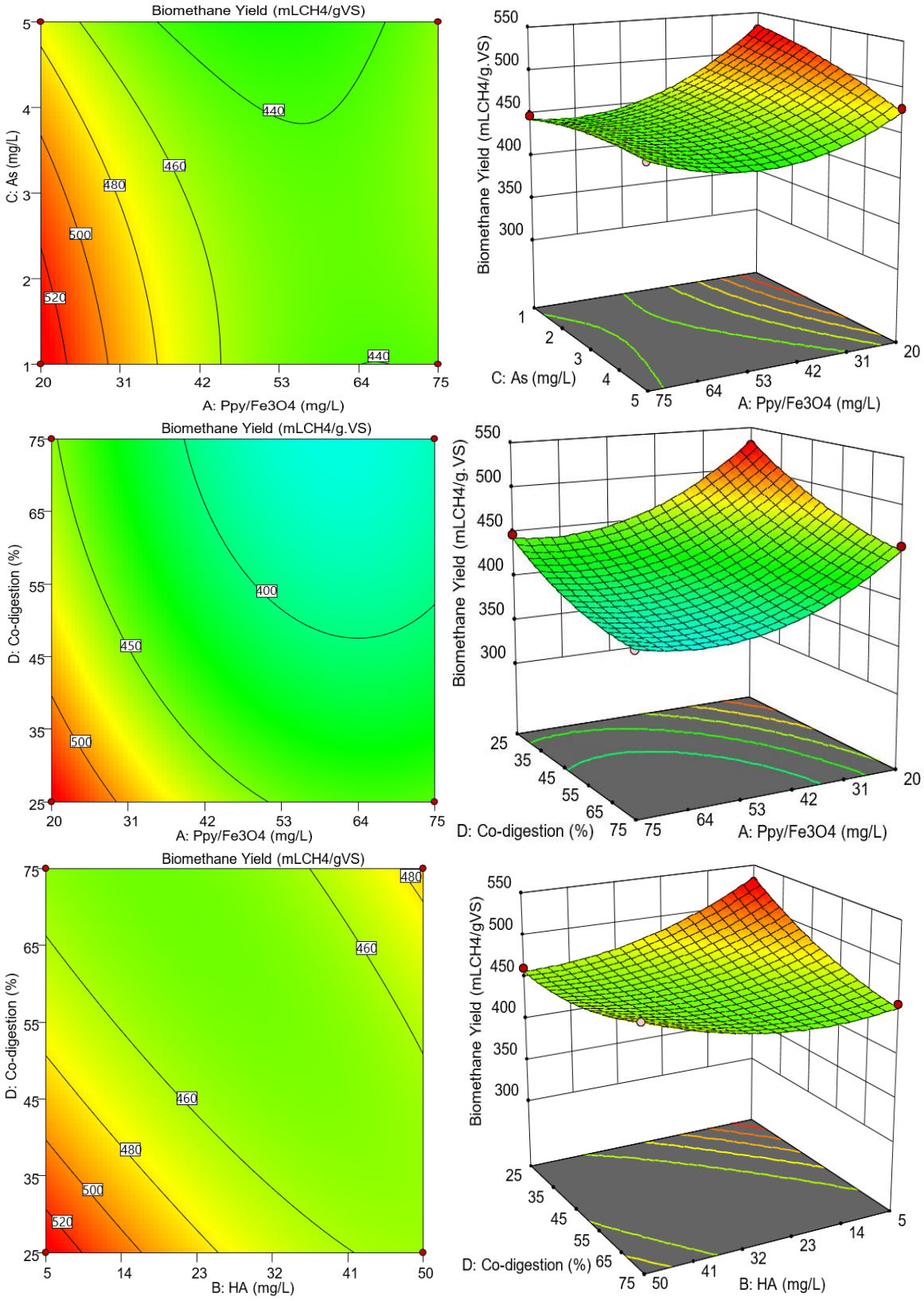
Biomethane Yield (mLCH4/gVS)
C: As (mg/L)
A: Ppy/Fe3O4 (mg/L)
440
460
480
500
520
Biomethane Yield (mLCH4/g.VS)
Biomethane Yield (mLCH4/g.VS)
C: As (mg/L)
A: Ppy/Fe3O4 (mg/L)
Biomethane Yield (mLCH4/g.VS)
D: Co-digestion (%)
A: Ppy/Fe3O4 (mg/L)
400
450
500
Biomethane Yield (mLCH4/g.VS)
D: Co-digestion (%)
A: Ppy/Fe3O4 (mg/L)
Biomethane Yield (mLCH4/gVS)
D: Co-digestion (%)
B: HA (mg/L)
460
480
500
520
Biomethane Yield (mLCH4/gVS)
D: Co-digestion (%)
B: HA (mg/L)

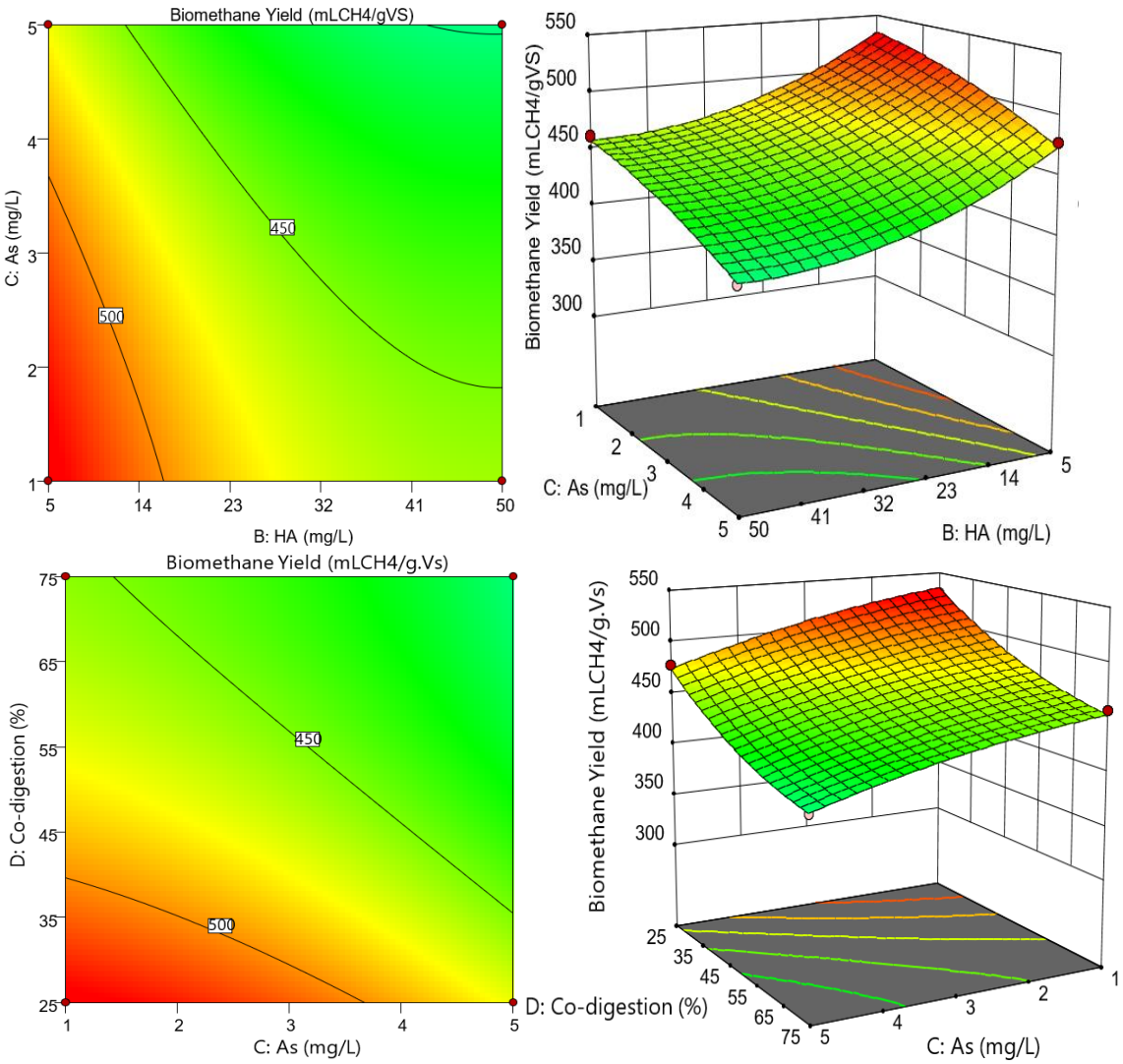

Fig.5. 5 Contour and response surfaces plots for biomethane yield

5.3.4 Phosphorus release from enhanced anaerobic digestion

In a bid to obtain the optimum release of phosphorus (P) from enhanced anaerobic digestion processes, four independent variables (Ppy/Fe_3O_4, HA, As and co-digestion) designed using CCD RSM to assess and analyze the influence (response) of these variables as shown in Fig. 5.3. The results of the experimental design and response were used to run a multi-regression RSM analysis to obtain a second-order equation (Equation 5.3). The model equation represented as coded factors of variables for P release (mg/L) is stated thus:

$$\text{P Release (mg/L)} = 243.71-5.32*A +3.25*B +8.81*C +7.40*D +1.85*AB +3.30*AC +15.20*AD +3.81*BC +5.43*BD +5.45*CD-30.70*A^2-26.48*B^2-29.46*C^2-24.46*D^2 \quad 5.3$$

This regression model (Equation 5.3) finds its relevance in the prediction of optimized P release. However, ANOVA analysis of the CCD-RSM response and design of experiment to determine the

quadratic model's goodness of fit was carried out and the result is as shown in Table 5.5. Model terms were considered statistically significant if the F-values had $p < 0.05$.

The quadratic model's F-value was 731.20, this implies that the model was highly significant at $p < 0.0001$(Anderson and Whitcomb, 2017). It also entails that the model appropriately fitted the measured data and could be suitable for understanding the influences of independent variables on P release (Ghaleb et al. 2020). A low F-value (0.02%) at a very high *p*-value of 1.0000 shows that the model's lack of Fit was not significant relative to the pure error. The coefficient of variation (CV) from the ANOVA analysis at 1.62 % implied high reliability and high accuracy level of the measured data. The model fitness was validated by the correlation coefficient R^2 value of 0.9985, this means that 99.85% of the P release prediction variability could be explained by the model and there was little difference between predicted and measured response data (Fig. 5.6) (Anderson and Whitcomb, 2017, Pei et al. 2014). In Table 5.5, the difference between predicted R^2 and adjusted R^2 is less than 0.2 and the adequate precision is greater than 4, which shows that the model with acceptable goodness of fits is suitable and appropriate for predicting P release during enhanced co-digestion process.

Table 5. 5 ANOVA result for the quadratic model of P Release

Source	**Sum of Squares**	**DF**	**Mean Square**	**F-value**	***p*-value**	
Model	73264.38	14	5233.17	731.20	< 0.0001	significant
A-Ppy/Fe3O4	596.34	1	596.34	83.32	< 0.0001	
B-HA	180.44	1	180.44	25.21	0.0002	
C-As	1441.84	1	1441.84	201.46	< 0.0001	
D-Co-digestion	1150.87	1	1150.87	160.80	< 0.0001	
AB	54.97	1	54.97	7.68	0.0143	
AC	173.76	1	173.76	24.28	0.0002	
AD	3695.60	1	3695.60	516.36	< 0.0001	
BC	232.53	1	232.53	32.49	< 0.0001	
BD	471.75	1	471.75	65.92	< 0.0001	
CD	475.73	1	475.73	66.47	< 0.0001	
A^2	17886.96	1	17886.96	2499.23	< 0.0001	
B^2	10863.32	1	10863.32	1517.86	< 0.0001	
C^2	13841.57	1	13841.57	1933.99	< 0.0001	
D^2	11353.04	1	11353.04	1586.29	< 0.0001	
Residual	107.35	15	7.16			
Lack of Fit	3.77	10	0.3770	0.0182	1.0000	not significant
Pure Error	103.58	5	20.72			
Cor Total	73371.74	29				
Std. Dev.	2.68		R^2	0.9985		
Mean	165.09		Adjusted R^2	0.9972		
C.V. %	1.62		Predicted R^2	0.9980		
			Adequate Precision	79.1949		

Further suitability of the model based on its diagnostic parameters was carried out; the residuals and prediction plots were plotted as shown in Fig. 5.6. The normality probability plot has all points scattered on both sides and relatively in a straight line. This shows that the residuals followed the normal distribution pattern. On the other hand, the plot of residual vs experimental runs (Fig. 5.6) showed random scatter on both sides. All residual values were in the range of ±4 without any outlier. This indicates according to Kainthola et al. (2020) and Deepanraj et al. (2020) that the model was appropriate without irregularity and that the model could check variables that can influence P release during the experiment. As shown in Fig. 5.6. very less difference exists between measured and predicted response data.

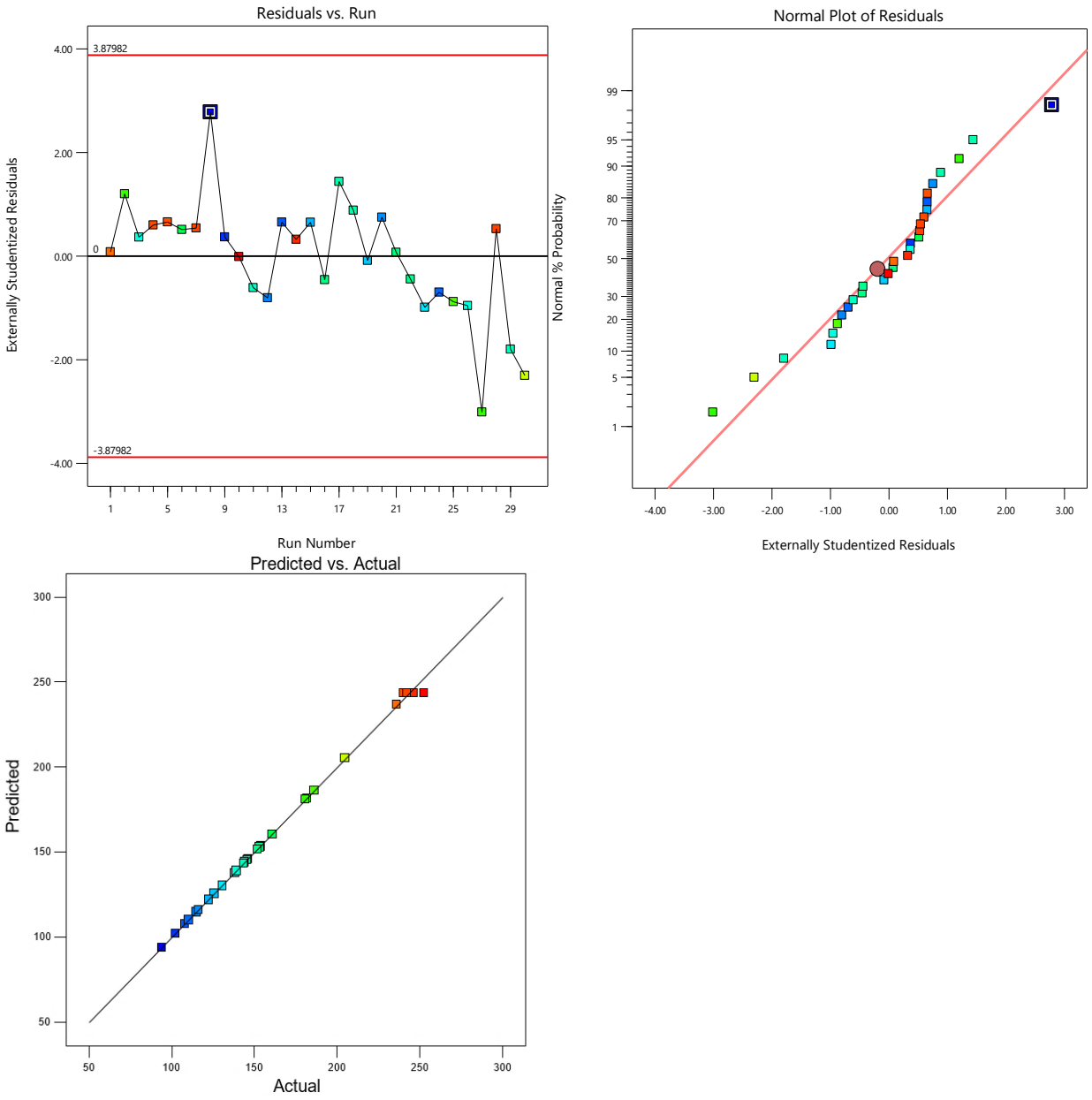

Fig.5. 6 Plot of Residuals and Predicted vs Actual of P release

Furthermore, the linear model terms (A, B, C and D), quadratic model values (A^2, B^2, C^2 and D^2) and interacting terms (AB, AC, AD, BC, BD and CD) were seen to be statistically significant at $p < 0.05$. It was observed that iron addition (Ppy/Fe_3O_4) (< 0.0001) had a significant negative linear and quadratic effect on P release. This negative linear correlation shows that when other variables are held constant and iron concentration increases, P release decreases. Humic acid (HA), arsenate (As), and co-digestion ($p < 0.05$) showed a significant positive linear effect on P release. All the interaction terms in the model were positively correlated ($p < 0.05$), implying synergistic influences of all independent variables on P release. As observed from Fig. 5.7, the negative quadratic correlation reflected on the surface plot parabola facing down, with maximum P release appearing at the ridges. The interactive effect of the four independent variables on P release was depicted and described using contour and 3-D surface plots (Fig. 5.7). Both response contour and surface plots represent the effect of two variables on P release when the other two are held constant at the center point (Ppy/Fe_3O_4 = 47.5 mg/L, HA = 27.5 mg/L, As = 3 mg/L or Co-digestion = 50%) (Deepanraj et al. 2020; Pei et al. 2014). Observation reveals in Fig. 5.7 that a decrease in Ppy/Fe_3O_4 concentration (20 mg/L), increased P release (between 240 and 252.425 mg/L), a percentage increase in pig manure content of the co-digestion, resulted in an increase in P availability in the digestate.

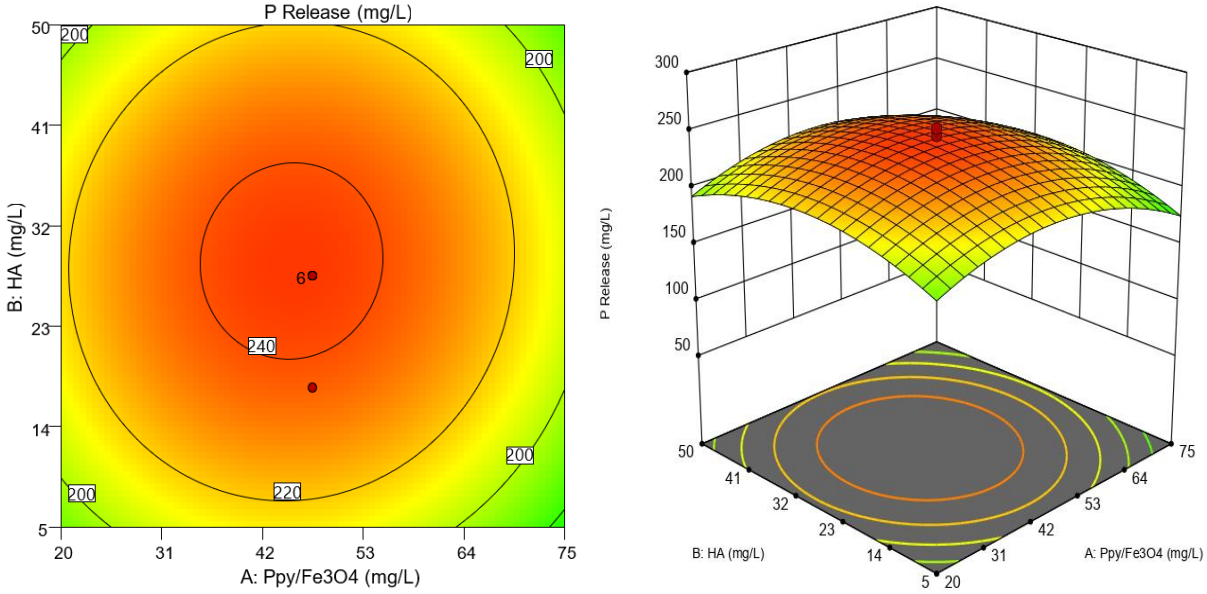

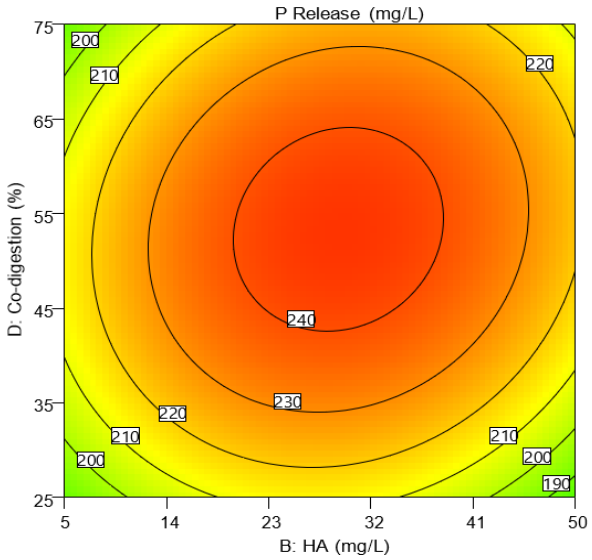
P Release (mg/L)
D: Co-digestion (%)
B: HA (mg/L)
75
65
55
45
35
25
5
14
23
32
41
50
200
210
220
240
230
190

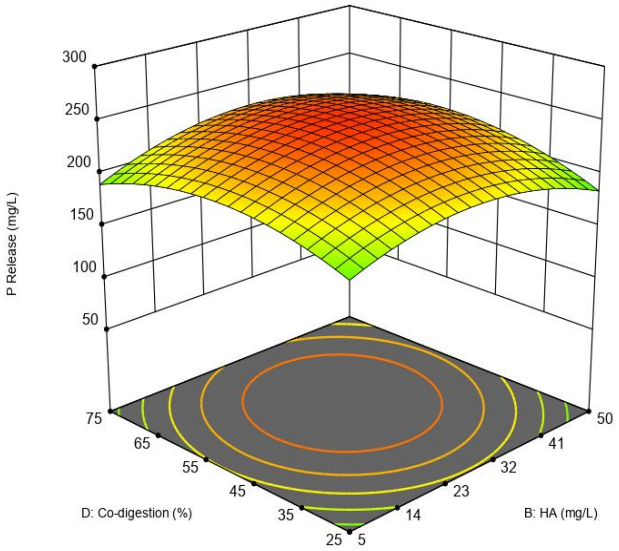
P Release (mg/L)
300
250
200
150
100
50
D: Co-digestion (%)
B: HA (mg/L)
75
65
55
45
35
25
5
14
23
32
41
50

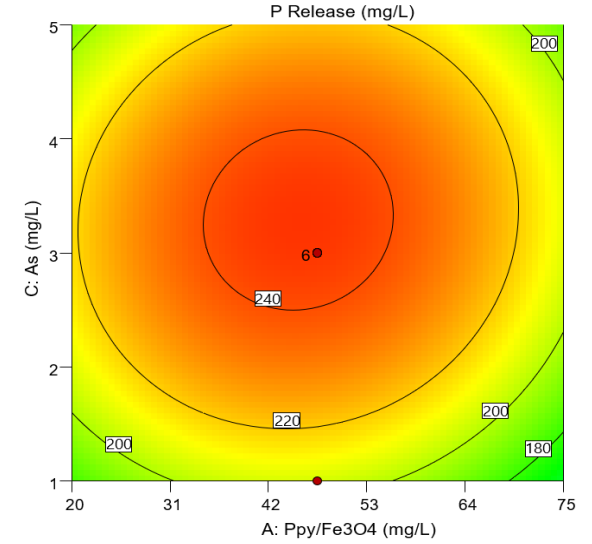
P Release (mg/L)
C: As (mg/L)
A: Ppy/Fe3O4 (mg/L)
5
4
3
2
1
20
31
42
53
64
75
200
240
220
180
6

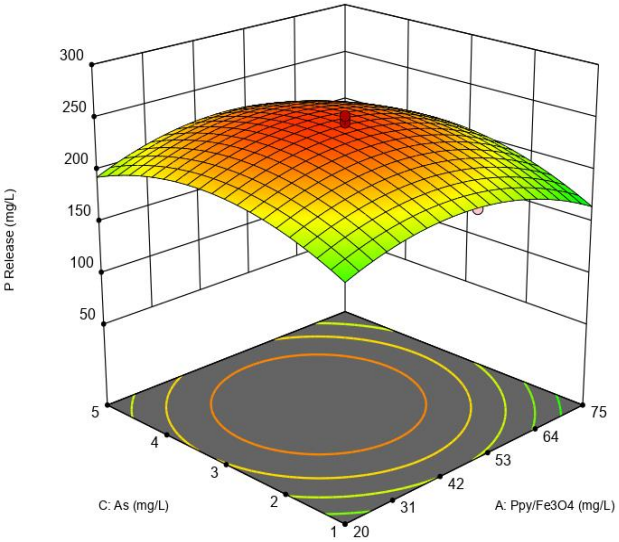
P Release (mg/L)
300
250
200
150
100
50
C: As (mg/L)
A: Ppy/Fe3O4 (mg/L)
5
4
3
2
1
20
31
42
53
64
75

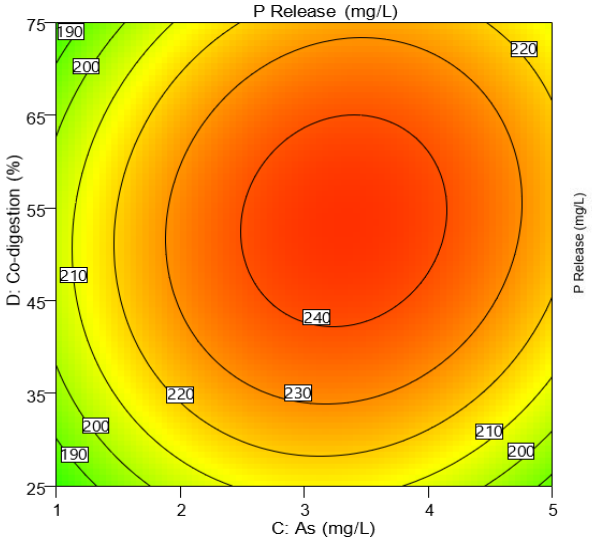
P Release (mg/L)
D: Co-digestion (%)
C: As (mg/L)
75
65
55
45
35
25
1
2
3
4
5
190
200
210
220
240
230

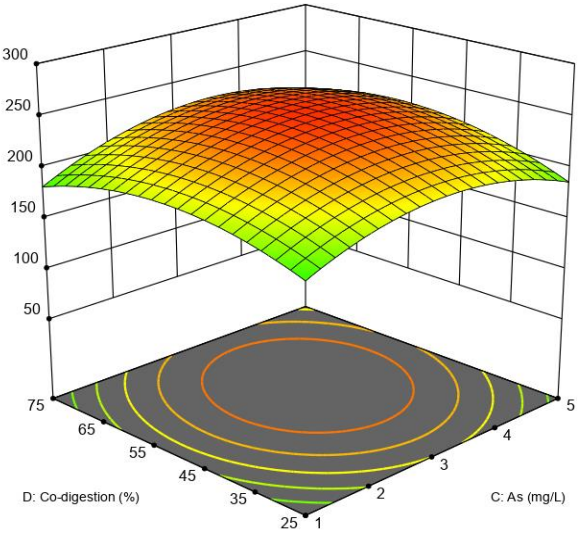
P Release (mg/L)
300
250
200
150
100
50
D: Co-digestion (%)
C: As (mg/L)
75
65
55
45
35
25
1
2
3
4
5

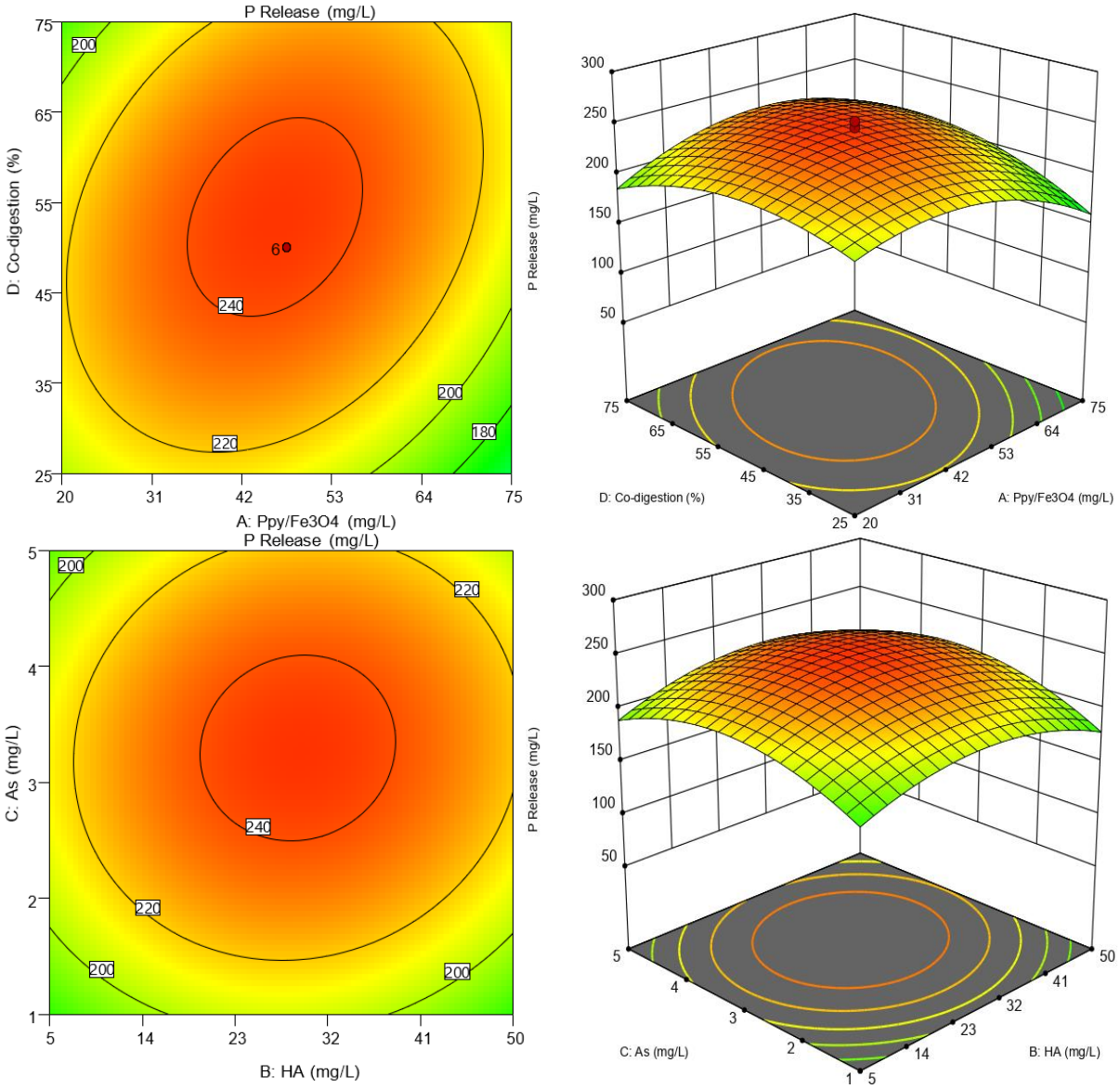

Fig.5. 7 Contour and response surfaces plots for P release

More so, the negative linear correlation (Equation 5.3, Fig. 5.7) implied that higher P release was due decreased Ppy/Fe_3O_4 concentration in the anaerobic digestion system, but the reverse was the case when iron supplementation is higher. This observed trend agrees with Puyol et al. (2018) and Xie et al. (2017) that increased supplementation of iron additives reacts with dissolved P to reduce soluble P availability. The positive interaction effects of Ppy/Fe_3O_4 with other variables revealed their synergy with each other for enhanced P release. Jeong (2017), Liu et al. (2011) and Lenoble et al. (2005) alluded to the iron interaction with HA and As separately and in combination as well as the antagonistic relationship between As and P (due to their similarity in the property), which altered their capability to absorb P, making P available in the digestate (instead of the usual Fe-P entrapment). A view at the interaction terms with co-digestion showed that solubilization of substrates during the

co-digestion for P release was enhanced by all other three additives (AD, BD and CD). Aligning with this observation, Yap et al (2018) and Azman et al. (2015) suggested that when these additives are used at appropriate concentrations (Ppy/Fe_3O_4 ≤20 mg/L, HA≤ 5 mg/L, As ≤1%), they synergistically interact to allow substrate hydrolysis and consequently influence P release.

5.3.5 Multi-objective optimization of CCD-RSM

The enhanced anaerobic digestion for both biomethane production and P release is a multi-input and output process, optimization of these process parameters simultaneously can be achieved using multi-objective optimization approach in RSM via desirability analysis (Deepanraj et al. 2020). This method involves the combination of goals into an overall desirability function using numerical optimization method by transforming estimated responses (Y_i) into a dimensionless bound ($0 < d_i < 1$), where $d_i \leq 1$ indicates that Y_i is more desirable and considered to be the optimum condition, $d_i = 0$ implies complete undesired response (Anderson and Whitcomb, 2017). The simultaneous objective function according to Deepanraj et al. (2020) is a geometric mean of all responses.

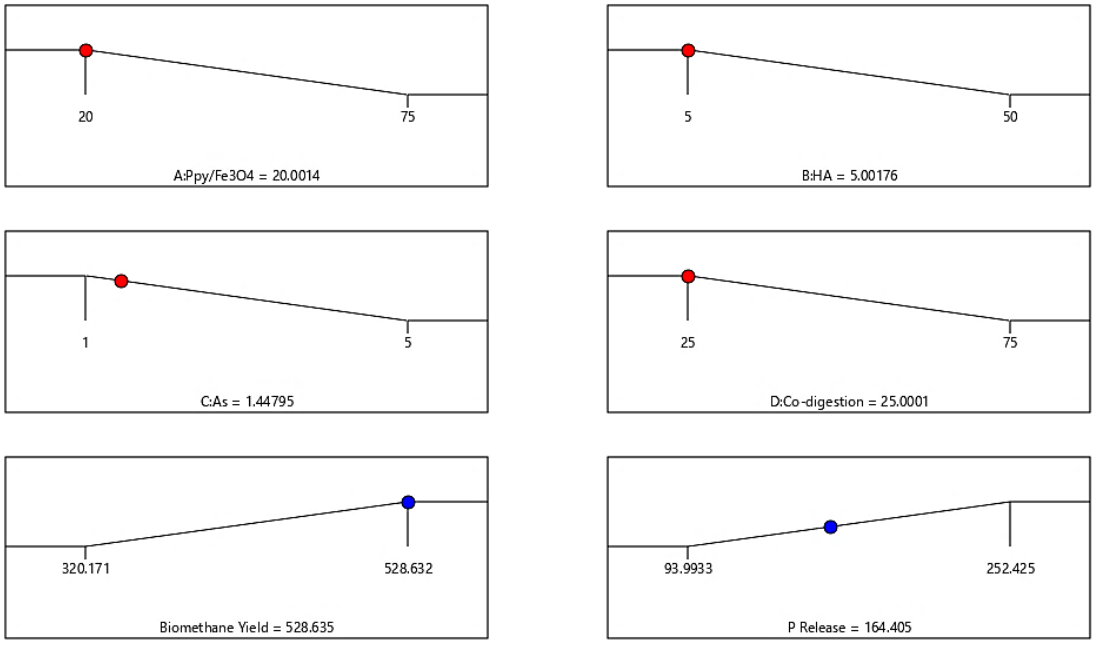

Fig.5. 8 Ramp plot for desirability analysis

Based on the numerical optimization of this studies, the optimum input parameter (Ppy/Fe_3O_4, HA As and co-digestion) was determined with the objective targeted at maximizing both biomethane yield and P release as shown in the ramp plot (Fig.5.8) and Table 5.6. The optimized input values include Ppy/Fe_3O_4 concentration of 20.0014 mg/L, HA concentration of 5.0018 mg/L, As the concentration of 1.448 mg/L and co-digestion of 25.0001% and the predicted responses from the

second-order polynomial model (Equations 5.2 and 5.3) are biomethane yield (528.635 $mLCH_4/gVS$) and P released (164.405 mg/L). The overall desirability value for the combined objective is 0.870 since this is closer to 1, it is adjudged a good measure. This agrees with the view of Siami et al. (2020) on desirability that objective function varies from 0 (zero) outside the limit to 1(one) on the goal. The multi-objective optimization desirability plot is shown in Fig. 5.9.

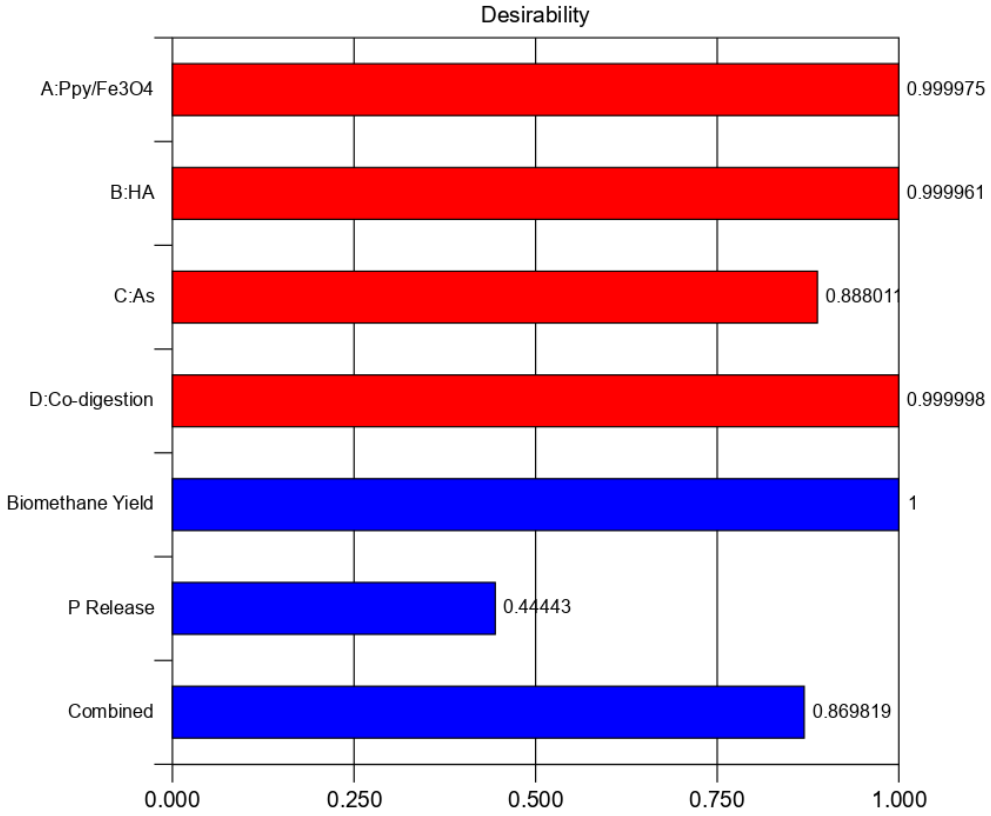

Fig.5. 9 The plot of multi-objective optimization desirability

However, with the optimum input values obtained through the multi-objective optimization process, validation of the optimum values was conducted to verify their performances and the adequacy predicted responses. Thereafter, confirmatory sets of experiment were conducted using the optimized independent variables and the same AMPTS II BMP Assay for biomethane yield and P release determination. Table 5.6 shows that the biomethane yield (502.743 $mLCH_4/gVS$) was 4.90% lower than the predicted value, while the measured P release (168.674 mg/L) was higher by 2.597%. Despite the prediction difference, according to Raposo et al. (2011) model prediction difference below 10% is acceptable for yield estimation, hence the CCD-RSM model is adjudged fit for further predication.

Table 5. 6 Optimum values of constraints and responses

Parameter and response	Lower Limit	Upper Limit	Optimum	Goal	Prediction difference %
Ppy/Fe3O4	20.00	75.00	20.00	minimize	-
Humic acid	5.00	50.00	5.00	minimize	-
Arsenate	1.00	5.00	1.45	minimize	-
Co-digestion	25.00	75.00	25.00	minimize	-
Biomethane Yield	320.17	528.63	528.64	maximize	4.90
P Release	93.99	252.43	164.41	maximize	2.60

5.4 Summary

Experimental study on the simultaneous biomethane production and P release during anaerobic digestion of organic waste was done through RSM optimization of additives (accelerants and P antagonist). The validated maximum biomethane yield and P releases were 502.743 mLCH4/gVS and 168.674 mg/L at the optimum conditions of Ppy/Fe_3O_4 (20.0014 mg/L), HA (5.0018 mg/L), As (1.448 mg/L) and co-digestion (25.0001%), while the predicted biomethane yield and P release were 528.635 mLCH_4/gVS and 164.405 mg/L respectively. All the response models were highly significant with appropriate goodness of fit and had prediction differences of 4.90% and 2.597% respectively for both biomethane yield and P release. All the additives (accelerants and antagonists) had influences on anaerobic digestion processes to achieve both increased biomethane production and P release. General high VFA reduction was also observed in all studies sample and this is attributable to the low TS% of all the substrates. Studies on the influence of long exposure of anaerobic digestion processes to these additives on both biomethane yield and P release in a continuous bioreactor setup is recommended for further investigation.

Chapter Six

Life cycle assessment of enhanced anaerobic digestion of agro-industrial waste for biogas production

6.1 Introduction

The current global challenge is the transitioning to a resource-efficient and sustainable energy supply. This is in the face of menacing environmental concerns and acute energy resources depletion (mainly fossil energy sources) (Longo et al. 2020; Cellura et al. 2013). Energy generation from renewable resources (such biomass or biowaste) is vital for the attainment of the desired low-carbon economy due to its numerous benefits, which include cheap energy provision for heating and power generation, easy off-grid energy access and reduction of fossil energy cost (Longo et al. 2020). Energy from biomass is expected to supply more than half of the global energy demand in the future (Ertem et al. 2017). Due to the challenges associated with over-exploitation of arable land for energy crop and its impact on food security as well as increasing greenhouse gas emissions, there is need for a more environmentally friendly and economically competitive bioenergy source (Ertem et al. 2017). As an aspect of the circular bioeconomy, bioenergy production from waste through anaerobic digestion is adjudged an efficient energy (biogas) and nutrient (biofertilizer) recovery strategy from biowastes/biomass (substrates) (Show et al. 2020). When compared to other techniques for emission abatement from these substrates such as land application of biowastes or composting, anaerobic digestion has proven emission mitigation approach to minimize the adverse impact of biowastes management on the environment (Abdelsalam et al. 2019; Samer, 2016).

However, these substrates, especially those of agro-industrial origin contain complex natural polymers which are difficult to breakdown by microbes due to their chemical compositions (Akunna, 2018). Although most of these substrates have high biomethane potential, their actual biogas production from the anaerobic digestion process is often lower due to structural configuration (Xiao et al. 2020). To this end, substrate enhancement becomes necessary for the rapid breakdown of the compact substrate structure and overall improvement of the biogas production. Pretreatment is one of such enhancement strategies undertaken before anaerobic digestion process to hydrolyze recalcitrant substrates (lignocellulosic wastes) and facilitate enzymatic activities microbial deconstruction of plant cell's complex structures (Xue et al. 2020; Ingle et al. 2019). Various pretreatment methods (chemical, physical, biological, combined method, among others) have been employed in biofuel studies for improvement of hydrolysis stage, which is the rate-limiting step of

anaerobic digestion process (Atelge et al. 2020; Salihu and Alam, 2016). Substrate pretreatment with alkaline is very efficient at solubilizing lignocellulose-rich biomass, Xue et al. (2020) reported that the use of 8% NaOH resulted in 56.92% increase in biogas production.

Furthermore, the use of nutrient supplementation as an anaerobic digestion intensification option has been widely reported as a cheap and successful means of increasing biogas production (Abdelsalam et al. 2017). In Hijazi et al. (2020a and b) and Kim et al. (2017), it was noted that additives are crucial for bacteria kinetics, increased biodigester stability, minimized toxin impacts and supply of deficient nutrients. Already studied additives for enhanced biogas production are in different forms such as organic or inorganic or biological or chemical and are in a macro, micro or nanoscale (Abdelwahab et al. 2020; Romero-Güiza et al. 2016; Mao et al. 2015). Amongst the most used additives (Fe, Co, Mo, Ni, Se, etc.), iron-based ones have proven to be effective in enhancing substrate solubilization, toxicity control, stimulation of anaerobes, nutrient availability, improvement of biogas yield, among others (Chen et al. 2018; Casals et al. 2014). Abdelsalam et al. (2016) reported that the addition of iron nanoparticle to anaerobic digestion at optimum concentration reduced the lag phase and digestion time. Ugwu and Enweremadu (2020) demonstrated that upon the addition of 20 mg/L of iron additive (Ppy/Fe_3O_4 Nanocomposite), biomethane yield was enhanced by 2.74%. Similarly, Yang et al. (2019) reported a 27.3% increase in biomethane yield with the addition of zero-valent iron to anaerobic digestion of pig manure. According to Hijazi et al. (2020a and b) and Martins et al. (2017), these environmentally friendly iron additives have been used in biogas plants even at commercial levels to ensure superior bioreactor performances and biogas production, but the iron nanoparticles despite their high reactivity, high specificity and increased surface area have not been used at large scale.

Moreover, these enhancement strategies involve energy and material exchanges with the surroundings; therefore, it is vital to assess the environmental and energetic performance these intensification methods in comparison with unenhanced digestion process (Moghaddam et al. 2016). Life cycle assessment (LCA) is most suited for understanding the environmental impacts of enhanced biomethane production and its utilization (Hijazi et al. 2016). LCA is an all-inclusive methodology deployed in the evaluation of environmental impacts of services, products, materials and energy flows from the beginning (cradle or raw material extraction), raw material processing, usage and end-stage (disposal, recycling or reuse) (Abdelsalam et al. 2019; Martins et al. 2017). It also aids in determining the influences of varying sub-processes on the entire system results (Moghaddam et al. 2016). The four-phased approach based on ISO 14040:2006 used in LCA evaluation is goal and scope definition,

data inventory collection, impact assessment and result interpretation (Ertem et al. 2017; ISO, 2006). While assessing the environmental effects of novel technologies, enhanced techniques and products, LCA can be used to quantify specific environmental concerns like eutrophication, greenhouse gas (GHG) emission, etc. (Hijazi et al. 2020b; Nasution et al., 2018).

On the other hand, LCA has been successfully used in several areas of biogas production for assessment of energy balance and environmental influences (Abdelsalam et al. 2019; Ramírez-Arpide et al. 2018). Several studies focusing on LCA analysis of enhanced biogas production processes have been conducted: (a) Ramírez-Arpide et al. (2018) analyzed the co-digestion of nopal cladodes and dairy cow manure to achieve lower global warming potentials, (b) Lijó et al. (2014) investigated the LCA of electricity production from co-digestion of pig slurry and energy crops, (c) Xiao et al. (2020) reported on the life cycle and economic assessments of hydrothermally pretreated microalgae for improved biogas yield, (d) In evaluating the environmental impacts of pretreated lignocellulosic biomass, Prasad et al. (2016) showed that pretreatment lowered the CO_2 emission, (e) Abdelsalam et al. (2019) reported on the LCA of laser pretreatment of animal manure for biogas production, (f) Hijazi et al. (2020a and b) investigated the environmental impacts of supplemented anaerobic digestion with nanoparticles and trace elements, (g) The assessment of biogas production from pig manure was also studies by Ramírez-Islas et al. (2020).

However, the environmental impacts of various enhancement options used in this study have not been evaluated. This study also seeks to address these issues: which enhancement technique is most environmentally friendly when compared to each other? and which option consumes more energy and materials (inputs and outputs) in the process of energy production? Therefore, the objective of this investigation is to carry out an environmental impact assessment of the implementation of such as Ppy/Fe_3O_4 NPs, NZVI, Fe_3O_4 NPs and alkaline pretreatment on biogas production from okra waste and pig manure through the anaerobic digestion (mono or co-digestion) process.

6.2. Materials and methods

In order to assess the potential environmental impacts associated with energy production from anaerobic digestion (mono or co-digestion) enhanced with additives (Ppy/Fe_3O_4 NPs, NZVI, Fe_3O_4 NPs) and alkaline pretreatment, the standard life cycle assessment methodology was used. This assessment was conducted in accordance with the stipulated LCA framework in ISO 14040 (ISO, 2006). The focus of the entire study was on these categorized waste management processes: waste

generation from okra and pig production, substrate processing, digestion process for biogas production, biogas utilization and digestate management. The LCA software SimaPro version 9.1 (PRé Sustainability, Netherlands) and data from the Ecoinvent version 3.6 database (Ecoinvent, Switzerland) were used for the assessment of enhanced anaerobic digestion.

6.2.1. Goal and scope definition

This study is aimed at performing the environmental impact assessment of the use of different enhancements in biogas production from anaerobic digestion of okra and pig wastes and utilization of produce biogas as an energy source. The goal also includes comparing LCAs of processes involved in waste management systems of the enhancement anaerobic digestion and baselines. The generated wastes (feedstocks) are fed into the bioreactor for biogas and digestate production. The produced biogas is used for energy (electricity and heat) production, while the digestate is separated into liquid and solid portions for further treatment and proper disposal (as organic fertilizer).

6.2.2. Description of biogas production and energy generation

For the entire life cycle assessment, the environmental footprints of all the material and energy input processes ranging from waste generation to digestate management were included in this study. The assessment processes considered the associated inputs and outputs, which include the following: materials and energies involved in okra and livestock (pig) production, okra production for biomass generation, transportation and preprocessing of substrates, feedstock pretreatment, mono-digestion, co-digestion and additive supplemented anaerobic digestion processes, biogas utilization, digestate management (Fig.6.1). The quantity of produced biogas production and generated energy were calculated for the various scenarios chosen in this study. These scenarios varied from each other based on the variation in substrates (okra and pig waste) and additive types (Ppy/Fe_3O_4 NPs, NZVI, Fe_3O_4 NPs and alkaline pretreatment). Data from Ugwu and Enweremadu (2019a and b), measured data from our unpublished research and other relevant literature on enhanced anaerobic digestion for production of biogas from okra wastes and pig manure formed the foundation for the yearly data computation used in this research. For each of the enhancement options, the biogas yield was computed based on the modified specifications of standard biogas plant reported in Abdelsalam et al. (2019). The overall energy (electric and heat energies) of each scenario were estimated from the data of biogas and biomethane produced as discussed in subsequent sections.

6.2.3. Functional unit and system boundaries

The functional unit, which according to (ISO, 2006) explains the quantification of the identified system's function and offers a necessary reference to which inputs and outputs can relate to each other. It can either be based on the output or input (Li et al. 2018b). Since the objective of this study is to investigate the environmental impacts of biogas production and utilization as an energy source, the functional unit of this assessment was chosen to be the useful bioenergy produced (1 MJ). The system boundaries shown in Fig.6.1 depicts the input (including raw materials and processes) and output variables that formed the life cycle inventory (LCI). However, pig slaughter, okra yield, digestate management and power usage were outside the system boundary.

6.2.4. Scenario description

The waste management systems within the boundaries were chosen based on the established enhancement options for anaerobic digestion of agro-wastes (Fig. 6.1). This study compares the baseline scenario (anaerobic digestion of okra and pig waste), which is the reference scenario based on obtained data from operational facilities. Alternative cases involving substrate pretreatment and additives supplementation aimed at improving performance parameters and yields were studied. The brief description of the analyzed scenarios in this study with their varying inputs and outputs attributes are shown in the block diagram (Fig. 6.1). More so, baseline systems: these scenarios are based on one-stage anaerobic digestion of okra waste and pig manure in a continuously stirred tank bioreactor system without any enhancement option (Hijazi et al. 2020a). For this system, the total solid of the mixed liquor (substrate, inoculum and water) was below 12%. The substrate to inoculum ratio was 2 (based on volatile solids (%VS)) (Li et al. 2018b). This process was conducted under mesophilic temperature since it was relevant for comparing alternative scenarios. Scenario 1 (Alkaline pretreatment) approach involved pretreating okra waste with 6% NaOH at room temperature for 15 minutes before its introduction to the biodigester (Ugwu and Enweremadu, 2019a). Other anaerobic digestion conditions and digester was the same as the one described in the baseline scenario. Other alternative scenarios (2 to 5) considered an additive enhancement of okra waste with 20 mg/L Ppy/Fe_3O_4 NPs, 1000 mg/L nZVI, 20 mg/L Fe_3O_4 NPs and 20 mg/L Ppy/Fe_3O_4 NPs for co-digestion (okra and pig waste) for improved biogas production (Ugwu and Enweremadu 2020a).

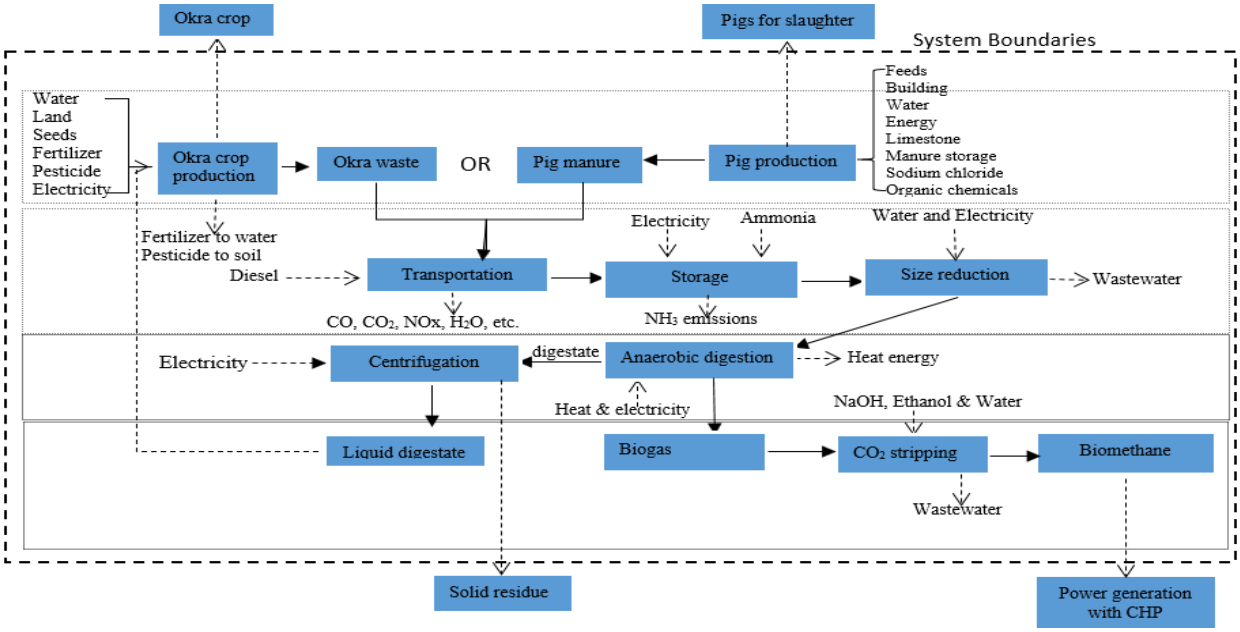

Baseline studies

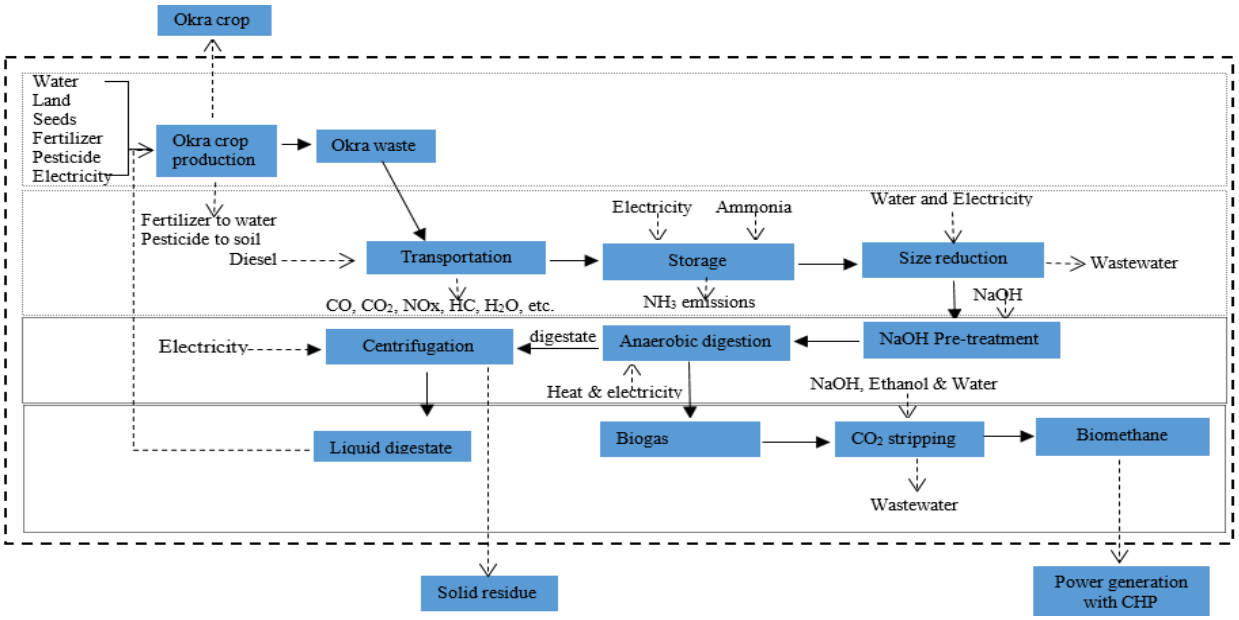

Option 1

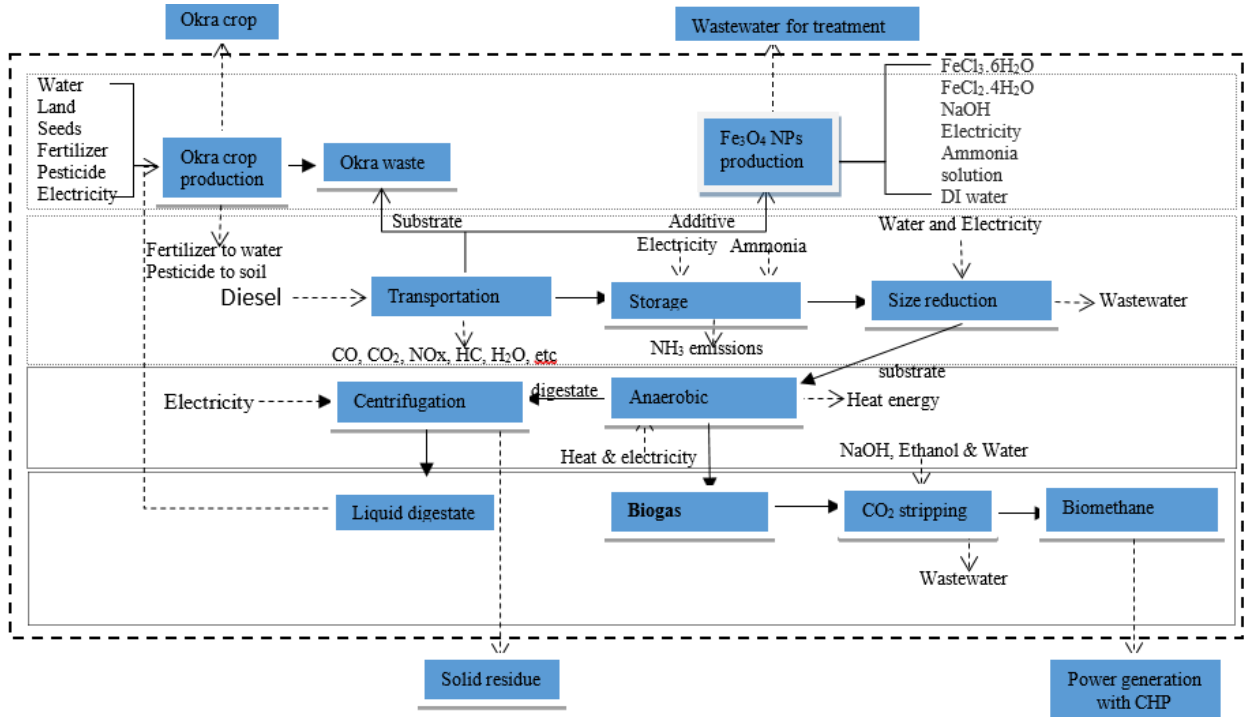

Option 2

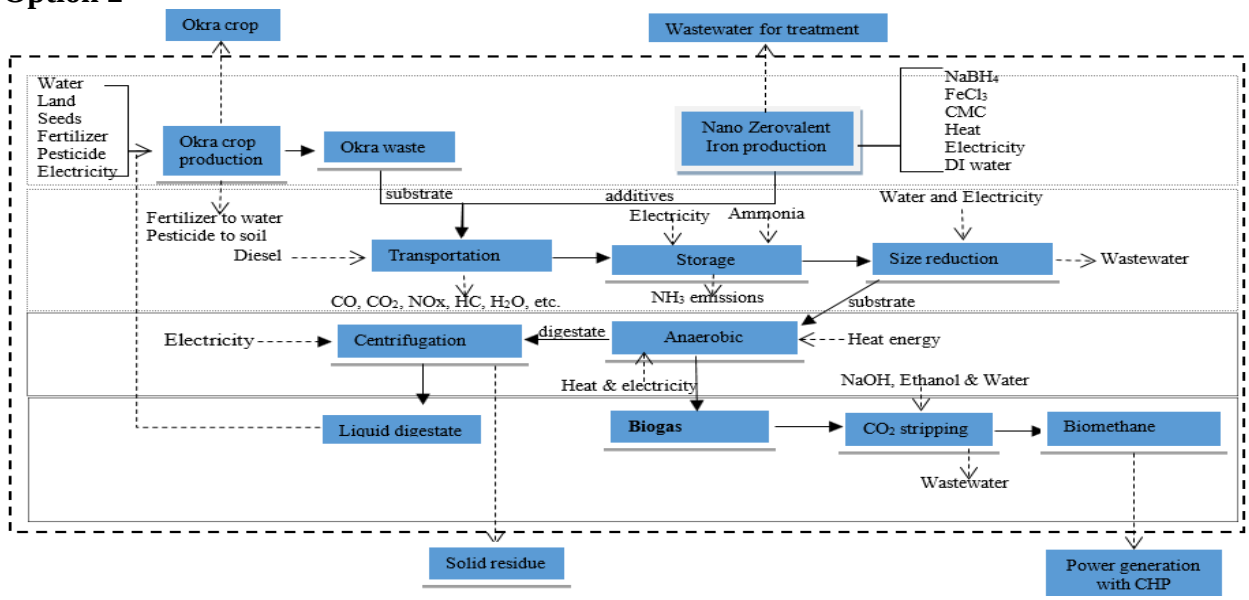

Option 3

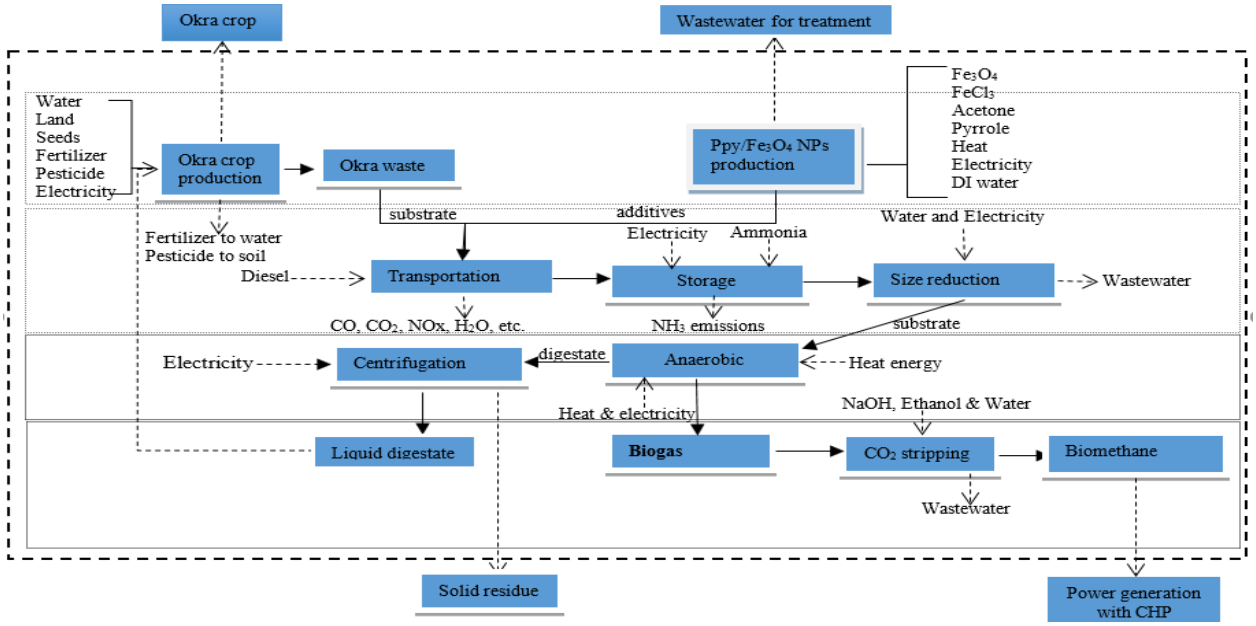

Option 4

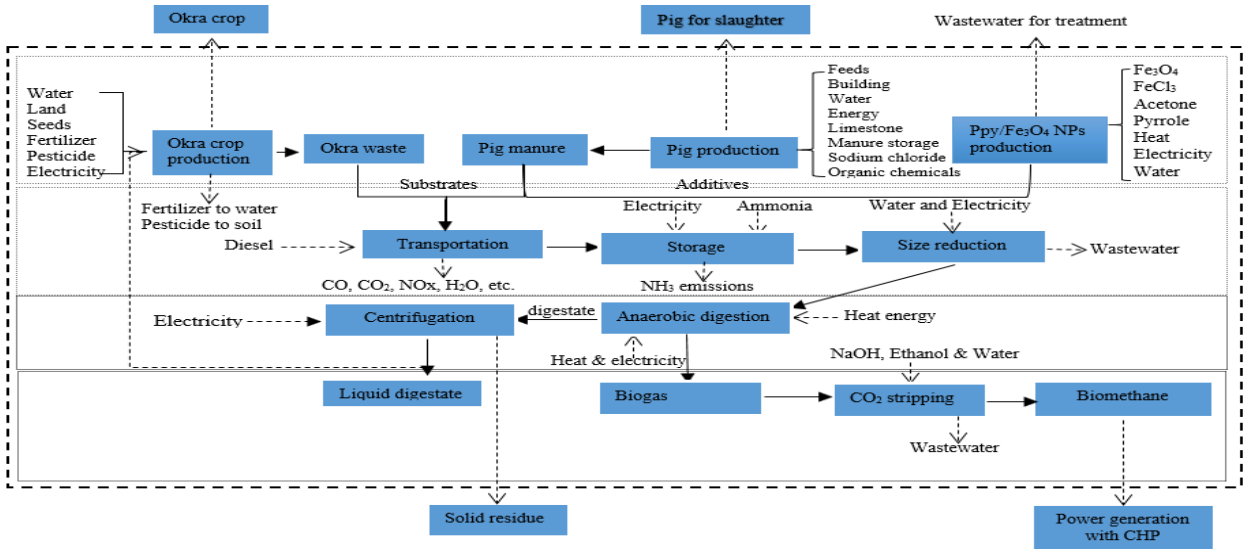

Option 5

Fig.6. 1 Baseline scenario: Product system and structure of biogas recovery without any enhancement; Option 1: Product system and structure of biogas recovery enhance with NaOH pretreatment; Option 2: Product system and structure of biogas recovery enhance with Fe_3O_4 NPs; Option 3: Product system and structure of biogas recovery enhance with NZVI; Option 4: Product system and structure of biogas recovery enhance with Ppy/Fe_3O_4 NPs; Option 5: Product system and structure of biogas recovery enhance with okra-pig waste co-digestion and Ppy/Fe_3O_4 NPs.

6.2.5. Life cycle inventory

For biogas production processes captured in this study, the inventory data that make up the life cycle inventory (LCI) are mostly data of raw materials and energy consumed obtained from previous studies, onsite data and databases in SimaPro 9.1. The LCI is discussed based on the management systems outlined earlier. The mass of the product was used for both input and output allocation

process. For this study, the used inventory data were shown in Tables 6.1 to 6.3 below.

6.2.5.1 Substrate production and characteristics

Okra production processes include land preparation and cultivation. Other farm management practices including nutrient supplementation with mineral fertilizer, pesticide and digestate application, as well as harvesting and transportation of both yields and wastes within the 1-hectare farm (FAO,2013; DAFF, 2012; National Research Council, 2006). The energy inputs and outputs at cultivation and harvesting with agricultural equipment and machinery are associated with diesel combustion and usage. The anaerobic digestion process generated a sizeable amount of digestate capable of lowering the quantity of inorganic fertilizer for okra cultivation. Similarly, part of the heat and electricity from the CHP co-generation unit is re-channeled to the anaerobic digestion processes. According to Moghaddam et al. (2016) and IPCC (2006), N_2O biogenic, which is emitted during crop production is calculated to be 967 kg CO_2-eq/FU. Nutrient leakage emissions from digestate and inorganic fertilizer emission were valued according to Moghaddam et al. (2016) and Börjesson and Tufvesson (2011) at 16 kg PO_4^{3-}eq/FU. Okra production data are determined and presented in Table 6.1.

Table 6. 1 Inventory of okra biomass production

Parameter	**Quantity**	**Sources**
Cultivation		
Water irrigation (m^3)	6,000	Calculated
Land (ha)	1	Calculated
Seeds (per hectare)	2500	National Research Council, 2006
Phosphate fertilizer (kg)	45	DAFF, 2012
Nitrogen fertilizer (kg)	43	DAFF, 2012
Pesticide (kg)	19	DAFF, 2012
Electricity (kWh)	70,000	FAO, 2013
Transportation within the farm	Within 1 hectare	Calculated
Outputs		
Okra yield (kg/ha)	11,000	National Research Council, 2006
Okra biomass (kg/ha)	27,000	National Research Council, 2006
leaching fraction (20%) (m^3) (containing fertilizers, pesticides, etc.)	1,200	FAO, 2013
Emissions to air from agronomic activities (kg)	2.688	Sampattagul et al. 2012

The data for material and energy inputs and emissions in pig waste generation, which was reported as a by-product was based on the datasets documented in Ecoinvent 3.6 (swine production- Global).

6.2.5.2. Substrate processing

The anaerobic digestion plant was assumed to be in proximity with the okra farm and piggery. The distance between digestion plant (Florida) and farm (Centurion) is 45.9 km, while from the piggery at ARC Irene and digestion plant (Florida) is 51.7 km. All raw materials were assumed to have been transported using diesel consuming trucks. Since the types of truck, speeds of the truck, weight of raw materials affect the amount of diesel, in this study, the two-way distance for raw material collection as well as the weight of raw materials were considered (Li et al. 2018b). The wastes transported to the digestion plant are kept in a controlled environment to minimize putrefaction. At the digestion plant, the sizes of okra biomass and pig manure are reduced and homogenized at $10m^3$ per hour for 7.5 kW and 4 kW respectively (Li et al. 2018b). The energy requirement for size reduction and homogenization operations depends on the type of machines. According to Li et al. (2018b), the pump capacity for transferring 25 m^3/h water and inoculum to the bioreactor was rated 4 kW. One controlled environment (for refrigeration with data from Ecoinvent 3.6) was used for storing substrates before being fed to the biodigester.

6.2.5.3. Production of additives for enhancement of biogas production

In this section, the production of additives for enhancement of anaerobic digestion for improved biogas yield was considered. Detailed inventory for production of 1g of nano zerovalent iron, iron (III) nanoparticles and polypyrrole magnetic nanocomposite are presented in Table 6.2. The data on alkaline pretreatment with sodium hydroxide (NaOH) were obtained from the Ecoinvent 3.6 database of SimaPro 9.1. The pretreatment was performed prior to actual anaerobic digestion.

Table 6. 2 Inventory data production of additives

Parameters	**[a]NZVI**	**[b]Fe3O4 NPs**	**[c]Ppy-Fe3O4 NPs**
$NaBH_4$ (kg)	2.71E-03	-	-
$FeCl_3$ (kg) ($FeCl_3.6H_2O$ (kg)	2.90E-03	0.00235	0.00600
$FeCl_2.4H_2O$ (kg)	-	0.00086	-
Fe_3O_4 (kg)	-	-	0.0004
Deionized water (m^3)	0.001	1.00E-04	8.00E-05
Stirring (kWh)	1.43E-01	1.43E-01	-
Filtration (kWh)	3.98E-02	-	-
Filter paper (kg)	2.49E-03	-	-
Heating below 100^oC (kWh)	-	1.2	1.2
Sonicating (kWh)	-	-	2.00E-01
Ethanol for washing (kg)	3.76E-03	-	-
NH_4OH (m^3)	5.00E-06	5.00E-06	-
Pyrrole (m^3)	-	-	8.00E-07
Acetone (m^3)	-	-	5.00E-04

Outputs			
Additive yield (kg)	0.001	0.001	0.001
Wastewater (m^3)	9.17E-04	8.16E-04	8.16-04
Solid waste (kg)	2.49E-03	1.53E-04	1.50E-04

Note: a = Martins et al. 2017, b = Mizutani et al. 2008, c = Aigbe et al. 2018

6.2.5.4. Anaerobic digestion and energy generation

At this stage, solid (proximate and ultimate) analysis are conducted; thereafter substrate(s), inoculum and water are introduced into the bioreactor to form mixed liquor of about 8% TS. However, the data of the solid (proximate and ultimate) analysis, as well as the biomethane content of the produced biogas, are presented in Table 6.3. In this study, mesophilic conditions (37^{o}C) were adopted for the anaerobic digestion process because of its proven track record of reliability, favourable energy usage, cost-effectiveness and overall satisfactory process performances (Li et al. 2018b). The hydraulic retention time of 30 days was adopted for the anaerobic digestion across all scenarios. The results of biogas production from anaerobic digestion and energy generation are shown in Table 6.3. The table also shows the calculated values of electrical energy, heat energy and overall energy from produced biogas via various scenarios (baselines and enhancement options). These computations were based on standard single-stage biodigester with about 1400 m^3 capacity and possible throughput of 10,000 m^3 per annum (Hijazi et al. 2020b). The biogas yield in m^3 was modified from Ecoinvent 3.6 database using Equation 6.1. Other outputs such as digestate yield and emissions were also computed based on guidelines provided in Ecoinvent 3.6 database and Li et al. (2018b).

$$Q = m \times TS \times VS \times Y_p \quad 6.1$$

Where: Q is biogas yield in m^3; m is mass of substrate (kg of wet mass); TS is total solid of substrates (kg of TS per kg wet mass); VS/TS is Volatile matter (kg of VS per kg of TS); Y_p is biogas yield potential (m3 biogas per kg of VS).

Table 6. 3 Data for biogas production and energy generation from standard biogas plant per year

Parameter	**Baseline 1**	**Baseline 2**	**Option 1**	**Option 2**	**Option 3**	**Option 4**	**Option 5**
	Okra waste	**Pig waste**	**Alkali Pretreated**	**Fe_3O_4 NPs**	**nZVI-1000**	**Ppy-Fe_3O_4**	**Pig +Okra + Ppy-Fe_3O_4**
Substrate Characteristics							
Total Solid (%)	7.82	9.78	7.82	7.82	7.82	7.82	8.55
VS of TS %	88.21	81.54	88.21	88.21	88.21	88.21	81.54
Carbon % TS	39.3	40.39	39.3	39.3	39.3	39.3	39.3
Hydrogen% TS	5.39	5.29	5.39	5.39	5.39	5.39	5.29
Nitrogen %TS	3.21	1.97	3.21	3.21	3.21	3.21	1.97
Oxygen% TS	45.74	45.03	45.74	45.74	45.74	45.74	45.03
Anaerobic Digestion							

[a]Mixing of mixed liquor during digestion kJ/m^3	300	300	300	300	300	300	300
Water (%)	16	16	16	16	16	16	16
Biogas yield (m^3/tonVS)	493.9	420.3	509.09	510.35	512.6	544.9	528.632
Biomethane production m^3	340519.36	289777.21	350992.11	351860.81	353412.07	375681.31	364465.33
Methane content (%)	55.9	65	56.2	57.2	56.5	59.5	60.1
Biogas production (m^3)	609158.06	445811.1	624541.1	615141.27	625508.09	631397.15	606431.5
Biogas Utilization							
Heat energy (kWh)	12197415	8926654	12505436	12317220	12524799	12642718	12142820
Electrical energy (kWh)	2365326.9	1731059.7	2425058.4	2388559.4	2428813.2	2451680.1	2354739.8
Overall energy (kWh)	14562742	10657714	14930495	14705779	14953612	15094398	14497560
Digestate management							
[a]Centrifugation (kWh/m^3)	1.26	1.26	1.26	1.26	1.26	1.26	1.26
Wastewater (m3)	8924.09	8734.34	8924.09	8924.09	8924.09	8924.09	8829.21
Solid waste (t)	757.07	946.82	757.07	757.07	757.07	757.07	851.94

Note: a = Xiao et al. 2020

6.2.5.5. Biogas utilization

After the conditioning of produced biogas, biomethane is then converted to both thermal and electrical energy with the use of internal combustion cogeneration engine (combined heat and power (CHP)). From the Ecoinvent 3.6, the used CHP for this study is a heat and power co-generation unit of 160kW electrical with common components for heat and electricity. The biogas conditioning (purification and dehumidification) was considered negligible since the volume of H_2S and emissions from both purification and dehumidification is very low (Li et al. 2018b; Evangelisti et al. 2014). As shown in Table 6.3, the biomethane yields for different scenarios considered in this study are 493.90 m^3/ton.VS, 420 m^3/ton.VS, 509.09 m^3/ton.VS, 510.35 m^3/ton.VS, 512.60 m^3/ton.VS, 544.90 m^3/ton.VS, and 528.63 m^3/ton.VS respectively for baseline 1, baseline 2, option 1, option 2, option 3, option 4 and option 5. The CHP engine biogas to energy (thermal and electricity) conversion efficiencies considered in his study was as reported in Li et al. (2018b). The overall energy outputs are based on the combined energy (electrical and thermal) conversion efficiencies from CHP internal combustion engine. In this study, thermal and electrical conversion efficiencies from Ecoinvent 3.6 database are 53% and 37% respectively. According to Li et al. (2018b), these efficiencies were computed with Equations 6.2 and 6.3.

$$E = \eta_1 \times (V \times e)/3.6 \quad 6.2$$

$$H = \eta_2 \times V \times e \quad 6.3$$

Where: E is the amount of produced electricity (kWh); η_1 is the conversion efficiency of electricity (37%); V is the quantity of methane combusted in the CHP engine (m3); e is the heating value of

methane (35.9 MJ/m^3); η_2 is the conversion efficiency of thermal energy (53%).

Similarly, in allocating greenhouse gas emission from the entire heat and power system, the exergetic allocation option was selected with electricity assigned 100% exergy (Abdelsalam et al. 2019; Nuorkivi, 2010). This entails that a major part of the greenhouse gas emission from the CHP system can be attributed to electricity while the heat component is considered negligible (Hijazi et al. 2020a).

6.2.5.6. Digestate management

The liquid digestate is used partly for enhancing substrate mix, irrigation of crop production lands and substituting inorganic fertilizer usage. The liquid digestate for irrigation and nutrient supply was transported to the farm (45.9 km). According to Moghaddam et al. (2016), the liquid digestate is applied via shallow injection to avert nitrogen loss as ammonia. The management (drying, storage or usage) of the solid digestate was not captured in this study. The anaerobic digestion plant has an average digestate output of about 9681.16 m^3. The produced digestate is phase-separated by centrifuging to yield 8883.43 m^3 of liquid digestate and 797.73 m^3 of solid digestate.

6.2.6. Life cycle impact indicators

These impact category indicators from electricity and heat generation from biogas were calculated using the ReCiPe 2016 method developed by Huijbregts et al. (2016), which is one of the methods in SimaPro 9.1 LCA software. The impact categories are largely grouped into three damage assessment endpoint level categories: damages to human health (HH), ecosystem quality (ED) and resource availability (RA) (Aziz and Hanafiah, 2020). The mid-point level of the impact categories in ReCiPe 2016 (Midpoint (H) V1.04 / World (2010) H) includes global warming (GWP, kg CO_2-eq to air), Stratospheric ozone depletion (ODP, kg CFC11-eq to air), ionizing radiation (IRP, kBq Co-60-eq to air), Ozone formation, Human health (HOFP, kg NOx-eq to air), particulate matter formation (PMFP, kg PM2.5-eq to air), Ozone formation, Terrestrial ecosystems (EOFP, kg NOx-eq to air), Terrestrial acidification (TAP, kg SO_2-eq to air), Freshwater eutrophication (FEP, kg P-eq to freshwater), marine eutrophication (MEP, kg N-eq to marine water), terrestrial ecotoxicity (TETP, kg 1,4-DCB-eq to industrial soil), marine ecotoxicity (METP, kg 1,4-DCB-eq to marine water), freshwater ecotoxicity (FETP, kg 1,4-DCB-eq to fresh water), human carcinogenic toxicity (HTPc, kg 1,4-DCB-eq to urban air), human non-carcinogenic toxicity (HTPnc, kg 1,4-DCB-eq to urban), land use change (LUC, m^2 x yr annual cropland-eq), mineral resources scarcity (SOP, kg Cu-eq), fossil resource scarcity (FFP, kg oil-eq) and water consumption (WCP, m^3 water-eq consumed).

6.3. Results and Discussions

6.3.1 Environmental indicators

At the mid-point level of the impact categories, the results are presented in different mass referenced units in kg of specific emission-based environmental indicators. In this study, the environmental indicators of the baselines and five other scenarios for electricity production from enhanced anaerobically digested agro-wastes are shown in Figs. 6.2 to 6.6 as computed. The results were discussed based on the impact categories with focus on the different contributing processes involved in the production and usage of biogas for electricity generation, which includes biomass production, substrate processing, enhancement production, biogas production, plant and machinery, utilization and digestate handling. Unlike in Hijazi et al. (2020a) and Abdelsalam et al. (2019) where enhancement options scored lower in all impact categories than those of the baseline studies, it could be observed that Scenario 1, 2 and 3 showed higher impacts for most of the impact categories. This may be due to the exclusion of enhancement (additives and alkaline) production and digestate handling processes. In addition, Harding et al. (2018) also suggested that this may be due to more input requirements (raw materials and energy) at each process stage for those scenarios. The overall LCA is exemplified by network representation of Baseline 1 shown in Fig S1(in appendix).

6.3.1.1. Global warming potential (GWP)

The GWP of electricity production expressed as carbon (IV) equivalent (CO_2-eq) to indicate the impact of climate change was analyzed and presented in Fig. 6.2 for all scenarios. The emissions are 0.005808, 0.005786, 0.005837, 0.006026, 0.006033, 0.005807 and 0.005300 kg CO_2-eq/MJ electrical for baseline 1, baseline 2, alkaline, NZVI NPs, Fe_3O_4 NPs, Ppy/Fe_3O_4 NPs and co-digestion-Ppy/Fe_3O_4 NPs respectively. Scenario 5 co-digestion-Ppy/Fe_3O_4 NPs) showed the lowest GWP when compared with other scenarios, while the highest GWP was given in the Fe_3O_4 NPs and NZVI enhanced productions. In Fig. 6.2, all the scenarios showed that utilization was the major contributor to the total GWP. Enhancement production had an appreciable contribution to the GWP, but the production of Ppy/Fe_3O_4 gave the least contribution. Generally, the lowest GWP result may be attributable to the combined enhancement (co-digestion of okra and pig waste and Ppy/Fe_3O_4) of the biogas production system. This is in line with the report of Ramírez-Arpide et al. (2018) that co-digestion of crop residue and animal waste resulted in lower GWP. Similarly, Ma et al. (2020) alluded to the numerous benefits of co-digestion between animal waste and crop biomass. On the contrary, Hijazi et al. (2020a) reported that additives supplementation showed lower GWP than the baselines. This may be that the authors did not capture production of both feedstock and additives in their study

goal. It was suggested in Ramírez-Arpide et al. (2018) and Van Stappen et al. (2016) that replacement of energy usage with electricity generation from biogas could reduce the GWP.

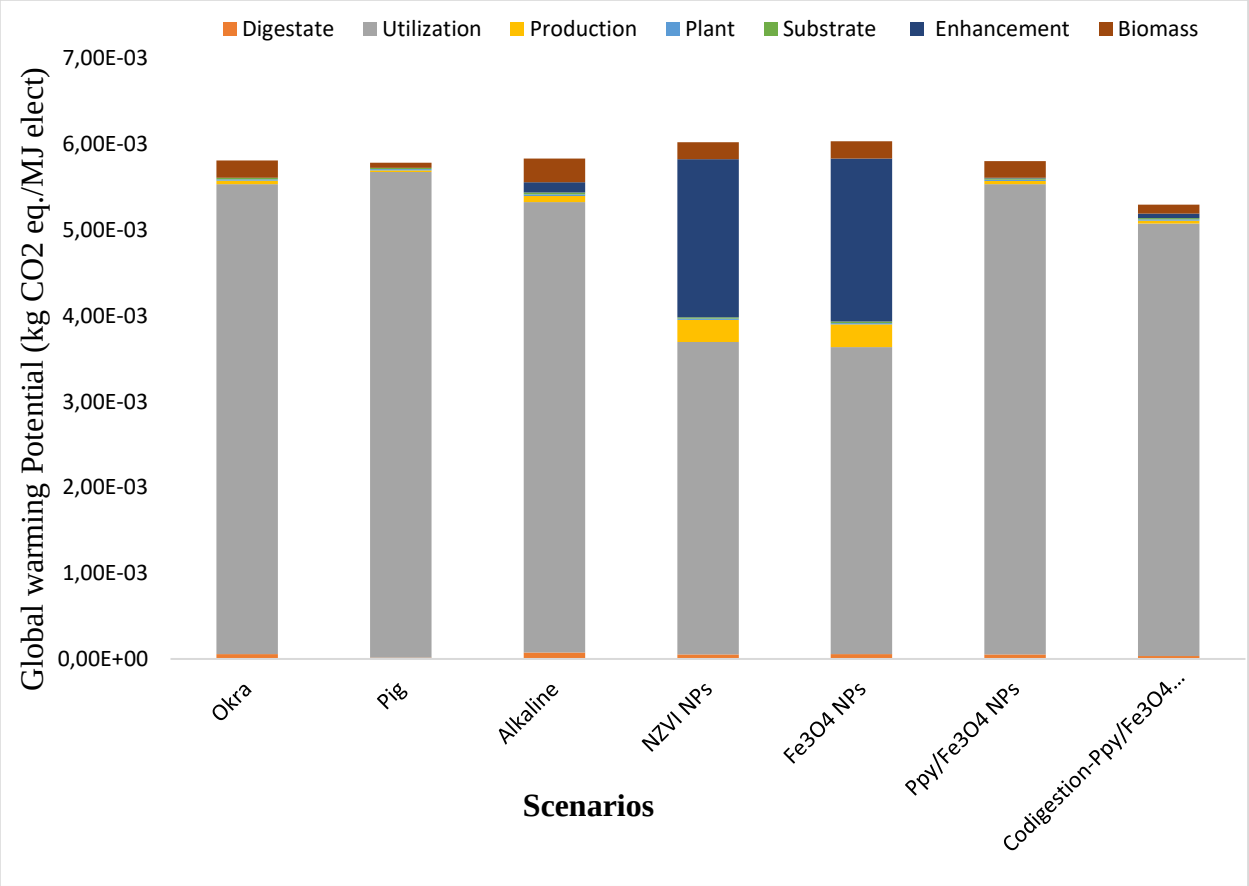

Fig.6. 2 Global warming potential (GWP) emissions from electricity production through different scenarios of anaerobic digestion of agrowastes.

6.3.1.2. Eutrophication potential

The addition of anthropogenic inputs such as nitrogen and phosphorus to the ecosystem causes eutrophication (nutrient enrichment). Eutrophication potential which is expressed in phosphate equivalent (P-eq) entails the potential impacts of nutrients (especially nitrogen and phosphorus) beyond environmental limits that may lead to adverse changes to the structure of the ecosystem and their functions (the composition of species and biomass production) (Li et al. 2018b; Prasad et al. 2016). The contribution of each process to the total eutrophication potential from electricity production from agro-wastes in kg PO_4^{3-}eq/MJ and kg N-eq/MJ were analyzed for all the scenarios are shown in Fig. 6.3a and b. For freshwater eutrophication, digestate handling was the main contributor, while biomass production was the highest contributor to marine eutrophication, this is logical because of the presence of ionized nutrients (phosphate, nitrogen, etc.) and possible leaching

and runoffs of PO_4^{3-} and NO_3^- mineral fertilizers during biomass production (Moghaddam et al. 2016; Prasad et al. 2016). The baseline 2 showed lowest eutrophication potential value of 1.54E-07 kg PO_4^{3-} eq/MJ and 1.95E-07 kg N-eq/MJ for freshwater and marine eutrophication respectively, which indicates the best scenario, while worst cases were observed from both scenario 2 (8.40E-07) and 3 (8.14E-07 kg PO_4^{3-}eq/MJ) for freshwater eutrophication. Scenario 1 (alkaline pretreat case) presented the worst case (highest value) for marine eutrophication at 7.42E-07 kg N-eq/MJ. The low value of all the eutrophication potentials for pig waste may be attributable to the amount (kg) of pig waste added to the digester due to its high volatile matter and considered in this study. The highest digestate contribution was from the alkaline pretreated scenario. This is in line with the assertion of Akunna (2018) that aside pretreatment cost, high sludge residue are the disadvantages of alkaline pretreatment option. Based on the high eutrophication potential of most of the scenarios, guided usage or disposal of digestate as well as the replacement of inorganic fertilizer usage for biomass production is suggested for lower eutrophication potential (Ramírez-Islas et al. 2020; Li et al. 2018b).

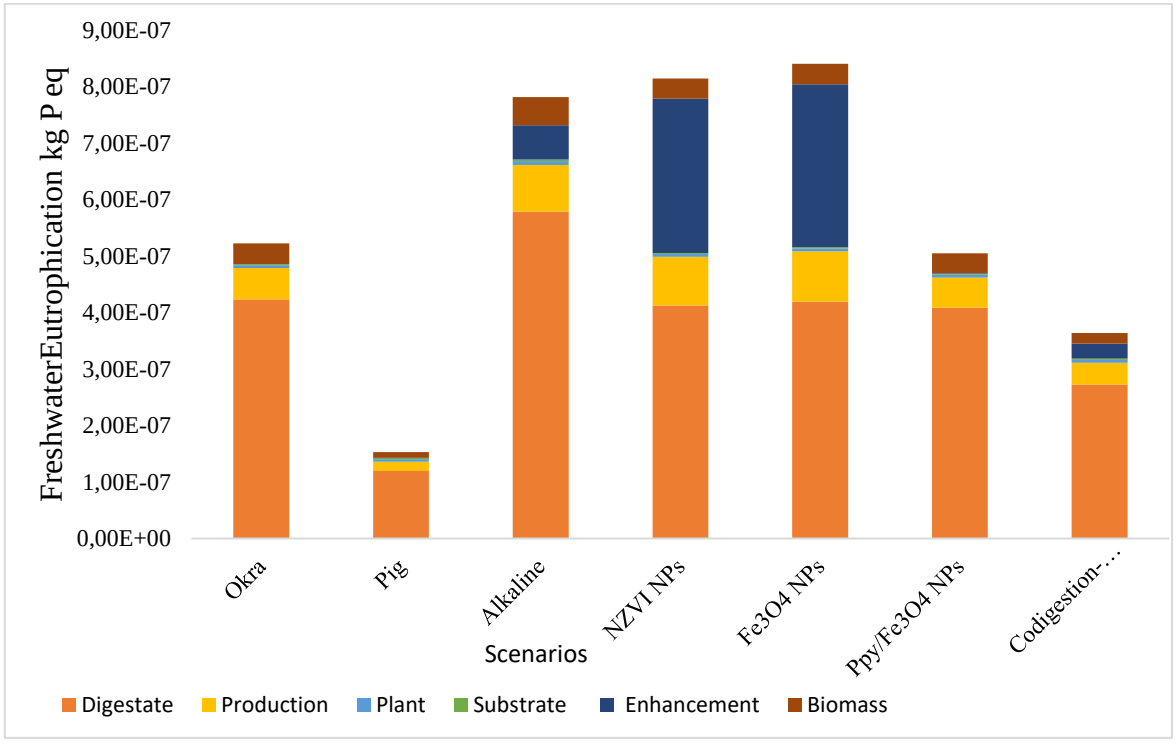

(a)

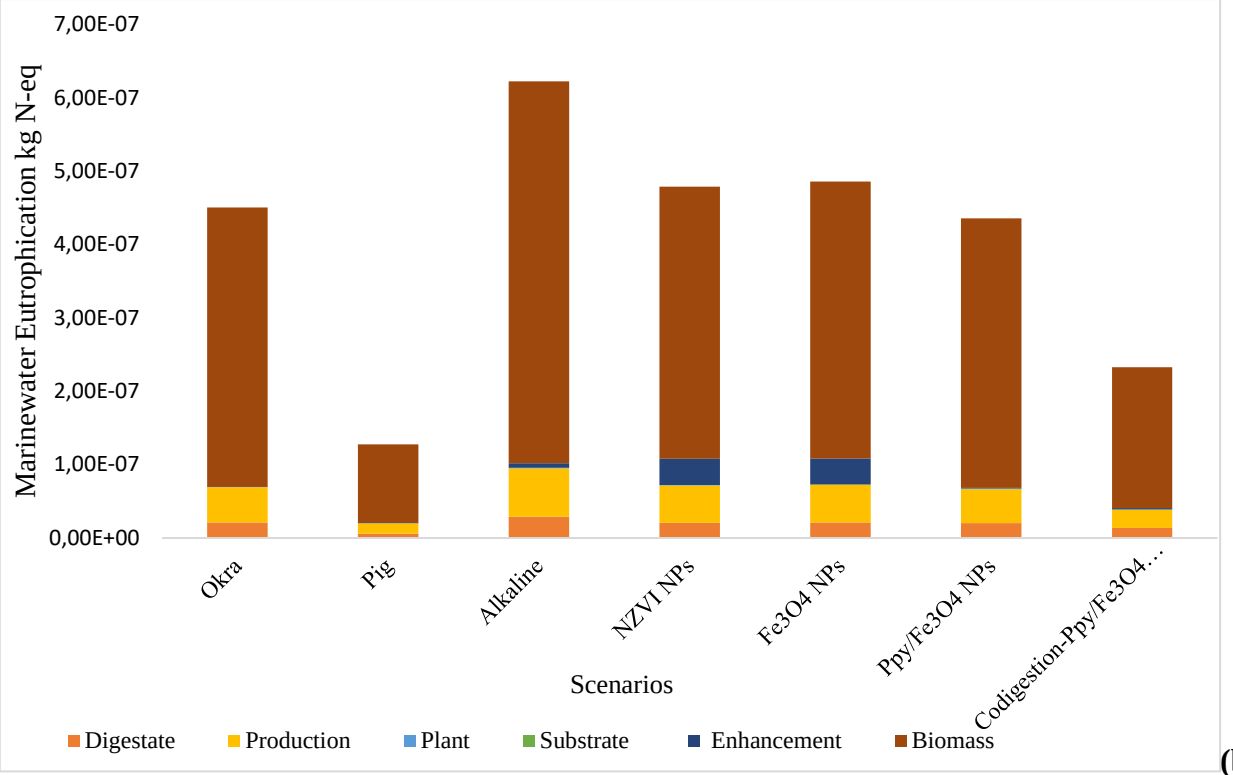

(b)

Fig.6. 3 Eutrophication Potentials ((a) Freshwater eutrophication and (b) Marine eutrophication) from electricity production through various scenarios of anaerobic digestion of agrowastes

6.3.1.3. Acidification potential

Terrestrial acidification potential is mainly related to atmospheric pollution by sulfur related emissions and expressed in kg SO_2-eq/MJ. According to Prasad et al. (2016), emitted sulfur dioxide (SO_2) to the atmosphere reacts with water to form acid rain via acid deposition process, causing impairment of the ecosystem when it falls. The contribution of each process to acidification potential of electricity production from anaerobic digestion of agrowastes was computed for all scenarios and shown in Fig. 6.4. Both scenario 2 and 3 at the value of 1.00787E-05 kg SO_2-eq showed the highest impact of acidification potentials. It could be observed that biogas utilization was the main contributor to terrestrial acidification potential. This agrees with Prasad et al. (2016) that electricity production contributed 86% to the overall acidification potential. Similarly, since biogas utilization involves the combustion of biogas for electricity and heat generation in CHP engines, Moghaddam et al. (2016) agreed that acidification potential is related to fuel combustion. The second largest emission of SO_2 was from enhancement production. This may likely be due to the combustion of fossil fuel during the extraction of minerals for additives production.

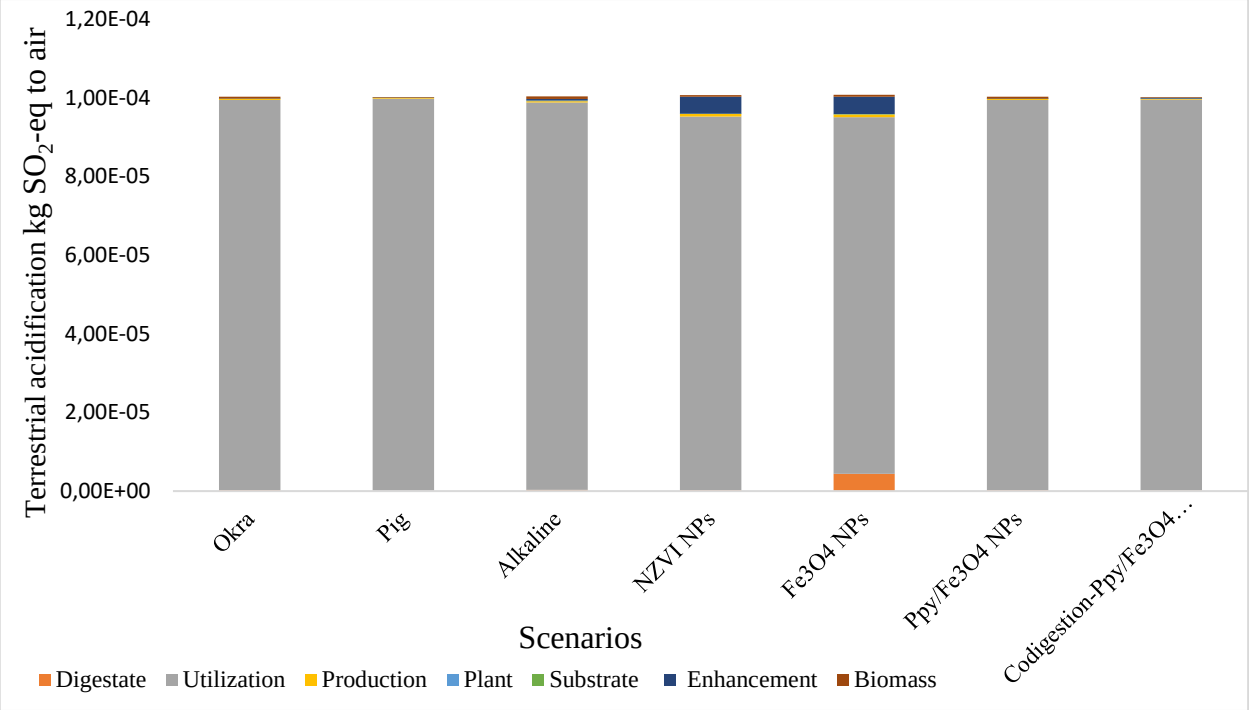

Fig.6. 4 Acidification from electricity generation from different anaerobic digestion of agrowastes scenarios.

6.3.1.4. Ecotoxicity and Toxicity potential

In this study, terrestrial ecotoxicity (TETP, kg 1,4-DCB-eq/MJ), marine ecotoxicity (METP, kg 1,4-DCB-eq/MJ), freshwater ecotoxicity (FETP, kg 1,4-DCB-eq/MJ), human carcinogenic toxicity (HTPc, kg 1,4-DCB-eq/MJ), human non-carcinogenic toxicity (HTPnc, kg 1,4-DCB-eq/MJ) impact categories for electricity production from anaerobic digestion of agrowastes showed a similar pattern of scenario 2 and 3 having the highest impact in Fig. 6.5a to e. The enhancement production was the major contributor to ecotoxicities and toxicities potentials of all impact categories, especially in scenario 2 and 3. This is consistent with several reports linking toxicities with chemical or fertilizer production (Ramírez-Arpide et al. 2018; Li et al. 2018b).

The process contribution to all scenarios of TETP is presented in Fig. 6.5a. The result showed that the baseline 2 (0.00049 kg 1,4-DCB-eq/MJ) and scenario 5 (0.00075 kg 1,4-DCB-eq/MJ) had lowest TETP value. Due to high emissions associated with chemical production and fuel combustion, Lansche and Müller (2017) reported that they contribute to TETP. In this study, aside enhancement production, anaerobic digestion had the next highest contribution to TETP. This also agrees with Ramírez-Arpide et al. (2018) that anaerobic digestion was a significant contributor to TETP. On the one hand, different processes that contributed to freshwater ecotoxicity potential (FETP) of the system expressed in kg 1,4-DCB-eq/MJ were computed for all scenarios and presented in Fig. 6.4b.

Baseline 2 with the least FETP value is the best case, while scenario 2 and 3 with the highest FETP values are considered the worst cases. Digestate handling was the next highest process contributor to FETP after enhancement production. This observation is in line with that of Guven et al. (2019) and Thomsen et al. (2018) effluent of nutrients and heavy metals could influence FETP. On the other hand, the results of process contributors to marine ecotoxicity (METP expressed in kg 1,4-DCB-eq/MJ) are calculated and presented in Fig. 6.5c. showed a similar trend as FETP with emissions from enhancement production and digestate having the greatest contributions to METP. In the enhanced categories, the combined enhancement option (co-digestion-Ppy/Fe_3O_4) had the least value of 0.00026875 kg 1,4-DCB-eq/MJ, unlike scenarios 2 and 3 with the worst case of METP. In alignment with these observations, Ramírez-Arpide et al. (2018) suggested that chemical production and digestate effluents may have contributed METP.

Finally, human toxicities (human carcinogenic toxicity (HTPc) and human non-carcinogenic toxicity (HTPnc)) expressed in kg 1,4-DCB-eq/MJ. As presented in Fig 6.5d and e, both HTPc and HTPnc presented a similar trend in their process contributions with enhancement, digestate and anaerobic digestion processes having the highest impact contribution. The least values of 1.04E-05 kg 1,4-DCB-eq/MJ and 0.000351 kg 1,4-DCB-eq/MJ were respectively for HTPc and HTPnc impact categories. They are the best scenarios, while the highest values (worst cases) are from scenario 2 and 3 for both HTPc and HTPnc.

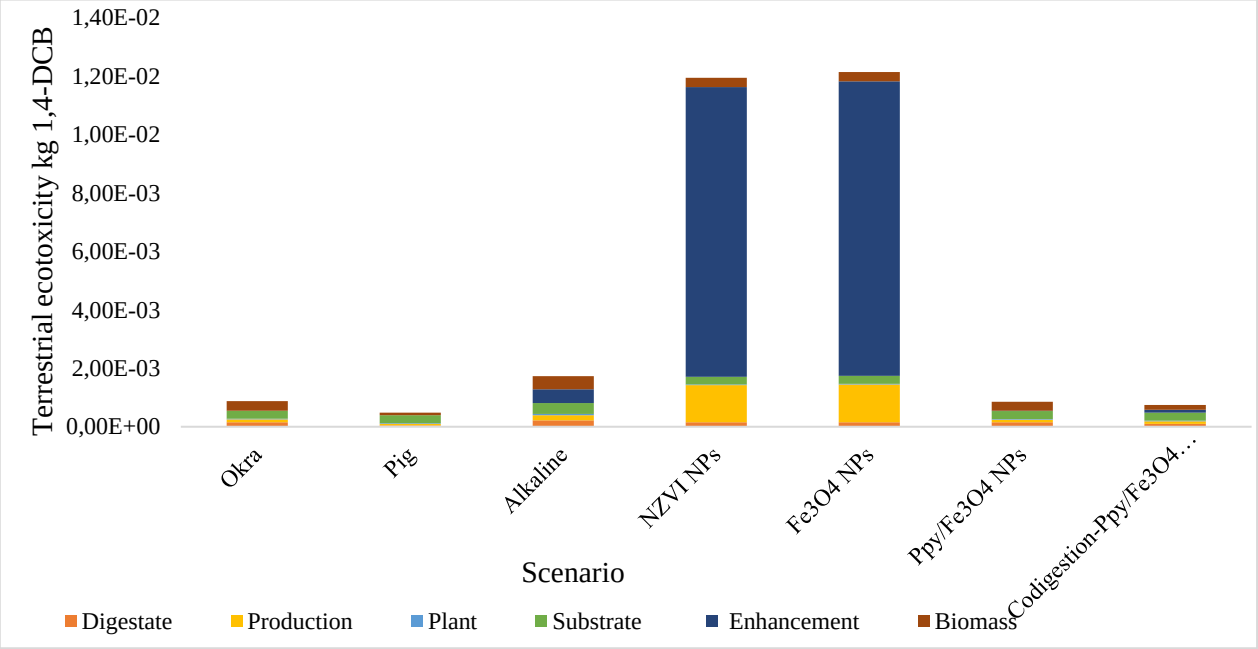

(a)

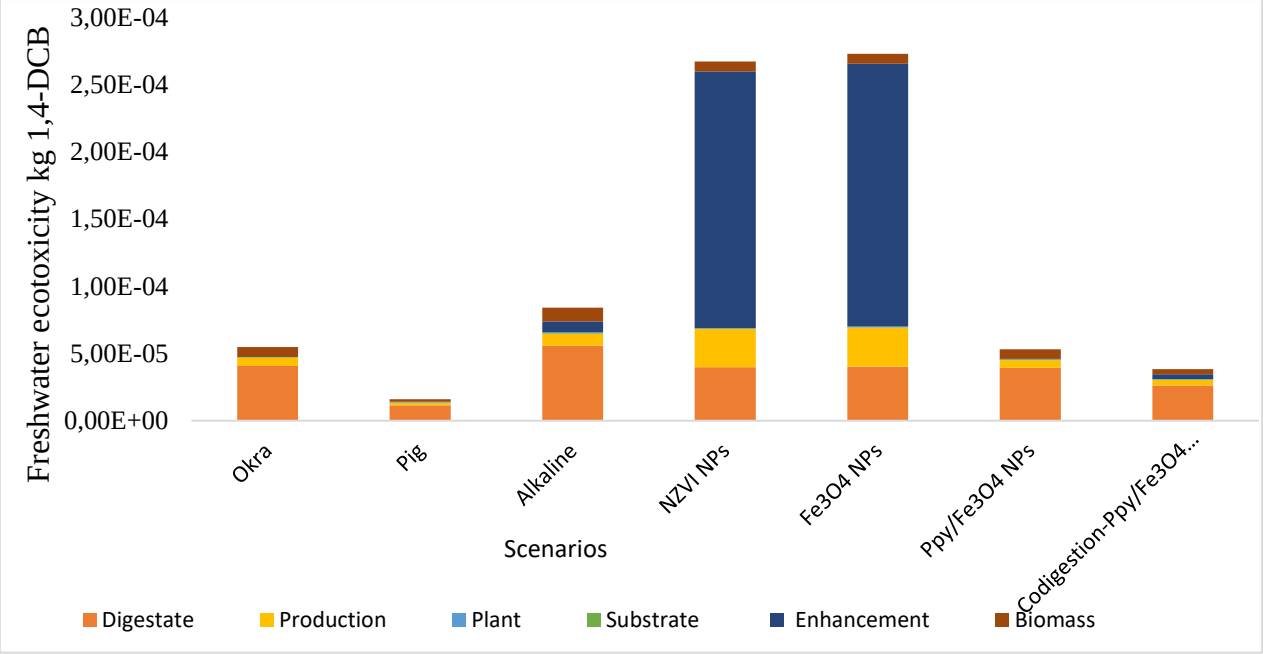
Freshwater ecotoxicity kg 1,4-DCB
3,00E-04
2,50E-04
2,00E-04
1,50E-04
1,00E-04
5,00E-05
0,00E+00
Okra
Pig
Alkaline
NZVI NPs
Fe3O4 NPs
Ppy/Fe3O4 NPs
Codigestion-Ppy/Fe3O4...
Scenarios
Digestate
Production
Plant
Substrate
Enhancement
Biomass

(b)

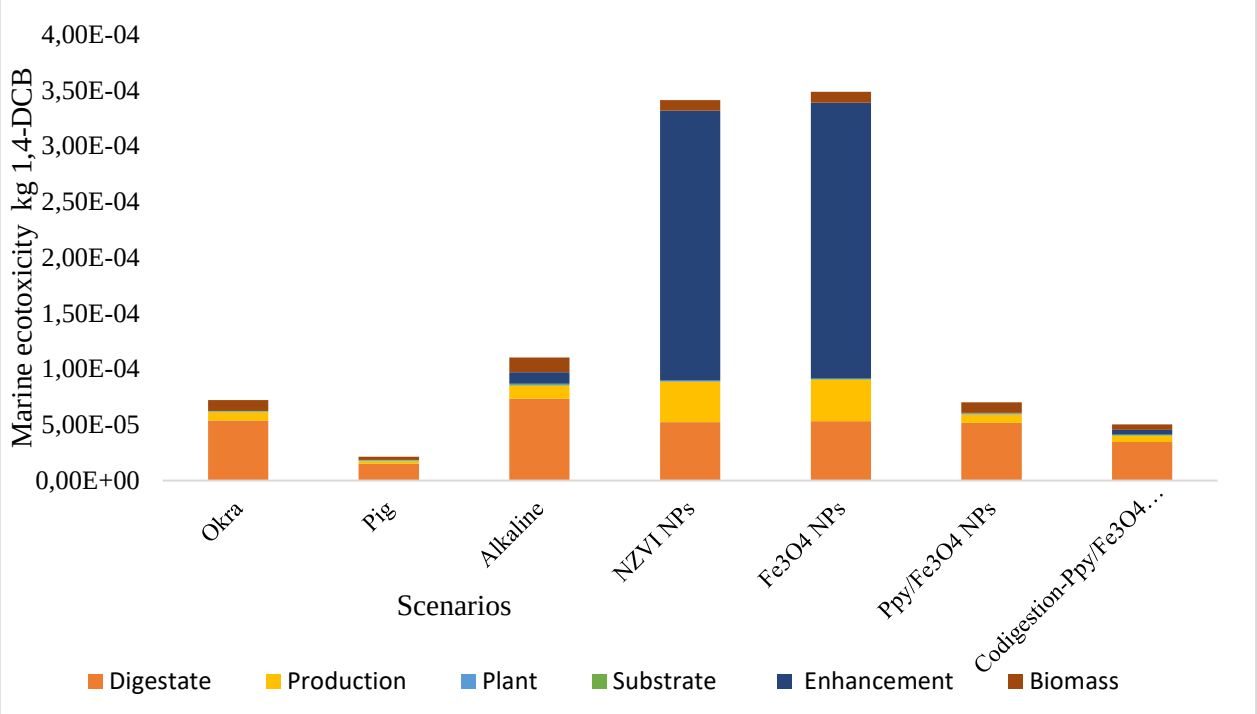
Marine ecotoxicity kg 1,4-DCB
4,00E-04
3,50E-04
3,00E-04
2,50E-04
2,00E-04
1,50E-04
1,00E-04
5,00E-05
0,00E+00
Okra
Pig
Alkaline
NZVI NPs
Fe3O4 NPs
Ppy/Fe3O4 NPs
Codigestion-Ppy/Fe3O4…
Scenarios
Digestate
Production
Plant
Substrate
Enhancement
Biomass

(c)

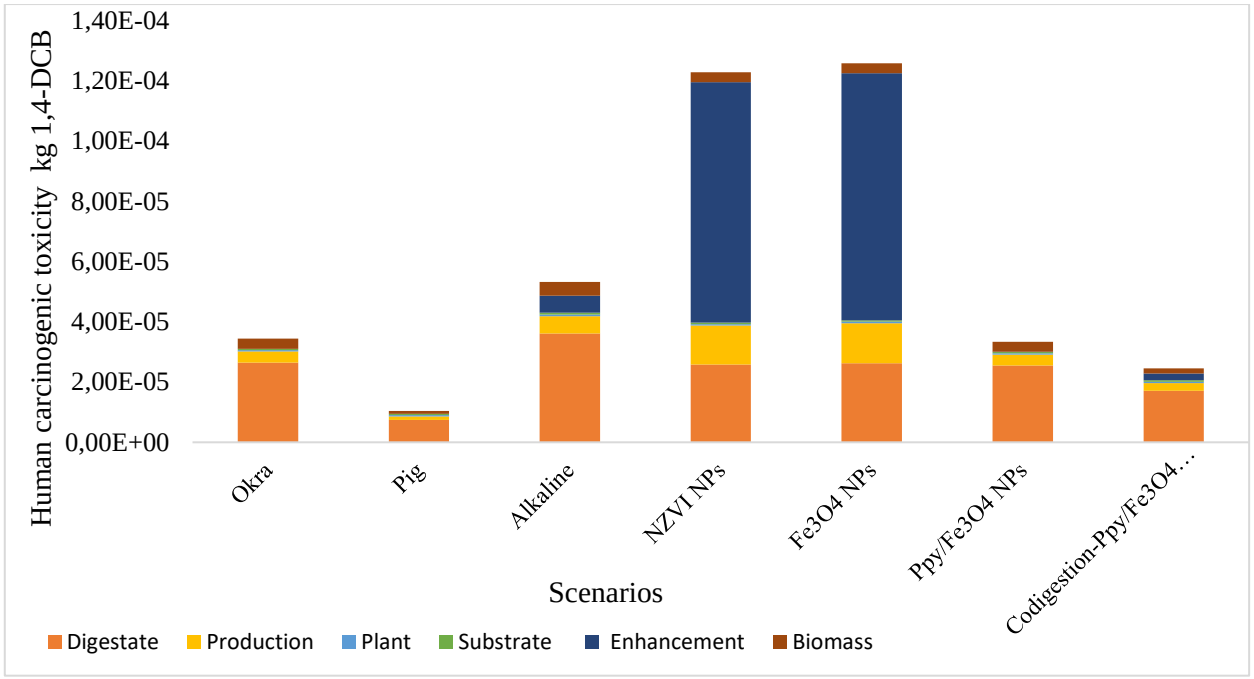

(d)

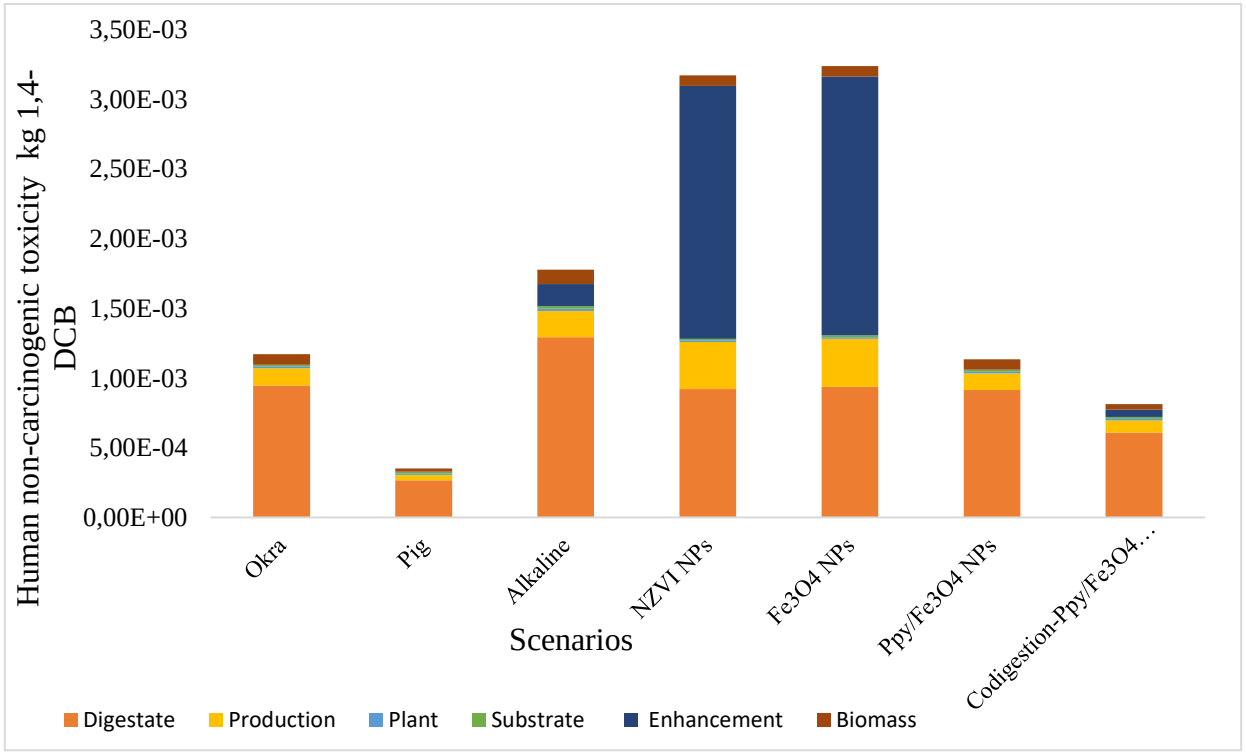

(e)

Fig.6. 5 Ecotoxicity and Toxicity Potentials ((a) Terrestrial ecotoxicity, (b) Freshwater ecotoxicity, (c) Marine ecotoxicity), (d) Human carcinogenic toxicity and (e) Human non-carcinogenic toxicity from electricity generation through various scenarios of anaerobic digestion of agrowastes

6.3.1.5. Resource depletion and land use change

The resources depletion potential also known as abiotic resource depletion refers to impact categories

covering consumption of resources (especially non-biological resources) such as usage of water usage, mineral and fossil resource scarcities. In this study, the impact categories considered are mineral resources scarcity (SOP, kg Cu-eq/MJ) and fossil resource scarcity (FFP, kg oil-eq/MJ) and water consumption (WCP, m^3-eq/MJ) for electricity production from anaerobic digestion. In Fig 6.6a, the highest value of 2.05E-05 kg Cu-eq/MJ and 2.02E-05 kg Cu-eq/MJ for scenario 2 and 3 respectively were observed for mineral resource scarcity with enhancement production and usage as the major process contributor of 38.7% (scenario 2) and 38.1% (scenario 3) of all the contributions to the impact category. Although iron supplementation of anaerobic digestion increases biogas yield (in quantity and quality), this result indicates that iron enhanced anaerobic digestion has the potential of impacting on the overall iron availability. Similarly, Fig 6.6b showed the process contribution of all scenarios for fossil resource scarcity impact category. Akin to mineral resource scarcity, the highest value of 6.69E-04 kg oil-eq/MJ and 6.50E-04 kg oil-eq/MJ for scenario 2 and 3 respectively were observed from the FFP impact category. The main contributor to FFP was from the enhancement production/usage. This result according to Hijazi et al. 2020a and Li et al. (2018b) may be attributable to high fossil energy input during extraction and production processes of enhancements and may also trigger some energy-environment concerns in the quest for cleaner energy production and environmentally friendliness.

More so, water, which is a vital resource is essential to determining environmentally sustainable scenario. Fig. 6.6c compares the water usage of different and their process contributions. Upon analyzing the process contributions to total WCP, the biomass production process contributed over 87.4% of the overall WCP for all the baselines and scenarios. Biogas production process (anaerobic digestion) was the next significant contributor to WCP. Scenario 1 recorded the highest value of 1.89E-04 m^3-eq/MJ. The observed main contribution from biomass production process agrees with Aziz and Hanafiah (2020) that palm oil plantation impacted WCP the most. Against this backdrop, Prasad et al. (2016) recommended reuse of wastewater from each process to minimize the potential impact of water consumption.

Finally, land use change (LUC), expressed in m^2 a-eq, evaluates the influence of various direct and indirect activities on this impact category. In this study, Fig. 6.6d showed the values of different process contribution to all the scenarios. It can be observed that biomass production process had the largest contribution to LUC, which aligns with Aziz and Hanafiah (2020) that LUC is related to agricultural land usage and practices as well as its influence on biodiversity and emissions. Scenario

3, 1 and 2 had the highest values of 1.32E-04 m^2 a-eq/MJ, 1.29E-03 m^2 a-eq/MJ and 1.28E-03 m^2 a-eq/MJ respectively for LUC of electricity production from anaerobic digestion of agrowastes, while baseline 2 recorded the lowest value.

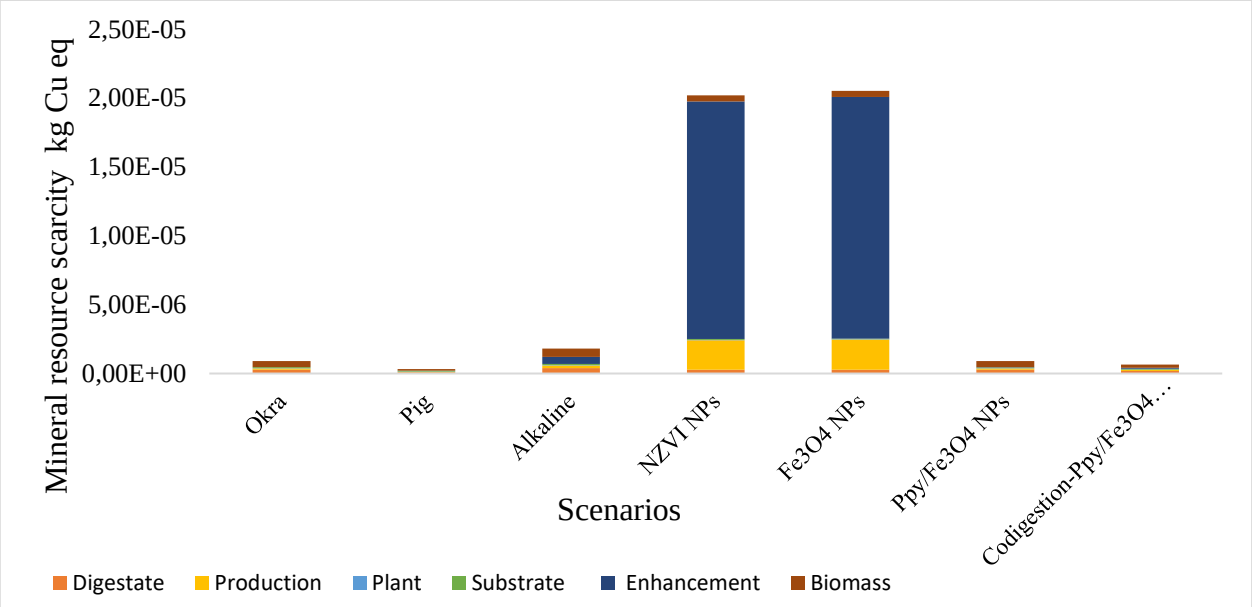

(a)

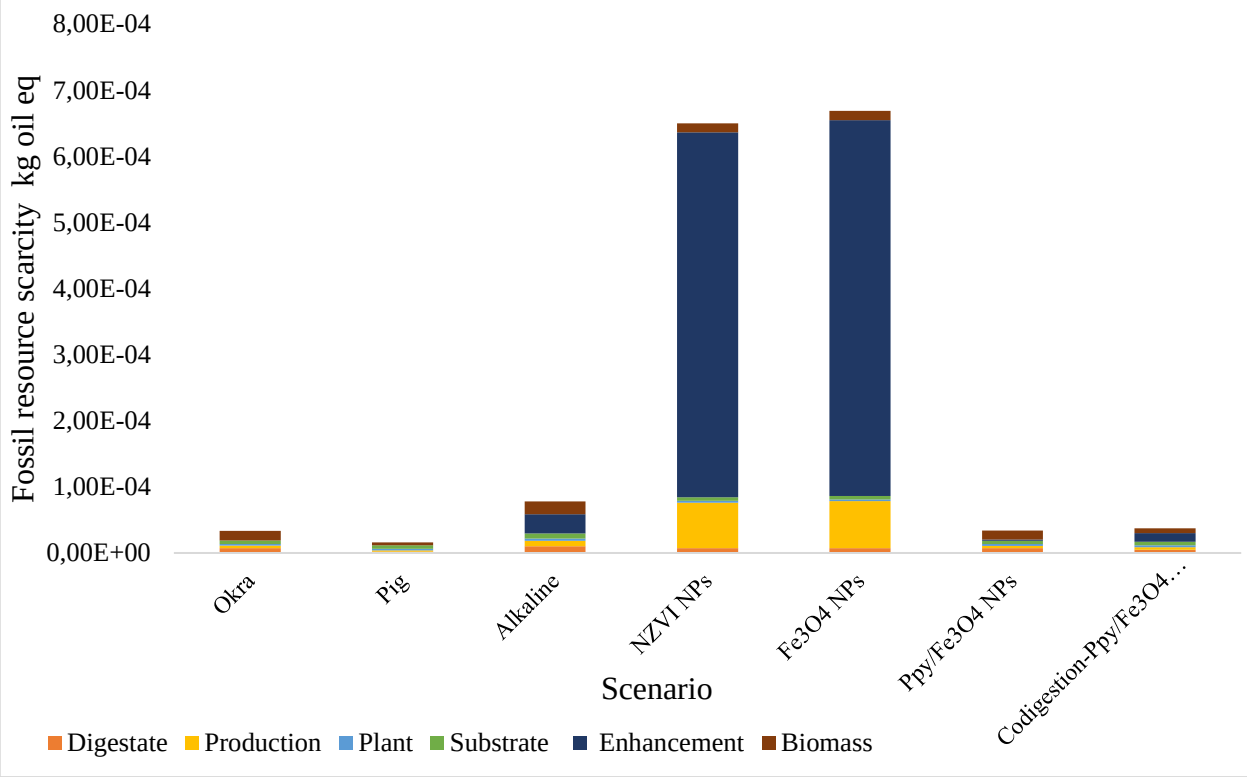

(b)

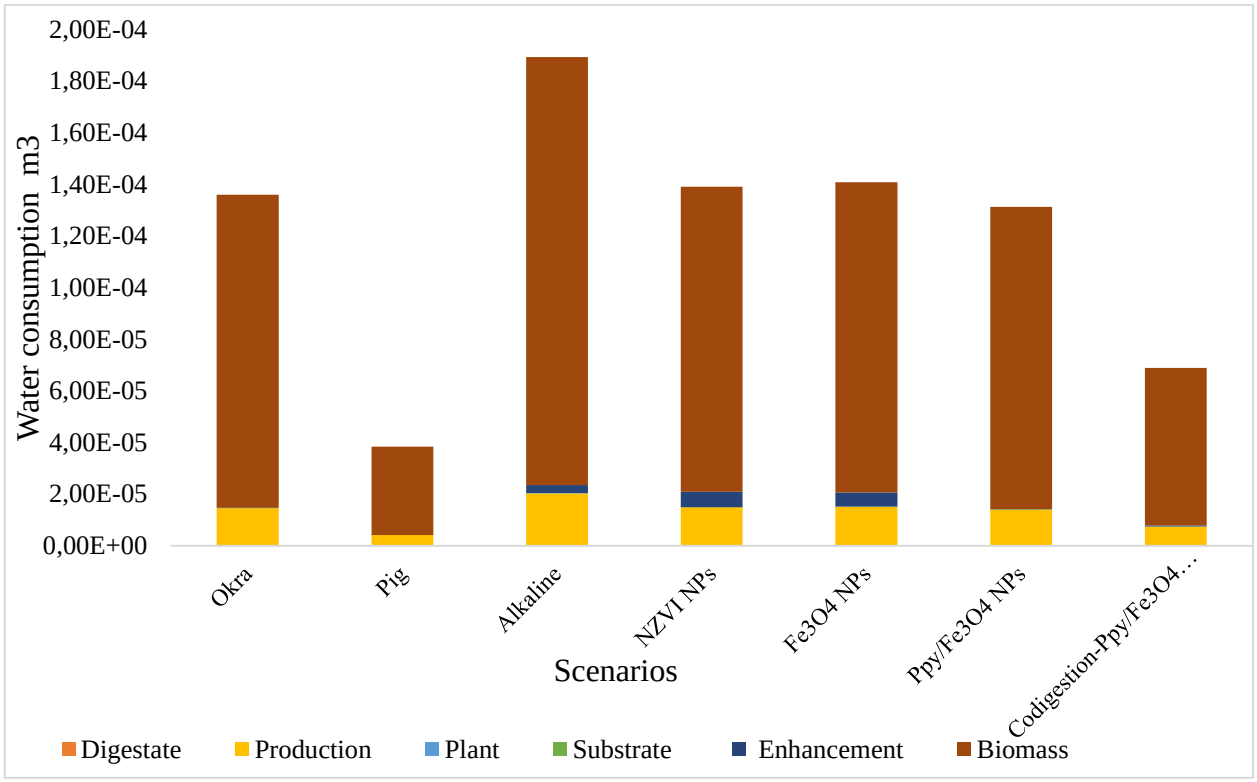

(c)

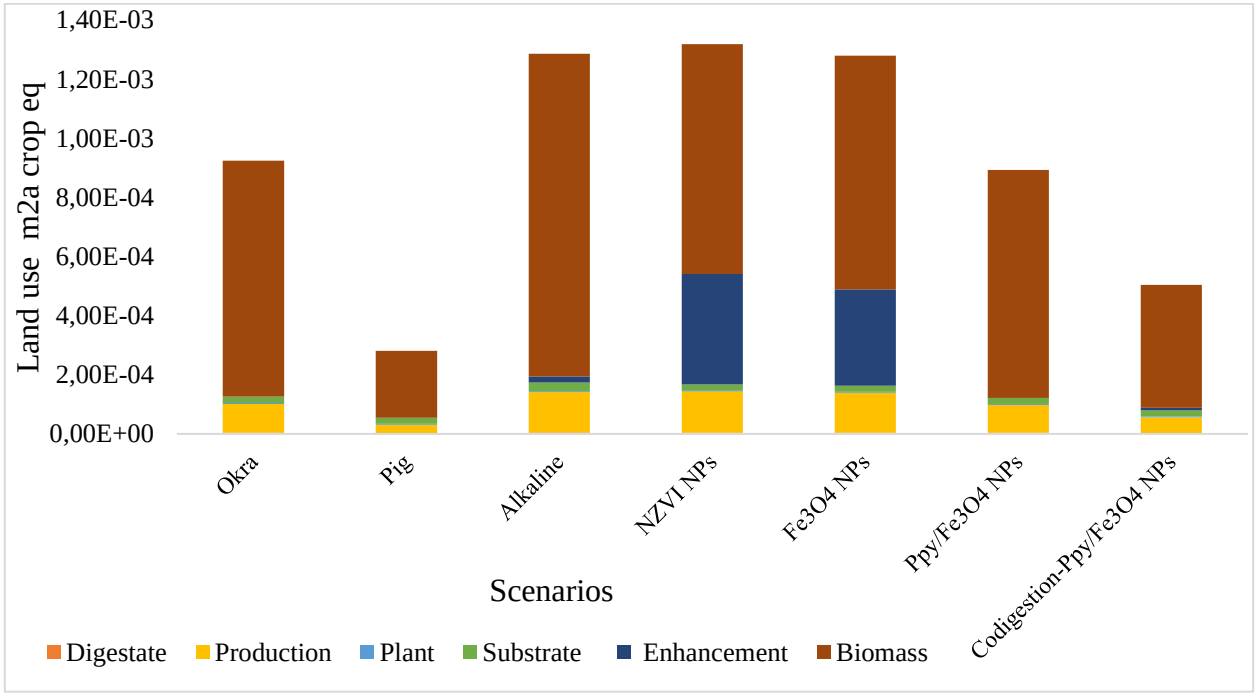

(d)

Fig.6. 6 Resource Depletion and Land Use Changes ((a) Mineral resource scarcity, (b) Fossil resource scarcity, (c) Water Consumption Potential and (e) Land Use Changes from electricity generation through various scenarios of anaerobic digestion of agrowastes

6.4 Summary

Various intensification strategies (eg. co-digestion, alkaline pretreatment, iron-based additives, etc.) have been reported as anaerobic digestion enhancement option for biogas production. The positive gains associated with increased biogas yield and the associated environmental trade-offs have triggered some concerns between higher clean energy production and environmentally sustainable process. Based on these concerns, the overall assessment of environmental impacts of electricity production from enhanced anaerobic digestion of agrowaste was conducted and conclusions made. From the assessment, combined enhancement (co-digestion and Ppy/Fe_3O_4) option (scenario 5) had the least global warming potential and overall low values on all impact categories. However, pig manure with the lowest raw material input and energy output gave the least value for most of the environmental indicators (eutrophication potential, acidification potential, toxicity and ecotoxicity, land use change and resource depletion potential) studied. It could be observed that scenario 4 (enhanced with Ppy/Fe_3O_4 NPs) with the highest biogas output, had the least environmental impact when compared with scenario 1,2 and 3. It could be concluded that the enhancement production process (especially scenario 2 and 3) was the major contributor to all impact categories. In a nutshell, based on the energy and environmental performances, the use of combined enhancement (co-digestion + Ppy/Fe_3O_4 NPs), followed by Ppy/Fe_3O_4 NPs only for enhanced biogas production is recommended to minimize the adverse impacts of electricity generation from biogas on the environment.

Chapter Seven
General Discussions and Future Perspective

7.1 General discussion

This chapter presents an abridged but holistic discussion on an integrated approach for biomethane recovery and phosphate release from anaerobic digestion of agro-industrial wastes relative to the stated objectives of this thesis.

7.1.1 Introduction

It has been established that due to global population rise, demand on important resources such as energy and phosphorus is on the increase (BP, 2019; Gurtekin, 2014). This demand-gaps can be handled through alternative resource recovery strategies like anaerobic digestion of wastes. There are wide varieties of substrates for anaerobic digestion, but due to their complex polymeric structures, some forms of enhancements (co-digestion, pretreatments or additive usage) are needed for increased profitability and maximize resource recovery from existing substrate-types (Akunna, 2018; Cai et al. 2017). Based on the substrate availability, yield enhancement and environmental impacts concerns, **Chapter 1 and Chapter 2** highlights the need to explore novel substrates and cheaper but effective enhancement options. The influence of the various enhancement options on process parameters of anaerobic digestion as well as their merits and demerits were reviewed from previous studies. It was also identified that the use of additives such as Ni, Fe, Co, Mo, Se, C, N, P, S, etc. among others, aid substrate solubilization, supply deficient nutrients, inhibits toxins, accelerate other anaerobic digestion processes (Chen et al. 2018; Mao et al. 2015). Due to the inherent advantages on anaerobes, process stability and the overall positive influences, iron-based additives have been widely used for enhancement of anaerobic digestion (Chen et al. 2018; Feng et al. 2014). It was revealed that despite the enhancement efforts of iron-based additives in aiding biodegradability, increasing biomethane production, etc., they react in ionic forms with other soluble nutrients, resulting in the formation of complex non-biodegradable substance, having adverse effects on phosphate release and impacting the environment negatively (Puyol et al. 2018 and Elijamal et al. 2020). This thesis was conducted through an integrated approach to identify and compare novel substrates and novel enhancement type with existing options based on biomethane yield, phosphorus release during the enhanced digestion process and environmental impacts.

The main aim of this thesis was to i) identify, characterize and rank potential agro-industrial wastes based on their energy and phosphorus potentials, ii) identify the most suitable enhancement techniques for increased biogas production during anaerobic digestion of selected agro-industrial waste, iii) optimize the iron enhanced anaerobic digestion of selected agro-waste for biomethane production and phosphate release with the addition of antagonists, iv) use Lifecycle Assessment (LCA) tool in evaluating the environmental footprints of different enhancement types for anaerobic digestion of selected agro-industrial waste.

7.1.2 Substrate identification and resource recovery potential

Due to the increasing interests in biomass-to-resource recovery technologies sustainable supply of conventional substrate-type for anaerobic digestion appears to remain a concern (Achinas and Euverink, 2016). There are debates on the appropriateness of some feedstock usage for energy generation in the face of mounting food insecurity and starvation in most developing climes (Muvhiiwa et al. 2017). However, issues of profitability due to low conversion efficiency and unavailability are still the challenges with biomass-to-resource recovery industries (Bharathiraja et al. 2018). In **Chapter 2**, the necessity of novel substrate identification and its enormous potentials for resource recovery when used singularly or with conventional feedstocks was highlighted. It was also observed that full characterization for the determination and ranking of their resource recoverability potentials (theoretically or experimentally) is necessary. The results of the identification, characterization and ranking of the eighteen selected (novel and conventional) biomass types of both plant and animal sources were shown in **Chapter 3** to be important in selecting suitable substrate types. Both the novel and conventional substrates were characterized to obtain the proximate and ultimate values as well as other chemical compositions, which are vital for determining, ranking energy and phosphate recovery potentials theoretically and experimentally. The identification, characterization and ranking of both novel and conventional substrates motivated the choice of anaerobic digestion as the most suited energy conversion option and the selection of substrate types. This agrees with Leng et al. (2020) and Raposo et al. (2011) that the determination of substrate compositions influences the choice of recovery technology. Consequently, okra waste as a novel substrate type with appreciable biomethane potential as shown in Fig. 3. 4 was chosen. Due to its high phosphate content (Fig. 3.2), pig waste was selected for co-digestion with okra for both biomethane yield and phosphate release.

7.1.3 Enhancement techniques for increased biogas production

Most available substrates for anaerobic digestion are affected by biodegradability challenges arising from the nature of the substrates, presence of inhibitors or other operational challenges (Akunna, 2018). This reduces biogas yield and impacts profitability; hence the anaerobic digestion enhancement (additive supplementation, substrate pretreatment and co-digestion) is required to achieve improved biodegradability ($B_{CH4} \geq 70\%$), elimination of inhibitions, supply of deficient nutrients and increase of biogas production (Choi et al. 2018; Casals et al. 2014; Browne and Murphy, 2013). After reviewing the potency of these enhancement options in **Chapter 2**, it was suggested that suitable enhancement types must be cheap, effective and environmentally friendly (Abdelsalam et al. 2016). In **Chapter 4,** series of anaerobic digestion enhancements with both novel and known were conducted and with a view to selecting the most effective option. From all the comparative assessments, it was observed that the addition of 20 mg/L of Ppy/Fe_3O_4 NPs achieved higher biomethane yield. This result agrees with Casals et al. (2014) and Abdelsalam et al. (2017) that conductive iron-based additives improve anaerobic digestion greatly.

7.1.4 Optimization of an integrated approach to biomethane recovery and phosphate release

From previous studies on anaerobic digestion enhancement, iron-based additives increase biomethane yield due to their ability to accept and donate electrons to methanogens, avail necessary nutrients to methanogens, acts as cofactors to enzymes, enhance substrate degradation, etc (Ugwu et al. 2020; Chen et al. 2018 Feng et al. 2014). As observed from reviewed literature in **Chapters 1 and 2,** iron-based additives ionize to form non-degradable complexes nutrients like phosphate (P) thereby lowering soluble P availability in the digestate for use as biofertilizer (Puyol et al. 2018; An et al. 2014). This contradiction makes iron ions unavailable for methanogenic activities and poses a serious environmental concern upon disposal (Heiberg et al. 2012). Based on the foregoing, **Chapter 5** of this thesis focused on an optimized integrated approach to achieving simultaneous enhanced biomethane recovery and P release through supplementation of anaerobic digestion with P-antagonists (HA and As) and accelerants (iron-based additives). The substrates (pig and okra wastes) identified in **Chapter 3** and the iron-based additive (Ppy/Fe_3O_4 NPs) selected in **Chapter 4** were digested together at varying proportions with the aim of optimizing these parameters and maximizing both biomethane yield and phosphate release. From the optimization process, 20.0014 mg/L, 5.0018 mg/L, 1.448 mg/L and 25.0001% respectively for Ppy/Fe_3O_4, HA, As and co-digestion were the optimum conditions.

7.1.5 Environmental footprints of different enhancement types for energy generation

Every activity of man on earth either enhances or diminishes our environment. Anaerobic digestion (enhanced or not) for electricity generation is not an exception to this concern (Moghaddam et al. 2016). Life cycle assessment (LCA) which is one of the internationally approved methods of identifying environmental impacts of novel and established processes, technologies, etc. As identified earlier in this study (in **Chapter 1**), enhancement of anaerobic digestion has notable environmental trade-offs. However, since **Chapter 5** of this study already showed the positive impacts of identified enhancement options on biomethane yield, conduct of LCA of all the options for selection of appropriate enhancement option based on energy-environmental consideration was the focus of **Chapter 6**. In this Chapter, comparative investigation of the environmental impact categories of different enhancements options was carried out; electricity generation processes from a conceptualized anaerobic digestion of 10,000 m^3 substrate slurry per annum using life cycle assessment approach. The results showed that the use of combined enhancement (codigestion + Ppy/Fe_3O_4 NPs) option for enhanced biogas production is most suited to reduce the adverse impacts of electricity generation from biogas on the environment.

7.2 Main conclusions

Based on the set objectives of this study, the following can be concluded:

- After screening, characterization and ranking of identified agro-industrial wastes, a novel substrate type (okra biomass) with appreciable biodegradability (B_{CH4} = 71.78 %) and good biomethane potentials were identified and selected as the main substrate for anaerobic digestion process in this thesis.
- The novel use of Ppy/Fe_3O_4 NPs for anaerobic digestion enhancement was discovered and when compared with other enhancement options, 20 mg/L Ppy/Fe_3O_4 NPs achieved higher biomethane yield.
- The proposed integrated approach to enhanced resource recovery was validated and optimized values of biomethane yield and P release obtained.
- The comparative environmental impacts of the different enhancement options (scenarios) were assessed with LCA tools and the impact categories determined.

7.3 Future research perspectives

Based on the result of the identification, screening and characterization of wastes, it was shown that the singularly assessed wastes have great potentials for resources recovery. However, co-digestion of high performing feedstocks with other substrates could ensure feedstock availability and improve overall resource recoverability, but furthertechno-economic evaluation is recommended.

Despite the efforts and achievements made in enhancing biodegradability and increasing resource recoverability, issues of optimum pretreatment time, additive dosages and possible toxicity/inhibition of methanogen activities remains serious concerns to full-scale deployment of these enhancement options and profitability. Through holistic feasibility analysis and process optimization, targeted use of any enhancement option for increased resource recovery is achievable.

Future studies should evaluate the adaptability of microbes to P antagonists (HA and As) and anaerobic digestion accelerants (iron-based additive) without adversely affecting anaerobic digestion activities. Continuous digestion in the presence of these additives at constant levels to monitor microbial population, obtain complete genomic information and to evaluate impacts on anaerobic digestion performance. More so, prolonged exposure of anaerobic digestion processes to HA, As and iron-based additives and their influence on resource recovery in a continuous biodigester should be further evaluated. Studies on speciation of iron-P in the digestates and recoverability potentials of P from iron enhanced anaerobic digestion process may be needed.

A comprehensive and detailed life cycle assessment (LCA) and techno-economic analysis of the entire integrated approach to biogas production and P release/recovery from enhanced anaerobic digestion of waste should be performed. This should aim at determining the minimum enhancement required to achieve environmental improvement and evaluating the efficiency of resource recovery processes. In order to ascertain the robustness of the life cycle model due to parametric variations, systems and scenarios should be subjected to sensitivity analysis.

References

Abbasi, T., Tauseef, S. M., and Abbasi, S. A., 2012. Biogas energy. Springer Briefs in Environmental Science 2: 1-184.

Abdelsalam, E., Hijazi, O., Samer, M., Yacoub, I.H., Ali, A.S., Ahmed, R.H. and Bernhardt, H., 2019. Life cycle assessment of the use of laser radiation in biogas production from anaerobic digestion of manure. *Renewable Energy*, *142*, pp.130-136.

Abdelsalam, E., Samer, M., Attia, Y.A., Abdel-Hadi, M.A., Hassan, H.E. and Badr, Y., 2016. Comparison of nanoparticles effects on biogas and methane production from anaerobic digestion of cattle dung slurry. Renewable Energy, *87*, pp. 592-598.

Abdelsalam, E., Samer, M., Attia, Y.A., Abdel-Hadi, M.A., Hassan, H.E. and Badr, Y., 2017. Influence of zero valent iron nanoparticles and magnetic iron oxide nanoparticles on biogas and methane production from anaerobic digestion of manure. *Energy*, *120*, pp.842-853.

Abdelwahab, T.A.M., Mohanty, M.K., Sahoo, P.K. and Behera, D., 2020. Application of nanoparticles for biogas production: Current status and perspectives. *Energy Sources, Part A: Recovery, Utilization, and Environmental Effects*, pp.1-13.

Acero, A.P., Rodríguez, C. and Ciroth, A., 2014. LCIA methods–Impact assessment methods in Life Cycle Assessment and their impact categories. *GreenDelta GmbH, Berlin, Germany*, *23*.

Achinas, S. and Euverink, G.J.W., 2016. Theoretical analysis of biogas potential prediction from agricultural waste. *Resource-Efficient Technologies*, *2*(3), pp.143-147.

Adelakun, O.E., Oyelade, O.J., Ade-Omowaye, B.I.O., Adeyemi, I.A., Van de Venter, M. and Koekemoer, T.C., 2009. Influence of pre-treatment on yield chemical and antioxidant properties of a Nigerian okra seed (Abelmoschus esculentus Moench) flour. *Food and Chemical Toxicology*, *47*(3), pp.657-661.

AgSTAR-EPA 430-B-20-001., 2020. Project Development Handbook A Handbook for Developing Anaerobic Digestion/Biogas Systems on Farms in the United States 3rd Edition.

Aguilar-Aguilar, F.A., Nelson, D.L., Pantoja, L.D.A. and Santos, A.S., 2017. Study of anaerobic co-digestion of crude glycerol and swine manure for the production of biogas. *Rev. Virtual Quim*, *9*(6), pp.2383-2403.

Ahn, H.K., Smith, M.C., Kondrad, S.L. and White, J.W., 2010. Evaluation of biogas production potential by dry anaerobic digestion of switchgrass–animal manure mixtures. *Applied Biochemistry and Biotechnology*, *160*(4), pp.965-975.

Aigbe, U.O., Das, R., Ho, W.H., Srinivasu, V. and Maity, A., 2018. A novel method for removal of Cr (VI) using polypyrrole magnetic nanocomposite in the presence of unsteady magnetic fields. *Separation and Purification Technology*, *194*, pp.377-387.

Ajay, C.M., Mohan, S., Dinesha, P. and Rosen, M.A., 2020. Review of impact of nanoparticle additives on anaerobic digestion and methane generation. *Fuel*, *277*, p.118234.

Akhtar, A., Ivanova, T., Jiříček, I. and Krepl, V., 2019. Detailed characterization of waste from date palm (Phoenix dactylifera) branches for energy production: Comparative evaluation of heavy metals concentration. *Journal of Renewable and Sustainable Energy*, *11*(1), p.013102.

Akunna, J.C., 2018. Anaerobic waste-wastewater treatment and biogas plants: a practical handbook. Boca Raton, FL: CRC Press, Taylor & Francis Group.

Al-Ahmad, A.E., Hiligsmann, S., Lambert, S., Heinrichs, B., Wannoussa, W., Tasseroul, L., Weekers, F. and Thonart, P., 2014. Effect of encapsulated nanoparticles on thermophillic anaerobic digestion. In: 19th National symposium on applied biological sciences, Gembloux, Belgium; 2014.

Alam, M.S. and Khan, G.A., 2007. Chemical analysis of okra bast fiber (Abelmoschus esculentus) and its physico-chemical properties. *Journal of Textile and Apparel Technology and Management*, *5*(4), pp.1-9

Ali, A., Mahar, R.B., Soomro, R.A. and Sherazi, S.T.H., 2017. Fe3O4 nanoparticles facilitated anaerobic digestion of organic fraction of municipal solid waste for enhancement of methane production. *Energy Sources, Part A: Recovery, Utilization, and Environmental Effects*, *39*(16), pp.1815-1822.

Al-Seadi, A. T., Rutz, D., Prassl, H., Köttner, M., Finsterwalder, T., Silke Volk, S. and Janssen, R., 2008. Biogas Handbook. *University of Southern Denmark*. Pp.1-136. http://lemvigbiogas.com

Ambuchi, J.J., Zhang, Z. and Feng, Y., 2016. Biogas enhancement using iron oxide nanoparticles and multi-wall carbon nanotubes. *International Journal of Chemical, Molecular, Nuclear, Materials and Metallurgical Engineering*, *10*, pp.1239-1246.

Ambuchi, J.J., Zhang, Z., Dong, Y., Huang, L. and Feng, Y., 2018. Hematite and multi-walled carbon nanotubes stimulate a faster syntrophic pathway during methanogenic beet sugar industrial wastewater degradation. *Applied Microbiology and Biotechnology*, *102*(16), pp.7147-7158.

Amen, T.W., Eljamal, O., Khalil, A.M. and Matsunaga, N., 2017. Biochemical methane potential enhancement of domestic sludge digestion by adding pristine iron nanoparticles and iron nanoparticles coated zeolite compositions. *Journal of Environmental Chemical Engineering*, *5*(5), pp. 5002-5013.

Amen, T.W., Eljamal, O., Khalil, A.M., Sugihara, Y. and Matsunaga, N., 2018. Methane yield enhancement by the addition of new novel of iron and copper-iron bimetallic nanoparticles. *Chemical Engineering and Processing-Process Intensification*, *130*, pp. 253-261.

American Biogas Council, Benefits of Biogas, https://americanbiogascouncil.org/resources/why-biogas/ (accessed March 2020).

Amini, A., 2014. Sustainable Energy and Nutrient Recovery from Swine Waste. Graduate Theses and Dissertations. http://scholarcommons.usf.edu/etd/4977

An, J.S., Back, Y.J., Kim, K.C., Cha, R., Jeong, T.Y. and Chung, H.K., 2014. Optimization for the removal of orthophosphate from aqueous solution by chemical precipitation using ferrous chloride. *Environmental Technology*, *35*(13), pp.1668-1675.

Anderson, M., Whitcomb, P. 2017). RSM Simplified. New York: Productivity Press, https://doi.org/10.1201/9781315382326

Angelidaki, I. and Sanders, W., 2004. Assessment of the anaerobic biodegradability of macropollutants. *Re/Views in Environmental Science & Bio/Technology*, *3*(2), pp.117-129.

Angelidaki, I., Alves, M., Bolzonella, D., Borzacconi, L., Campos, J.L., Guwy, A.J., Kalyuzhnyi, S., Jenicek, P. and Van Lier, J.B., 2009. Defining the biomethane potential (BMP) of solid organic wastes and energy crops: a proposed protocol for batch assays. *Water Science and Technology*, *59*(5), pp.927-934.

Angelonidi, E. and Smith, S.R., 2015. A comparison of wet and dry anaerobic digestion processes for the treatment of municipal solid waste and food waste. *Water and Environment Journal*, *29*(4), pp.549-557.

Anwar, F., Rashid, U., Ashraf, M. and Nadeem, M., 2010. Okra (Hibiscus esculentus) seed oil for biodiesel production. *Applied Energy*, *87*(3), pp.779-785.

APHA. 2005. Standard methods for the examination of water and wastewater, 21st ed. Washington, DC: American Public Health Association/American Water Works Association/Water Environment Federation.

ARC, 2016. Estimating the Biogas Potential for Electricity Generation from the Agro-Waste Industry: A Resource Assessment for South Africa. South African-German Energy Programme (SAGEN). South Africa - October 2016. Pp.1-32. www.giz.de/southafrica%0A.

Archer, D.B. and Kirsop, B.H., 1990. The microbiology and control of anaerobic digestion. *Anaerobic digestion: a waste treatment technology. Elsevier Science Publishing Ltd., London, England*, pp.43-89.

Arif, S., Liaquat, R. and Adil, M., 2018. Applications of materials as additives in anaerobic digestion technology. *Renewable and Sustainable Energy Reviews*, *97*, pp.354-366.

Ashley, K., Cordell, D. and Mavinic, D., 2011. A brief history of phosphorus: from the philosopher's stone to nutrient recovery and reuse. *Chemosphere*, *84*(6), pp.737-746.

Ashraf, A., Sattar, H. and Munir, S., 2019. Thermal decomposition study and pyrolysis kinetics of coal and agricultural residues under non-isothermal conditions. *Fuel*, *235*, pp.504-514.

Atelge, M.R., Atabania, A.E., Banu, J.R., Krisa, D., Kaya, M., Eskicioglu, C., Kumar, G., Lee, C., Yildiz, Y.Ş., Unalan, S., Mohanasundaram, R. and Duman. F., 2020. A critical review of pretreatment technologies to enhance anaerobic digestion and energy recovery. *Fuel*, *270*, p.117494.

AU (2019). The African Union Bioenergy Development in Africa Programme. https://au.int/sites/default/files/newsevents/workingdocuments/33313-wd-african_union_bioenergy_development_in_africa_programme_e.pdf (accessed: 4/7/2020)

Auffan, M., Achouak, W., Rose, J., Roncato, M.A., Chaneac, C., Waite, D.T., Masion, A., Woicik, J.C., Wiesner, M.R. and Bottero, J.Y., 2008. Relation between the redox state of iron-based nanoparticles and their cytotoxicity toward Escherichia coli. *Environmental Science & Technology, 42*(17), pp.6730-6735.

Aziz, N.I.H.A. and Hanafiah, M.M., 2020. Life cycle analysis of biogas production from anaerobic digestion of palm oil mill effluent. *Renewable Energy, 145*, pp.847-857.

Azman, S., Khadem, A.F., Van Lier, J.B., Zeeman, G. and Plugge, C.M., 2015a. Presence and role of anaerobic hydrolytic microbes in conversion of lignocellulosic biomass for biogas production. *Critical Reviews in Environmental Science and Technology*, *45*(23), pp.2523-2564.

Azman, S., Khadem, A.F., Zeeman, G., Van Lier, J.B. and Plugge, C.M., 2015b. Mitigation of humic acid inhibition in anaerobic digestion of cellulose by addition of various salts. *Bioengineering*, *2*(2), pp.54-65.

Banerjee, G., 2010. Treatment of arsenic-laden water plant sludge by anaerobic digestion. *Practice Periodical of Hazardous, Toxic, and Radioactive Waste Management*, *14*(2), pp.124-131.

Banfield, J.F. and Zhang, H., 2001. Nanoparticles in the environment. *Reviews in Mineralogy and Geochemistry*, *44*(1), pp.1-58.

Barbeau, E. M., Krieger, N., Soobader, M. J., 2014. The American Journal of Public Health (AJPH) from the American Public Health Association (APHA) publications. 2014. *American Journal of Public Health. 93*, 10, p.1699.

Baredar, P., Suresh, S., Kumar, A. and Krishnakumar, P., 2016. A Review on Enhancement of Biogas Yield by Pre-treatment and addition of Additives. In *MATEC Web of Conferences,* 62 (06002), pp.1-5.

Barker, H.A., 1956. *Bacterial fermentations* (No. 589.9 B37). New York: Wiley.

Barton, L. E., Auffan, M., Durenkamp, M., McGrath, S., Bottero, J. Y. and Wiesner, M, R., 2015. Monte Carlo simulations of the transformation and removal of Ag, TiO2, and ZnO nanoparticles in wastewater treatment and land application of biosolids, *Science of the Total Environment*, 511, pp. 535–543.

Barua, V.B., Goud, V.V. and Kalamdhad, A.S., 2018. Microbial pretreatment of water hyacinth for enhanced hydrolysis followed by biogas production. *Renewable Energy, 126*, pp.21-29.

Basu, P., 2010. Biomass gasification and pyrolysis: practical design and theory. *Academic Press*. doi:10.1016/B978-0-12-374988-8.00001-5

Basu, P., 2018. Biomass gasification, pyrolysis and torrefaction: practical design and theory. *Academic Press*. doi:10.1016/b978-0-12-812992-0.00011-x

Bhange, V.P., William, S.P., Sharma, A., Gabhane, J., Vaidya, A.N. and Wate, S.R., 2015. Pretreatment of garden biomass using Fenton's reagent: influence of Fe 2+ and H 2 O 2 concentrations on lignocellulose degradation. *Journal of Environmental Health Science and Engineering*, *13*(1), p.12.

Bharathiraja, B., Sudharsana, T., Jayamuthunagai, J., Praveenkumar, R., Chozhavendhan, S. and Iyyappan, J., 2018. Biogas production–A review on composition, fuel properties, feed stock and principles of anaerobic digestion. *Renewable and Sustainable Energy Reviews*, *90*(C), pp. 570-582.

Bharti, V., 2019. India's Programmes and Incentives Being Implemented to Support Biogas Systems. Online training on Bioenergy-biogas policy and practices in India and Denmark. September 2019. https://ccacoalition.org/en/file/6375/download?token=lTBiOKVA

Bhaumik, M., Maity, A., Srinivasu, V.V. and Onyango, M.S., 2011. Enhanced removal of Cr (VI) from aqueous solution using polypyrrole/Fe3O4 magnetic nanocomposite. *Journal of Hazardous Materials*, *190*(1-3), pp.381-390.

Borja, R. and Rincón, B., 2017. Biogas production. Reference Module in Life Sciences. Pp.1-24. doi:10.1016/b978-0-12-809633-8.09105-6

Boulamanti, A.K., Maglio, S.D., Giuntoli, J. and Agostini, A., 2013. Influence of different practices on biogas sustainability. *Biomass and Bioenergy*, *53*, pp.149-161.

Box, G.E. and Draper, N.R., 1987. Empirical model-building and response surfaces. *John Wiley & Sons*.

Boyle, W.C., 1977. Energy recovery from sanitary landfills-a review. In *Microbial energy conversion* (pp. 119-138). Pergamon.

BP (2019). BP Statistical Review of World Energy 2019. 68th Edition, June 2019. Pp.1-64. Pureprint, UK. https://www.bp.com/content/dam/bp/business-sites/en/global/corporate/pdfs/energy-economics/statistical-review/bp-stats-review-2019-full-report.pdf

BP. 2018. BP Statistical Review of World Energy 2018. 67th Edition, June 2018. Pp.1-56. Pureprint, UK. https://www.bp.com/content/dam/bp/en/corporate/pdf/energy-economics/statistical-review/bp-stats-review-2018-renewable-energy.pdf

Braun, R., Drosg, B., Bochmann, G., Weiß, S. and Kirchmayr, R., 2010. Recent developments in bio-energy recovery through fermentation. In *Microbes at Work* (pp. 35-58). Springer, Berlin, Heidelberg.

Braz, C.E.M. and Crnkovic, P.C.G.M., 2014. Physical-chemical characterization of biomass samples for application iin pyrolysis process. *Chemical Engineering Transactions*, pp.523-528.

Browne, J.D. and Murphy, J.D., 2013. Assessment of the resource associated with biomethane from food waste. *Applied Energy*, *104*, pp.170-177.

Budiyono, I.S. and Sumardiono, S., 2014. Kinetic model of biogas yield production from vinasse at various initial pH: comparison between modified Gompertz model and first order kinetic model. *Research Journal of Applied Sciences, Engineering and Technology*, *7*(13), pp.2798-2805.

Buswell, A.M. and Boruff, C.S., 1933. Mechanical equipment for continuous fermentation of fibrous materials. *Industrial & Engineering Chemistry*, *25*(2), pp.147-149.

Buswell, A.M. and Mueller, H.F., 1952. Mechanism of methane fermentation. *Industrial & Engineering Chemistry*, *44*(3), pp.550-552.

Cai, F., Yan, H., Zhang, R., Liu, G. and Chen, C., 2019. Prediction of methane production performances based on determination of organic components for different vegetable wastes. *International Journal of Agricultural and Biological Engineering*, *12*(3), pp.154-159.

Cai, J., He, Y., Yu, X., Banks, S.W., Yang, Y., Zhang, X., Yu, Y., Liu, R. and Bridgwater, A.V., 2017. Review of physicochemical properties and analytical characterization of lignocellulosic biomass. *Renewable and Sustainable Energy Reviews*, 76, pp. 309-322.

Campos Cuellar, A.A., 2014. Development of a process for the enhanced phosphorus recovery from the organic matrix of agricultural residues. Stuttgart: FRAUNHOFER VERLAG. http://verlag.fraunhofer.de.

Capodaglio, A.G., Ranieri, E. and Torretta, V., 2016. Process enhancement for maximization of methane production in codigestion biogas plants. *Management of Environmental Quality*, *27*(3), pp.289-298.

Carlsson, M., 2015. When and why is Pre-treatment of Substrates for Anaerobic Digestion Useful? (Doctoral dissertation, Luleå tekniska universitet). http://urn.kb.se/resolve?urn=urn:nbn:se:ltu:diva-17712

Casals, E., Barrena, R., García, A., González, E., Delgado, L., Busquets-Fité, M., Font, X., Arbiol, J., Glatzel, P., Kvashnina, K. and Sánchez, A., 2014. Programmed iron oxide nanoparticles disintegration in anaerobic digesters boosts biogas production. *Small*, *10*(14), pp. 2801-2808.

Cellura, M., Guarino, F., Longo, S., Mistretta, M. and Orioli, A., 2013. The role of the building sector for reducing energy consumption and greenhouse gases: An Italian case study. *Renewable Energy*, *60*, pp.586-597.

Chasnyk, O., Sołowski, G. and Shkarupa, O., 2015. Historical, technical and economic aspects of biogas development: Case of Poland and Ukraine. *Renewable and Sustainable Energy Reviews*, *52*, pp.227-239.

Chauhan, A.K., 2020. Biofuel: Types and Process Overview. In *Nanomaterials in Biofuels Research* (1-28). Springer, Singapore.Doi:10.1007/978-981-13-9333-4_1

Chen, H., Luo, H., Lan, Y., Dong, T., Hu, B. and Wang, Y., 2011. Removal of tetracycline from aqueous solutions using polyvinylpyrrolidone (PVP-K30) modified nanoscale zero valent iron. *Journal of hazardous materials*, *192*(1), pp.44-53.

Chen, N.Y., Degnan, T.F. and Koenig, L.R., 1986. Liquid fuel from carbohydrates. *Chemtech*, *16*(8), pp.506-511.

Chen, R., Konishi, Y. and Nomura, T., 2018. Enhancement of methane production by Methanosarcina barkeri using Fe3O4 nanoparticles as iron sustained release agent. *Advanced Powder Technology*, *29*(10), pp.2429-2433.

Chen, Y.C., Chen, W.H., Lin, B.J., Chang, J.S. and Ong, H.C., 2017. Fuel property variation of biomass undergoing torrefaction. *Energy Procedia*, *105*, pp.108-112.

Cheng, X., Chen, B., Cui, Y., Sun, D. and Wang, X., 2015. Iron (III) reduction-induced phosphate precipitation during anaerobic digestion of waste activated sludge. *Separation and Purification Technology*, *143*, pp.6-11.

Chiappero, M., Norouzi, O., Hu, M., Demichelis, F., Berruti, F., Di Maria, F., Mašek, O. and Fiore, S., 2020. Review of biochar role as additive in anaerobic digestion processes. *Renewable and Sustainable Energy Reviews*, *131*, p.110037.

Choi, J.M., Han, S.K. and Lee, C.Y., 2018. Enhancement of methane production in anaerobic digestion of sewage sludge by thermal hydrolysis pretreatment. *Bioresource Technology*, *259*, pp.207-213.

Chow, W.L., Chong, S., Lim, J.W., Chan, Y.J., Chong, M.F., Tiong, T.J., Chin, J.K. and Pan, G.T., 2020. Anaerobic Co-Digestion of Wastewater Sludge: A Review of Potential Co-Substrates and Operating Factors for Improved Methane Yield. *Processes*, *8*(1), p.39.

Cioabla, A.E., Ionel, I., Dumitrel, G.A. and Popescu, F., 2012. Comparative study on factors affecting anaerobic digestion of agricultural vegetal residues. *Biotechnology for Biofuels*, *5*(1), pp.1-9.

Cremiato, R., Mastellone, M.L., Tagliaferri, C., Zaccariello, L. and Lettieri, P., 2018. Environmental impact of municipal solid waste management using Life Cycle Assessment: The effect of anaerobic digestion, materials recovery and secondary fuels production. *Renewable Energy*, *124*, pp.180-188.

Crolla, A.M., 2017. *Anaerobic Digestion of Dairy Manure with Food and Industry Wastes–Enhanced Biogas Production and Digestate Quality* (Doctoral dissertation, Université d'Ottawa/University of Ottawa).

CSIR, 2016. Forecasts for electricity demand in South Africa (2010 – 2035) using the CSIR sectoral regression model. Pretoria.

Cucina, M., Zadra, C., Marcotullio, M.C., Di Maria, F., Sordi, S., Curini, M. and Gigliotti, G., 2017. Recovery of energy and plant nutrients from a pharmaceutical organic waste derived from a fermentative biomass: Integration of anaerobic digestion and composting. *Journal of Environmental Chemical Engineering*, *5*(3), pp.3051-3057.

Damm, O. and Triebel, R., 2008. A synthesis report on biomass energy consumption and availability in South Africa. *GTZ (Gesellschaft für Technische Zusammenarbeid) Programme for basic energy and conservation (ProBEC). ProBEC and LHA Management Consultants, Pretoria, South Africa*.

Dar, R.A., Arora, M. and Phutela, U.G., 2019. Optimization of cultural factors of newly isolated microalga Spirulina subsalsa and its co-digestion with paddy straw for enhanced biogas production. *Bioresource Technology Reports*, *5*, pp.185-198.

De Rosa, I.M., Kenny, J.M., Puglia, D., Santulli, C. and Sarasini, F., 2010. Morphological, thermal and mechanical characterization of okra (Abelmoschus esculentus) fibres as potential reinforcement in polymer composites. *Composites Science and Technology*, *70*(1), pp.116-122.

DEA (Department of Environmental Affairs and Tourism), 2000. White Paper on Integrated Pollution and Waste Management for South Africa, *Government Gazette*, 417(20978), pp. 10–11.

DEA, 2012. National Waste Information Baseline Report,. Department of Environmental Affairs. Pretoria, South Africa. pp. 1–28.

DEA/GIZ, 2014. South Africa's Greenhouse Gas (GHG) Mitigation Potential Analysis, Pretoria South Africa. 1-32.

Deepanraj, B., Senthilkumar, N., Ranjitha, J., Jayaraj, S. and Ong, H.C., 2020. Biogas from food waste through anaerobic digestion: optimization with response surface methodology. *Biomass Conversion and Biorefinery*, pp.1-13.

Deepanraj, B., Sivasubramanian, V. and Jayaraj, S., 2015. Experimental and kinetic study on anaerobic digestion of food waste: The effect of total solids and pH. *Journal of Renewable and Sustainable Energy*, *7*(6), p.063104.

del Valle-Zermeño, R., Romero-Güiza, M.S., Chimenos, J.M., Formosa, J., Mata-Alvarez, J. and Astals, S., 2015. Biogas upgrading using MSWI bottom ash: An integrated municipal solid waste management. *Renewable Energy*, *80*, pp.184-189.

Demirel, B. and Scherer, P., 2011. Trace element requirements of agricultural biogas digesters during biological conversion of renewable biomass to methane. *Biomass and Bioenergy*, *35*(3), pp.992-998.

Desmidt, E., Ghyselbrecht, K., Zhang, Y., Pinoy, L., Van der Bruggen, B., Verstraete, W., Rabaey, K. and Meesschaert, B., 2015. Global phosphorus scarcity and full-scale P-recovery techniques: a review. *Critical Reviews in Environmental Science and Technology*, *45*(4), pp.336-384.

Deublein, D. and Steinhauser, A., 2010. Biogas. *Biogas from waste and renewable resources*, pp.85-95.

Dima, A.D., Pârvulescu, O.C., Mateescu, C. and Dobre, T., 2020. Optimization of substrate composition in anaerobic co-digestion of agricultural waste using central composite design. *Biomass and Bioenergy*, *138*, p.105602.

Ding, H.H., Chang, S. and Liu, Y., 2017. Biological hydrolysis pretreatment on secondary sludge: Enhancement of anaerobic digestion and mechanism study. *Bioresource technology*, *244*, pp.989-995.

Dobre, P., Nicolae, F. and Matei, F., 2014. Main factors affecting biogas production-an overview. *Romanian Biotechnological Letters*, *19*(3), pp.9283-9296.

DoE, 2016. Department of Energy Annual Report 2015/2016. Vote 26. Pretoria: Department of Energy. Available at: www.energy.gov.za.

DOE., 2020. Department of Environmental Affairs. Facilitation of Large-Scale Uptake of Alternative Transport Fuels in South Africa – The Case for Biogas. Biogas reports. (accessed: 4/7/2020). https://www.environment.gov.za/sites/default/files/reports/bioagas_report.pdf

DOET., 2000. Department of Environmental Affairs and Tourism White Paper on Integrated Pollution Waste Management for South Africa No. 20978. Government Gazette, 17 March 2000. Pp.1-79.

Donoso-Bravo, A. and Fdz-Polanco, M., 2013. Anaerobic co-digestion of sewage sludge and grease trap: assessment of enzyme addition. *Process Biochemistry*, *48*(5-6), pp.936-940.

Drosg, B., Fuchs, W., Al Seadi, T., Madsen, M. and Linke, B., 2015. *Nutrient recovery by biogas digestate processing* (Vol. 2015, p. 711). Dublin: IEA Bioenergy. http://www.iea-biogas.net/files/daten-redaktion/download/Technical

Duan, N., Khoshnevisan, B., Lin, C., Liu, Z. and Liu, H., 2020. Life cycle assessment of anaerobic digestion of pig manure coupled with different digestate treatment technologies. *Environment International*, *137*, p.105522.

Dudek, M., Świechowski, K., Manczarski, P., Koziel, J.A. and Białowiec, A., 2019. The effect of biochar addition on the biogas production kinetics from the anaerobic digestion of brewers' spent grain. *Energies*, *12*(8), p.1518.

Duman, M.N., Kocak, E.M.İ.N.E., Merdan, D.N. and Mistik, I., 2017, October. Nonwoven production from agricultural okra wastes and investigation of their thermal conductivities. In *17th world textile conference AUTEX*.

Dwivedi, A.D., Dubey, S.P., Sillanpää, M., Kwon, Y.N., Lee, C. and Varma, R.S., 2015. Fate of engineered nanoparticles: implications in the environment. *Coordination Chemistry Reviews*, *287*, pp. 64-78.

EBA (2019). Annual Report 2019. https://www.europeanbiogas.eu/wp-content/uploads/2020/01/EBA-AR-2019-digital-version.pdf

Eduok, S., Ferguson, R., Jefferson, B., Villa, R. and Coulon, F., 2017. Aged-engineered nanoparticles effect on sludge anaerobic digestion performance and associated microbial communities. *Science of the Total Environment*, *609*,pp. 232-241.

Edwiges, T., Frare, L., Mayer, B., Lins, L., Triolo, J.M., Flotats, X. and de Mendonça Costa, M.S.S., 2018. Influence of chemical composition on biochemical methane potential of fruit and vegetable waste. *Waste Management*, *71*, pp.618-625.

Elbeshbishy, E., Nakhla, G. and Hafez, H., 2012. Biochemical methane potential (BMP) of food waste and primary sludge: influence of inoculum pre-incubation and inoculum source. *Bioresource Technology*, *110*, pp.18-25.

Eljamal, O., Mokete, R., Matsunaga, N. and Sugihara, Y., 2018. Chemical pathways of nanoscale zero-valent iron (NZVI) during its transformation in aqueous solutions. *Journal of Environmental Chemical Engineering*, *6*(5), pp.6207-6220.

Eljamal, O., Thompson, I.P., Maamoun, I., Shubair, T., Eljamal, K., Lueangwattanapong, K. and Sugihara, Y., 2020. Investigating the design parameters for a permeable reactive barrier consisting of nanoscale zero-valent iron and bimetallic iron/copper for phosphate removal. *Journal of Molecular Liquids*, *299*, p.112144.

Elsayed, M., Andres, Y., Blel, W., Gad, A. and Ahmed, A., 2016. Effect of VS organic loads and buckwheat husk on methane production by anaerobic co-digestion of primary sludge and wheat straw. *Energy Conversion and Management*, *117*, pp.538-547.

Emerson, D., Fleming, E.J. and McBeth, J.M., 2010. Iron-oxidizing bacteria: an environmental and genomic perspective. *Annual Review of Microbiology*, *64*, pp.561-583.

Energy Information Administration. 2010. International Energy Outlook 2010. National Energy Information Center, US Energy Information Administration, Washington, DC, http://www.eia.gov/oiaf/ieo/pdf/0484%282010%29.pdf; 2010 [retrieved 17.09.10].

Ertem, F.C., Neubauer, P. and Junne, S., 2017. Environmental life cycle assessment of biogas production from marine macroalgal feedstock for the substitution of energy crops. *Journal of cleaner production*, *140*, pp.977-985.

Esteves, E.M.M., Herrera, A.M.N., Esteves, V.P.P. and Morgado, C.D.R.V., 2019. Life cycle assessment of manure biogas production: A review. *Journal of Cleaner Production*, *219*, pp.411-423.

EU-RED (2018). Renewable Energy – Recast to 2030 (RED II) Directive (EU) 2018/2001 of The European Parliament and of The Council. https://eur-lex.europa.eu/legal-content/EN/TXT/PDF/?uri=CELEX:32018L2001&from=EN

Evangelisti, S., Lettieri, P., Borello, D., Clift, R., 2014. Life cycle assessment of energy from waste via anaerobic digestion: A UK case study. Waste Management. 34, pp. 226–237.

FAO (2013). Good Agricultural Practices for greenhouse vegetable crops: *Principles for Mediterranean climate areas.* FAO plant production and protection paper 217, Rome. http://www.fao.org/3/a-i3284e.pdf

FAO, 2013. *Food wastage footprint summary report*. France: FAO. Available at: www.fao.org/nr/sustainability.

FAOSTAT. 2017. Global Food data. http://www.fao.org/faostat/en/#data/QC. Accessed: 25/06/2019

FAOSTAT., 2013. Database of greenhouse gas emissions from agriculture. *Environmental Research Letters*, *8*(1), p.015009.

FAOSTAT., 2016. Okra, production quantity – for all countries. Rome: Food and Agriculture Organization of the United Nations; 2016. Available from: www.fao.org/faostat/en/#data/QC

Feng, Y., Zhang, Y., Quan, X. and Chen, S., 2014. Enhanced anaerobic digestion of waste activated sludge digestion by the addition of zero valent iron. *Water Research, 52*, pp. 242-250.

Foged, H., Flotats Ripoll, X., Bonmatí Blasi, A., Palatsi Civit, J., Magrí Aloy, A. and Schelde, K.M., 2012. Inventory of manure processing activities in Europe. In Technical Report to the European Commission: Tjele

Folk, E., 2020. Biogas Sector in India: Perspectives. Bioenergy consult https://www.bioenergyconsult.com/biogas-india/

Food and Agriculture Organization of the United Nations (FAO), 2019. World Fertilizer Trends and Outlook to 2022. Rome

Fox, T. and Fimeche C. 2013. Global Food Waste Not, Want Not. ImechE, England.
Fu, S.F., Chen, K.Q., Zhu, R., Sun, W.X., Zou, H. and Guo, R.B., 2018. Improved anaerobic digestion performance of Miscanthus floridulus by different pretreatment methods and preliminary economic analysis. *Energy Conversion and Management*, *159*, pp.121-128.

Gaballah, E.S., Abomohra, A.E.F., Xu, C., Elsayed, M., Abdelkader, T.K., Lin, J. and Yuan, Q., 2020. Enhancement of biogas production from rape straw using different co-pretreatment techniques and anaerobic co-digestion with cattle manure. *Bioresource Technology*, p.123311.

Ganzoury, M.A. and Allam, N.K., 2015. Impact of nanotechnology on biogas production: a mini-review. *Renewable and Sustainable Energy Reviews*, *50*, pp.1392-1404.

Gao, N., Zhang, L. and Wu, C., 2018. Biomass and Wastes for Bioenergy: Thermochemical Conversion and Biotechnologies. *BioMed Research International*. pp. 1-2. doi:10.1155/2018/9638380

Gao, P., Gu, C., Wei, X., Li, X., Chen, H., Jia, H., Liu, Z., Xue, G. and Ma, C., 2017. The role of zero valent iron on the fate of tetracycline resistance genes and class 1 integrons during thermophilic anaerobic co-digestion of waste sludge and kitchen waste. *Water Research, 111*, pp.92-99.

Gent, S., Twedt, M., Gerometta, C. and Almberg, E., 2017. *Theoretical and applied aspects of biomass torrefaction: for biofuels and value-added products*. Butterworth-Heinemann, Pp. 17-39.

Ghaleb, A.A.S., Kutty, S.R.M., Ho, Y.C., Jagaba, A.H., Noor, A., Al-Sabaeei, A.M. and Almahbashi, N.M.Y., 2020. Response Surface Methodology to Optimize Methane Production from Mesophilic Anaerobic Co-Digestion of Oily-Biological Sludge and Sugarcane Bagasse. *Sustainability*, *12*(5), p.2116.

Ghasimi, D.S., Tao, Y., de Kreuk, M., Zandvoort, M.H. and van Lier, J.B., 2015. Microbial population dynamics during long-term sludge adaptation of thermophilic and mesophilic sequencing batch digesters treating sewage fine sieved fraction at varying organic loading rates. *Biotechnology for Biofuels*, *8*(1), pp.1-15.

Ghosh, P., Sengupta, S., Singh, L. and Sahay, A., 2020. Life cycle assessment of waste-to-bioenergy processes: a review. In *Bioreactors* (pp. 105-122). Elsevier.

Giasuddin, A.B., Kanel, S.R. and Choi, H., 2007. Adsorption of humic acid onto nanoscale zerovalent iron and its effect on arsenic removal. *Environmental Science & Technology*, *41*(6), pp.2022-2027.

Giwa, A., 2017. Comparative cradle-to-grave life cycle assessment of biogas production from marine algae and cattle manure biorefineries. *Bioresource Technology*, *244*, pp.1470-1479.

Guedes, P., Couto, N., Mateus, E.P. and Ribeiro, A.B., 2017. Phosphorus recovery in sewage sludge by Electrokinetic based technologies: a multivariate and circular economy view. *Waste and Biomass Valorization*, *8*(5), pp.1587-1596.

Guo, X., Liu, S., Wang, Z., Zhang, X.X., Li, M. and Wu, B., 2014. Metagenomic profiles and antibiotic resistance genes in gut microbiota of mice exposed to arsenic and iron. *Chemosphere*, *112*, pp.1-8.

Gurtekin. E., 2014. Phosphorus Recovery in Sustainability Frame. 2nd ISEM 2014 Conference. Adiyaman University 24-26 Oct, 2014, Turkey. *Akademik Platform*, pp.453-462

Guven, H., Wang, Z., and Eriksson, O., 2019. Evaluation of future food waste management alternatives in Istanbul from the life cycle assessment perspective. *Journal of Cleaner Production*, 239, pp.117999

Hansen, K.H., Angelidaki, I. and Ahring, B.K., 1999. Improving thermophilic anaerobic digestion of swine manure. *Water Research*, *33*(8), pp.1805-1810.

Hao, X., Wei, J., van Loosdrecht, M.C. and Cao, D., 2017. Analysing the mechanisms of sludge digestion enhanced by iron. *Water Research*, 117, pp. 58-67.

Harding, K.G., Dennis, J.S., and Harrison, T. L., 2018. Generic flowsheeting approach to generating first estimate material and energy balance data for Life Cycle Assessment (LCA) of Penicillin V production. *Sustainable Production and Consumption*,15, pp. 89–95.

Haroon, B., Abbasi, A.M., Faridullah, An, P., Pervez, A. and Irshad, M., 2018. Chemical characterization of cow manure and poultry manure after composting with privet and cypress residues. *Communications in Soil Science and Plant Analysis*, *49*(22), pp.2854-2866.

Hashimoto, A.G., 2004. Pretreatment of wheat straw for fermentation to methane. *Biotechnology and Bioengineering*, *28*(12), pp.1857-1866.

He, C.S., He, P.P., Yang, H.Y., Li, L.L., Lin, Y., Mu, Y. and Yu, H.Q., 2017. Impact of zero-valent iron nanoparticles on the activity of anaerobic granular sludge: From macroscopic to microcosmic investigation. *Water Research*, *127*, pp.32-40.

Heiberg, L., Koch, C.B., Kjaergaard, C., Jensen, H.S. and Hansen, H.C.B., 2012. Vivianite precipitation and phosphate sorption following iron reduction in anoxic soils. *Journal of Environmental Quality*, *41*(3), pp.938-949.

Hijazi, O., Abdelsalam, E., Samer, M., Amer, B.M.A., Yacoub, I.H., Moselhy, M.A., Attia, Y.A. and Bernhardt, H., 2020b. Environmental impacts concerning the addition of trace metals in the process of biogas production from anaerobic digestion of slurry. *Journal of Cleaner Production*, *243*, p.118593.

Hijazi, O., Abdelsalam, E., Samer, M., Attia, Y.A., Amer, B.M.A., Amer, M.A., Badr, M. and Bernhardt, H., 2020a. Life cycle assessment of the use of nanomaterials in biogas production from anaerobic digestion of manure. *Renewable Energy*, *148*, pp.417-424.

Hiloidhari, M., Baruah, D.C., Singh, A., Kataki, S., Medhi, K., Kumari, S., Ramachandra, T.V., Jenkins, B.M. and Thakur, I.S., 2017. Emerging role of Geographical Information System (GIS), Life Cycle Assessment (LCA) and spatial LCA (GIS-LCA) in sustainable bioenergy planning. *Bioresource Technology*, *242*, pp.218-226.

Hiloidhari, M., Das, D. and Baruah, D.C., 2014. Bioenergy potential from crop residue biomass in India. *Renewable and Sustainable Energy Reviews*, *32*, pp.504-512.

Holliger, C., Alves, M., Andrade, D., Angelidaki, I., Astals, S., Baier, U., Bougrier, C., Buffière, P., Carballa, M., De Wilde, V. and Ebertseder, F., 2016. Towards a standardization of biomethane potential tests. *Water Science and Technology*, *74*(11), pp.2515-2522.

Hosokai, S., Matsuoka, K., Kuramoto, K. and Suzuki, Y., 2016. Modification of Dulong's formula to estimate heating value of gas, liquid and solid fuels. *Fuel Processing Technology*, *152*, pp.399-405.

Hotze, E.M., Phenrat, T. and Lowry, G.V., 2010. Nanoparticle aggregation: challenges to understanding transport and reactivity in the environment. *Journal of Environmental Quality*, *39*(6), pp.1909-1924.

Hu, Z.H., Yue, Z.B., Yu, H.Q., Liu, S.Y., Harada, H. and Li, Y.Y., 2012. Mechanisms of microwave irradiation pretreatment for enhancing anaerobic digestion of cattail by rumen microorganisms. *Applied Energy*, *93*, pp.229-236.

Huang, C.H., Liu, S.M. and Hsu, N.Y., 2020. Understanding Global Food Surplus and Food Waste to Tackle Economic and Environmental Sustainability. *Sustainability*, 12(7),2892.

Huijbregts, M.A., Steinmann, Z.J., Elshout, P.M., Stam, G., Verones, F., Vieira, M., Zijp, M., Hollander, A. and van Zelm, R., 2017. ReCiPe2016: a harmonised life cycle impact assessment method at midpoint and endpoint level. *The International Journal of Life Cycle Assessment*, *22*(2), pp.138-147.

Hungría, J., Siles, J.A., Chica, A.F., Gil, A. and Martín, M.A., 2020. Anaerobic co-digestion of winery waste: Comparative assessment of grape marc waste and lees derived from organic crops. *Environmental Technology*, pp.1-9.

IEA (2020b). Outlook for biogas and biomethane. https://www.euneighbours.eu/sites/default/files/publications/2020-03/Outlook_for_biogas_and_biomethane.pdf

IEA 2020a. Outlook for biogas and biomethane: Prospects for organic growth, IEA, Paris https://www.iea.org/reports/outlook-for-biogas-and-biomethane-prospects-for-organic-growth

IEA, 2019. Electricity final energy consumption in South Africa by scenario,2018-2040, IEA, Paris https://www.iea.org/data-and-statistics/charts/electricity-final-energy-consumption-in-south-africa-by-scenario-2018-2040

Ingle, A.P., Chandel, A.K., Antunes, F.A., Rai, M. and da Silva, S.S., 2019. New trends in application of nanotechnology for the pretreatment of lignocellulosic biomass. *Biofuels, Bioproducts and Biorefining*, *13*(3), pp.776-788.

International Organization for Standardization, 2006. *Environmental Management: Life Cycle Assessment; Principles and Framework* (No. 2006). Geneva, ISO.

IPCC (2018). Summary for Policymakers. In: Global warming of 1.5 C. An IPCC Special Report on the impacts of global warming of 1.5ºC. Masson-Delmotte, V. et al.(eds.) Geneva, Switzerland. https://www.ipcc.ch/sr15/chapter/spm/

IRENA (2017). Biogas for domestic cooking: Technology brief, International Renewable Energy Agency, Abu Dhabi. https://www.irena.org/-/media/Files/IRENA/Agency/Publication/2017/Dec/IRENA_Biogas_for_domestic_cooking_2017.pdf (accessed: 4/7/2020)

ISO (International Standards Organisation), 2006. ISO 14.040. Environmental Management: Life Cycle Assessment, Principles and Framework. Geneva, p. 10

Jeong, S., 2017. *Effect of Humic Acid on Arsenic (III),(V) Sorption onto Zero-valent Iron, Hematite, and Magnetite* (Doctoral dissertation, Department of Civil and Environmental Engineering). The Graduate School Seoul National University.

Jia, T., Wang, Z., Shan, H., Liu, Y. and Gong, L., 2017. Effect of nanoscale zero-valent iron on sludge anaerobic digestion. *Resources, Conservation and Recycling*, *127*, pp.190-195.

Jiang, D., Hu, X., Wang, R. and Yin, D., 2015. Oxidation of nanoscale zero-valent iron under sufficient and limited dissolved oxygen: Influences on aggregation behaviors. *Chemosphere*, *122*, pp.8-13.

Jin, W., Singh, K. and Zondlo, J., 2013. Pyrolysis kinetics of physical components of wood and wood-polymers using isoconversion method. *Agriculture*, *3*(1), pp.12-32.

Jingura, R.M. and Kamusoko, R., 2017. Methods for determination of biomethane potential of feedstocks: a review. *Biofuel Research Journal*, *4*(2), pp.573-586.

Kadar, E., Rooks, P., Lakey, C. and White, D.A., 2012. The effect of engineered iron nanoparticles on growth and metabolic status of marine microalgae cultures. *Science of the Total Environment*, *439*, pp.8-17.

Kafle, G.K. and Chen, L., 2016. Comparison on batch anaerobic digestion of five different livestock manures and prediction of biochemical methane potential (BMP) using different statistical models. *Waste Management*, *48*, pp.492-502.

Kafle, G.K. and Kim, S.H., 2012. Kinetic study of the anaerobic digestion of swine manure at mesophilic temperature: a lab scale batch operation. *Journal of Biosystems Engineering*, *37*(4), pp.233-244.

Kafle, G.K., Kim, S.H. and Sung, K.I., 2013. Ensiling of fish industry waste for biogas production: a lab scale evaluation of biochemical methane potential (BMP) and kinetics. *Bioresource Technology*, *127*, pp.326-336.

Kalia, S., Kaith, B.S. and Kaur, I., 2009. Pretreatments of natural fibers and their application as reinforcing material in polymer composites—a review. *Polymer Engineering & Science*, *49*(7), pp.1253-1272.

Kampman, B., Leguijt, C., Scholten, T., Tallat-Kelpsaite, J., Brückmann, R., Maroulis, G., Lesschen, J.P., Meesters, K., Sikirica, N. and Elbersen, B., 2017. Optimal use of biogas from waste streams: an assessment of the potential of biogas from digestion in the EU beyond 2020, pp. 1–158.

Karlsson, T. and Persson, P., 2012. Complexes with aquatic organic matter suppress hydrolysis and precipitation of Fe (III). *Chemical Geology*, *322*, pp.19-27.

Karunanithi, R., Szogi, A. A., Bolan, N., Naidu, R., Loganathan, P., Hunt, P. G., Vanotti, M. B., Saint, C. P. and Ok, Y. S., 2015. Phosphorus Recovery and Reuse from Waste Streams, *Advances in Agronomy*, 131, pp. 173–250

Kataki, S., West, H., Clarke, M. and Baruah, D.C., 2016. Phosphorus recovery as struvite from farm, municipal and industrial waste: Feedstock suitability, methods and pre-treatments. *Waste Management*, *49*, pp.437-454.

Kemausuor, F., Adaramola, M.S. and Morken, J., 2018. A review of commercial biogas systems and lessons for Africa. *Energies*, *11*(11), p.2984.

Khan, N., le Roes-Hill, M., Welz, P.J., Grandin, K.A., Kudanga, T., Van Dyk, J.S., Ohlhoff, C., Van Zyl, W.H. and Pletschke, B.I., 2015. Fruit waste streams in South Africa and their potential role in developing a bioeconomy. *South African Journal of Science*, *111*(5-6), pp.1-11.

Kigozi, R., Muzenda, E. and Aboyade, A.O., 2014, November. Biogas technology, current trends, opportunities and challenges. In *Proceedings of the 6th International Conference GREEN Technology, Renewable Energy & Environmental Engineering, Cape Town, South Africa* (pp. 27-28).

Kim, M., Li, D., Choi, O., Sang, B.I., Chiang, P.C. and Kim, H., 2017. Effects of supplement additives on anaerobic biogas production. *Korean Journal of Chemical Engineering*, *34*(10), pp. 2678-2685.

Kim, N.J., Lim, S.J. and Chang, H.N., 2018. Volatile fatty acid platform: Concept and application. *Emerging Areas in Bioengineering*, *1*, pp.173-190.

Kim, Y.S. and Kim, Y.H., 2003. Application of ferro-cobalt magnetic fluid for oil sealing. *Journal of Magnetism and Magnetic Materials*, *267*(1), pp.105-110.

Kipli, K., Muhammad, M.S., Masra, S.M.W., Zamhari, N., Lias, K. and Mat, D.A.A., 2012, March. Performance of Levenberg-Marquardt backpropagation for full reference hybrid image quality metrics. In *Proceedings of International Conference of Muti-Conference of Engineers and Computer Scientists (IMECS'12)* (pp. 704-707).

Kjerstadius, H., Haghighatafshar, S. and Davidsson, Å., 2015. Potential for nutrient recovery and biogas production from blackwater, food waste and greywater in urban source control systems. *Environmental Technology*, *36*(13), pp.1707-1720.

Klüpfel, L., Piepenbrock, A., Kappler, A. and Sander, M., 2014. Humic substances as fully regenerable electron acceptors in recurrently anoxic environments. *Nature Geoscience*, *7*(3), pp.195-200.

Komiyama, T. and Ito, T., 2019. The characteristics of phosphorus in animal manure composts. *Soil Science and Plant Nutrition*, *65*(3), pp.281-288.

Kong, X., Yu, S., Xu, S., Fang, W., Liu, J. and Li, H., 2018. Effect of Fe0 addition on volatile fatty acids evolution on anaerobic digestion at high organic loading rates. *Waste Management*, *71*, pp. 719-727.

Koniuszewska, I., Korzeniewska, E., Harnisz, M. and Czatzkowska, M., 2020. Intensification of biogas production using various technologies: A review. *International Journal of Energy Research*, pp. 1-19. DOI: 10.1002/er.5338

Kougias, P.G. and Angelidaki, I., 2018. Biogas and its opportunities—A review. *Frontiers of Environmental Science & Engineering*, *12*(3), p.14.

Kreuger, E., Sipos, B., Zacchi, G., Svensson, S.E. and Björnsson, L., 2011. Bioconversion of industrial hemp to ethanol and methane: the benefits of steam pretreatment and co-production. *Bioresource Technology*, 102(3), pp. 3457-3465.

Kumar, V., Kumar, P., Kumar, P. and Singh, J., 2020. Anaerobic digestion of Azolla pinnata biomass grown in integrated industrial effluent for enhanced biogas production and COD reduction: Optimization and kinetics studies. *Environmental Technology & Innovation*, *17*, p.100627.

Kuttner, P., Weißböck, A.D., Leitner, V. and Jäger, A., 2015. Examination of commercial additives for biogas production. *Agron Res*, *13*(2), pp.337-347.

Labatut, R.A., Angenent, L.T. and Scott, N.R., 2014. Conventional mesophilic vs. thermophilic anaerobic digestion: a trade-off between performance and stability? *Water Research*, *53*, pp.249-258.

Lansche, J., and Müller, J., 2017. Life cycle assessment (LCA) of biogas versus dung combustion household cooking systems in developing countries e a case study in Ethiopia. *Journal of Cleaner Production*, 165, pp. 828-835.

Lee, C., Kim, J.Y., Lee, W.I., Nelson, K.L., Yoon, J. and Sedlak, D.L., 2008. Bactericidal effect of zero-valent iron nanoparticles on Escherichia coli. *Environmental Science & Technology*, *42*(13), pp.4927-4933.

Lee, U., Han, J. and Wang, M., 2017. Evaluation of landfill gas emissions from municipal solid waste landfills for the life-cycle analysis of waste-to-energy pathways. *Journal of Cleaner Production*, *166*, pp.335-342.

Leng, L., Bogush, A.A., Roy, A. and Stegemann, J.A., 2019. Characterisation of ashes from waste biomass power plants and phosphorus recovery. *Science of The Total Environment*, *690*, pp.573-583.

Lenoble, V., Laclautre, C., Deluchat, V., Serpaud, B. and Bollinger, J.C., 2005. Arsenic removal by adsorption on iron (III) phosphate. *Journal of Hazardous Materials*, *123*(1-3), pp.262-268.

Levis, J.W. and Barlaz, M.A., 2013. Anaerobic Digestion Process Model Documentation. *North Carolina State University Raleigh, NC* 27695-7908 (September), pp. 1-44.

Li, B., Dinkler, K., Zhao, N., Sobhi, M., Merkle, W., Liu, S., Dong, R., Oechsner, H. and Guo, J., 2020. Influence of anaerobic digestion on the labile phosphorus in pig, chicken, and dairy manure. *Science of the Total Environment*, *737*, p.140234.

Li, J., Hao, X., van Loosdrecht, M.C., Luo, Y. and Cao, D., 2019b. Effect of humic acids on batch anaerobic digestion of excess sludge. *Water Research*, *155*, pp.431-443.

Li, Q., Li, H., Wang, G. and Wang, X., 2017. Effects of loading rate and temperature on anaerobic co-digestion of food waste and waste activated sludge in a high frequency feeding system, looking in particular at stability and efficiency. *Bioresource Technology*, *237*, pp.231-239.

Li, W., Khalid, H., Zhu, Z., Zhang, R., Liu, G., Chen, C. and Thorin, E., 2018a. Methane production through anaerobic digestion: Participation and digestion characteristics of cellulose, hemicellulose and lignin. *Applied Energy*, 226, pp.1219-1228.

Li, X.Q., Brown, D.G. and Zhang, W.X., 2007. Stabilization of biosolids with nanoscale zero-valent iron (nZVI). *Journal of Nanoparticle Research*, *9*(2), pp.233-243.

Li, Y., Chen, Y. and Wu, J., 2019a. Enhancement of methane production in anaerobic digestion process: A review. *Applied Energy*, *240*, pp.120-137.

Li, Y., Jin, Y., Li, H., Borrion, A., Yu, Z. and Li, J., 2018. Kinetic studies on organic degradation and its impacts on improving methane production during anaerobic digestion of food waste. *Applied Energy*, *213*, pp.136-147.

Li, Y., Manandhar, A., Li, G. and Shah, A., 2018b. Life cycle assessment of integrated solid state anaerobic digestion and composting for on-farm organic residues treatment. *Waste Management*, *76*, pp.294-305.

Li, Y., Zhang, R., Liu, G., Chen, C., He, Y. and Liu, X., 2013. Comparison of methane production potential, biodegradability, and kinetics of different organic substrates. *Bioresource Technology*, *149*, pp.565-569.

Liao, X. and Li, H., 2015. Biogas production from low-organic-content sludge using a high-solids anaerobic digester with improved agitation. *Applied Energy*, *148*, pp.252-259.

Lijó, L., González-García, S., Bacenetti, J., Fiala, M., Feijoo, G., Lema, J.M. and Moreira, M.T., 2014. Life Cycle Assessment of electricity production in Italy from anaerobic co-digestion of pig slurry and energy crops. *Renewable Energy*, *68*, pp.625-635.

Linville, J.L., Shen, Y., Schoene, R.P., Nguyen, M., Urgun-Demirtas, M. and Snyder, S.W., 2016. Impact of trace element additives on anaerobic digestion of sewage sludge with in-situ carbon dioxide sequestration. *Process Biochemistry*, *51*(9), pp.1283-1289.

Liu, G., Fernandez, A. and Cai, Y., 2011. Complexation of arsenite with humic acid in the presence of ferric iron. *Environmental Science & Technology*, *45*(8), pp.3210-3216.

Liu, K., Chen, Y., Xiao, N., Zheng, X. and Li, M., 2015a. Effect of humic acids with different characteristics on fermentative short-chain fatty acids production from waste activated sludge. *Environmental Science & Technology*, *49*(8), pp.4929-4936.

Liu, L., Zhang, T., Wan, H., Chen, Y., Wang, X., Yang, G. and Ren, G., 2015b. Anaerobic co-digestion of animal manure and wheat straw for optimized biogas production by the addition of magnetite and zeolite. *Energy Conversion and Management*, *97*, pp.132-139.

Liu, R., Hao, X. and Wei, J., 2016. Function of homoacetogenesis on the heterotrophic methane production with exogenous H_2/CO_2 involved. *Chemical Engineering Journal*, 284, pp.1196-1203.

Liu, X.Y., Wang, J.J., Nie, J.M., Wu, N., Yang, F. and Yang, R.J., 2018. Biogas production of Chicken Manure by Two-stage fermentation process. In *E3S Web of Conferences* (Vol. 38, p. 01048). EDP Sciences.

Longo, S., Cellura, M., Guarino, F. and Mistretta, M., 2020. A life cycle assessment of tri-generation from biomass waste: The experience of the "agro-combined" of Thibar. In *Biofuels for a More Sustainable Future* (pp. 213-226). Elsevier.

Lovley, D.R., 2017. Syntrophy goes electric: direct interspecies electron transfer. *Annual review of microbiology*, *71*, pp.643-664.

Lozano, J., 2010. Enhanced anaerobic digestion using Fenton reagent. *Proceedings of the Water Environment Federation*, *2010*(12), pp.4885-4897.

Lu, D., Liu, X., Apul, O.G., Zhang, L., Ryan, D.K. and Zhang, X., 2019. Optimization of biomethane production from anaerobic Co-digestion of microalgae and septic tank sludge. *Biomass and Bioenergy*, *127*, p.105266.

Lu, X., Wang, H., Ma, F., Zhao, G. and Wang, S., 2017. Enhanced anaerobic digestion of cow manure and rice straw by the supplementation of an iron oxide–zeolite system. *Energy & Fuels*, *31*(1), pp.599-606.

Lusk, P., 1998. *Methane recovery from animal manures the current opportunities casebook* (No. NREL/SR-580-25145). National Renewable Energy Lab., Golden, CO (US). Work performed by Resource Development Associates, Washington, DC.

Lv, W., Schanbacher, F.L. and Yu, Z., 2010. Putting microbes to work in sequence: recent advances in temperature-phased anaerobic digestion processes. *Bioresource Technology*, *101*(24), pp.9409-9414.

Ma, G., Ndegwa, P., Harrison, J.H. and Chen, Y., 2020. Methane yields during anaerobic co-digestion of animal manure with other feedstocks: meta-analysis. Science of the Total Environment, 788, pp. 138224.

Maamir, W., Ouahabi, Y., Poncin, S., Li, H.Z. and Bensadok, K., 2017. Effect of Fenton pretreatment on anaerobic digestion of olive mill wastewater and olive mill solid waste in mesophilic conditions. *International Journal of Green Energy*, *14*(6), pp.555-560.

Mahanty, B., Zafar, M., Han, M.J. and Park, H.S., 2014. Optimization of co-digestion of various industrial sludges for biogas production and sludge treatment: Methane production potential experiments and modeling. *Waste Management*, *34*(6), pp.1018-1024.

Maletta, E. and Díaz-Ambrona, C.H., 2020. Lignocellulosic Crops as Sustainable Raw Materials for Bioenergy. Green Energy to Sustainability: *Strategies for Global Industries*. pp. 489-514.

Manyi-Loh, C.E., Mamphweli, S.N., Meyer, E.L., Okoh, A.I., Makaka, G. and Simon, M., 2013. Microbial anaerobic digestion (bio-digesters) as an approach to the decontamination of animal wastes in pollution control and the generation of renewable energy. *International Journal of Environmental Research and Public Health*, *10*(9), pp.4390-4417.

Mao, C., Feng, Y., Wang, X. and Ren, G., 2015. Review on research achievements of biogas from anaerobic digestion. *Renewable and Sustainable Energy Reviews*, *45*, pp. 540-555.

Mayer, B.K., Baker, L.A., Boyer, T.H., Drechsel, P., Gifford, M., Hanjra, M.A., Parameswaran, P., Stoltzfus, J., Westerhoff, P. and Rittmann, B.E., 2016. Total value of phosphorus recovery. *Environmental science & Technology*, *50*(13), pp.6606-6620.

Melia, P.M., Cundy, A.B., Sohi, S.P., Hooda, P.S. and Busquets, R., 2017. Trends in the recovery of phosphorus in bioavailable forms from wastewater. *Chemosphere*, *186*, pp.381-395.

Meng, X., Zhang, Y., Li, Q. and Quan, X., 2013. Adding Fe0 powder to enhance the anaerobic conversion of propionate to acetate. *Biochemical Engineering Journal*, *73*, pp.80-85.

Menon, A., Wang, J.Y. and Giannis, A., 2017. Optimization of micronutrient supplement for enhancing biogas production from food waste in two-phase thermophilic anaerobic digestion. *Waste Management*, *59*, pp.465-475.

Michalska, K., Miazek, K., Krzystek, L. and Ledakowicz, S., 2012. Influence of pretreatment with Fenton's reagent on biogas production and methane yield from lignocellulosic biomass. *Bioresource Technology*, *119*, pp.72-78.

Moghaddam, E. A., Ahlgren, S., and Nordberg, Å., 2016. Assessment of novel routes of biomethane utilization in a life cycle perspective. *Frontiers in Bioengineering and Biotechnology*, 4, (89), pp.1-13.

Mokete, R., Eljamal, O. and Sugihara, Y., 2020. Exploration of the reactivity of nanoscale zero-valent iron (NZVI) associated nanoparticles in diverse experimental conditions. *Chemical Engineering and Processing-Process Intensification*, *150*, p.107879.

Montgomery, L.F. and Bochmann, G., 2014. Pretreatment of feedstock for enhanced biogas production, pp. 1-20. Ireland*: IEA Bioenergy*.

Mshandete, A., Björnsson, L., Kivaisi, A.K., Rubindamayugi, M.S. and Mattiasson, B., 2006. Effect of particle size on biogas yield from sisal fibre waste. *Renewable Energy*, *31*(14), pp.2385-2392.

Muvhiiwa, R., Hildebrandt, D., Chimwani, N., Ngubevana, L. and Matambo, T., 2017. The impact and challenges of sustainable biogas implementation: moving towards a bio-based economy. *Energy, Sustainability and Society*, *7*(1), p.20.

Naidu, R., Lamb, D.T., Bolan, N.S. and Gawandar, J., 2012. Recovery and reuse of phosphorus from wastewater sources. *Advanced nutrient management: gains from the past—goals for the future. http://flrc. massey. ac. nz/publications. html. Occasional Report*, (25).

Najafi, B. and Ardabili, S.F., 2018. Application of ANFIS, ANN, and logistic methods in estimating biogas production from spent mushroom compost (SMC). *Resources, Conservation and Recycling*, *133*, pp.169-178.

Nassar, N.N., 2012. Iron oxide nanoadsorbents for removal of various pollutants from wastewater: an overview. *Application of Adsorbents for Water Pollution Control*, pp.81-118.

Nasution, M.A., Wibawa, D.S., Ahamed, T. and Noguchi, R., 2018. Comparative environmental impact evaluation of palm oil mill effluent treatment using a life cycle assessment approach: A case study based on composting and a combination for biogas technologies in North Sumatera of Indonesia. *Journal of Cleaner Production*, *184*, pp.1028-1040.

National Research Council (NRC)., 2006. Lost crops of Africa: Volume II: Vegetables. "Chapter 16 Okra." *The National Academies Press*. Washintgon D.C, pp. 287–354. Doi: 10.17226/11763.

Nguyen, D., Visvanathan, C., Jacob, P. and Jegatheesan, V., 2015. Effects of nano cerium (IV) oxide and zinc oxide particles on biogas production. *International Biodeterioration & Biodegradation*, *102*, pp.165-171.

Nhuchhen, D.R. and Salam, P.A., 2012. Estimation of higher heating value of biomass from proximate analysis: A new approach. *Fuel*, *99*, pp.55-63.

Noonari, A.A., Mahar, R.B., Sahito, A.R. and Brohi, K.M., 2019. Anaerobic co-digestion of canola straw and banana plant wastes with buffalo dung: effect of Fe3O4 nanoparticles on methane yield. *Renewable Energy*, *133*, pp.1046-1054.

Noubactep, C.J.W.S., 2010. The fundamental mechanism of aqueous contaminant removal by metallic iron. *Water Sa*, *36*(5).

Nuorkivi, A., 2010. Allocation of Fuel Energy and Emissions to Heat and Power in CHP. Final Report. Energy-AN Consulting.

Obileke, K., Nwokolo, N., Makaka, G., Mukumba, P. and Onyeaka, H., 2020. Anaerobic digestion: Technology for biogas production as a source of renewable energy—A review. *Energy & Environment*, p.0958305X20923117.

Oechsner, H., Khanal, S.K. and Taherzadeh, M., 2015. Advances in biogas research and application. *Bioresource Technology*, 178, p.177.

Ogejo, J.A., Wen, Z., Ignosh, J., Bendfeldt, E.S. and Collins, E., 2009. Biomethane technology. Virginia Coop Ext: 442–881 http://pubs.ext.vt.edu/442/442-881/442-881 pdf.pdf

Oladejo, O.S., Dahunsi, S.O., Adesulu-Dahunsi, A.T., Ojo, S.O., Lawal, A.I., Idowu, E.O., Olanipekun, A.A., Ibikunle, R.A., Osueke, C.O., Ajayi, O.E. and Osueke, N., 2020. Energy generation from anaerobic co-digestion of food waste, cow dung and piggery dung. *Bioresource Technology*, *313*, p.123694.

Olaniyan, A.M. and Omoleyomi, B.D., 2013. Characteristics of okra under different process pretreatments and different drying conditions. *Journal of Food Processing and Technology*, *4*(6), p.237.

Omelianski, W., 1906. Über Methanbildung in der Natur bei biologischen Prozessen. *Zentralblatt fuèr Bakteriol. Parasitenkd. II*.

Osborn, D., Cutter, A. and Ullah, F., 2015. Universal Sustainable Development Goals: Understanding the transformational challenge for developed countries. In *Report of a study by Stakeholder Forum*, pp. 5-20.

Otero-González, L., Field, J. A. and Sierra-Alvarez, R., 2014. Fate and long-term inhibitory impact of ZnO nanoparticles during high-rate anaerobic wastewater treatment, *Journal of Environmental Management*, 135, pp. 110–117.

Pagliari, P.H., Wilson, M., Waldrip, H.M. and He, Z., 2020. Nitrogen and phosphorus characteristics of beef and dairy manure. *Animal Manure: Production, Characteristics, Environmental Concerns, and Management*, *67*, pp.45-62.

Pant, D., Singh, A., Van Bogaert, G., Gallego, Y.A., Diels, L. and Vanbroekhoven, K., 2011. An introduction to the life cycle assessment (LCA) of bioelectrochemical systems (BES) for sustainable energy and product generation: relevance and key aspects. *Renewable and Sustainable Energy Reviews*, *15*(2), pp.1305-1313.

Parsons, S.A. and Smith, J.A., 2008. Phosphorus removal and recovery from municipal wastewaters. *Elements*, *4*(2), pp.109-112.

Pazera, A., Slezak, R., Krzystek, L., Ledakowicz, S., Bochmann, G., Gabauer, W., Helm, S., Reitmeier, S., Marley, L., Gorga, F. and Farrant, L., 2015. Biogas in Europe: food and beverage (FAB) waste potential for biogas production. *Energy & Fuels*, *29*(7), pp.4011-4021.

Peeters, K., Lespes, G., Zuliani, T., Ščančar, J. and Milačič, R., 2016. The fate of iron nanoparticles in environmental waters treated with nanoscale zero-valent iron, FeONPs and Fe3O4NPs. *Water Research*, *94*, pp.315-327.

Pei, P., Zhang, C., Li, J., Chang, S., Li, S., Wang, J., Zhao, M., Li, J., Yu, M. and Chen, X., 2014. Optimization of NaOH pretreatment for enhancement of biogas production of banana pseudo-stem fiber using response surface methodology. *BioResources*, *9*(3), pp.5073-5087.

Piepenbrock, A., Schröder, C. and Kappler, A., 2014. Electron transfer from humic substances to biogenic and abiogenic Fe (III) oxyhydroxide minerals. *Environmental Science & Technology*, *48*(3), pp.1656-1664.

Podstawczyk, D., Witek-Krowiak, A., Dawiec-Liśniewska, A., Chrobot, P. and Skrzypczak, D., 2017. Removal of ammonium and orthophosphates from reject water generated during dewatering of digested sewage sludge in municipal wastewater treatment plant using adsorption and membrane contactor system. *Journal of Cleaner Production*, *161*, pp.277-287.

Powell, J.J., Faria, N., Thomas-McKay, E. and Pele, L.C., 2010. Origin and fate of dietary nanoparticles and microparticles in the gastrointestinal tract. *Journal of Autoimmunity*, *34*(3), 226-233.

Prasad, A., Sotenko, M., Blenkinsopp, T. and Coles, S.R., 2016. Life cycle assessment of lignocellulosic biomass pretreatment methods in biofuel production. *The International Journal of Life Cycle Assessment*, *21*(1), pp.44-50.

Pruden, A., Pei, R., Storteboom, H. and Carlson, K.H., 2006. Antibiotic resistance genes as emerging contaminants: studies in northern Colorado. *Environmental Science & Technology*, *40*(23), pp.7445-7450.

Puyol, D., Flores-Alsina, X., Segura, Y., Molina, R., Jerez, S., Gernaey, K.V., Melero, J.A. and Martinez, F., 2017, May. ZVI addition in continuous anaerobic digestion systems dramatically decreases P recovery potential: dynamic modelling. In *Frontiers international conference on wastewater treatment and modelling* (pp. 211-217). Springer, Cham.

Puyol, D., Flores-Alsina, X., Segura, Y., Molina, R., Padrino, B., Fierro, J.L.G., Gernaey, K.V., Melero, J.A. and Martinez, F., 2018. Exploring the effects of ZVI addition on resource recovery in the anaerobic digestion process. *Chemical Engineering Journal*, *335*, pp.703-711.

Qin, Y., Chen, L., Wang, T., Ren, J., Cao, Y. and Zhou, S., 2019. Impacts of ferric chloride, ferrous chloride and solid retention time on the methane-producing and physicochemical characterization in high-solids sludge anaerobic digestion. *Renewable Energy*, *139*, pp.1290-1298.

Quan, C. and Gao, N., 2016. Copyrolysis of biomass and coal: a review of effects of copyrolysis parameters, product properties, and synergistic mechanisms. *BioMed Research International*, *2016*.

Rahman, K.M., Melville, L., Huq, S.I. and Khoda, S.K., 2016. Understanding bioenergy production and optimisation at the nanoscale–a review. *Journal of Experimental Nanoscience*, *11*(10), pp.762-775.

Ram, M.S., Singh, L., Suryanarayana, M.V.S. and Alam, S.I., 2000. Effect of iron, nickel and cobalt on bacterial activity and dynamics during anaerobic oxidation of organic matter. *Water, Air, and Soil Pollution*, *117*(1-4), pp.305-312.

Ramírez-Arpide, F.R., Demirer, G.N., Gallegos-Vázquez, C., Hernández-Eugenio, G., Santoyo-Cortés, V.H. and Espinosa-Solares, T., 2018. Life cycle assessment of biogas production through anaerobic co-digestion of nopal cladodes and dairy cow manure. *Journal of Cleaner Production*, *172*, pp.2313-2322.

Ramírez-Islas, M.E., Güereca, L.P., Sosa-Rodriguez, F.S. and Cobos-Peralta, M.A., 2020. Environmental assessment of energy production from anaerobic digestion of pig manure at medium-scale using life cycle assessment. *Waste Management*, 102, pp. 85–96.

Raposo, F., Borja, R., Martín, M.A., Martín, A., De la Rubia, M.A. and Rincón, B., 2009. Influence of inoculum–substrate ratio on the anaerobic digestion of sunflower oil cake in batch mode: process stability and kinetic evaluation. *Chemical Engineering Journal*, *149*(1-3), pp.70-77.

Raposo, F., Fernández-Cegrí, V., De la Rubia, M.A., Borja, R., Béline, F., Cavinato, C., Demirer, G.Ö.K.S.E.L., Fernández, B., Fernández-Polanco, M., Frigon, J.C. and Ganesh, R., 2011. Biochemical methane potential (BMP) of solid organic substrates: evaluation of anaerobic biodegradability using data from an international interlaboratory study. *Journal of Chemical Technology & Biotechnology*, *86*(8), pp.1088-1098.

Rea, J., 2014. *Kinetic Modeling and experimentation of anaerobic digestion* (Doctoral dissertation, Massachusetts Institute of Technology), pp. 1–58.

Remy, C. and Jossa, P., 2015. Sustainable Sewage Sludge Management Fostering Phosphorus Recovery and Energy Efficiency. Life Cycle Assessment of Selected Processes for P Recovery from Sewage Sludge, Sludge Liquor or Ash. EU P-REX Project. Report Deliverable D 9.2.

Rincón, B., Heaven, S., Banks, C.J. and Zhang, Y., 2012. Anaerobic digestion of whole-crop winter wheat silage for renewable energy production. *Energy & Fuels*, *26*(4), pp.2357-2364.

Rodriguez, C., Alaswad, A., El-Hassan, Z. and Olabi, A.G., 2017. Mechanical pretreatment of waste paper for biogas production. *Waste Management*, *68*, pp.157-164.

Romero-Güiza, M.S., Vila, J., Mata-Alvarez, J., Chimenos, J.M. and Astals, S., 2016. The role of additives on anaerobic digestion: a review. *Renewable and Sustainable Energy Reviews*, *58*, pp.1486-1499.

Roopnarain, A. and Adeleke, R., 2017. Current status, hurdles and future prospects of biogas digestion technology in Africa. *Renewable and Sustainable Energy Reviews*, *67*, pp.1162-1179.
Salihu, A. and Alam, M.Z., 2016. Pretreatment methods of organic wastes for biogas production. *Journal of Applied Science*, *16*(3), pp.124-137.

Sam, A., Bi, X., and Farnsworth, D. (2017). How incentives affect the adoption of anaerobic digesters in the United States. Sustainability, 9(7), 1221.

Samer, M., 2016. *Abatement techniques for reducing emissions from livestock buildings*. Springer International Publishing.

Santos, L.H., Araújo, A.N., Fachini, A., Pena, A., Delerue-Matos, C. and Montenegro, M.C.B.S.M., 2010. Ecotoxicological aspects related to the presence of pharmaceuticals in the aquatic environment. *Journal of Hazardous Materials*, *175*(1-3), pp.45-95.

Selvam, A., Xu, D., Zhao, Z. and Wong, J.W., 2012. Fate of tetracycline, sulfonamide and fluoroquinolone resistance genes and the changes in bacterial diversity during composting of swine manure. *Bioresource Technology*, *126*, pp.383-390.

Shafiee, S. and Topal, E., 2008. An econometrics view of worldwide fossil fuel consumption and the role of US. *Energy Policy*, *36*(2), pp.775-786.

Shahriari, H., Warith, M., Hamoda, M. and Kennedy, K.J., 2012. Anaerobic digestion of organic fraction of municipal solid waste combining two pretreatment modalities, high temperature microwave and hydrogen peroxide. *Waste Management*, *32*(1), pp.41-52.

Sharp, R., Fiore, A., Fok, A., Mahoney, K., Galst, S., Lin, T. and Horne, M. V. 2015. Comprehensive Evaluation of Food Waste Co-Digestion'.Clear Water, Winter 2015 New York Department of Environmental Protection (NYCDEP), pp. 19-25. https://nywea.org/clearwaters/uploads/5ComprehensiveEvaluation.pdf

Shi, H., Mahinpey, N., Aqsha, A. and Silbermann, R., 2016. Characterization, thermochemical conversion studies, and heating value modeling of municipal solid waste. *Waste Management*, *48*, pp.34-47.

Shi, X.S., Dong, J.J., Yu, J.H., Yin, H., Hu, S.M., Huang, S.X. and Yuan, X.Z., 2017. Effect of hydraulic retention time on anaerobic digestion of wheat straw in the semicontinuous continuous stirred-tank reactors. *BioMed Research International*, *2017*.

Show, K.Y., Yan, Y., Yao, H., Guo, H., Li, T., Show, D.Y., Chang, J.S. and Lee, D.J., 2020. Anaerobic granulation: A review of granulation hypotheses, bioreactor designs and emerging green applications. *Bioresource Technology*, *300*, p.122751.

Siami, S., Aminzadeh, B., Karimi, R. and Hallaji, S.M., 2020. Process optimization and effect of thermal, alkaline, H 2 O 2 oxidation and combination pretreatment of sewage sludge on solubilization and anaerobic digestion. *BMC Biotechnology*, *20*, pp.1-12.

Sikosana, M., Randall, D.G., Petrie, D.J., Oelofse, M., Russo, V. and Von Blottnitz, H. (2016) Nutrient and Energy Recovery From Sewage : Towards an Integrated Approach, *Extended Report to the Water Research Commission*, WRC Report, pp. 1–177.

Singh, Y.D., Mahanta, P. and Bora, U., 2017. Comprehensive characterization of lignocellulosic biomass through proximate, ultimate and compositional analysis for bioenergy production. *Renewable Energy*, *103*, pp.490-500.

Smith, A.D. and Holtzapple, M.T., 2011. Investigation of the optimal carbon–nitrogen ratio and carbohydrate–nutrient blend for mixed-acid batch fermentations. *Bioresource Technology*, *102*(10), pp.5976-5987.

So, D., Oo, F. and Eo, Y., 2020. Bioenergy technologies adoption in Africa: A review of past and current status. *Journal of Cleaner Production*, p.121683.

Söhngen, N.L., 1906. Über bakterien, welche methan als kohlenstoffnahrung und energiequelle gebrauchen. *Zentrabl Bakteriol Parasitenk Infektionskr*, *15*, pp.513-517.

Song, Z., Liu, X., Yan, Z., Yuan, Y. and Liao, Y., 2014. Comparison of seven chemical pretreatments of corn straw for improving methane yield by anaerobic digestion. *PloS One*, *9*(4), p.e93801.

South African Biogas Industry Association (SABIA)., 2015. Paper presented at: National Biogas Conference, Standards and Regulations; 2015 March 05; South Africa. www.energy.gov.za/files/biogas/2015-Biogas-Conference/Day-1/SABIA-Standards-and-Regulations-25March2015.pdf

Sreekrishnan, T.R., Kohli, S. and Rana, V., 2004. Enhancement of biogas production from solid substrates using different techniques—a review. *Bioresource Technology*, *95*(1), pp.1-10.

Stams, A.J. and Plugge, C.M., 2009. Electron transfer in syntrophic communities of anaerobic bacteria and archaea. *Nature Reviews Microbiology*, *7*(8), pp.568-577.

StatsSA. 2018. www.statssa.gov.za/?p=11527. Accessed: 29/06/2019

Steven, V. K. J., 2010. World phosphate rock reserves and resources (p. 48). Muscle Shoals: IFDC. https://pdf.usaid.gov/pdf_docs/Pnadw835.PDF

Strömberg, S., Nistor, M. and Liu, J., 2014. Towards eliminating systematic errors caused by the experimental conditions in Biochemical Methane Potential (BMP) tests. *Waste Management*, *34*(11), pp.1939-1948.

Suanon, F., Sun, Q., Li, M., Cai, X., Zhang, Y., Yan, Y. and Yu, C.P., 2017. Application of nanoscale zero valent iron and iron powder during sludge anaerobic digestion: Impact on methane yield and pharmaceutical and personal care products degradation. *Journal of Hazardous Materials*, *321*, pp.47-53.

Suanon, F., Sun, Q., Mama, D., Li, J., Dimon, B. and Yu, C.P., 2016. Effect of nanoscale zero-valent iron and magnetite (Fe3O4) on the fate of metals during anaerobic digestion of sludge. *Water Research*, *88*, pp.897-903.

Sun, Q., Li, H., Yan, J., Liu, L., Yu, Z. and Yu, X., 2015. Selection of appropriate biogas upgrading technology-a review of biogas cleaning, upgrading and utilisation. *Renewable and Sustainable Energy Reviews*, *51*, pp.521-532.

Surendra, K.C., Takara, D., Hashimoto, A.G. and Khanal, S.K., 2014. Biogas as a sustainable energy source for developing countries: Opportunities and challenges. *Renewable and Sustainable Energy Reviews*, *31*, pp.846-859.

Taha, M.R., Ibrahim, A.H., Amat, R.C. and Azhari, A.W., 2014. Applicability of nano zero valent iron (nZVI) in sono–Fenton process. In *Journal of Physics: Conference Series*, 495, 1, 012010.

Takashima, M., 2019. Enhanced phosphate release from anaerobically digested sludge through sulfate reduction. *Waste and Biomass Valorization*, *10*(11), pp.3419-3425.

Talha, Z., Hamid, A., Guo, D., Hassan, M., Mehryar, E., Okinda, C. and Ding, W., 2018. Ultrasound assisted alkaline pre-treatment of sugarcane filter mud for performance enhancement in biogas production. *International Journal of Agric & Biological Engineering*, *11*(1), pp.226-231.

Tan, J., Wang, J., Xue, J., Liu, S.Y., Peng, S.C., Ma, D., Chen, T.H. and Yue, Z., 2015. Methane production and microbial community analysis in the goethite facilitated anaerobic reactors using algal biomass. *Fuel*, *145*, pp.196-201.

Tang, S.C. and Lo, I.M., 2013. Magnetic nanoparticles: essential factors for sustainable environmental applications. *Water Research*, *47*(8), pp.2613-2632.

Thanos, D., Maragkaki, A., Venieri, D., Fountoulakis, M. and Manios, T., 2020. Enhanced Biogas Production in Pilot Digesters Treating a Mixture of Olive Mill Wastewater and Agro-industrial or Agro-livestock By-Products in Greece. *Waste and Biomass Valorization*, pp.1-9.

Thiruselvi, D., Yuvarani, M., Amudha, T., Sneha, R., Mariselvam, A.K., Anil Kumar, M., Shanmugam, P. and Sivanesan, S., 2018. Synthesis of iron nano-catalyst using Acalypha indica leaf extracts for biogas production from mixed liquor volatile suspended solids. *Energy Sources, Part A: Recovery, Utilization, and Environmental Effects*, *40*(7), pp. 772-779.

Thomsen, M., Romeo, D., Caro, D., Seghetta, M., Cong, R.-G., 2018. Environmental economic analysis of integrated organic waste and wastewater management systems: a case study from Aarhus city (Denmark). *Sustainability*, 10 (10).

Tian, T. and Yu, H.Q., 2020. Iron-assisted biological wastewater treatment: Synergistic effect between iron and microbes. *Biotechnology Advances*, p.107610.

Tsapekos, P., Kougias, P.G., Egelund, H., Larsen, U., Pedersen, J., Trénel, P. and Angelidaki, I., 2017. Mechanical pretreatment at harvesting increases the bioenergy output from marginal land grasses. *Renewable Energy*, *111*, pp.914-921.

Twinomunuji, E., Kemausuor, F., Black, M., Roy, A., Leach, M., Sadhukhan, R.O.J. and Murphy, R., 2020. The potential for bottled biogas for clean cooking in Africa. February 2020 Working Paper. University of Surrey, KNUST, UCPC, Engas UK and MECS. Available at https://www.mecs.org.uk/working-papers/.

U.S. Environmental Protection Agency (USEPA), 2017. U.S. Environmental Protection Agency (EPA)Inventory of U.S. Greenhouse Gas Emissions and Sinks: 1990–2015. EPA 430-P-17-001, Washington, D.C

Ugwu, S.N. and Enweremadu, C.C., 2019. Effects of pre-treatments and co-digestion on biogas production from Okra waste. *Journal of Renewable and Sustainable Energy*, *11*(1), p.013101.

Ugwu, S.N. and Enweremadu, C.C., 2020. Enhancement of biogas production process from biomass wastes using iron-based additives: types, impacts, and implications. *Energy Sources, Part A: Recovery, Utilization, and Environmental Effects*, pp.1-23.

Ugwu, S.N., Biscoff, R.K. and Enweremadu, C.C., 2020. A meta-analysis of iron-based additives on enhancements of biogas yields during anaerobic digestion of organic wastes. *Journal of Cleaner Production*, 269 (2020) 122449.

Uman, A.E., Usack, J.G., Lozano, J.L. and Angenent, L.T., 2018. Controlled experiment contradicts the apparent benefits of the Fenton reaction during anaerobic digestion at a municipal wastewater treatment plant. *Water Science and Technology*, *78*(9), pp. 1861-1870.

UNDP (2020). Mitigation through reducing emissions and increasing carbon storage https://www.undp.org/content/undp/en/home/2030-agenda-for-sustainable-development/planet/climate-change/reducing-emissions--promoting-clean-energy-and-protecting-forest.html

UNSTAT, 2020. Composition of Municipal Waste. https://unstats.un.org/unsd/envstats/Questionnaires/2019/Tables/Composition%20of%20Municipal%20Waste%20(latest%20year).xlsx

UNSTATS (2019). 7 Affordable and Clean Energy. https://unstats.un.org/sdgs/report/2019/goal-07/ (accessed: 12/06/2020)

USGS (2019). U.S. Geological Survey: mineral commodity summaries., 2019. p122-123.

Van Haandel, A. and Van Der Lubbe, J., 2007. Handbook biological wastewater treatment-design and optimisation of activated sludge systems. *Quist Publishing, Leidschendam*, Netherlands, ISBN: 978-90-77983-22-5.

Van Stappen, F., Mathot, M., Decruyenaere, V., Loriers, A., Delcour, A., Planchon, V., Goffart, J.-P., Stilmant, D., 2016. Consequential environmental life cycle assessment of a farm-scale biogas plant. *Journal of Environmental Management*, 175, pp. 20-32.

Wagner, T., Watanabe, T. and Shima, S., 2018. Hydrogenotrophic methanogenesis. *Biogenesis of hydrocarbons. Handbook of hydrocarbon and lipid microbiology*, pp.1-29.

Wan, S., Sun, L., Douieb, Y., Sun, J. and Luo, W., 2013. Anaerobic digestion of municipal solid waste composed of food waste, wastepaper, and plastic in a single-stage system: performance and microbial community structure characterization. *Bioresource Technology*, *146*, pp.619-627.

Wang, B., 2016. Factors that influence the biochemical methane potential (BMP) test: *steps towards the standardisation of BMP test*. *Lund University*.

Wang, H., Lim, T.T., Duong, C., Zhang, W., Xu, C., Yan, L., Mei, Z. and Wang, W., 2020. Long-Term Mesophilic Anaerobic Co-Digestion of Swine Manure with Corn Stover and Microbial Community Analysis. *Microorganisms*, *8*(2), p.188.

Wang, X., Duan, X., Chen, J., Fang, K., Feng, L., Yan, Y. and Zhou, Q., 2016. Enhancing anaerobic digestion of waste activated sludge by pretreatment: effect of volatile to total solids. *Environmental Technology*, *37*(12), pp.1520-1529.

Wang, Y., Wang, D. and Fang, H., 2018. Comparison of enhancement of anaerobic digestion of waste activated sludge through adding nano-zero valent iron and zero valent iron. *RSC Advances*, *8*(48), pp.27181-27190.

Wang, Y., Zhang, Y., Wang, J. and Meng, L., 2009. Effects of volatile fatty acid concentrations on methane yield and methanogenic bacteria. *Biomass and Bioenergy*, *33*(5), pp.848-853.

Ward, A.J., Hobbs, P.J., Holliman, P.J. and Jones, D.L., 2008. Optimisation of the anaerobic digestion of agricultural resources. *Bioresource Technology*, 99(17), pp.7928-7940.

Ware, A. and Power, N., 2017. Modelling methane production kinetics of complex poultry slaughterhouse wastes using sigmoidal growth functions. *Renewable Energy*, *104*, pp.50-59.

Webster, T.M., Reddy, R.R., Tan, J.Y., Van Nostrand, J.D., Zhou, J., Hayes, K.F. and Raskin, L., 2016. Anaerobic disposal of arsenic-bearing wastes results in low microbially mediated arsenic volatilization. *Environmental Science & Technology*, *50*(20), pp.10951-10959.

Weiland, P., 2010. Biogas production: current state and perspectives. *Applied Microbiology and Biotechnology*, *85*(4), pp.849-860.

WERF, 2011. Nutrient Recovery Research Challenge: State of the Knowledge, Water Environment & Technology Report, (December, 2011). pp. 1-44.

Wilfert, P., Kumar, P.S., Korving, L., Witkamp, G.J. and van Loosdrecht, M.C., 2015. The relevance of phosphorus and iron chemistry to the recovery of phosphorus from wastewater: a review. *Environmental Science & Technology*, *49*(16), pp.9400-9414.

Wong, P. Y., 2016. A novel approach for biological recovery of phosphorus, PhD thesis (June, 2016) University of Western Australia School of Pathology and Laboratory Medicine. pp. 191

World bank (2020). Trends in Solid Waste Management. In What a Waste 2.0 A Global Snapshot of Solid Waste Management to 2050. https://datatopics.worldbank.org/what-a-waste/trends_in_solid_waste_management.html (accessed 26/08/2020)

World Bioenergy Association (WBA) (2019) Global Bioenergy Statistics 2019 Summary Report https://worldbioenergy.org/global-bioenergy-statistics. Accessed on 26 May 2020.

Worldbank. 2015. The Future of the World's Population in 4 Charts. Worldbank.org.

Worldometers, 2020. World Population Projections. https://www.worldometers.info/world-population/

Wu, Y., Wang, S., Liang, D. and Li, N., 2020. Conductive materials in anaerobic digestion: From mechanism to application. *Bioresource Technology*, *298*, p.122403.

Xiao, C., Fu, Q., Liao, Q., Huang, Y., Xia, A., Chen, H. and Zhu, X., 2020. Life cycle and economic assessments of biogas production from microalgae biomass with hydrothermal pretreatment via anaerobic digestion. *Renewable Energy*, *151*, pp.70-78.

Xiao, Y., Zhang, E., Zhang, J., Dai, Y., Yang, Z., Christensen, H.E., Ulstrup, J. and Zhao, F., 2017. Extracellular polymeric substances are transient media for microbial extracellular electron transfer. *Science Advances*, *3*(7), p.e1700623.

Xie, Y., Dong, H., Zeng, G., Tang, L., Jiang, Z., Zhang, C., Deng, J., Zhang, L. and Zhang, Y., 2017. The interactions between nanoscale zero-valent iron and microbes in the subsurface environment: A review. *Journal of Hazardous Materials*, *321*, pp. 390-407.

Xu, F., Wang, Z.W. and Li, Y., 2014. Predicting the methane yield of lignocellulosic biomass in mesophilic solid-state anaerobic digestion based on feedstock characteristics and process parameters. *Bioresource Technology*, *173*, pp.168-176.

Xu, S., He, C., Luo, L., Lü, F., He, P. and Cui, L., 2015. Comparing activated carbon of different particle sizes on enhancing methane generation in upflow anaerobic digester. *Bioresource Technology*, *196*, pp.606-612.

Xu, Y., Lu, Y., Zheng, L., Wang, Z. and Dai, X., 2020. Perspective on enhancing the anaerobic digestion of waste activated sludge. *Journal of Hazardous Materials*, *389*, p.121847.

Xue, S., Song, J., Wang, X., Shang, Z., Sheng, C., Li, C., Zhu, Y. and Liu, J., 2020. A systematic comparison of biogas development and related policies between China and Europe and corresponding insights. Renewable and Sustainable Energy Reviews, 117, p.109474.

Xue, Y., Li, Q., Gu, Y., Yu, H., Zhang, Y. and Zhou, X., 2020b. Improving biodegradability and biogas production of miscanthus using a combination of hydrothermal and alkaline pretreatment. *Industrial Crops and Products*, *144*, p.111985.

Yadav, A.K., Jena, S., Acharya, B.C. and Mishra, B.K., 2012. Removal of azo dye in innovative constructed wetlands: Influence of iron scrap and sulfate reducing bacterial enrichment. *Ecological Engineering*, *49*, pp. 53-58.

Yadav, K. and Jagadevan, S., 2019. Influence of process parameters on synthesis of biochar by pyrolysis of biomass: an alternative source of energy. In *Recent Advances in Pyrolysis*. IntechOpen.

Yadvika, S.S., Sreekrishnan, T.R., Kohli, S., and Rana, V., 2004. Enhancement of biogas production from solid substrates using different techniques-a review. *Bioresource Technology*, *95*, pp. 1–10.

Yan, H., Zhao, C., Zhang, J., Zhang, R., Xue, C., Liu, G. and Chen, C., 2017. Study on biomethane production and biodegradability of different leafy vegetables in anaerobic digestion. *AMB Express*, *7*(1), p.27.

Yang, Y., Guo, J. and Hu, Z., 2013. Impact of nano zero valent iron (NZVI) on methanogenic activity and population dynamics in anaerobic digestion. *Water Research*, *47*(17), pp.6790-6800.

Yang, Y., Wang, J. and Zhou, Y. (2019). Enhanced anaerobic digestion of swine manure by the addition of zero-valent iron. *Energy & Fuels*, 33(12), pp.12441-12449.

Yap, S.D., Astals, S., Lu, Y., Peces, M., Jensen, P.D., Batstone, D.J. and Tait, S., 2018. Humic acid inhibition of hydrolysis and methanogenesis with different anaerobic inocula. *Waste Management*, *80*, pp.130-136.

Ye, J., Hu, A., Ren, G., Chen, M., Tang, J., Zhang, P., Zhou, S. and He, Z., 2018. Enhancing sludge methanogenesis with improved redox activity of extracellular polymeric substances by hematite in red mud. *Water Research*, *134*, pp.54-62.

Ye, J., Hu, A., Ren, G., Chen, M., Tang, J., Zhang, P., Zhou, S. and He, Z., 2018. Enhancing sludge methanogenesis with improved redox activity of extracellular polymeric substances by hematite in red mud. *Water Research*, *134*, pp.54-62.

Yılmaz, Ş. and Şahan, T., 2020. Utilization of pumice for improving biogas production from poultry manure by anaerobic digestion: A modeling and process optimization study using response surface methodology. *Biomass and Bioenergy*, *138*, p.105601.

Yu, B., Shan, A., Zhang, D., Lou, Z., Yuan, H., Huang, X., Zhu, N. and Hu, X., 2015. Dosing time of ferric chloride to disinhibit the excessive volatile fatty acids in sludge thermophilic anaerobic digestion system. *Bioresource Technology*, *189*, pp.154-161.

Yu, T., Deng, Y., Liu, H., Yang, C., Wu, B., Zeng, G., Lu, L. and Nishimura, F., 2017. Effect of alkaline microwaving pretreatment on anaerobic digestion and biogas production of swine manure. *Scientific Reports*, *7*(1), pp.1-8.

Zahra, Z., Arshad, M., Ali, M.A., Farooqi, M.Q.U. and Choi, H.K., 2020. Phosphorus Phytoavailability upon Nanoparticle Application. In *Sustainable Agriculture Reviews 41* (pp. 41-61). Springer, Cham.

Zaidi, A.A., Feng, R., Malik, A., Khan, S.Z., Shi, Y., Bhutta, A.J. and Shah, A.H., 2019. Combining microwave pretreatment with iron oxide nanoparticles enhanced biogas and hydrogen yield from green algae. *Processes*, *7*(1), p.24.

Zaidi, A.A., Khan, S.Z. and Shi, Y., 2020. Optimization of nickel nanoparticles concentration for biogas enhancement from green algae anaerobic digestion. *Materials Today: Proceedings*.

Zaidi, A.A., RuiZhe, F., Shi, Y., Khan, S.Z. and Mushtaq, K., 2018. Nanoparticles augmentation on biogas yield from microalgal biomass anaerobic digestion. *International Journal of Hydrogen Energy*, *43*(31), pp.14202-14213.

Zhai, N., Zhang, T., Yin, D., Yang, G., Wang, X., Ren, G. and Feng, Y., 2015. Effect of initial pH on anaerobic co-digestion of kitchen waste and cow manure. *Waste Management*, *38*, pp.126-131.

Zhai, W., Qin, T., Guo, T., Khan, M.I., Tang, X. and Xu, J., 2017. Arsenic Transformation in Swine Wastewater with Low-Arsenic Content during Anaerobic Digestion. *Water*, *9*(11), p.826.

Zhang, D., Chen, Y., Zhao, Y. and Zhu, X., 2010. New sludge pretreatment method to improve methane production in waste activated sludge digestion. *Environmental Science & Technology*, *44*(12), pp.4802-4808.

Zhang, J., Chen, M., Sui, Q., Tong, J., Jiang, C., Lu, X., Zhang, Y. and Wei, Y., 2016b. Impacts of addition of natural zeolite or a nitrification inhibitor on antibiotic resistance genes during sludge composting. *Water Research*, *91*, pp.339-349.

Zhang, J., Sui, Q., Zhong, H., Meng, X., Wang, Z., Wang, Y. and Wei, Y., 2018. Impacts of zero valent iron, natural zeolite and Dnase on the fate of antibiotic resistance genes during thermophilic and mesophilic anaerobic digestion of swine manure. *Bioresource Technology*, *258*, pp.135-141.

Zhang, J., Zhang, Y., Quan, X. and Chen, S., 2013. Effects of ferric iron on the anaerobic treatment and microbial biodiversity in a coupled microbial electrolysis cell (MEC)–anaerobic reactor. *Water Research*, *47*(15), pp. 5719-5728.

Zhang, L., He, X., Zhang, Z., Cang, D., Nwe, K.A., Zheng, L., Li, Z. and Cheng, S., 2017. Evaluating the influences of ZnO engineering nanomaterials on VFA accumulation in sludge anaerobic digestion. *Biochemical Engineering Journal*, *125*, pp.206-211.

Zhang, Q., Hu, J. and Lee, D.J., 2016. Biogas from anaerobic digestion processes: Research updates. *Renewable Energy*, *98*, pp.108-119.

Zhang, S., Chang, J., Lin, C., Pan, Y., Cui, K., Zhang, X., Liang, P. and Huang, X., 2017b. Enhancement of methanogenesis via direct interspecies electron transfer between Geobacteraceae and Methanosaetaceae conducted by granular activated carbon. *Bioresource Technology*, *245*, pp.132-137.

Zhang, T., Yang, Y. and Pruden, A., 2015b. Effect of temperature on removal of antibiotic resistance genes by anaerobic digestion of activated sludge revealed by metagenomic approach. *Applied Microbiology and Biotechnology*, *99*(18), pp.7771-7779.

Zhang, W., Zhang, L. and Li, A., 2015. Enhanced anaerobic digestion of food waste by trace metal elements supplementation and reduced metals dosage by green chelating agent [S, S]-EDDS via improving metals bioavailability. *Water Research*, *84*, pp. 266-277.

Zhang, Y., Feng, Y., Yu, Q., Xu, Z. and Quan, X., 2014b. Enhanced high-solids anaerobic digestion of waste activated sludge by the addition of scrap iron. *Bioresource Technology*, *159*, pp. 297-304.

Zhang, Z., Li, W., Zhang, G. and Xu, G., 2014a. Impact of pretreatment on solid state anaerobic digestion of yard waste for biogas production. *World Journal of Microbiology and Biotechnology*, *30*(2), pp.547-554.

Zhao, B.H., Chen, J., Yu, H.Q., Hu, Z.H., Yue, Z.B. and Li, J., 2017b. Optimization of microwave pretreatment of lignocellulosic waste for enhancing methane production: Hyacinth as an example. *Frontiers of Environmental Science & Engineering*, *11*(6), p.17.

Zhao, C., Yan, H., Liu, Y., Huang, Y., Zhang, R., Chen, C. and Liu, G., 2016. Bio-energy conversion performance, biodegradability, and kinetic analysis of different fruit residues during discontinuous anaerobic digestion. *Waste Management*, *52*, pp.295-301.

Zhao, Z., Li, Y., Quan, X. and Zhang, Y., 2017. Towards engineering application: Potential mechanism for enhancing anaerobic digestion of complex organic waste with different types of conductive materials. *Water Research*, *115*, pp.266-277.

Zhao, Z., Zhang, Y., Li, Y., Quan, X. and Zhao, Z., 2018. Comparing the mechanisms of ZVI and Fe3O4 for promoting waste-activated sludge digestion. *Water Research*, *144*, pp.126-133.

Zhen, G., Lu, X., Li, Y.Y., Liu, Y. and Zhao, Y., 2015. Influence of zero valent scrap iron (ZVSI) supply on methane production from waste activated sludge. *Chemical Engineering Journal*, *263*, pp.461-470.

Zheng, L., Chen, J., Zhao, M., Cheng, S., Wang, L., Mang, H.P. and Li, Z., 2020b. What could China give to and take from other countries in terms of the development of the biogas industry? *Sustainability*, *12*(4), p.1490.

Zheng, L., Cheng, S., Han, Y., Wang, M., Xiang, Y., Guo, J., Cai, D., Mang, H.P., Dong, T., Li, Z. and Yan, Z., 2020a. Bio-natural gas industry in China: Current status and development. *Renewable and Sustainable Energy Reviews*, *128*, p.109925.

Zheng, W., Li, X.M., Wang, D.B., Yang, Q., Luo, K., Jing, Y.G. and Zeng, G.M., 2013. Remove and recover phosphorus during anaerobic digestion of excess sludge by adding waste iron scrap. *Journal of the Serbian Chemical Society*, *78*(2), pp.303-312.

Zhu, H., Seto, P. and Parker, W.J., 2014. Enhanced dark fermentative hydrogen production under the effect of zero-valent iron shavings. *International Journal of Hydrogen Energy*, *39*(33), pp.19331-19336.

Zhuang, L., Tang, J., Wang, Y., Hu, M. and Zhou, S., 2015. Conductive iron oxide minerals accelerate syntrophic cooperation in methanogenic benzoate degradation. *Journal of Hazardous Materials*, *293*, pp.37-45.

Appendices

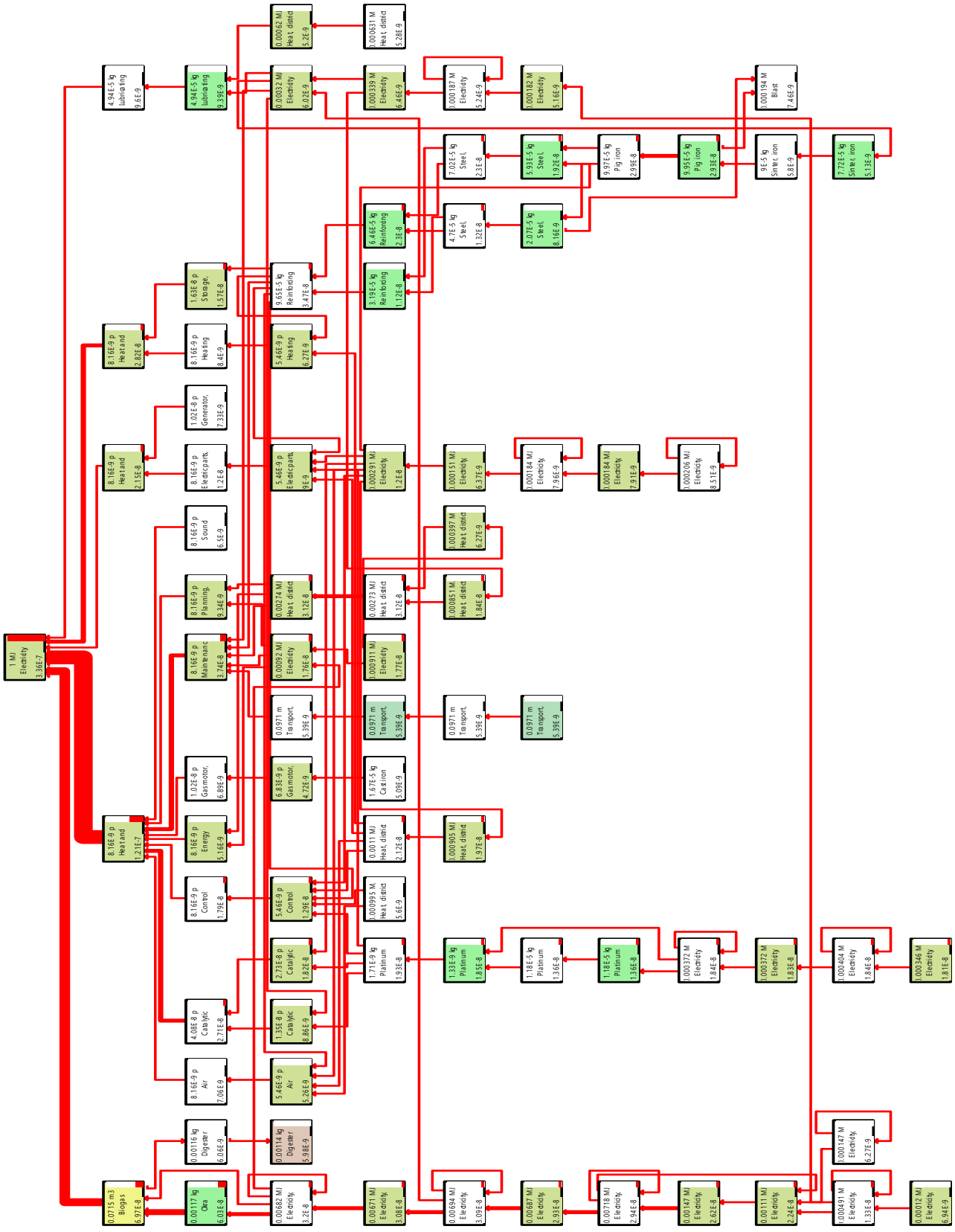

(a)

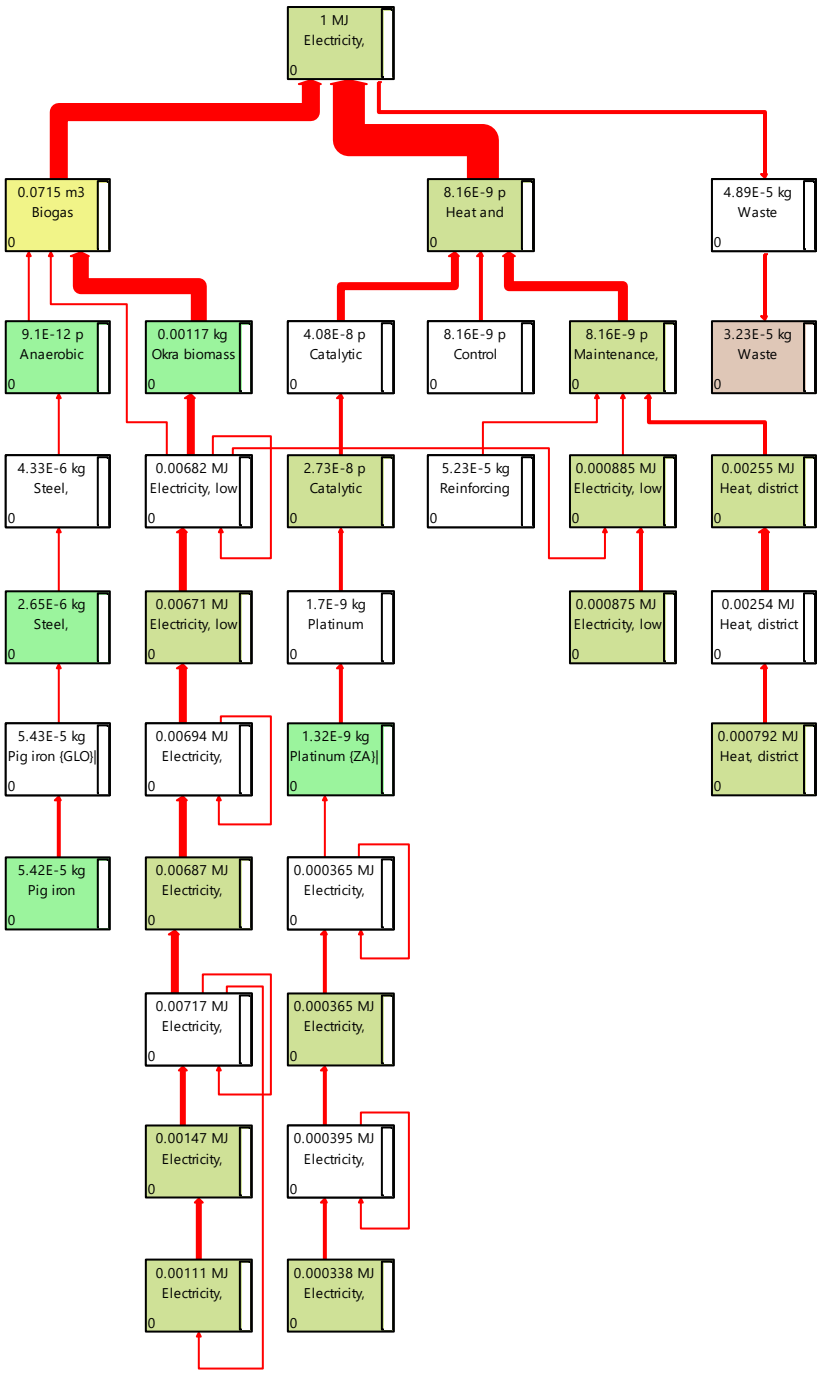

Fig. S1. Life cycle network of baseline 1 (a) 1.5 % cutoff and (b) (4 % cutoff)

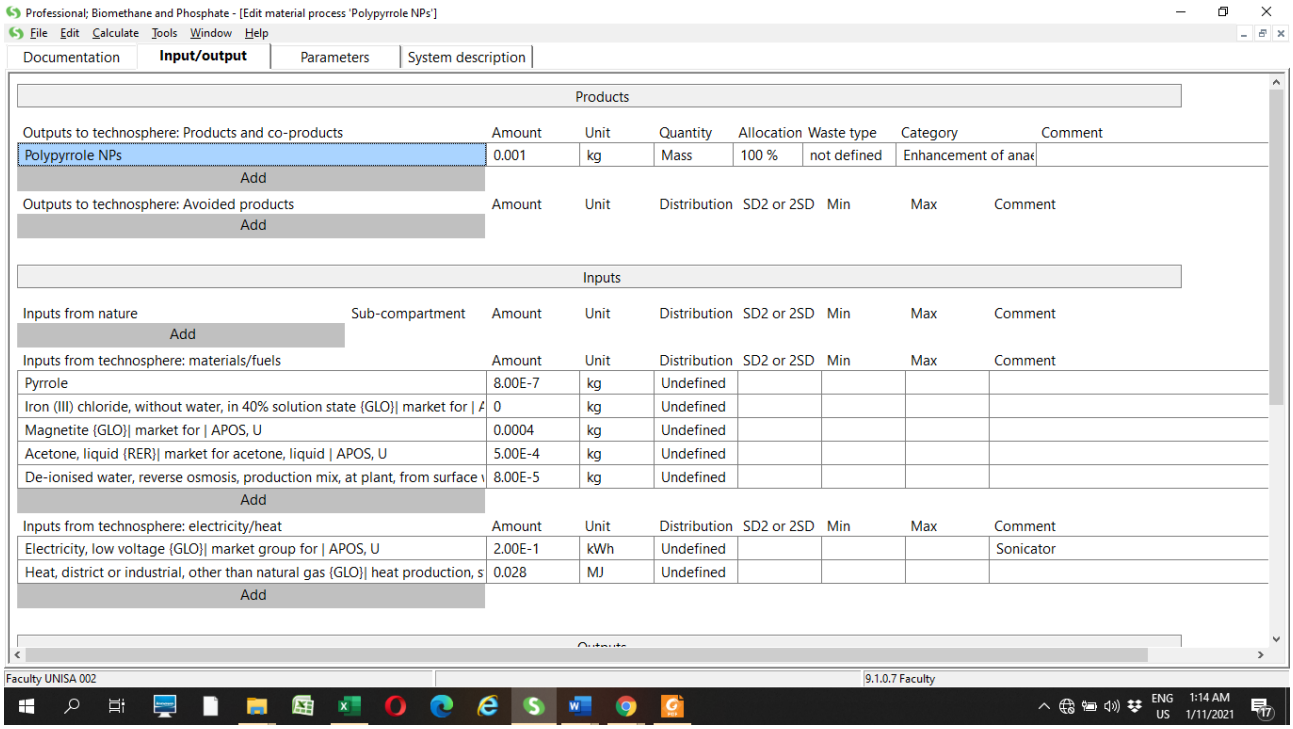

Graphical user interface sample of Simpro 9.1